

MASSACHUSETTS INSTITUTE OF TECHNOLOGY

# APOLLO

## GUIDANCE, NAVIGATION AND CONTROL

R-577

GUIDANCE SYSTEM OPERATIONS PLAN  
FOR MANNED CM EARTH ORBITAL AND  
LUNAR MISSIONS USING  
PROGRAM COLOSSUS 2E

SECTION 3 DIGITAL AUTOPILOTS  
(Rev. 11)

JUNE 1970

**MIT**

CAMBRIDGE MASSACHUSETTS 02139

**CHARLES STARK DRAPER  
LABORATORY**

# APOLLO

## GUIDANCE, NAVIGATION AND CONTROL

Submitted by: Donald C Fraser Date: 10 June 1970  
 D. C. FRASER, DIR., CONTROL AND FLIGHT DYNAMICS  
 APOLLO GUIDANCE AND NAVIGATION PROGRAM

Approved: Stephen L. Copps Date: 18 June 1970  
 S. L. COPPS, COLOSSUS PROJECT MANAGER  
 APOLLO GUIDANCE AND NAVIGATION PROGRAM

Approved: R. H. Battin Date: 17 June 1970  
 R. H. BATTIN, DIRECTOR, MISSION DEVELOPMENT  
 APOLLO GUIDANCE AND NAVIGATION PROGRAM

Approved: David G. Hoag Date: 19 June 70  
 D. G. HOAG, DIRECTOR  
 APOLLO GUIDANCE AND NAVIGATION PROGRAM

Approved: Ralph R. Ragan Date: 19 June 70  
 R. R. RAGAN, DEPUTY DIRECTOR  
 CHARLES STARK DRAPER LABORATORY

R-577

GUIDANCE SYSTEM OPERATIONS PLAN  
 FOR MANNED CM EARTH ORBITAL AND  
 LUNAR MISSIONS USING  
 PROGRAM COLOSSUS 2E

SECTION 3 DIGITAL AUTOPILOTS  
 (Rev. 11)

JUNE 1970

**MIT**

**CHARLES STARK DRAPER  
 LABORATORY**

CAMBRIDGE MASSACHUSETTS 02139

INDEXING DATA

DATE	OPR	#	T	PGM	SUBJECT	SIGNATOR	LOC
6-30-70	MIT	R-577	R	APD	*	MIT	084-63

## ACKNOWLEDGEMENT

This report was prepared under DSR Project 55-23870, sponsored by the Manned Spacecraft Center of the National Aeronautics and Space Administration through Contract NAS 9-4065 with the Massachusetts Institute of Technology.

R-577

GUIDANCE SYSTEM OPERATIONS PLAN  
FOR MANNED CM EARTH ORBITAL AND  
LUNAR MISSIONS USING  
PROGRAM COLOSSUS

SECTION 3 DIGITAL AUTOPILOTS

Signatures appearing on this page designate  
approval of this document by NASA/MSC.

Approved: Thomas F. Gibson Date: 7/13/64  
Thomas F. Gibson  
Asst. Chief, Flight Software Branch  
Manned Spacecraft Center, NASA

Approved: James C. Stokes, Jr. Date: 7/23/64  
James C. Stokes, Jr.  
Chief, Flight Software Branch  
Manned Spacecraft Center, NASA

Approved: Lynwood C. Dunseith Date: 7-30-64  
Lynwood C. Dunseith  
Chief, Flight Support Division  
Manned Spacecraft Center, NASA





















REVISION INDEX COVER SHEET  
GUIDANCE SYSTEM OPERATIONS PLAN

GSOP No. R-577 Title: For Manned CM Earth Orbital and Lunar Missions Using Program COLOSSUS 2E

Section No. 3 Title: Digital Autopilots (Revision 10)

Revision 10 incorporates the following NASA/MSC approved changes and becomes the control document for COLOSSUS 2E.

<u>PCR (PCN*)</u>	<u>TITLE</u>	<u>PAGES AFFECTED</u>
289	Addition of MIN. IMP. from RHC	xix, 3.2-1, 11, 18, 19, 40
292	Add Time Display to V79	3.2-5, 6, 7
822	Delete Stroke Test	xvii, xx, 3.3-4, 6, 55, 56
867	Make R64Y Rotation Fix	3.2-6, 8
869	Rate-Aided Optics Drive	3.3-5
1020	Change Initial TVCEXEC Delay	3.3-6, 8, 34
1003*	GSOP Section 3 (Rev. 10) Editorial Changes	(See Below)

NOTE: A solid bar, █, in the margin indicates a change in specification authorized by the PCR (PCN\*) listed at the bottom of the page. A series of dots, ●, indicates a document improvement change as authorized by PCN 1003\*.

Date: June 1970

REVISION INDEX COVER SHEET  
GUIDANCE SYSTEM OPERATIONS PLAN

GSOP No. R-577 Title: For Manned CM Earth Orbital and Lunar  
Missions Using Program COLOSSUS 2E

Section No. 3 Title: Digital Autopilots (Revision 11)

Revision 11 is published as change pages to Section 3, Revision 10. With the pages substituted, it becomes the control document for COLOSSUS 2E (Revision 108). The following NASA/MSC approved changes are included in this revision.

<u>PCR (PCN*)</u>	<u>TITLE</u>	<u>PAGES AFFECTED</u>
1041	Add AVEGFLAG check in implementation of PCR 984	3.5-2

NOTE: A solid bar, **|**, indicates a change in specification authorized by the PCR (PCN\*) listed at the bottom of the page.

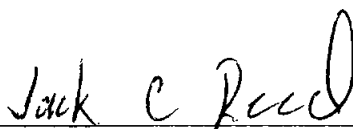
## FOREWORD

The Guidance System Operations Plan (GSOP) for Program COLOSSUS 2E is published in six sections as separate volumes:

1. Prelaunch
2. Data Links
3. Digital Autopilots
4. Operational Modes
5. Guidance Equations
6. Control Data

With this issue, Section 3 is revised from the previous issue of COLOSSUS GSOP (Rev. 10, February 1970 for COLOSSUS 2E) in order to reflect the NASA/MSC-approved changes listed on the "Revision Index Cover Sheet" at the beginning of this volume.

This volume is published as a control document governing digital autopilot programs for COLOSSUS 2E. Revisions constituting changes to the COLOSSUS Program require NASA approval.



---

Jack C. Reed  
APOLLO Documentation Group



TABLE OF CONTENTS

<u>Section</u>	<u>Page</u>
3.1 INTRODUCTION . . . . .	3.1-1
3.1.1 Astronaut Interface . . . . .	3.1-1
3.1.2 Automatic Transitions in Operating Mode . . . . .	3.1-2
3.2 REACTION CONTROL SYSTEM DIGITAL AUTOPILOT . . . . .	3.2-1
3.2.1 Modes of Operation . . . . .	3.2-1
3.2.2 Crew Control of RCS DAP Configuration . . . . .	3.2-2
3.2.3 RCS DAP Implementation . . . . .	3.2-11
3.2.4 RCS DAP Program Design . . . . .	3.2-20
3.2.5 Restart Behavior of the RCS DAP . . . . .	3.2-45
3.3 THRUST VECTOR CONTROL AUTOPILOT . . . . .	3.3-1
3.3.1 TVC DAP Design Requirements . . . . .	3.3-1
3.3.2 Operating Procedures . . . . .	3.3-3
3.3.3 TVC DAP Filters: Design and Implementation . . . . .	3.3-7
3.3.4 TVC DAP Variable Gains . . . . .	3.3-24
3.3.5 Trim Estimation . . . . .	3.3-29
3.3.6 TVC ROLL DAP . . . . .	3.3-33
3.3.7 TVC DAP Interfaces . . . . .	3.3-43
3.3.8 Restart Protection of the TVC DAP . . . . .	3.3-52
3.4 ENTRY AUTOPILOT AND MISSION CONTROL PROGRAMS . . . . .	3.4-1
3.4.1 Atmospheric Reentry -- an Overall View . . . . .	3.4-1
3.4.2 Reentry -- System Point of View . . . . .	3.4-6
3.4.3 Reentry -- Mission Oriented View . . . . .	3.4-9
3.4.4 ENTRY Autopilot -- Introduction . . . . .	3.4-20
3.4.5 Aerodynamic Attitude and Body Rate Estimation . . . . .	3.4-22

TABLE OF CONTENTS (cont.)

<u>Section</u>	<u>Page</u>
3.4.6 Extra-atmospheric DAP . . . . .	3.4-34
3.4.7 Atmospheric DAP. . . . .	3.4-41
3.4.8 Roll Attitude Control -- CM/RCS. . . . .	3.4-46
3.4.9 DAP Displays and Telemetry. . . . .	3.4-52
3.4.10 Restart Protection of ENTRY DAP . . . . .	3.4-53
3.4.11 DAP Flow Chart Summary. . . . .	3.4-53
3.4.12 Symbol Table. . . . .	3.4-68
 3.5 TAKEOVER OF SATURN STEERING	 3.5-1
3.5.1 Automatic Mode . . . . .	3.5-1
3.5.2 Manual Mode. . . . .	3.5-2
3.5.3 Coarse Align Avoidance During SATURN Steering . . . . .	3.5-2
3.5.4 Restarts. . . . .	3.5-2
3.5.5 S-IVB Engine-off Signal . . . . .	3.5-4
 3.6 COASTING-FLIGHT ATTITUDE MANEUVER ROUTINE	 3.6-1
3.6.1 Introduction . . . . .	3.6-1
3.6.2 R60 Executive . . . . .	3.6-3
3.6.3 VECPOINT. . . . .	3.6-6
3.6.4 KALCMANU Maneuver-Parameters Calculation . . . . .	3.6-16
3.6.5 KALCMANU Steering . . . . .	3.6-21

ILLUSTRATIONS

<u>Figure</u>		<u>Page</u>
3.2.1	PGNCS RCS Attitude-Control Attitude-Error Display . . . . .	3.2-10
3.2.2	PGNCS RCS Attitude Hold Logic . . . . .	3.2-13
3.2.3	PGNCS RCS Automatic Control Logic . . . . .	3.2-14
3.2.4	PGNCS RCS Manual Rate Control . . . . .	3.2-16
3.2.5	PGNCS RCS Attitude Control Free Mode Control . . . . .	3.2-19
3.2.6	CSM - RCS Digital Autopilot Rate Filter . . . . .	3.2-29
3.2.7	Filter Responses . . . . .	3.2-30
3.2.8	Phase Plane . . . . .	3.2-32
3.2.9	Apollo Spacecraft . . . . .	3.2-34
3.2.10	DAP Timing -- Initialization . . . . .	3.2-46
3.2.11	DAP Timing -- Normal Run . . . . .	3.2-48
3.3.1	Gimbal Drive Test/Trim . . . . .	3.3-5
3.3.2	TVC DAP Startup . . . . .	3.3-8
3.3.3	CSM/LM, High-bandwidth Mode; Rigid-body Open-loop function, Magnitude vs Phase. . . . .	3.3-17
3.3.4	CSM/LM, Low-bandwidth Mode; Rigid-body Open-loop function, Magnitude vs Phase. . . . .	3.3-18
3.3.5	CSM; Rigid-body Open-loop function, Magnitude vs Phase . . . . .	3.3-19
3.3.6	Generalized Sixth-Order Filter . . . . .	3.3-21
3.3.7	Mathematical Block Diagram of the CSM/LM and CSM DAP Filter Configurations . . . . .	3.3-23
3.3.8	Sketch of Curves Used by Program TVCMASPROP to Calculate $I_{xx}$ , $I_{AVG}$ and $I_{AVG}/T_x$ . . . . .	3.3-26
3.3.9	Mass Properties Approximations: CSM Docked With LM Ascent Stage Only . . . . .	3.3-27
3.3.10	Block Diagram of Pitch-axis Thrust Misalignment Correction (TMC) Loop . . . . .	3.3-32
3.3.11	Equivalent s-Domain Transfer Function of Thrust-misalignment Estimator Loop . . . . .	3.3-35
3.3.12	TVC ROLL Digital Autopilot . . . . .	3.3-37
3.3.13	Phase-plane Switching Lines for the TVC ROLL DAP . . . . .	3.3-38
3.3.14	Analytic Switching Lines and Control Regions in the TVC ROLL DAP Phase Plane . . . . .	3.3-40
3.3.15	TVC ROLL DAP Phase-plane Switching Logic. . . . .	3.3-41
3.3.16	TVC ROLL DAP Jet-selection Logic . . . . .	3.3-44
3.3.17	Interface Between Cross-product Steering and TVC DAP . . . . .	3.3-47

ILLUSTRATIONS (cont'd)

<u>Figure</u>		<u>Page</u>
3.3.18	CDU Rates to Body Rates Transformation . . . . .	3.3-48
3.3.19	FDAI Needle Variables . . . . .	3.3-49
3.3.20	Error Needles Interface for TVC DAP . . . . .	3.3-50
3.3.21	TVC Actuator Command Interface: Pitch Channel . . . . .	3.3-53
3.4.1	Typical Entry Events . . . . .	3.4-2
3.4.2	Block Diagram for ENTRY DAP . . . . .	3.4-7
3.4.3	Timing Diagram for ENTRY DAP . . . . .	3.4-8
3.4.4	Events in Mission Control Program . . . . .	3.4-10
3.4.5	Transition From Program P62 to P63 . . . . .	3.4-11
3.4.6	ENTRY Digital Autopilot Initialization . . . . .	3.4-13
3.4.7	ENTRY DAP Starting Sequence . . . . .	3.4-16
3.4.8	Milestones in Reentry Steering . . . . .	3.4-17
3.4.9	Termination of Entry Control (P60s) . . . . .	3.4-19
3.4.10	CM Thruster Schematic . . . . .	3.4-21
3.4.11	ENTRY Autopilot Coordinate Triads . . . . .	3.4-23
3.4.12	Platform to Body Transformation . . . . .	3.4-24
3.4.13	CM Body Attitude Angles -- Definition . . . . .	3.4-25
3.4.14	Computation of CM Body Attitude Angles . . . . .	3.4-26
3.4.15	Gamma Dot Correction to CM Body Rates . . . . .	3.4-28
3.4.16	Initialization of Body Attitude Calculation (CM/POSE) . . . . .	3.4-30
3.4.17	Calculation of Attitude Angles . . . . .	3.4-31
3.4.18	Attitude Calculation -- Continued . . . . .	3.4-32
3.4.19	ENTRY Autopilot Attitude Modes . . . . .	3.4-35
3.4.20	Phase-plane Logic for CM Attitude DAP . . . . .	3.4-36
3.4.21	Phase-plane Logic (Without BIAS) for CM Attitude DAP . . . . .	3.4-39
3.4.22	CM Pitch Rate Autopilot . . . . .	3.4-44
3.4.23	CM Yaw Rate Autopilot . . . . .	3.4-45
3.4.24	Dual-gain Roll-attitude Phase Plane With Control Line . . . . .	3.4-47
3.4.25	Roll System Deadzone . . . . .	3.4-51
3.4.26	Buffer Zone . . . . .	3.4-51
3.4.27	ROLL DAP Synchronizer . . . . .	3.4-54
3.4.28	Gimbal-angle Rates and Body-rate Initialization . . . . .	3.4-55
3.4.29	CM Body Rates . . . . .	3.4-56
3.4-30	CM Attitude Angles: Pitch and Yaw Dampers . . . . .	3.4-57
3.4-31	Exoatmospheric Attitude CM DAP . . . . .	3.4-58

ILLUSTRATIONS (cont'd)

<u>Figure</u>		<u>Page</u>
3.4.32	Biased DZ and Rate DZ for CM Attitude DAP . . . . .	3.4-59
3.4.33	CM Body-rate Estimation . . . . .	3.4-60
3.4.34	Dual-gain ROLL DAP -- Error Calculation . . . . .	3.4-61
3.4.35	Dual-gain ROLL DAP -- Initial Logic . . . . .	3.4-62
3.4.36	Dual-gain ROLL DAP -- Time Calculations . . . . .	3.4-63
3.4.37	ROLL DAP -- Time Interval Processing . . . . .	3.4-64
3.4.38	ROLL DAP -- Time Interval Execution Logic . . . . .	3.4-65
3.4.39	ENTRY DAP Display and Telemetry Interface . . . . .	3.4-66
3.5.1	Logic Diagram of CMC Takeover of Saturn IU Autopilot . . . . .	3.5-3
3.6.1	R60 Information Flow . . . . .	3.6-2
3.6.2	R60 Executive . . . . .	3.6-4
3.6.3	The Coordinate Frames and Transformations Used in VECPOINT . . . . .	3.6-9
3.6.4	VECPOINT Logic Flow . . . . .	3.6-11
3.6.5	Rotation to Correct for Gimbal Lock . . . . .	3.6-13
3.6.6	Geometry for Computing the Maximum Value of the Angle A . . . . .	3.6-15
3.6.7	Calculation of KALCMANU Maneuver Parameters . . . . .	3.6-18
3.6.8	Maneuver Phase-Plane Trajectories . . . . .	3.6-24
3.6.9	KALCMANU Steering Logic . . . . .	3.6-25

TABLES

<u>Table</u>		<u>Page</u>
3.2-I	DAP Filter Gains . . . . .	3.2-26
3.2-II	Phase-plane Summary of Decision Areas . . . . .	3.2-32
3.2-III	Jet Selection for Pitch Rotations -- Quads AC . . . . .	3.2-37
3.2-IV	Jet Selection for Yaw Rotations -- Quads BD . . . . .	3.2-37
3.2-V	Jet Selection for Roll Rotations -- Quads AC . . . . .	3.2-38
3.2-VI	Jet Selection for Roll Rotations -- Quads BD . . . . .	3.2-38
3.2-VII	X-translations -- Quads AC . . . . .	3.2-39
3.2-VIII	X-translations -- Quads BD . . . . .	3.2-39
3.2-IX	Y-translations -- Quads AC . . . . .	3.2-39
3.2-X	Z-translations -- Quads BD . . . . .	3.2-39
3.3-I	W-Transform of the High-Bandwidth Filter . . . . .	3.3-13
3.3-II	W-Transform of the Low-Bandwidth Filter . . . . .	3.3-14
3.3-III	Z-Transform of the High-Bandwidth Filter . . . . .	3.3-15
3.3-IV	Z-Transform of the Low-Bandwidth Filter . . . . .	3.3-16
3.3-V	TVC DAP Filter Coefficients and Gains . . . . .	3.3-22
3.3-VI	Parameters of Thrust-misalignment Estimator Loop . . . . .	3.3-34
3.3-VII	Equivalent s-Domain Transfer Function for Thrust-misalignment Estimator Loop . . . . .	3.3-35
3.3-VIII	ROLL DAP Parameters . . . . .	3.3-45
3.4-I	Outline of Entry Events . . . . .	3.4-5
3.4-II	Table of Jet Codes . . . . .	3.4-42
3.4-III	ENTRY DAP Constants . . . . .	3.4-67

## SECTION 3

### DIGITAL AUTOPILOTS

#### 3.1 INTRODUCTION

by Jack C. Reed

Within separate sections of the command-module computer (CMC), COLOSSUS Program, three digital autopilots (DAPs) perform the stabilization and control required for CSM coasting flight, CSM powered flight, and CM entry:

- a. The reaction-control-system digital autopilot is described in subsection 3.2. The RCS DAP is the means by which the primary guidance, navigation, and control system (PGNCS) maneuvers the command and service module (CSM) during the free-fall phases of the mission -- with, and without, the lunar module (LM) attached.
- b. The thrust-vector-control digital autopilot is described in subsection 3.3. The TVC DAP is the means by which PGNCS stabilizes and controls the attitude of the CSM (or CSM/LM) during service-propulsion-system (SPS) thrusting.
- c. The ENTRY DAP (subsection 3.4) provides the means for controlling the attitude of the command module (CM) after separation from the service module (SM).

In addition to the primary autopilots, a SATURN takeover function (subsection 3.5) is provided by which PGNCS can issue rate-command signals to the S-IVB autopilot.

##### 3.1.1 Astronaut Interface

The activation of any DAP or SATURN-control function, as well as its interfaces with other programs, is governed by the major mission program in progress. (See COLOSSUS GSOP, Section 4. ) Astronaut initiation of a DAP function, except for the RCS DAP FREE mode, requires that the PGNCS inertial subsystem (ISS) be in the inertial mode (evidenced by the absence of the NO ATTITUDE indication) and that the SC CONT switch be in the CMC position. The RCS DAP can be used in the FREE mode, independent of ISS status. In addition, crew control of DAP operation is effected as follows:

##### CMC MODE Switch Position. --

AUTO . . . . . Commands RCS DAP automatic mode  
HOLD . . . . . Commands RCS DAP attitude-hold mode  
FREE . . . . . Commands RCS DAP free mode

Rotational Hand Controller (RHC). -- Six discrettes command angular rotation during operation of RCS DAP and during SATURN control.

Translation Hand Controller (THC). -- Six discrettes command translation accelerations during operation of RCS DAP.

Minimum Impulse Controller (MIC). -- Six discrettes command rotational minimum impulses during operation of RCS DAP in the free mode.

Note that the RCS DAP responds to all three hand controllers, as well as to mode-switch selection; the SATURN-control function responds only to the RHC. All other

DAPs operate independent of CMC MODE selection and of manual inputs. Should the SC CONT switch be moved from the CMC position, PGNCS control will terminate and will attempt to resume when the switch is returned to CMC. Steering accuracy, however, may be downgraded.

The crew also has access to DAP padload erasables: as normal procedure, the crew will be responsible for selecting MANEUVER rates and deadbands for the RCS DAP; in certain instances, the crew may be responsible for changing gains and filter coefficients for the TVC DAP.

For normal activity, the DAP data input, display, and verification are mechanized through a single extended verb (V48). This verb sequences through three noun displays (N46, N47, N48), comprising all data that the crew is normally responsible for. These nouns are described in detail in the appropriate subsections for the individual DAPs.

### 3.1.2 Automatic Transitions in Operating Mode

RCS DAP turn on is a manual procedure via the DSKY and is described in subsection 3.2.

TVC DAP operation is governed by program control (P40). At ignition time, the SPS-thrusting program automatically suspends RCS DAP control and initiates the TVC DAP. At burn termination, the program transfers control back to the RCS DAP.

ENTRY DAP operation is governed by the P60 programs. Once the RCS DAP has positioned the spacecraft in the CM-SM separation attitude, separation has occurred, and this has been acknowledged by the crew via the DSKY, the mission program automatically suspends RCS DAP operation, and ENTRY DAP controls CM attitude during the remainder of the mission. (For the definitive and up-to-date description of the mission-control sequence, see COLOSSUS GSOP Section 4. )



### 3.2 REACTION CONTROL SYSTEM DIGITAL AUTOPILOT

by Donald W. Keene and Joseph F. Turnbull

The Reaction Control System Digital Autopilot (RCS DAP) provides attitude and translation control for all three axes of the CSM during nonthrusting phases of flight. The DAP receives and processes data from various internal and external sources. Included among these are the keyboard routines that affect the autopilot, the panel switches and hand controllers, the IMU-CDU angles, and the internal steering commands for controlling automatic maneuvers. The DAP, in turn, issues jet-on and jet-off commands to the reaction jets on the service module, through output channels 5 and 6, and generates attitude-error signals for display on the flight-director-attitude-indicator (FDAI) error meters.

#### 3.2.1 Modes of Operations

The RCS DAP may operate in one of three modes selected by the crew via the CMC MODE switch. These modes can be summarized as follows:

i. FREE Mode

a. Rotational hand controller (RHC) commands are treated as minimum impulse commands. Each time the RHC is moved out of detent, a single 14 ms firing of the control jets results on each of the axes commanded.

b. If there are no RHC commands, minimum-impulse controller (MIC) commands are processed. Each time the MIC is moved out of detent, a single 14-ms firing of the control jets results on each of the axes commanded.

c. If neither RHC nor MIC commands are present, the S/C will drift freely.

ii. HOLD Mode

a. If there are no RHC commands, the S/C will be held about the attitude reached upon switching to HOLD or upon termination of a manual rotation.

b. RHC commands override attitude hold and result in rotations at a predetermined rate (as specified by N46) on each of the appropriate control axes\* for as long as the RHC remains out of detent. When the RHC returns to detent in all three axes, all angular rates are driven to within a deadband; attitude hold is then established about the new S/C attitude.

c. MIC commands are ignored.

---

\*The control axes are rotated, with respect to the navigation base axes, by  $-7.25$  deg about  $X_{NAV}$ . This rotation aligns the control axes with the RCS jet axes. Specifically, the Y-control axis is parallel to a line joining RCS jet Quads B and D, and the Z-control axis is parallel to a line joining RCS jet Quads A and C.

iii. AUTO Mode

- a. If there are no RHC commands, the DAP accepts rate and attitude commands from the automatic steering routines to bring the S/C to the desired attitude at the specified rate.
- b. RHC commands override automatic maneuvers and are interpreted as rate commands (as in ii.b. above). When RHC command ceases, automatic maneuvers are not immediately resumed, but rather attitude hold is established about the new orientation. The automatic maneuver can be resumed only by astronaut action via the DSKY.
- c. In the absence of automatic-maneuver commands, the DAP functions exactly as in the attitude-hold mode.
- d. MIC commands are ignored.

Translation hand controller (THC) commands will be accepted in any mode and will be combined with the rotation commands whenever possible. In the event of a quad failure, however, rotation control will assume priority over translation; i.e., translations will be ignored if they would induce rotations that cannot be compensated by RHC (or automatic) commands or if they would cancel a desired rotation. The crew is responsible for performing ullage with the THC and by the selection and management of  $\pm X$ -translation quads as described below.

3.2.2 Crew Control of RCS DAP Configuration

3.2.2.1 DSKY Operation

VERB 48: Load DAP Data

Most of the DAP variables over which the crew has control are loaded by means of Verb 48, which is normally executed before the DAP is turned on for the first time and any time thereafter that the crew wishes to change or update the data. (Changing the rate data, however, has no effect on KALCMANU once the maneuver begins.) Verb 48 will display, successively, three nouns for loading and verification: NOUN 46, NOUN 47, and NOUN 48.

NOUN 46 -- Registers 1 and 2 each display five octal digits (Register 3 is blank):

Register 1	Config.	XTAC	XTBD	DB	RATE
------------	---------	------	------	----	------

- Configuration:
- 0 -- no DAP is requested
  - 1 -- CSM alone
  - 2 -- CSM and LM
  - 3 -- SIVB, CSM and LM (SIVB control)
  - 6 -- CSM and LM (ascent stage only)

**XTAC: X-translations using Quads AC**

0 -- Do not use AC

1 -- Use AC

**XTBD: X-translations using Quads BD**

0 -- Do not use BD

1 -- Use BD

**DB: Angular Deadband for Attitude Hold and Automatic Maneuvers**

0 --  $\pm 0.5$  deg

1 --  $\pm 5.0$  deg

**RATE: Rate Specification for RHC in HOLD or AUTO Mode and for KALCMANU-supervised Automatic Maneuvers**

0 -- 0.05 deg/sec

1 -- 0.2 deg/sec

2 -- 0.5 deg/sec

3 -- 2.0 deg/sec

Register 2

AC Roll	Quad A	Quad B	Quad C	Quad D
---------	--------	--------	--------	--------

**AC Roll: Roll-Jet Selection**

1 -- Use AC Roll

0 -- Use BD Roll

**A, B, C, D: Quad Fails**

1 -- Quad operational

0 -- Quad has failed

**NOUN 47 -- Two-decimal components**

**Register 1: CSM weight in pounds.**

**Register 2: LM weight in pounds.**

The moments of inertia and other pertinent parameters are stored in the CMC as a function of the keyed-in weights.

NOUN 48 -- Two-decimal components, used for TVC DAP only.

Register 1: Pitch-trim gimbal offset, in 1/100 degree

Register 2: Yaw-trim gimbal offset, in 1/100 degree

To initialize or change the operation of the DAP, the Verb 48 procedure is normally used. The logic of Verb 48 decodes each of the nouns and, on the basis of its value, initializes a number of DAP variables. Direct loading of one of the nouns (via Verb 24, for instance) would not cause the noun to be decoded and, therefore, would not be an effective means of altering DAP operation.

Verb 48 should not be executed while the TVC DAP is on (during powered flight). An attempt to execute Verb 48 while the TVC DAP is running will cause the operator-error light to go on and will have no further effect.

VERB 46: Establish G&N Control

After Verb 48 has been completed, Verb 46 may be executed to establish autopilot control of the S/C. If the configuration digit is "1," "2," or "6," and if the TVC DAP is not running, the RCS DAP will begin initialization. Should the IMU be on and usable, the RCS DAP will become fully operational in slightly over 1.7 second. If the configuration digit is "3," RHC commands are sent to the SIVB autopilot and steering jets for manual rate control. If the configuration digit is "0," execution of Verb 46 will terminate the RCS DAP and the SATURN Takeover Function.

During TVC DAP operation, execution of Verb 46 will not affect the RCS DAP, which is not then operational. The significance of executing Verb 46 during TVC operation is described in subsection 3.3.

VERB 49: Start Crew-Defined Maneuver

Verb 49 calls R62, the crew-defined maneuver routine. As described in Section 4 of this GSOP, R62 provides the crew with the ability to specify a final vehicle attitude. This attitude can be achieved by means of a KALCMANU-supervised attitude maneuver. (A detailed description of the coasting-flight attitude maneuver routine is presented in Subsection 3.6.)

VERB 58: Resume Tracking Attitude

Routine 61, the tracking attitude routine, provides the DAP with the information required to automatically track the LM during P20. Whenever R61 requires an attitude maneuver resulting in any gimbal-angle change of 10 degrees or more it will check the V50N18FL flagbit and if it is set, R61 will call the attitude maneuver routine (R60). If the V50N18FL flagbit is not set, the uplink activity light will be lit, new tracking commands will not be communicated to the DAP, and the DAP will continue to maneuver with the last computed tracking commands. V50N18FL is set by calling P20 initially (rendezvous flag not set or V37E20E keyed when P20 is the present major mode) or by keying V58E. It is reset by all R61 exits.

When R60 is called, it produces a flashing V50N18 and displays the desired gimbal angles. A PROCEED in response to the V50N18 will result in an execution

of the VECPOINT routine followed by a check to verify that the SC CONT switch is in CMC and the mode switch is in AUTO. If these two switches are so placed, the maneuver is executed via KALCMANU; otherwise R60 is exited.

If automatic tracking is interrupted by RHC activity, the flag bit STIKFLAG is set. This inhibits tracking commands and puts the DAP into an attitude-hold mode when the stick is undeflected. Verb 58, in addition to setting V50N18FL, also resets STIKFLAG; thus, the use of Verb 58 after RHC activity will re-enable automatic tracking. If there is no gimbal-angle change greater than 10 deg, automatic tracking will resume immediately without an R60 automatic maneuver.

#### VERB 79: Start Barbecue Mode Routine

Verb 79 calls R64, the barbecue mode routine. R64 is described from an operational viewpoint in Section 4 of this GSOP. Since this routine is closely related to utilization of the RCS DAP, it will also be described in some detail here.

A R64 enables the crew to perform 1) PTC (X-axis roll), 2) ORBRATE\*, and 3) deadband changing without having to do direct erasable loading. ORBRATE has only one restriction on attitude which is that CDUZ should be close to zero. If this condition is met, the CDUY axis (that is, the inner gimbal axis) will lie in the Y - Z RCS control axis plane. This is necessary because the ORBRATE option is implemented by incrementing the desired CDUY value every DAP cycle and commanding, as a function of the desired value of CDUX, rates about the Y and Z RCS control axes.

If no other extended verb is active and if a program other than P00 is running, keying V79E results in a flashing V06 N16 display with all zeros in R1, R2, and R3. The astronaut can load into N16 the ground elapsed time (GET) at which he wants the PTC or ORBRATE to begin. Leaving all zeros in N16 indicates that the astronaut wants maneuvering to begin immediately upon PROCEEDing on the V06N79 display which is described next.

In programs other than P00 a PROCEED in response to V06 N16 will cause R64 to sequence to a flashing V06 N79 display. In P00, R64 has no time option and the first display of R64 will be the flashing V06 N79. The first component of N79 is the commanded rate, displayed to 0.0001 deg/sec. The second component is the RCS-DAP deadband, displayed to 0.01 deg. The third component is the axis code: axis code  $\pm$  00000 implies the X axis (that is, the PTC option); nonzero implies the Y axis (that is, the ORBRATE option).

Once N79 is configured as desired, a PROCEED in response to the flashing V06 N79 will result in one of two alternatives. If P00 is the active program; or if P00 is not active but either N16 was left all zeros or the actual GET is greater \*ORBRATE is the name applied to a rate-drive procedure about the Y stable-member axis.

than that loaded in N16, the R64 coding which actually starts the maneuver will be executed immediately. If a non-P00 program is active and if the N16 time is greater than the actual GET, a "long call" will be setup such that the maneuver starting segment of R64 coding will be executed at the time loaded in N16.

The portion of R64 coding which starts the maneuver will, when it is executed:

1. Change the DAP deadband to the magnitude specified by the second component of N79.
2. If the PTC option is selected, generate a commanded rate about the vehicle X axis equal to that specified in the first component of N79 and also generate the appropriate increment to be added every DAP cycle to the desired CDUX.
3. If the ORBRATE option is selected, generate a commanded rate about the Y RCS control axis equal to the value specified in the first component of N79 times  $\cos(\text{CDUX} - 7.25^\circ)$ , generate a commanded rate about the Z RCS control axis equal to the value specified in the first component of N79 times  $-\sin(\text{CDUX} - 7.25^\circ)$ , and also generate the appropriate increment to be added every DAP cycle to the desired CDUY.
4. Configure a DAP erasable location such that a) if the PTC option is selected, a roll firing will be forced during the next DAP cycle, independent of whether the DAP phase-plane point is outside the roll deadzone, or b) if the ORBRATE option is selected, pitch and yaw firings will be forced during the next DAP cycle, independent of whether the DAP phase-plane point is outside the pitch deadzone.

It is important to remember that the erasable locations used for N79 are locations shared with the VECPOINT and KALCMANU computations for automatic maneuvering so data in N79 is not necessarily saved from the previous use of R64. Therefore, in general, it will be necessary to load N79 using V25 every time R64 is used. Moreover, once R64 is used to set up a "long call" to start maneuvering in the future, no R60, R61, or R63 maneuvering can be done. If it is, garbage will be left in N79 and any maneuver started by R64 would be completely random in rate and direction.

As is the case with all routines and programs involving automatic maneuvering, the maneuvering commands will be communicated to the DAP only if the S/C CONT switch is in CMC and the CMC MODE switch is in AUTO. If such is the case, the physical response to the execution of the maneuver starting segment of R64 will be an immediate forced roll firing or forced pitch and yaw firings (depending on the axis option selected in N79) that will reduce the difference between the commanded rate and the actual rate by about 80%. Additional firings to further refine the S/C rate will be commanded when the phase-plane point eventually leaves the deadzone. If a large deadband has been chosen, the time between the initial forced firing and the first additional firing may be very long - perhaps 10 or 20 minutes.

3.2-6

Revised

Added

GSOP # R-577

PCR # 292,867

Rev. 10

Date 2/70

When the first component of N79 is zero, the commanded rates and the CDU increments generated by a PROCEED on V06 N79 are identically zero. In this situation, the effect of doing R64 will be to set the deadband to the value specified in the second component of N79.

Once R64 has initiated maneuvering, the mode of operation established by it can be altered in various ways. The following tabulation presents the possible actions and their respective effects.

ACTION	EFFECTS		
	Zero the Commanded Rate	Return to the Deadband Specified by R03	Zero the DAP Attitude Error
V46E	✓	✓	✓
S/C Control Switch Cycled CMC → SCS → CMC	✓	✓	✓
CMC Mode Switch to HOLD	✓		✓
Rotational-Hand-Controller Activity	✓		✓
V37EXXE	✓	✓	
KALCMANU	*		✓
* KALCMANU generates new commanded rates.			

Operationally, several potential uses of R64 are envisioned:

1. Automatic PTC Initiation

The availability of R64 means that direct loading of erasable memory in order to initiate PTC or to widen the deadband is no longer necessary. Also, the V49 automatic maneuver to PTC attitude (which, in addition to maneuvering the S/C, assured that various erasables were properly configured prior to direct erasable loading) is no longer essential since R64 properly initializes all the necessary erasable locations. Still required, however, is the wait period between maneuvering to PTC attitude and PTC initiation, so that residual rates will be damped out before PTC is begun.

The roll forced firing will bring the S/C up to about 80% of the rate specified in the first component of N79. If a wide deadband is used, it will be a long time before the next roll firing occurs. Consequently, it may be desirable procedurally to load a rate in N79 that is 25 to 30 percent higher

than the desired PTC rate. The single forced firing should then produce a rate rather close to the actually desired PTC rate. The rest of the PTC checklist (disabling roll jets, etc.) can then be executed without waiting for additional firings to bring the S/C up to the desired rate.

## 2. Deadband Changing

If all zeros are loaded in the first component of N79, the effect of executing R64 will be to change the DAP deadband to that specified in the second component of N79. R64 does not change the attitude reference. Thus, if R64 were used to decrease the deadband, an attitude maneuver might be performed to get the S/C to within the new decreased deadband of the reference.

Also, the logic involved with R64 will produce either a forced firing about the roll axis or forced firings about the pitch and yaw axes (depending on the axis option selected in N79), even if the command rate is zero. This forced firing can be inhibited external to the DAP by switching the roll or pitch MAN ATT switch to ACCEL CMD before PROCEEDing on V06 N79. The switch can be returned to RATE CMD almost immediately (0.1 sec) after keying PROCEED.

## 3. Y-Axis Rate Drive

Program COLOSSUS does not have a local-vertical tracking routine. As a substitute for such a routine, R64 can be used to drive the S/C at orbital rate.

The accuracy of the rate drive is affected by decimal-to-octal conversion and quantization. It is estimated that if a rate on the order of 0.05 deg/sec is loaded in the first component of N79, then the long-term average value of the S/C rate will be within 1 deg/hr of the desired value. In other words, if the S/C is aligned initially so that some reference vector in the S/C is aligned with the local vertical and the accurate value of the orbital rate is loaded in the first component of N79, then after one hour it is possible that the DAP will be commanding the reference vector to point as much as one degree from the true local vertical.

The use of R64 to control a Y-axis rate may also be of help elsewhere; for example, in landmark tracking during P22. It should be kept in mind that V37 will do a STOPRATE which will terminate automatic maneuvering.

### 3.2.2.2 Attitude-Error Displays

The RCS autopilot generates three types of attitude errors for display on the FDAI error meters. The modes of operation are designated as Mode 1, Mode 2, and Mode 3, and display the following quantities:

Mode 1) Autopilot phase-plane errors -- selected through the DSKY by V61E.

Mode 2) Total attitude errors with respect to the angles in N22 -- selected by V62E.

Mode 3) Total astronaut attitude errors with respect to the angles in N17 -- selected by V63E.



Mode 1 is provided as a monitor of the RCS DAP and its ability to track automatic-steering commands. In this mode, the display will be zeroed when the CMC MODE switch is placed in the FREE position.

Mode 2 is provided to assist the crew in manually maneuvering the spacecraft to the attitude (gimbal angles) specified in N22. The attitude errors with respect to these angles and the current CDU angles are resolved into RCS control axes.

Mode 3 is provided to assist the crew in manually maneuvering the spacecraft to the attitude (gimbal angles) specified in N17. The attitude errors with respect to these angles and the current CDU angles are resolved into RCS control axes.

In all three modes, the errors are updated every 200 milliseconds.

Verb 60 is provided to load N17 with a snapshot of the current CDU angles, synchronizing the Mode 3 display with the current S/C attitude. This verb can be used at any time. N17 can also be loaded with values chosen by the crew, using V25N17E.

It should be noted that the erasable locations identified as N17 are the same as those identified as N96. N96 is used by R61 and R63 to store +X attitude angles. Thus, although V60 can be used any time, it should not be used at a time when it is undesirable to change N96 information. Conversely, R61 or R63 should not be allowed at a time when it is undesirable to change N17 information.

These displays will be available in any mode of operation (AUTO, HOLD, FREE) and under either SCS or CMC control once the RCS DAP has been initiated via V46E. Mode 1, however, will be meaningful only in CMC AUTO or HOLD, and all display modes assume that the IMU is on and inertially stabilized. The crew can preset an attitude reference (desired gimbal angles) into N17 at any time. A functional diagram of the attitude-error display modes is presented in Fig. 3.2.1.

### 3.2.2.3 Autopilot Operational Procedures

3.2.2.3.1 Autopilot Turn-on Sequence. -- Before turning on the autopilot, the crew should perform the DAP data load routine V48 (R03) and review or modify the data displayed. For CSM-RCS DAP operation, the configuration code must be a "1," a "2," or a "6." To activate the RCS DAP, the crew must then establish guidance and navigation (G&N) control with V46E. If the SC CONT switch is in CMC and the IMU is on and usable, the DAP will become fully operational within 1.7 sec after V46E. If the SC CONT switch is placed in SCS or if the THC is rotated clockwise, the DAP will revert to an idle mode. In this mode, the DAP will not respond to any inputs, but will display attitude errors, provided that the IMU is on and usable. When the SC CONT switch is returned to CMC, or the THC is returned to detent, the DAP will perform its start-up sequence and become fully operational within 1.1 sec, provided the IMU is on and usable.

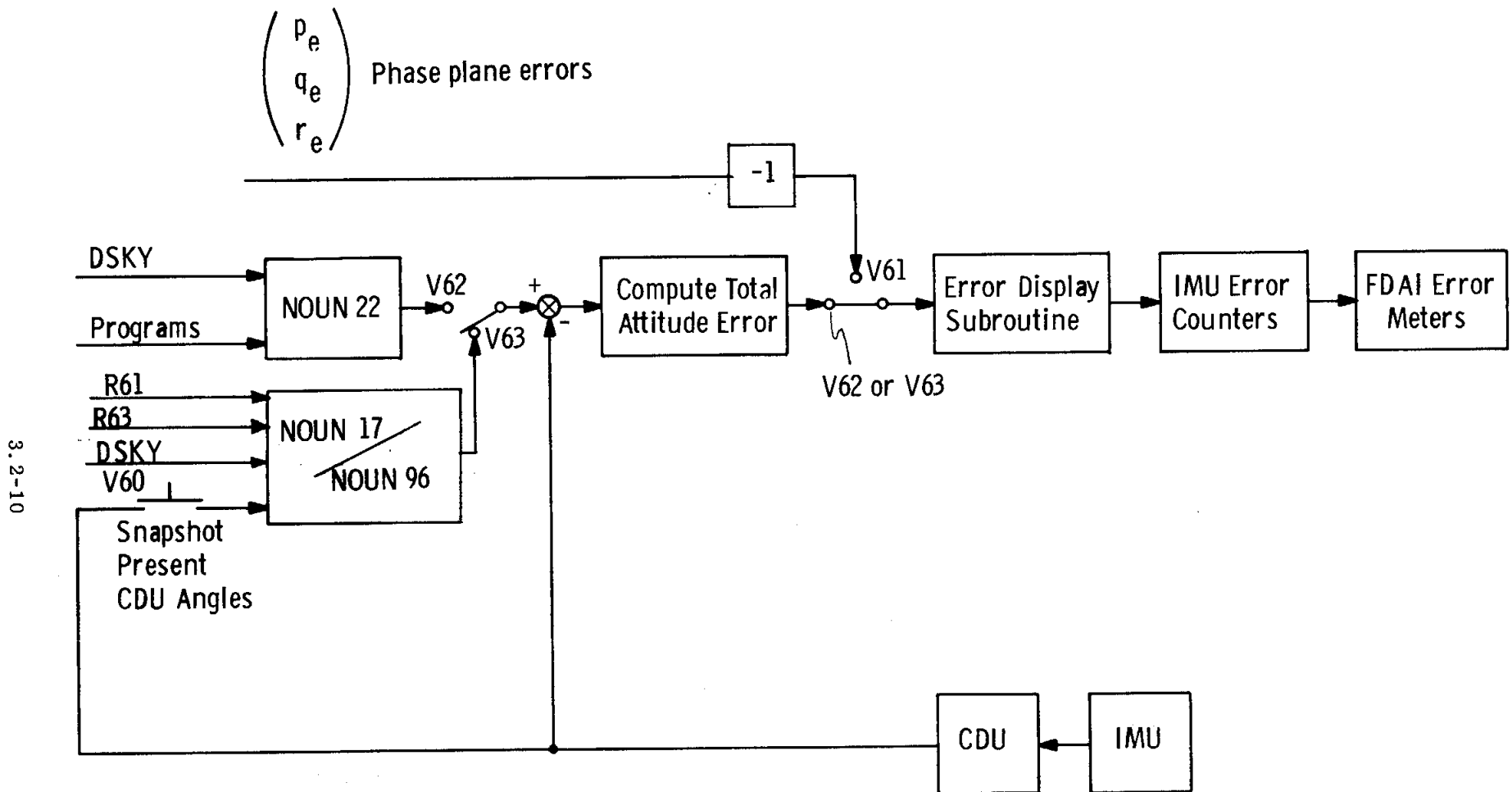


Fig. 3.2.1 PGNS RCS Attitude-Control Attitude-Error Display

If IMU power is off or if the IMU is on but is in the coarse-align or CDU-zero mode, computer-initiated jet firings will be inhibited when the CMC MODE switch is in AUTO or HOLD. The AUTO and HOLD modes are disabled, therefore, under the conditions stated, and the DAP will not respond, even to RHC inputs. The autopilot sets a flag bit indicating that re-initialization is required before the DAP can become fully operational in the AUTO or HOLD mode. The FREE mode does not require an attitude reference in order to operate, and therefore the autopilot can be used in the FREE mode whether the IMU is OFF or ON in any operational mode.

3.2.2.3.2 Autopilot Transitions. -- Switch-over to the TVC DAP when performing an SPS burn is accomplished under program control. Note that ullage must be initiated and controlled by the crew, using the THC. During the transition to TVC, the ullage jets will continue to fire until P40 shuts them off. At the end of the burn, RCS control is automatically re-established with wide angular deadband. The transition to the ENTRY autopilot is also performed under program control.

3.2.2.3.3 Deadband Selection. -- Various programs in the CMC will select the angular deadband of the autopilot. When switching to minimum deadband, the programs will zero the attitude error before collapsing the deadband, in order to save propellant. Note, however, that the attitude hold reference may be changed. The programs also update the deadband code in N46. When any program terminates, the RCS-DAP deadband will be restored to the value specified during the most recent DAP data load (Verb 48).

If the crew wants to select the deadband, they may do so by displaying N46 via V48 and by changing the deadband code with V21. This procedure, however, does not change the attitude reference. Therefore, when switching to minimum deadband, the MODE switch should be placed in FREE, in order to avoid the additional fuel expenditure, and returned to HOLD or AUTO after setting the deadband.

Routine 64, the barbecue mode routine, provides another means of modifying the RCS-DAP deadband. This method is described in the Subsection 3.2.2.1 description of Verb 79.

3.2.2.3.4 Autopilot Turn-off. -- Normally, the DAP need not be deactivated once it is turned on. For checkout, however, executing V46E with a "0" in the N46 configuration code turns off any jets that are on, turns off the T6 clock, and idles the autopilot control interrupt (T5) in order that no DAP coding will be executed -- a result also achieved by a computer fresh start (V36E). Executing V46E with a "3" in the N46 configuration code turns off jets that are on, turns off the T6 clock, and activates the SATURN takeover function.

### 3.2.3 RCS DAP Implementation

The RCS autopilot has four control functions:

- a. Attitude Hold and Rate Limiting
- b. Automatic Maneuvering
- c. Manual Rate Control
- d. Minimum Impulse Control

The first of these control functions is shown by the block diagram of Fig. 3.2.2. The input to the logic is a set of reference angles ( $\theta_{d_j}$ ,  $j = 1, 2, 3$ ) corresponding to desired outer-, inner-, and middle-gimbal angles. These angles are then differenced with the current CDU angles, and the result is resolved into the three control axes, using the small-angle difference approximation in order to yield a set of body attitude errors ( $\theta_{e_j}$ ). The next step in the computation is to compare the attitude errors with a set of estimated body rates ( $\hat{\omega}_j$ ), also resolved into control axes. These rates are derived from IMU gimbal-angle differences, which are transformed into corresponding body-angle differences and smoothed by a second-order filter. For greater accuracy, the commanded angular acceleration of the RCS jets ( $\alpha_j$ ) is included in this computation. As a function of attitude error and attitude rate, nonlinear switching functions in the phase-plane logic are used to generate RCS jet-on time ( $\tau_j$ ) for each control axis. The rate-limiting function is incorporated in the phase plane. A jet-selection logic is then used to combine the rotation commands with the translation commands from the THC and to select the individual jets to be fired. The actual control and timing of the RCS jets is accomplished with the aid of the T6-interrupt structure of the computer.

Attitude maneuvers are implemented with exactly the same logic as that used in attitude hold, except for the additional inputs shown in Fig. 3.2.3. One important difference is that the reference angles ( $\theta_{d_j}$ ) will, in general, be functions of time. Since the steering programs, such as the attitude maneuver routine, generate these desired gimbal angles with an interval ( $\Delta T_c$ ) that is much greater than the autopilot sample rate ( $\Delta T_s = 0.1$  sec), a set of incremental angles ( $\Delta\theta_{d_j}$ 's) are computed as follows:

$$\Delta\theta_{d_j}(t_n) = [\theta_{d_j}(t_{n+1}) - \theta_{d_j}(t_n)] \frac{\Delta T_s}{\Delta T_c} . \quad (3.2-1)$$

The autopilot will then perform the following angle additions every 100 ms:

$$\begin{aligned} \theta_{d_x}(N) &= \theta_{d_x}(N-1) + \Delta\theta_{d_x}(t_n) \\ \theta_{d_y}(N) &= \theta_{d_y}(N-1) + \Delta\theta_{d_y}(t_n) \\ \theta_{d_z}(N) &= \theta_{d_z}(N-1) + \Delta\theta_{d_z}(t_n). \end{aligned} \quad (3.2-2)$$

The steering programs also compute a set of command S/C rates ( $\omega_{d_j}$ ), which are subtracted from the measured body rates by the autopilot, and the results are used in the phase-plane computations. This procedure allows the autopilot to maneuver the spacecraft smoothly at the required rate. For proper attitude control, the desired gimbal-angle rates should be consistent with  $\omega_{d_j}$ . In addition, the steering program may generate a set of attitude-error biases ( $\beta_j$ ), which are added to the attitude errors in order to provide additional lead and prevent overshoot when starting and stopping an automatic maneuver (especially KALCMANU-supervised maneuvers). Normally, the required lead is only 1 to 2 degrees, but during high-rate maneuvers it can be as much as 3.33 degrees. The biases remain fixed until the maneuver is completed, when they are reset to zero.

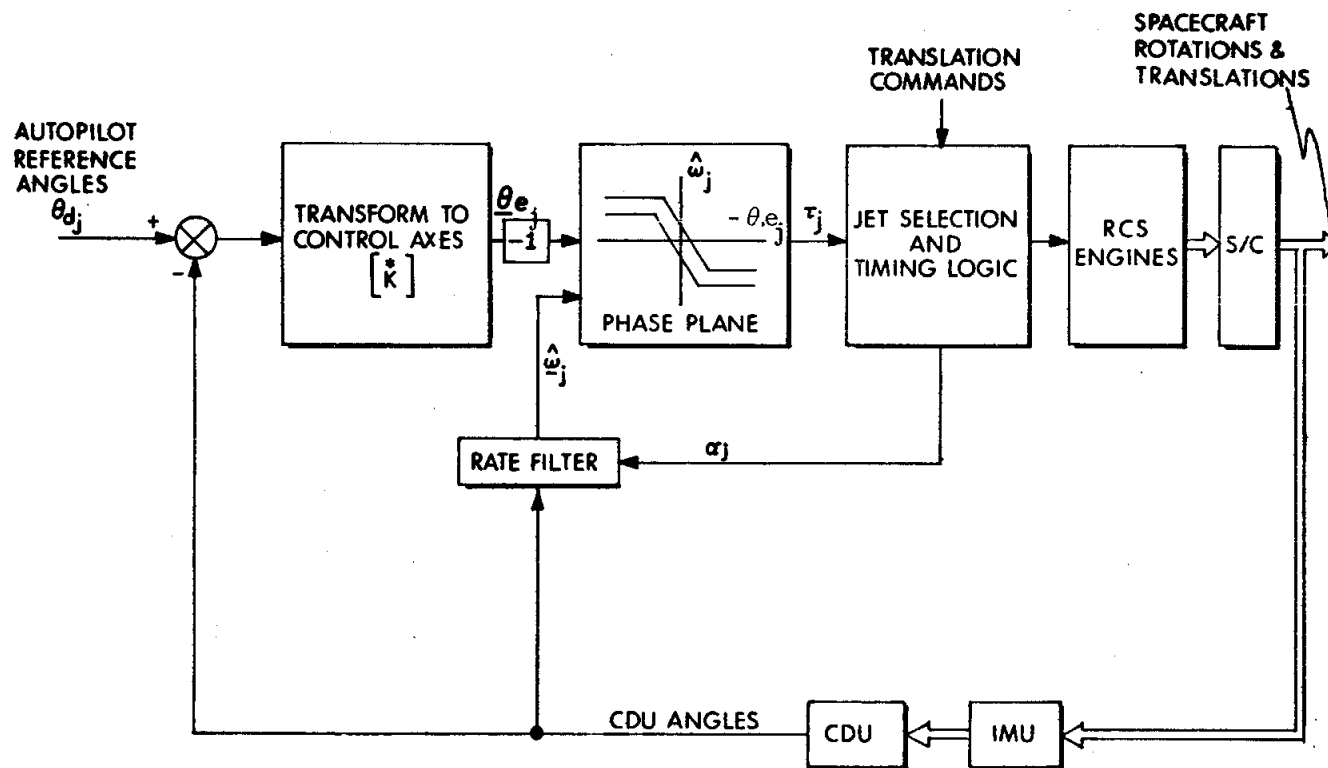


Fig. 3.2.2 PGNCS RCS Attitude Hold Logic.

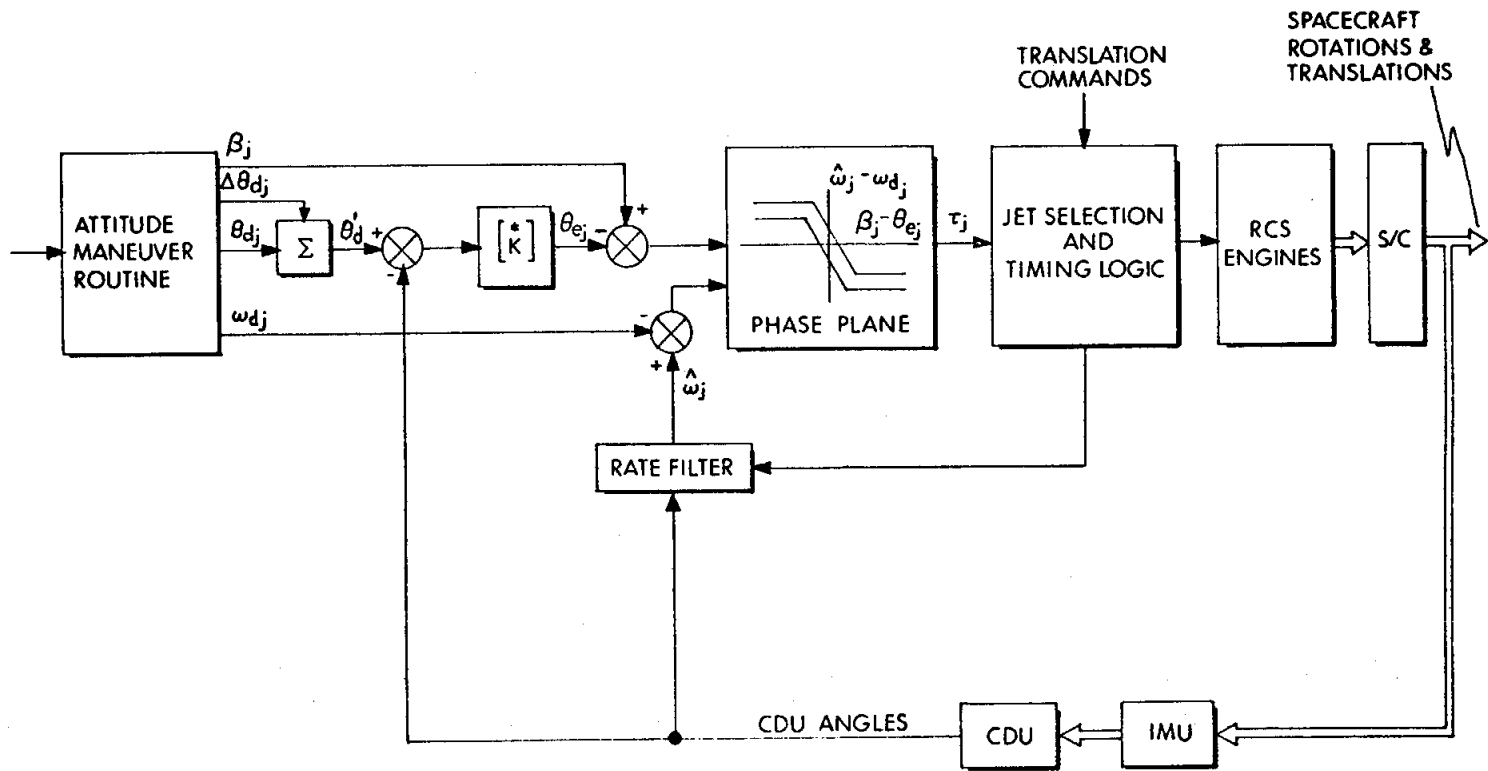


Fig. 3.2.3 PGNCS RCS Automatic Control Logic

Note that when steering is completed,  $\omega_{d_j}$ ,  $\Delta\theta_{d_j}$ , and  $\beta_j$  are reset to zero, and, in effect, the autopilot reverts to attitude hold about the final, desired gimbal angles.

The manual-rate mode (as shown in Fig. 3.2.4) is implemented such that it will also utilize the phase-plane logic. Command rates ( $\omega_{c_j}$ ), resolved into control axes, are computed on the bases of the rate magnitude selected in N46 and of the position of the RHC. Estimates of the actual body rates ( $\hat{\omega}_j$ ), also resolved into control axes, are provided by the rate filter. Command rate is subtracted from estimated rate in order to give rate error ( $\omega_{e_j}$ ):

$$\omega_{e_j} = \hat{\omega}_j - \omega_{c_j}.$$

The rate error is then used as one input to the phase plane.

The computation of attitude-error inputs for the phase plane is controlled by three rate-damping flags, one for each control axis. Whenever there is any change in RHC position, all three flags are set. The flag for any axis is reset to zero when the phase-plane point for that axis falls within the phase-plane deadzone for the first time since the flag was set. While any one of the three flags is set, the phase-plane attitude-error inputs for all three control axes are set to zero. When all three rate-damping flags are finally reset, the difference between command rate and unfiltered measurement of S/C rate is integrated for all three axes in order to give a set of cumulative attitude error ( $\theta_{e_j}$ ), which will be used as the attitude-error input to the phase plane:

$$\theta_{e_j} = \int (\omega_{c_j} - \omega_j) dt = \int \omega_{c_j} dt - \int \omega_j dt.$$

This integration is done incrementally in the AGC. A set of commanded body-axis angular increments ( $\Delta\theta_{d_j}$ ) over one DAP cycle is computed on the basis of the rate magnitude selected in N46 and the position of the RHC:

$$\Delta\theta_{d_j} = \omega_{c_j} \Delta t,$$

where

$\Delta t = 0.1$  sec, the DAP cycle time.

Measured gimbal-angle changes ( $\Delta\phi$ ,  $\Delta\theta$ , and  $\Delta\psi$ ) over one DAP cycle are transformed, using the K-matrix, into control axes in order to obtain a set of measured body-angle changes ( $\Delta A_j$ ), which are used as the integral of unfiltered S/C rates over a DAP cycle:

$$\begin{pmatrix} \int \omega_x dt \\ \int \omega_y dt \\ \int \omega_z dt \end{pmatrix} = \begin{pmatrix} \Delta A_x \\ \Delta A_y \\ \Delta A_z \end{pmatrix} = K \begin{pmatrix} \Delta\phi \\ \Delta\theta \\ \Delta\psi \end{pmatrix}, \quad (3.2-3)$$

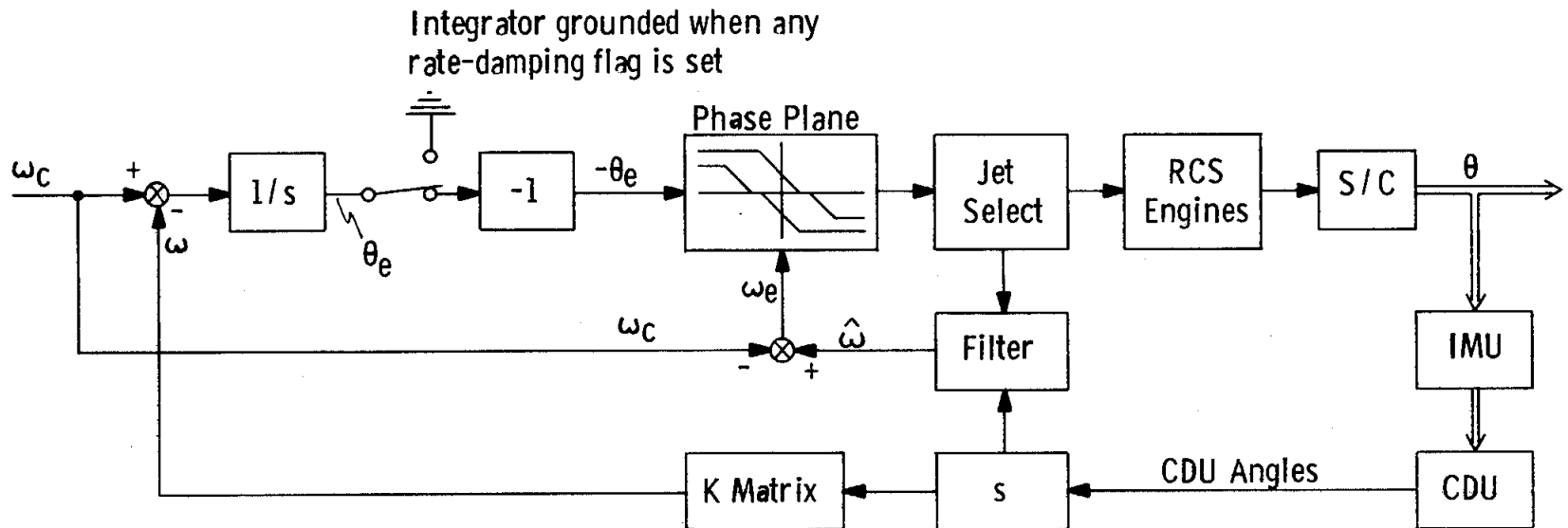


Fig. 3.2.4 PGNC RCS Manual Rate Control



where

$$* K = \begin{pmatrix} 1 & \sin \psi & 0 \\ 0 & \cos \psi \cos \phi' & \sin \phi' \\ 0 & -\cos \psi \sin \phi' & \cos \phi' \end{pmatrix}$$

$$\phi' = \phi - 7.25 \text{ deg (cf., footnote p. 3.2-1)}$$

$\phi$ ,  $\theta$ ,  $\psi$  are the outer-, inner- and middle-gimbal angles.

The set of cumulative attitude errors ( $\theta_{e_j}$ ) is computed recursively:

$$\theta_{e_j}(t + \Delta t) = \theta_{e_j}(t) + \Delta \theta_{d_j} - \Delta A_j.$$

All the  $\theta_{e_j}$ 's are initialized to zero before the integration is initiated by the resetting of the damping flags.

$\theta_{e_j}$  is used as the attitude-error input for the phase plane of each axis. As is done in attitude hold and automatic maneuvers, the phase-plane logic generates jet-on times ( $\tau_j$ ) for each axis; these are used as inputs to the jet-selection logic as described above.

Qualitatively, the action of the DAP after receiving a new RHC command is (1) to rate damp, i.e., drive S/C rate about each control axis to within a deadband of the command rate, and (2), once this is done, to incorporate in the forward loop an extra integration that will eliminate residual rate errors.

One particular consequence of the rate-damping feature is that, upon release of the RHC, the angular velocity of the S/C is driven to near zero before attitude-hold reference angles are picked up. This eliminates the fuel-consuming overshoot-and-return characteristic of high-rate manual maneuvers using the SUNDISK DAP.

Another feature of the manual-rate mode is that of forced firings. Ordinarily, when the phase-plane point lies in the deadzone, no jet firings are commanded. If either the 0.2-deg/sec or 0.05-deg/sec rate is selected, the phase-plane point initially will fall within the two-dimensional deadzone. Unless some special provision is made, there will be a lag between command and response, since no firing will be commanded until the attitude error has been integrated to a value large enough to move the phase-plane point outside the deadzone. For narrow attitude deadband and 0.2-deg/sec rate, the lag will be about 0.2 sec. For the same attitude deadband and the 0.05-deg/sec rate, the lag will be on the order of 10 sec. To eliminate this lag, the following provision has been made: Whenever there is a change in RHC position, bits indicating which axes have had a change in command are set for one, and only one, DAP cycle; whenever these bits are set for an axis, a firing will be forced in a direction such

as to reduce the rate error for that axis, even should the error fall within the deadzone. The effect of this provision is to provide the astronaut with immediate response for all RHC changes at all rates.

The manual-rate mode can be activated by RHC action when the CMC MODE switch is in either AUTO or HOLD. Note that the manual-rate mode will take priority over any automatic maneuver in progress, even should the CMC MODE switch be in AUTO. When the stick is released, the automatic maneuver is not immediately resumed, but rather the S/C remains in attitude hold about the manually acquired attitude. The automatic steering can be re-established by proper DSKY procedures.

The minimum impulse control mode is the simplest of all the operational modes. The logic is shown in Figure 3.2.5. RHC deflections are treated as minimum impulse commands. If RHC commands are present the appropriate jet-on commands ( $\tau_j$ ) are set to the minimum impulse time (14 ms). Each deflection of the RHC will produce another minimum impulse on the appropriate axes.

If MIC commands are present (and RHC in detent), the corresponding  $\tau_j$ 's are set equal to the minimum impulse time (14 ms). Each deflection of the MIC will produce another minimum impulse on the appropriate axes.

The mechanism for establishing the control reference of the autopilot is a multiple-purpose switch called HOLDFLAG. It has the following three states:

- i. (+) Sample the CDU angles and store in  $\theta_{d_j}$  (autopilot reference angles) before resuming attitude hold and resetting HOLDFLAG to "+0"
- ii. (+0) Remain in attitude hold about previously established reference angles ( $\theta_{d_j}$ )
- iii. (-) Enable automatic steering.

HOLDFLAG is set to the "+" state by

- a. occurrence of RHC commands,
- b. turn-on (freshstart) of autopilot,
- c. SCS MODE selection,
- d. FREE mode selection,
- e. switch-over to HOLD mode from AUTO mode when performing automatic maneuvers\*, or by
- f. improper IMU mode condition.

---

\*In this case, HOLDFLAG is never actually set to "+," but the logic functions as if it were.

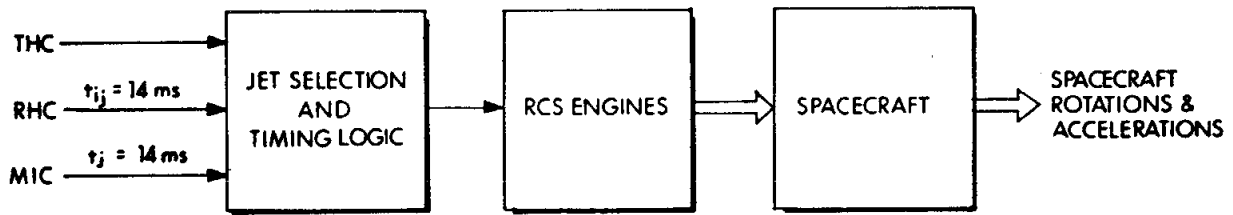


Fig. 3.2.5 PGNC's RCS Attitude Control Free Mode Control

3.2-19

Revised  
 Added

COLOSSUS 2E  
 GSOP # R-577

PCR # 289

Rev. 10

Date 2/70

To enable automatic control of the autopilot, the steering programs set HOLDFLAG to the "-" state, but this is done only after the mode switch has been set to AUTO, the astronaut has indicated his desire to allow automatic control, and the initial values of  $\omega_{d_j}$ ,  $\theta_{d_j}$ ,  $\Delta\theta_{d_j}$ ,  $\beta_j$  have been loaded by the automatic-maneuver routine (with interrupt inhibited). Thereafter, HOLDFLAG is monitored by the steering program in order to determine whether the automatic sequence has been interrupted and, if so, to take appropriate action. For automatic maneuvers initiated by R60, the DSKY will flash a request to trim the S/C attitude to the required angles. For automatic tracking of the LM during P20, however, the preferred tracking-attitude routine, R61 will automatically re-establish tracking unless the steering has been interrupted by the occurrence of RHC commands. Should steering have been interrupted, a V58E will re-establish the automatic tracking, provided that the CMC AUTO mode has been selected.

### 3.2.4 RCS DAP Program Design

#### 3.2.4.1 Computation of Attitude Errors

For automatic maneuvers and attitude hold, desired attitude is expressed in gimbal angles  $\theta_d$ ,  $\psi_d$ , and  $\phi_d$ . These angles are compared with the actual gimbal angles, and the differences computed to yield gimbal-angle errors.

Since the RCS jets work in the control axes p, q, and r, it is necessary to resolve the gimbal-angle errors into control axes. For small errors, the K-matrix used for angular-velocity transformation is also valid for angular differences:

$$\begin{bmatrix} p_e \\ q_e \\ r_e \end{bmatrix} = K^* \begin{bmatrix} \phi - \phi_d \\ \theta - \theta_d \\ \psi - \psi_d \end{bmatrix} \quad (3.2-4)$$

This yields formulas:

$$\begin{aligned} p_e &= (\phi - \phi_d) + (\theta - \theta_d) \sin \psi && \text{(Roll Error)} \\ q_e &= (\theta - \theta_d) \cos \psi \cos \phi' + (\psi - \psi_d) \sin \phi' && \text{(Pitch Error)} \\ r_e &= -(\theta - \theta_d) \cos \psi \sin \phi' + (\psi - \psi_d) \cos \phi' && \text{(Yaw Error)}. \end{aligned} \quad (3.2-5)$$

The small-angle approximation involved is sufficiently accurate for the purposes of the DAP, even though the K-matrix is updated only once per second. During automatic maneuvers, a set of biases ( $\beta_x$ ,  $\beta_y$ , and  $\beta_z$ ) is added to the attitude errors in order to compensate for the time required for the S/C to change angular rate. The biases eliminate the problem of rate overshoot, when a maneuver is started, and the problem of attitude overshoot, when the maneuver is stopped. Thus, for automatic maneuvers,

$$\begin{bmatrix} p_e \\ q_e \\ r_e \end{bmatrix} = K^* \begin{bmatrix} \phi - \phi_d \\ \theta - \theta_d \\ \psi - \psi_d \end{bmatrix} + \begin{bmatrix} \beta_x \\ \beta_y \\ \beta_z \end{bmatrix} \quad (3.2-6)$$

During manual-rate maneuvers, measured gimbal-angle changes over one DAP cycle are transformed, using the K-matrix, into control axes in order to obtain a set of measured body-angle changes. A set of desired changes ( $\Delta\theta_{d_j}$ ) for these control-axis quantities is computed on the bases of the rate magnitude selected in N46 and the position of the RHC:

$$\Delta\theta_{d_j} = \omega_{d_j} \Delta t,$$

where

$\Delta t = 0.1$  sec, the DAP cycle time.

Whenever rate damping, described above, is not in progress, a set of cumulative attitude errors is computed recursively:

$$\begin{bmatrix} p_e(t+\Delta t) \\ q_e(t+\Delta t) \\ r_e(t+\Delta t) \end{bmatrix} = \begin{bmatrix} p_e(t) \\ q_e(t) \\ r_e(t) \end{bmatrix} - \begin{bmatrix} \Delta\theta_{dp} \\ \Delta\theta_{dq} \\ \Delta\theta_{dr} \end{bmatrix} + K * \begin{bmatrix} \phi(t+\Delta t) - \phi(t) \\ \theta(t+\Delta t) - \theta(t) \\ \psi(t+\Delta t) - \psi(t) \end{bmatrix}.$$

### 3.2.4.2 Display of Attitude Errors

The DAP provides inputs to the FDAI needles in order to permit monitoring of its operation during automatic maneuvers and attitude hold. There are three display modes available:

Display Mode 1. -- The negatives of the attitude errors computed above are displayed on the needles. For automatic maneuvers, this display is sometimes called "maneuver following error." If the DAP is functioning properly, these errors should remain within the deadband selected during attitude hold, automatic maneuvers, and manual-rate maneuvers.

Display Mode 2. -- The attitude errors displayed are computed as the difference between the measured gimbal angles and the contents of Noun 22 ( $\phi_c$ ,  $\theta_c$ , and  $\psi_c$ ). These differences are resolved into control coordinates:

$$\begin{bmatrix} p_d \\ q_d \\ r_d \end{bmatrix} = K * \begin{bmatrix} \phi_c - \phi \\ \theta_c - \theta \\ \psi_c - \psi \end{bmatrix}. \quad (3.2-7)$$

During automatic maneuvers, the contents of N22 are set to the terminal attitude of the maneuver in order that the needles will indicate angles to be gained to completion of the maneuver.

Display Mode 3. -- The attitude errors displayed are computed as the difference between measured gimbal angles and the contents of Noun 17 ( $\phi_a$ ,  $\theta_a$ , and  $\psi_a$ ). The differences are resolved into control coordinates:

$$\begin{bmatrix} p_d \\ q_d \\ r_d \end{bmatrix} = K^* \begin{bmatrix} \phi_a - \phi \\ \theta_a - \theta \\ \psi_a - \psi \end{bmatrix}.$$

Verb 60, which can be executed at any time, loads Noun 17 with a snapshot of the current CDU angles. Noun 17 can also be loaded directly by the execution of V25N17. The attitude specified in Noun 17 can be regained by manually steering the S/C such as to null the error needles.

It should be noted that the erasable locations identified as N17 are the same as those identified as N96. N96 is used by R61 and R63 to store +X attitude angles. Thus, although V60 can be used anytime, it should not be used at a time when it is undesirable to change N96 information. Conversely, R61 or R63 should not be allowed at a time when it is undesirable to change N17 information.

#### 3.2.4.3 Angular-rate Filter

The RCS digital autopilot is, by the very nature of digital machines, a sampled-data process. Thus it must infer or estimate angular velocity from a series of samples of the environment at discrete intervals. The inputs to the rate estimator include gimbal angles (attitude) and estimates of the control forces applied to the S/C by the RCS jets (control acceleration). Both of these quantities must be considered "noisy": IMU angles are perturbed by uncertainties in the CDU counters and by quantization effects; S/C accelerations are perturbed by uncertainties in RCS jet thrust and by random forces -- vehicle bending, vibration, fuel slosh, etc.

The design of the rate filter can be viewed in terms of Kalman filtering techniques and can be derived as a set of recursive difference equations using this approach. Given the derived attitude  $\hat{\theta}$  and the derived velocity  $\hat{\omega}$  at time  $t_0$ , the state at some later time ( $t_1$ ) is estimated by extrapolation:

$$\hat{\theta}'(t_1) = \hat{\theta}(t_0) + \hat{\omega}(t_0) \Delta T + \int_{t_0}^{t_1} \int_0^t u(\tau) d\tau, \quad (3.2-8)$$

$$\hat{\omega}'(t_1) = \hat{\omega}(t_0) + \int_{t_0}^{t_1} u(\tau) d\tau, \quad (3.2-9)$$

where  $u(\tau)$  = the control acceleration caused by jet firings, and

$$\Delta T = t_1 - t_0 = 0.1 \text{ sec for the DAP.}$$

The prime notation indicates the estimation just before the incorporation of the measurement of current attitude.

After the state estimate is updated by this extrapolation, the estimated attitude is compared to the measured angles ( $\tilde{\theta}$ ), and the state estimate is revised on the basis of the difference between the two values:

$$\hat{\theta}(t_1) = \hat{\theta}'(t_1) + W_1(t_1) [\tilde{\theta}(t_1) - \hat{\theta}'(t_1)], \quad (3.2-10)$$

$$\hat{\omega}(t_1) = \hat{\omega}'(t_1) + W_2(t_1) [\tilde{\omega}(t_1) - \hat{\omega}'(t_1)]. \quad (3.2-11)$$

The parameters  $W_1$  and  $W_2$  are weighting factors applied to the error in adjusting the extrapolated values. These weighting factors represent a measure of the relative confidence that one has in the extrapolated values as opposed to the measured attitude figures. The selection of values for  $W_1$  and  $W_2$  to yield optimum performance depends on the statistical measures of variance of  $\tilde{\theta}$  and  $\hat{\theta}$ , and is beyond the scope of this discussion. For the DAP, the values can be selected in advance. After initialization (the first 1.1 sec of operation), the gains remain constant such that  $W_1(t) = K_1$ , and  $W_2(t) = K_2$ , for  $t \geq 1.1$ . The exception is that during translations and high-rate automatic or manual rotations the gains are set equal to higher, but still constant, values. Translation gains take precedence over rotation gains. The numerical values of the filter gains are shown in Table 3.2-I.

As implemented in the RCS DAP, Eq. 3.2-10 and Eq. 3.2-11 appear in slightly different form. If we define

$$X(t_1) = \int_{t_0}^{t_1} u(\tau) d\tau, \quad (3.2-12)$$

$$Y(t_1) = \int_{t_0}^{t_1} \int_0^t u(\tau) d\tau, \quad (3.2-13)$$



then Eq. 3.2-8 and Eq. 3.2-9 become

$$\hat{\theta}'(t_1) = \hat{\theta}(t_0) + \hat{\omega}(t_0) \Delta T + Y(t_1), \quad (3.2-14)$$

$$\hat{\omega}'(t_1) = \hat{\omega}(t_0) + X(t_1). \quad (3.2-15)$$

If we also define

$$\rho(t_1) = \tilde{\theta}(t_1) - \hat{\theta}'(t_1) = \tilde{\theta}(t_1) - \hat{\theta}(t_0) - \hat{\omega}(t_0) \Delta T - Y(t_1), \quad (3.2-16)$$

then Eq. 3.2-10 and Eq. 3.2-11 become

$$\hat{\theta}(t_1) = \hat{\theta}'(t_1) + W_1(t_1) \rho(t_1); \quad (3.2-17)$$

$$\hat{\omega}(t_1) = \hat{\omega}'(t_1) + W_2(t_1) \rho(t_1). \quad (3.2-18)$$

If we add  $-\tilde{\theta}(t_1)$  to both sides of Eq. 3.2-17, we obtain

$$\hat{\theta}(t_1) - \tilde{\theta}(t_1) = \hat{\theta}'(t_1) - \tilde{\theta}(t_1) + W_1(t_1) \rho(t_1),$$

or referring to Eq. 3.2-16, we have

$$\tilde{\theta}(t_1) - \hat{\theta}(t_1) = [1 - W_1(t_1)] \rho(t_1). \quad (3.2-19)$$

Substituting  $t_0$  for  $t_1$  in Eq. 3.2-19, we obtain

$$\tilde{\theta}(t_0) - \hat{\theta}(t_0) = [1 - W_1(t_0)] \rho(t_0). \quad (3.2-20)$$

If we solve Eq. 3.2-16 for  $\hat{\theta}(t_0)$  and substitute this result in Eq. 3.2-20, we obtain

$$\rho(t_1) = [1 - W_1(t_0)] \rho(t_0) - \hat{\omega}(t_0) \Delta T - Y(t_1) + [\tilde{\theta}(t_1) - \tilde{\theta}(t_0)]. \quad (3.2-21)$$

The computation of  $\rho(t_1)$  can be greatly simplified if we neglect the contribution due to  $Y(t_1)$ . If we do this, the filter equations become:

$$\rho(t_1) = [1 - W_1(t_0)] \rho(t_0) - \hat{\omega}(t_0) \Delta T + [\tilde{\theta}(t_1) - \tilde{\theta}(t_0)]; \quad (3.2-22)$$

$$\hat{\omega}(t_1) = \hat{\omega}(t_0) + W_2(t_1) \rho(t_1) + \int_{t_0}^{t_1} u(\tau) d\tau. \quad (3.2-23)$$

TABLE 3.2-1

## DAP FILTER GAINS

## 1) Kalman Filter Gains

<u>Time</u>	<u>W<sub>1</sub></u>	<u>W<sub>2</sub></u>	<u><math>\omega_n</math></u>	<u><math>\zeta</math></u>
0.1	0.9342	8.683		
0.2	0.8151	4.817		
0.3	0.6933	2.955		
0.4	0.5970	1.985		
0.5	0.5223	1.422		
0.6	0.4634	1.069		
0.7	0.4161	0.832		
0.8	0.3774	0.666		
0.9	0.3452	0.545		
1.0	0.3180	0.454		
<u>t ≥ 1.1</u>	0.0640	0.016	0.40	0.80

## 2) Normal Filter Gains

0.0640	0.016	0.40	0.80
--------	-------	------	------

## 3) High-rate-rotation Filter Gains

0.2112	0.1742	1.32	0.80
--------	--------	------	------

## 4) CSM-alone Translation Filter Gains

0.8400	3.6000	6.00	0.70
--------	--------	------	------

## 5) CSM-docked LM Translation Filter Gains

0.2112	0.1742	1.32	0.80
--------	--------	------	------

Measured gimbal-angle changes ( $\Delta\phi$ ,  $\Delta\theta$ , and  $\Delta\psi$ ) over one DAP cycle are transformed, using the K-matrix, into control axes in order to obtain a set of measured body-angle changes.

Although Eq. 3.2-22 and Eq. 3.2-23 were derived for a planar problem, they can be expanded to three axes if we make the small-angle approximation:

$$\begin{bmatrix} \Delta A_x \\ \Delta A_y \\ \Delta A_z \end{bmatrix} = K^*(t_0) \begin{bmatrix} \phi(t_1) - \phi(t_0) \\ \theta(t_1) - \theta(t_0) \\ \psi(t_1) - \psi(t_0) \end{bmatrix}, \quad (3.2-24)$$

where

$$K^*(t_0) = \begin{bmatrix} 1 & \sin \psi(t_0) & 0 \\ 0 & \cos \psi(t_0) \cos \phi'(t_0) & \sin \phi'(t_0) \\ 0 & -\cos \psi(t_0) \sin \phi'(t_0) & \cos \phi'(t_0) \end{bmatrix},$$

$$\phi' = \phi - 7.25 \text{ deg},$$

and

$\phi$ ,  $\theta$ ,  $\psi$  are the measured outer-, inner- and middle-gimbal angles.

Substituting  $\Delta A$  for  $\tilde{\theta}(t_1) - \tilde{\theta}(t_0)$  in Eq. 3.2-22, we obtain the filter equations as programmed in the autopilot:

$$\rho_x(t_1) = (1 - W_1(t_0)) \rho_x(t_0) - \hat{\omega}_x(t_0) \Delta T + \Delta A_x; \quad (3.2-25)$$

$$\hat{\omega}_x(t_1) = \hat{\omega}_x(t_0) + W_2(t_1) \rho_x(t_1) + \int_{t_0}^{t_1} u_x(\tau) d\tau, \quad (3.2-26)$$

with similar equations for the Y and Z axes.

Since the thrust of an RCS jet is assumed to be constant, the control acceleration integral reduces to  $C\Delta t_f$ , where  $C$  is a constant and  $\Delta t_f$  is the single-jet operation jet-on time\* calculated during the interval  $t_0 < t < t_1$ . The K-matrix is updated every 10 cycles, or once per second.

The result of this estimation procedure can be represented as a second-order linear sampled-data system with the block diagram of Fig. 3.2.6. The input  $[\Delta A(Z)]$  is the measured "body angle" difference over the previous sample period. The output is  $\hat{\omega}(Z)$ , the estimated body rate; and  $X(Z)$  is defined by the Z-transform of Eq. 3.2-12. In steady-state operation, one can define an equivalent damping ratio ( $\zeta$ ) and a natural frequency ( $\omega_n$ ) for this filter. To a good approximation, they may be defined:

$$\zeta = \frac{W_1}{2\sqrt{W_2} \Delta T} ,$$

$$\omega_n = \sqrt{\frac{W_2}{\Delta T}} .$$

The filter gains used by the DAP are shown in Table 3.2.-I. The Kalman gains are used during the first second of operation in order to speed up the initialization of the filter. The bandpass is initially set very high and gradually reduced to the nominal value. For normal operation,  $\omega_n = 0.4$  radian/sec, and  $\zeta = 0.8$ . The higher filter gains are used when performing maneuvers at the 2-deg/sec rate and, also, during translation. During 2-deg/sec maneuvers and CSM-LM Docked translations,  $\omega_n = 1.32$  radians/sec and  $\zeta = 0.8$ ; during CSM alone translations,  $\omega_n = 6.0$  radians/sec and  $\zeta = 0.7$ . Figure 3.2.7 shows the filter response obtained from an all-digital simulation for a step input of 4 deg/sec. The four curves represent the response for each of the filter modes of operation.

The rate filter provides virtual isolation of the DAP from various noise sources and undesirable perturbations, including S/C vibration, vehicle bending, and CDU quantization, and enables the autopilot to establish extremely low-rate minimum-impulse limit cycles. Although a penalty is paid in terms of a rather slow response time, performance is, in fact, adequate for the maneuver rates involved.

\*  $\Delta t_f$  is the duration that a single jet must be fired in order to attain a desired rotational impulse about a given axis. If two jets are used for the rotation, both will be fired for a duration  $\Delta t_f/2$ . When one jet is used,  $\Delta t_f$  can range between 14 and 100 ms. When two jets are used, however, the firing time ( $\Delta t_f/2$ ) must still be in the range 14 to 100 ms; the value of  $\Delta t_f$  would, therefore, range between 28 and 200 ms.

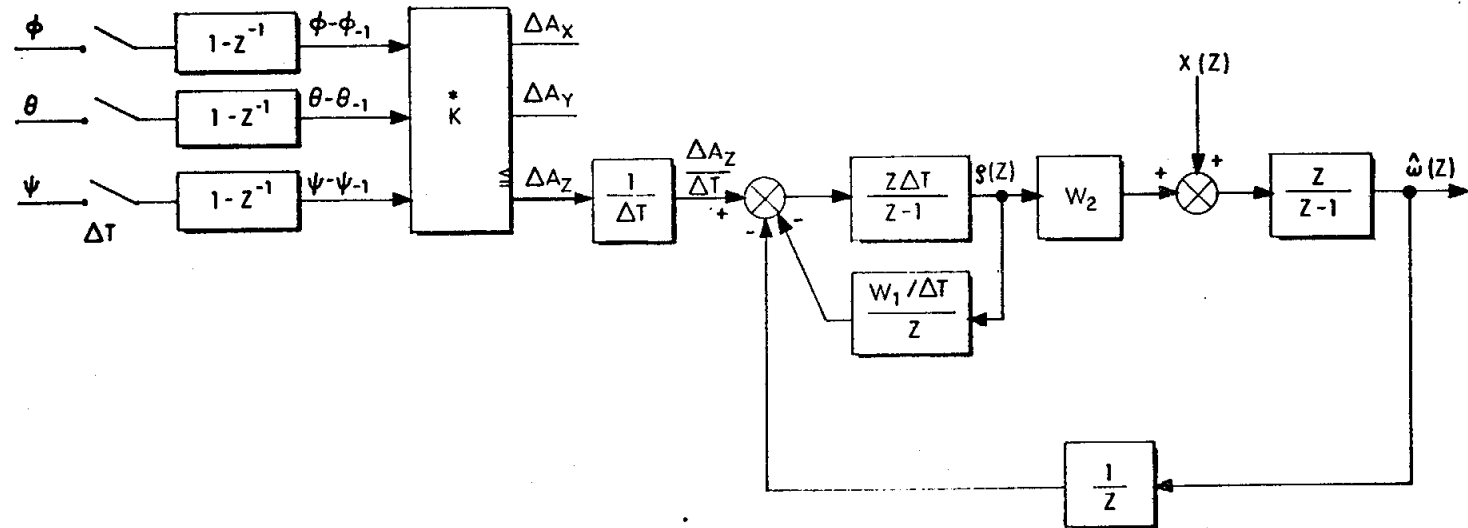


Fig. 3.2.6 CSM-RCS Digital Autopilot Rate Filter

3.2-30

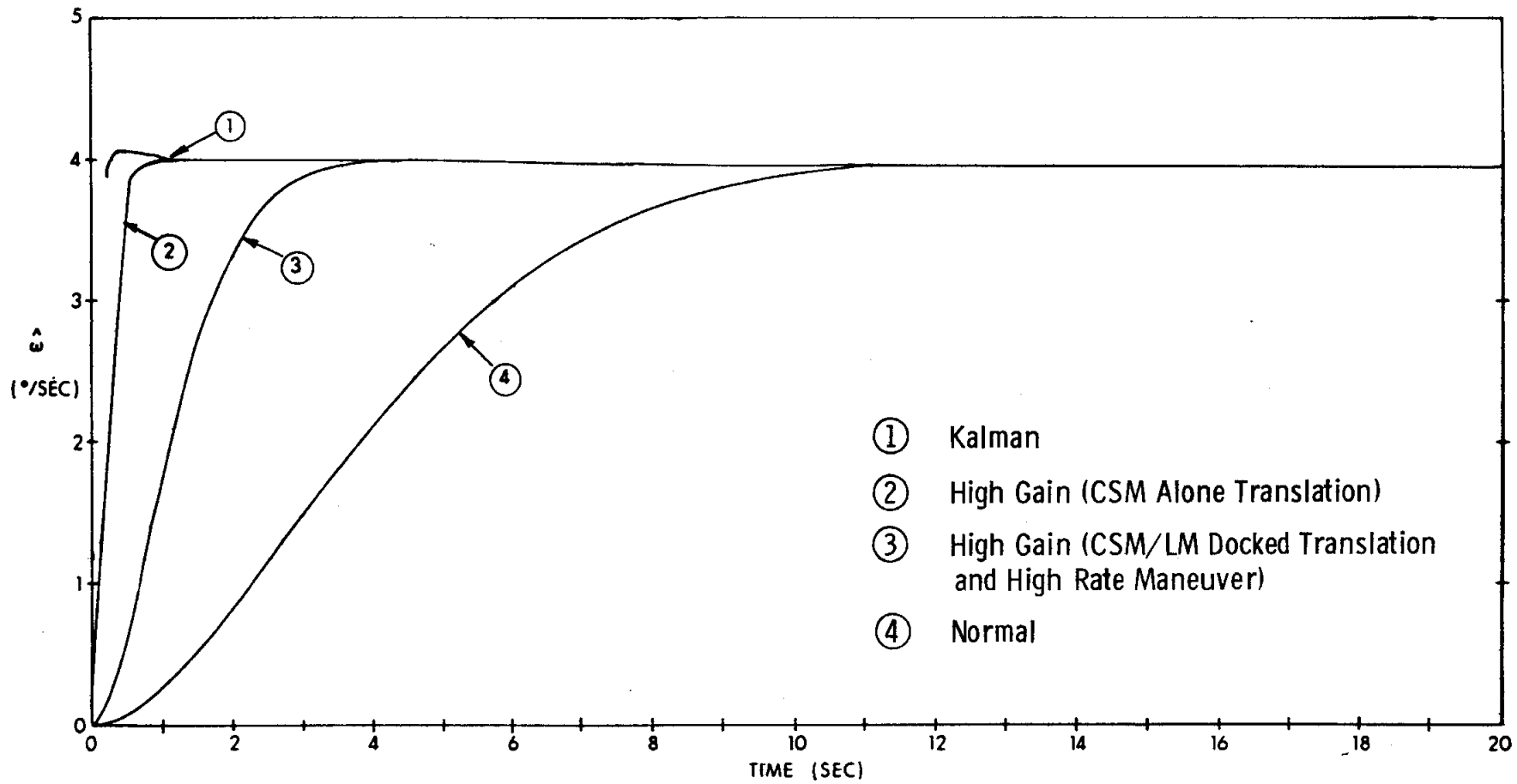


Fig. 3.2.7 Filter Responses

#### 3.2.4.4 Phase-plane Switching Logic

For attitude hold, automatic maneuvers, and manual-rate maneuvers, rate limiting and attitude control are performed by a nonlinear switching logic. Attitude errors, which are assumed to be small, are calculated and resolved into control axes. Rates are derived in control axes by the rate filter.

The dynamics of the switching logic for a single axis can best be understood by interpretation in the phase plane (See Fig. 3.2.8). The horizontal axis is attitude error; the vertical axis is angular-rate error. Paths of zero acceleration are horizontal lines, and paths of constant acceleration are parabolas.

In attitude-hold mode, consider what happens when the vehicle begins in the state represented by the point A. Since the velocity is positive, the state moves to the right until it reaches the decision line at B. The DAP then fires RCS jets to drive the rate to zero. To allow for vehicle torque-to-inertia ratios that are greater than those assumed by the autopilot and to prevent overshoot in this case, the desired impulse is intentionally reduced by 20 per cent. In the normal case, this means that the rate change falls short of the desired rate line, producing an over-damped response. The state drops only to point C and moves more slowly toward the decision line. Due to delays in the rate filter, line CD will not be perfectly straight, but will approach the correct rate value gradually. When the decision line is hit again, at point D, the cycle repeats. Because the firing time can never be less than 14 ms, the state will eventually cross the decision line close enough to zero to overshoot on the next jet firing. The state will then move left (since the velocity is now negative) all the way across the deadband to point F. Jets will fire to drive the rate in the opposite direction, overshooting again to point G. The end result is the minimum-impulse limit cycle EFGH. This limit cycle is encouraged by the flat region in the decision lines where they cross the attitude-error axis.

A summary of decision areas and responses is given in Table 3.2-II of Fig. 3.2.8 for the top half of the phase plane. The bottom half functions symmetrically with respect to the origin. Note that from decision areas 2 and 5 the rate is driven to the hysteresis lines +HSLOPE or -HSLOPE in order to ensure that the deadband is entered even should the impulse be short by as much as 20 per cent.

The width of the rate-limit deadband is fixed at 0.2 deg per second. The astronaut can either select maximum (5.0 deg) or minimum (0.5 deg) angular deadband through the DSKY, by executing Verb 48 and changing the appropriate component of Noun 46 when it is displayed.

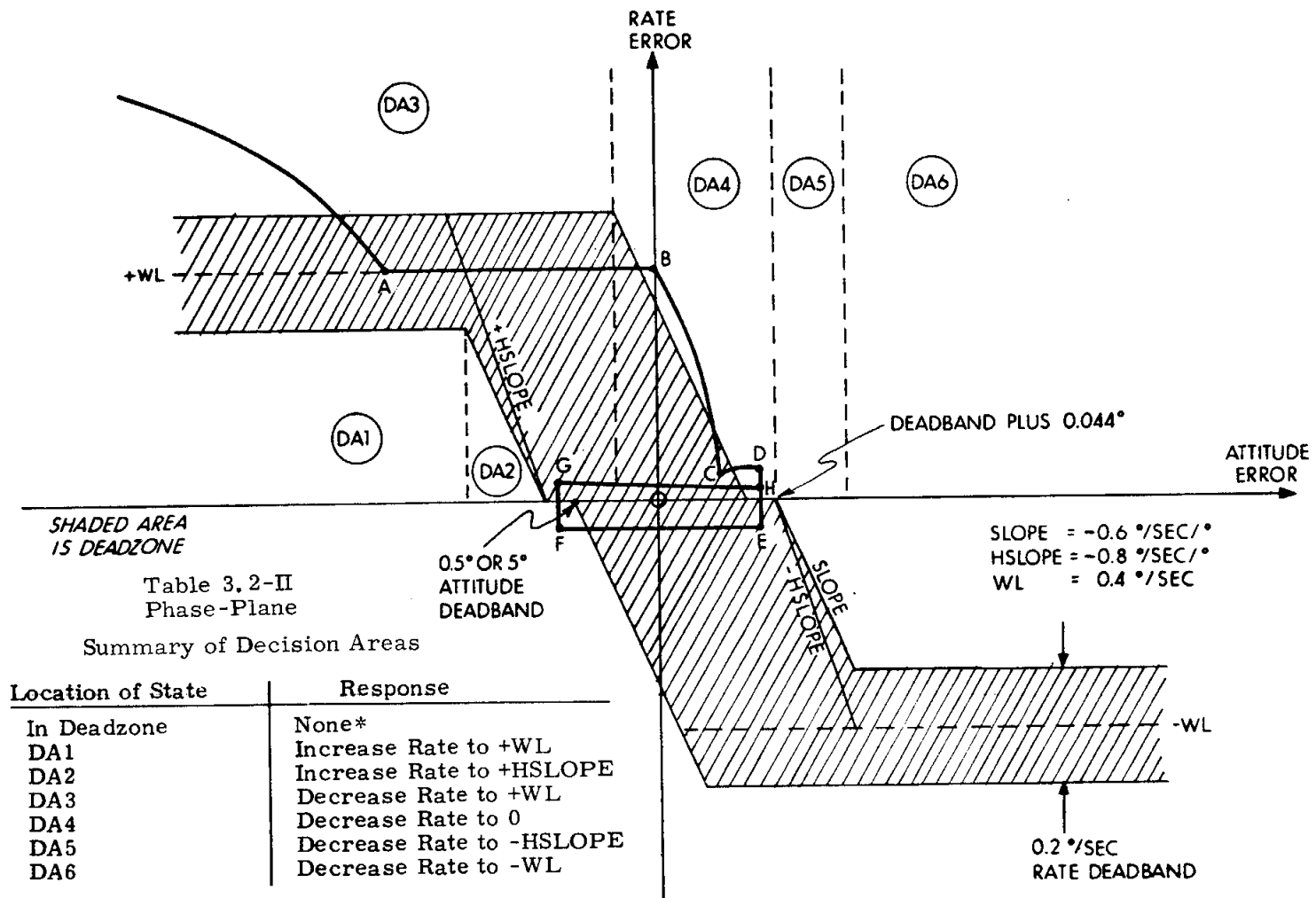


Table 3.2-II  
Phase-Plane  
Summary of Decision Areas

Location of State	Response
In Deadzone	None*
DA1	Increase Rate to +WL
DA2	Increase Rate to +HSLOPE
DA3	Decrease Rate to +WL
DA4	Decrease Rate to 0
DA5	Decrease Rate to -HSLOPE
DA6	Decrease Rate to -WL

\* See forced-firing exception (pp. 3.2-6, -17, -18)

Fig. 3.2.8 Phase Plane



Automatic maneuvers are implemented by exactly the same logic as that used in attitude hold, except that the inputs are rate error and attitude error. The rate coordinate represents the difference between the actual rate and the rate specified by the maneuver routine. Of course, the desired attitude will change for each cycle of the DAP during execution of a maneuver. In practice, the automatic-maneuver routines calculate new attitudes only periodically. A set of angle increments is also calculated. The DAP uses these incremental angles to interpolate desired attitude angles between computation cycles of the maneuver routines, such that smooth transition from one attitude to the next is achieved.

Manual rate maneuvers also use the phase-plane logic, with rate error and attitude error as inputs. The computation of error quantities during manual rate maneuvers is described in paragraph 3.2.3.

#### 3.2.4.5 RCS DAP Jet Selection Logic

The RCS DAP executes rotations and translations of the S/C by means of the 16 RCS jets located on the forward end of the service module. These jets are clustered in four quads, lettered A-D, four jets to a quad. Quads A and C are aligned with the yaw-control (Z) axis. (See footnote on page 3.2-1.) Quads B and D are aligned with the pitch-control (Y) axis. Jet configuration and numbering is shown in Fig. 3.2.9.

Rotations alone, about a given axis, or translations alone, along a given axis, are normally executed with a pair of jets -- one each on opposing quads (AC or BD). A single jet firing will result in both a rotation and a translation. Thus, fuel is conserved by combining rotations with translations whenever possible. Figure 3.2.9 shows that X-translations can be combined with pitch-axis rotations, using Quads AC; X-translations can be combined with yaw-axis rotations, using Quads BD; Y-translations can be combined with roll-axis rotations, using Quads AC; and Z-translations can be combined with roll-axis rotations, using Quads BD.

Pitch and yaw rotations and Y- and Z-translations are peculiar to a single pair of quads. Roll and X-translations can be performed using either quad pair. The crew can select either or both quad pairs for X-translation and can select one pair or the other, but not both, for roll.

Provision is made for informing the computer, via Verb 48, of quad failures when one or more of the jets in a quad have failed. In the event of a quad failure, the computer will not attempt to fire the jets in that quad, but will compensate for the reduction of control torque when performing

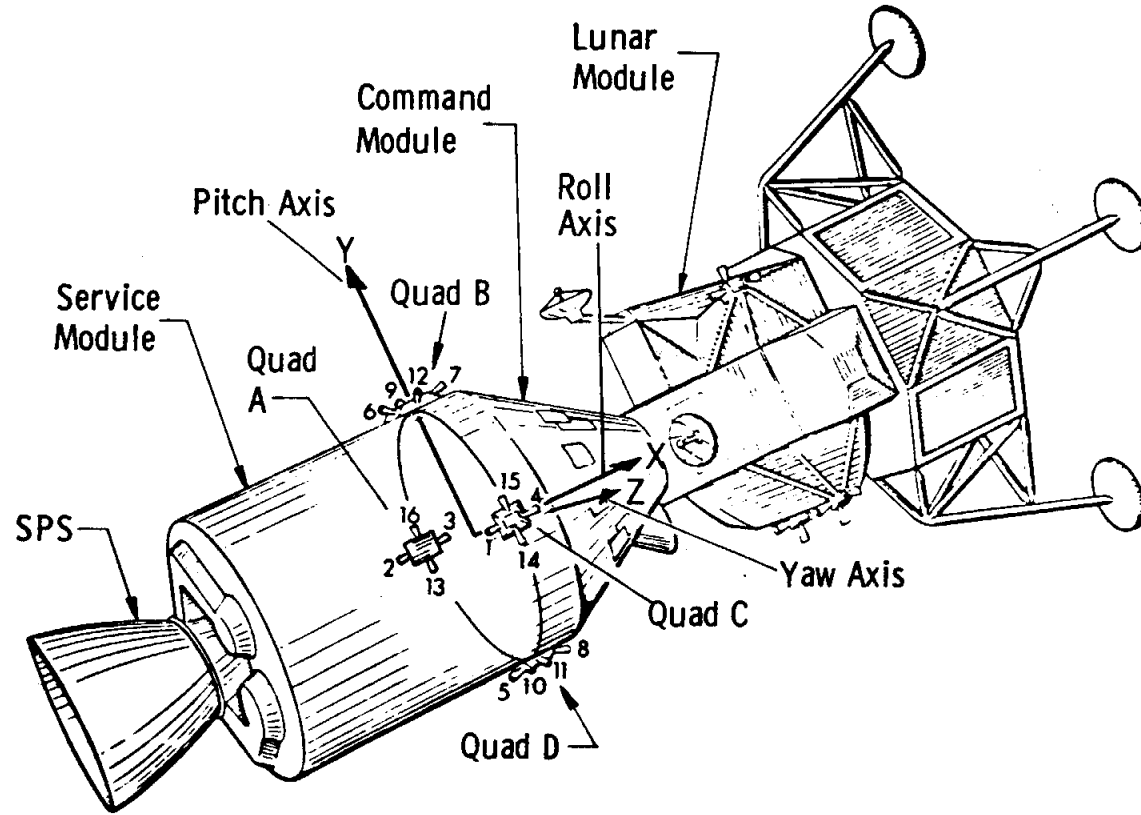


Fig. 3.2.9 Apollo Spacecraft

attitude maneuvers. This feature of the quad-fail logic can be used for fuel management and the attainment of single-jet rotational control for minimizing propellant consumption in attitude hold. Because of the reduction in overall control authority, however, some of the translational capabilities of the system must be sacrificed to permit attitude stabilization. Should one or more jets in a quad be disabled or failed and it be desired not to inactivate the entire quad, quad-failure information need not be communicated to the computer. The autopilot will continue to function but at reduced efficiency.

The logic that combines rotations with translations generates two control words during each autopilot cycle: Word 1 contains jet commands for rotations and translations combined; Word 2 contains jet commands for translation only. The logic incorporates the quad-failure information as follows:

- i. Command Word 1, --Rotations and Translations Combined
  - a. Pitch Word. -- X-translations are ignored if Quad A or C has failed; astronaut should shift to BD quads for X-translations.
  - b. Yaw Word. -- X-translations are ignored if Quad B or D has failed; astronaut should shift to AC quads for X-translations.
  - c. AC Roll
    1. Y-translations are ignored if Quad A or C has failed. A shift to BD roll may make the translation possible. (See below.)
    2. Z-translations are accepted in spite of Quad B or D failure unless the resulting torque cancels desired roll torque. This can happen only if a single jet is used for roll:
      - a) Case 1. -- Should one-jet roll be a result of failure on Quad A or C, the Z-translation cannot be done until the roll maneuver has been completed.
      - b) Case 2. -- Should one-jet roll be a result of combining roll with a Y-translation, the Y-translation must be completed before the Z-translation can be done.
  - d. BD Roll
    1. Z-translations are ignored if Quad B or D has failed. A shift to AC roll may make the translation possible. (See above.)
    2. Y-translations are accepted in spite of Quad A or C fail unless the resulting torque cancels desired roll torque. This can happen only if a single jet is used for roll:

- a) Case 1. -- Should one-jet roll be a result of failure of Quad B or D, the Y-translation cannot be done until the roll maneuver has been completed.
- b) Case 2. -- Should one-jet roll be a result of combining roll with a Z-translation, the Z-translation must be completed before the Y-translation can be done.

The net result of the logic of command-word 1 is that rotations will be attempted regardless of quad fails. Translations are accepted only if their execution will not adversely affect the execution of rotations. In some cases, translations can be enabled by judicious choice of roll quads and X-translation quads. In other cases, quad fails can force the postponement or rejection of translations. The logic of command-word 2 is somewhat simpler, since only translations are involved:

ii. Command-Word 2.-- Translations Only

a. Y- and Z-translations

- 1. Should AC roll be selected, Z-translations would be accepted regardless of Quad B or D fails; Y-translations would be rejected in the case of Quad A or C fails.
- 2. Should BD roll be selected, Y-translations would be accepted regardless of Quad A or C fails; Z-translations would be rejected in the case of Quad B and D fails.

b. X-Translations

- 1. Were one quad of a pair failed by the astronaut, neither quad would fire in response to X-translation requests. The astronaut should select unfailed quads for X-translations.

Implementation of jet selection in the jet-selection phase of the DAP is by means of a table look-up procedure. Two sets of four tables each are provided. The first set (Tables 3.2-III through 3.2-VI) gives rotations and translations combined; the second set (Tables 3.2-VII through 3.2-X) gives translations only. Entries are included for quad fails, where appropriate, and a torque parameter is included to indicate the direction and magnitude of the resultant torque. This parameter is used both in the calculation of jet-on time in terms of the actual number of jets fired and in evaluating the effects of quad fails on the resultant torque.

TABLE 3.2-III

## JET SELECTION FOR PITCH ROTATIONS -- QUADS AC

Item	Pitch	X-Translation	Quad Fail	Jets	Torque
1	0	0		None	0
2	+	0		1, 3	2
3	-	0		2, 4	-2
4	0	+		1, 2	0
5	+	+		1	1
6	-	+		2	-1
7	0	-		3, 4	0
8	+	-		3	1
9	-	-		4	-1
10	0		A	None	0
11	+		A	1	1
12	-		A	4	-1
13	0		C	None	0
14	+		C	3	1
15	-		C	2	-1

TABLE 3.2-IV

## JET SELECTION FOR YAW ROTATIONS -- QUADS BD

Item	Yaw	X-Translation	Quad Fail	Jets	Torque
1	0	0		None	0
2	+	0		5, 7	2
3	-	0		6, 8	-2
4	0	+		5, 6	0
5	+	+		5	1
6	-	+		6	-1
7	0	-		7, 8	0
8	+	-		7	1
9	-	-		8	-1
10	0		B	None	0
11	+		B	5	1
12	-		B	8	-1
13	0		D	None	0
14	+		D	7	1
15	-		D	6	-1

TABLE 3.2-V

## JET SELECTION FOR ROLL ROTATIONS -- QUAD AC

Item	Roll	Y-Translation	Quad Fail	Jets	Torque
1	0	0		None	0
2	+	0		13, 15	2
3	-	0		14, 16	-2
4	0	+		13, 14	0
5	+	+		13	1
6	-	+		14	-1
7	0	-		16, 15	0
8	+	-		15	1
9	-	-		16	-1
10	0		A	None	0
11	+		A	15	1
12	-		A	14	-1
13	0		C	None	0
14	+		C	13	1
15	-		C	16	-1

TABLE 3.2-VI

## JET SELECTION FOR ROLL ROTATIONS -- QUADS BD

Item	Roll	Z-Translation	Quad Fail	Jets	Torque
1	0	0		None	0
2	+	0		9, 11	2
3	-	0		10, 12	-2
4	0	+		9, 10	0
5	+	+		9	1
6	-	+		10	-1
7	0	-		11, 12	0
8	+	-		11	1
9	-	-		12	-1
10	0		B	None	0
11	+		B	11	1
12	-		B	10	-1
13	0		D	None	0
14	+		D	9	1
15	-		D	12	-1

TABLE 3.2-VII  
X-TRANSLATIONS -- QUADS AC

Item	X-Translation	Jets
1	0	None
2	+	1, 2
3	-	3, 4

TABLE 3.2-VIII  
X-TRANSLATIONS -- QUADS BD

Item	X-Translation	Jets
1	0	None
2	+	5, 6
3	-	7, 8

TABLE 3.2-IX  
Y-TRANSLATIONS -- QUADS AC

Item	Y Translation	Quad Fail	Jets	Net Roll Torque
1	0		None	0
2	+		13, 14	0
3	-		15, 16	0
4	0	A	None	0
5	+	A	14	-1
6	-	A	15	+1
7	0	C	None	0
8	+	C	13	+1
9	-	C	16	-1

TABLE 3.2-X  
Z-TRANSLATIONS -- QUADS BD

Item	Z Translation	Quad Fail	Jets	Net Roll Torque
1	0		None	0
2	+		9, 10	0
3	-		11, 12	0
4	0	B	None	0
5	+	B	10	-1
6	-	B	11	+1
7	0	D	None	0
8	+	D	9	+1
9	-	D	12	-1

### 3.2.4.6 Program Logic

The RCS DAP operates at a basic sample rate of 10 cps. Within each sample period, three distinct sets of operations are performed by the autopilot. In principle, Phase 1 samples the state of the S/C environment, Phase 2 calculates rotation commands, and Phase 3 adds translation commands and generates jet timing and selection commands.

Phase 1. In Phase 1 during nominal operation, the CDUs are read and the gimbal-angle differences converted to body-axis angle differences by use of a transformation matrix (K). From these readings, new estimates of vehicle angular rates are made by a filter system. The K-matrix, itself, is dependent on vehicle attitude and, therefore, is updated periodically. In practice this is done once every 10 sample periods. Finally, the FDAI needles are updated.

Phase 2. Phase 2 calculates rotational-control output in terms of impulses to be applied to each of the control axes by the RCS jets. These outputs are designated as  $\tau_0$  (impulse about the X-axis, roll),  $\tau_1$  (impulse about the Y-axis, pitch), and  $\tau_2$  (impulse about the Z-axis, yaw). These impulses are expressed as jet-on times, and designate the amount of time a single RCS jet must be fired to produce the desired impulse. For these calculations, the DAP takes into account the average thrust of the RCS jets, the moment arm, and S/C moment of inertia about each axis.

To handle adequately the requirements of the various modes of the autopilot, Phase 2 calculates jet impulse in one of three ways. In all cases, a negative  $\tau$  designates an impulse in the negative direction; the jet-on time is equal to  $|\tau|$ :

1. For RHC control in the FREE mode, Phase 2 generates impulses that will turn on the appropriate jets for 14 ms, this being the minimum jet-on time.
2. For MIC control in the FREE mode, Phase 2 generates impulses that will turn on the appropriate jets for 14 ms.
3. For attitude hold, automatic maneuvers, and manual-rate maneuvers, Phase 2, using the phase-plane logic, generates impulses to establish and maintain S/C rate and attitude within deadbands of desired values.

Case 3 requires that S/C attitude and angular rate be known. For this reason, attitude hold, automatic maneuvers, and manual-rate maneuvers require the IMU be operating and in fine align before any commands can be accepted, or any impulses calculated.

Phase 3. Phase 3 of the RCS DAP processes the tau's from Phase 2 and, in addition, accepts and processes translation commands from the THC. The output of Phase 3 consists of the jet command words and timing words. The jet command words are AGC data words suitable to be loaded into output Channels 5 and 6 in order to turn the required jets on or off. Two command words are generated for each axis. Word 1 enables jets both for rotations and for translations. Word 2 enables jets for translations only. The timing



word is a jet firing time for rotations, which is the tau value from Phase 2 divided by the number of jets contributing to the requested rotation.

Should  $\tau$  divided by the number of jets used be less than 14 ms, however, the firing time will be set to 14 ms; should  $\tau$  divided by the number of jets be greater than 100 ms, the firing time will be set to 100 ms.

After processing  $\tau$  and generating the jet-command words, Phase 3 resets  $\tau$  to zero if the required firing can be completed before the next Phase 3, i. e., within 0.1 sec. If the required firing cannot be completed within 0.1 sec, however, Phase 3 resets  $\tau$  to a value that will produce the firing required in excess of 0.1 sec. For example, if the initial  $\tau$  were 270 ms and two jets were to be used, Phase 3 would command the appropriate jet pair to fire for 100 ms (the duration of one cycle) and then reset  $\tau$  to 70 ms. This excess 70 ms would either be replaced during the next Phase 2 or be saved for the next Phase 3.

During normal operation, Phase 1 computes a phase-plane point every cycle; should the point lie outside the deadzone, Phase 2 computes a new  $\tau$  to replace any  $\tau$  heldover from the last Phase 3. Should the new phase-plane point lie within the deadzone, however, Phase 2 leaves the existing value of  $\tau$  unchanged. The existing value of  $\tau$  will be zero or nonzero, depending upon whether, at the last execution of Phase 3, there was a firing requirement in excess of 0.1 sec. For the example given (original  $\tau$  of 270 ms), the existing value of  $\tau$  would be 70 ms.

The logic of this phase is equipped to deal with failures of one or more of the RCS jet quads and to honor astronaut requests for preferred quads for roll and X-translations. Under certain conditions, the execution of a translation would cancel a desired rotation or would induce rotations that cannot be compensated by RHC (or automatic) commands. In such cases, the translation requests are ignored: rotations always take precedence over translations.

Actual jet turn-on and turn-off is performed by a separate program (T6 Program) with its own timing clock. This program is described in paragraph 3.2.4.11.

#### 3.2.4.7 DAP Idling Sequence

If the DAP is running with the SC CONT switch in SCS (computer not directing guidance, control, and navigation) and with the CMC MODE switch in AUTO or HOLD, the DAP is not fully operational. Phase 2 and Phase 3 are not executed at all. Once every 0.1 sec, an abbreviated form of Phase 1 is executed to update the FDAI needles and, at 1.0-sec intervals, to update the K-matrix, which is used in updating the needles. No other autopilot functions are operational. If the CMC MODE switch is in FREE, however, all these phases are executed. This is done because the channel bit that the DAP checks and the SCS selection resets is also reset when IMU power is off. Therefore, to ensure the providing of FREE mode control when the SC CONT switch is in CMC but the IMU is off, all DAP phases are executed whenever the CMC MODE switch is in FREE.

#### 3.2.4.8 DAP Turn-on Sequence

To establish DAP control of the S/C, an initialization sequence is executed. This sequence is entered whenever the SC CONT switch is turned to CMC while the DAP is on, or whenever the DAP is started (through V46) while the SC CONT switch is in CMC.

The rate estimate is initialized by means of a Kalman-filter procedure. The filter gains are initially set very high and gradually reduced to nominal values in the course of the first 1.1 second of operation. During this first 1.1 second, Phase 3 is omitted entirely since no jet commands can be calculated while the filter is being initialized. Normal Phase-2 operation is disabled, and Phase 2 functions only to count down the tables of filter gains for the Kalman filter. Phase 1 updates the rate estimation, the error needles, and the K-matrix when necessary.

#### 3.2.4.9 Initialization Phase

The initialization sequence begins with an initialization phase, which stops any jets that may be firing, initializes a number of variables, and calculates the K-matrix for the first time. Phase 2 is executed next, in order to select the first set of Kalman gains. Following these initial two steps, the sequence is thus: Phase 1, to update rate estimate, displays, and K-matrix; Phase 2, to select the gains for the next Phase-1 pass. This sequence is executed once every 0.1 sec for 1.1 sec. At the end of 1.1 sec, the rates are properly initialized, and normal DAP operation begins.

For the rate estimate to be valid, the above initialization sequence requires that the IMU be usable. If the IMU is not usable, rate-estimate initialization is not possible. Operation without valid rates depends on the mode. In AUTO or HOLD, no control can be provided; therefore, Phase 1 exits at once. Initialization is attempted every 0.2 sec thereafter until successful. In the FREE mode, normal Phase-2 and Phase-3 operation is permitted, such that manual control by the RHC, MIC, and THC is possible. Phase 1 bypasses all operations requiring the IMU, and the error needles are not updated. As long as the DAP is kept in the FREE mode, no further attempt will be made to initialize the rates, even though the IMU become usable. As soon as the DAP is switched into AUTO or HOLD, initialization will be attempted, and the attempt will be repeated every 0.2 sec until successful.

Should the IMU become disabled for any reason, after rate initialization, the rates immediately become invalid. Operation reverts to the without-valid-rates condition described above, just as though the rates had never been initialized.

#### 3.2.4.10 Program Timing

Adequate performance of the RCS DAP depends on the maintenance of accurate timing between the various phases. The mechanism for this timing is the TIME5 register. This register is incremented every 10 ms and, upon overflow, initiates an interrupt. When the interrupt occurs, all normal operation is suspended, and control is transferred to an address contained in a variable-address register. The interrupt takes precedence over any job, regardless of priority, and therefore can be delayed only by another interrupt, which hopefully will be brief and occur but rarely. The scheduling process consists of setting the TIME 5 register to overflow at the desired instant and loading the variable-address register (T5LOC) with the starting address of the phase to be executed.

In practice, the initialization phase, Phase 1, and Phase 2 all have the same starting address, and are selected within the DAP by the setting of a flagword. The jet-selection phase (Phase 3) does have its own starting address. Since the TIME 5 register cannot be shut off, an idling address is also available. This address is the start of a short program that merely resets the interrupt for the maximum time interval possible (163.84 sec) and then returns to the program active at the time of the interrupt.

Turning on the DAP consists of setting the flagword to "+", setting the TIME5 counter to overflow in a suitably short time (typically 10 ms), and loading the starting address of the DAP into the address register. To turn the DAP off requires only the loading of the idling address into the address register.

In the implementation of the DAP, it is the responsibility of each phase of the DAP to schedule the phase to follow by setting the flagword, loading the address register, and setting the TIME5 register.

If we designate the start of Phase 1 as time 0.0, beginning the 100-ms cycle period, then the timing of the various phases within the cycle period typically will be as follows:

1. During DAP idle (DAP on, SC CONT switch in SCS, and CMC MODE switch in AUTO or HOLD), Phase 1 merely reschedules itself to begin again in 100 ms.
2. For the initialization sequence, the initialization phase schedules Phase 2 for time 60 ms in order to select the filter gains; Phase 2 schedules Phase 1 for time 100 ms in order that Phase 1 will fall at the beginning of the next cycle period.
3. Thereafter, during filter initialization, Phase 1 begins at time 0; Phase 2 begins at time 20 ms.
4. During normal operation, Phase 1 begins at time 0, Phase 2 at time 20 ms, and jet-selection phase at time 40 ms.

Matrix updating is not done during Phase 1 itself, but is scheduled as a separate job with relatively high priority. In the absence of waiting interrupts or jobs with high priority, the update job will begin immediately following completion of Phase 1, whenever it has been scheduled.

The timing of the DAP phases may be clarified by the graphs of Figs. 3.2.10 and 3.2.11. Figure 3.2.10 shows the first 2 seconds of DAP initialization and run following turn-on at time 6.0 seconds. Figure 3.2.11 shows a typical 2 seconds of normal DAP run: one-jet firing was initiated at time 39.26 and terminated at time 39.3. The typical timing described above and shown in Figs. 3.2.10 and 3.2.11 will, at times, be altered slightly. DAP computer interrupts can be delayed by other interrupts already in progress. Delays, however, should be short and infrequent and, consequently, should not degrade DAP performance.

#### 3.2.4.11 Jet Timing

Jet timing is handled by a program initiated by underflow of the TIME6 counter. This counter differs from the TIME5 counter in that it is decremented rather than incremented, its time increment is 0.625 ms rather than 10 ms, and it may be shut off when not in use.

The jet-selection phase produces two command words and a time word for each control axis. Command-word 1 contains jet commands for rotations and translations; command-word 2 contains jet commands for translations alone. The time word designates the desired duration of the rotational impulse--ranging from a minimum of 14 ms to a maximum of 100 ms. For certain rotation-translation combinations, rotational commands for 86- to 100-ms firings can result in one or more jets firing for less than the 14-ms minimum. To prevent this, the logic is structured such that all firing commands for the 86- to 100-ms range produce actual firing times of 100 ms. The original firing-command value, however, is fed back to the rate filter--introducing, infrequently, a slight error. The jet timing program is scheduled by the jet-selection phase for time 55 ms. When this first interrupt occurs, the timing program places Word 1 into the appropriate output channels and sets the TIME6 counter to underflow again at the end of the time period specified by the time word. This initiates all impulses--rotations and translations. When the second interrupt occurs, the timing program replaces command-word 1 with command-word 2 in order that rotations cease while translations continue.

In actual practice, there are three sets of command and time words. On the first interrupt, firing begins for all three axes. There are then up

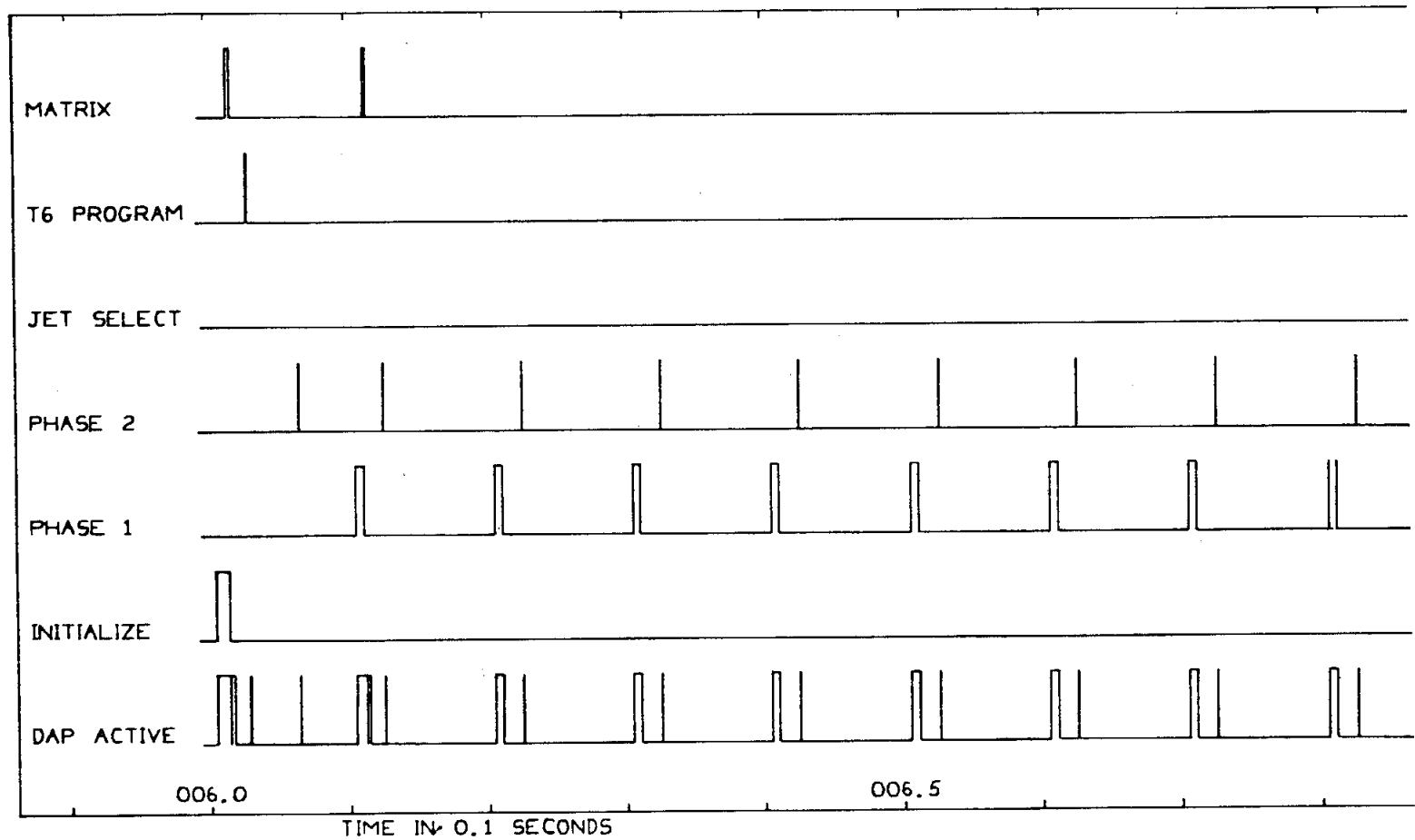
to three more interrupts to turn off the rotational jets at the appropriate time during the cycle period for each axis. After all rotations have ceased, the TIME6 counter is shut off. The result is that rotational impulses may have a duration of from 14 to 100 ms per cycle, but translational impulses continue for the entire 100-ms cycle, and are ceased only by generation of new command words by Phase 3 of the DAP.

#### 3.2.5 Restart Behavior of the RCS DAP

Should a restart occur during RCS DAP operation, any jets that happen to be on will be turned off, and re-initialization of the RCS DAP will be scheduled. This re-initialization is the same as the initialization caused by RCS DAP turn on using V46, with exception that the attitude reference angles are not changed.

Automatic maneuvers governed by R60 that were in progress at the time of a restart will not automatically be resumed. Rather, attitude hold will be established following re-initialization. The automatic maneuver can be resumed by appropriate DSKY action.

### DAP TIMING -- INITIALIZATION



3.2-46

Fig. 3.2.10 DAP Timing -- Initialization

3.2-47

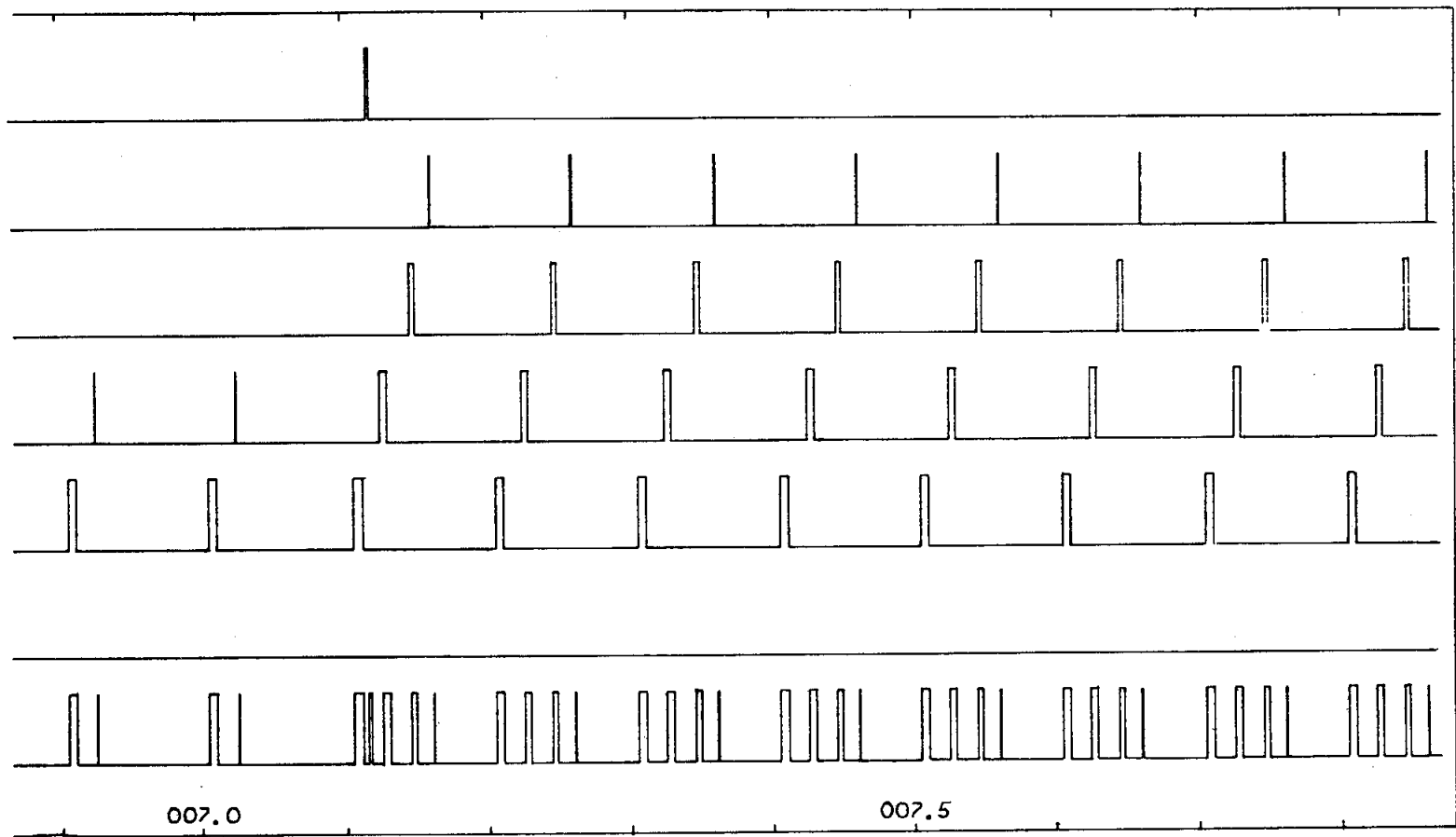


Fig. 3.2.10 DAP Timing -- Initialization (Cont'd)

### DAP TIMING - NORMAL RUN

3.2-48

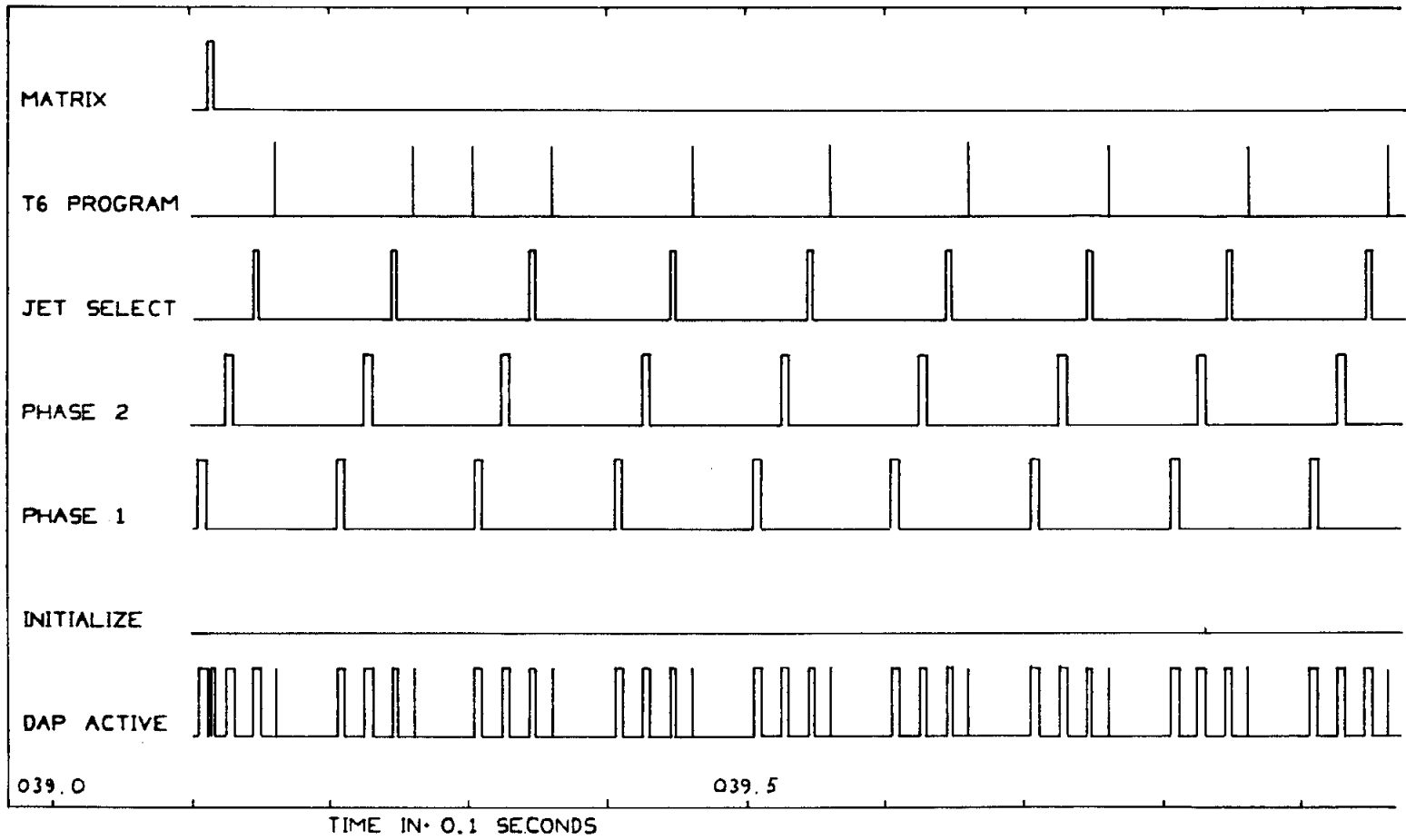


Fig. 3.2.11 DAP Timing -- Normal Run



3.2-49

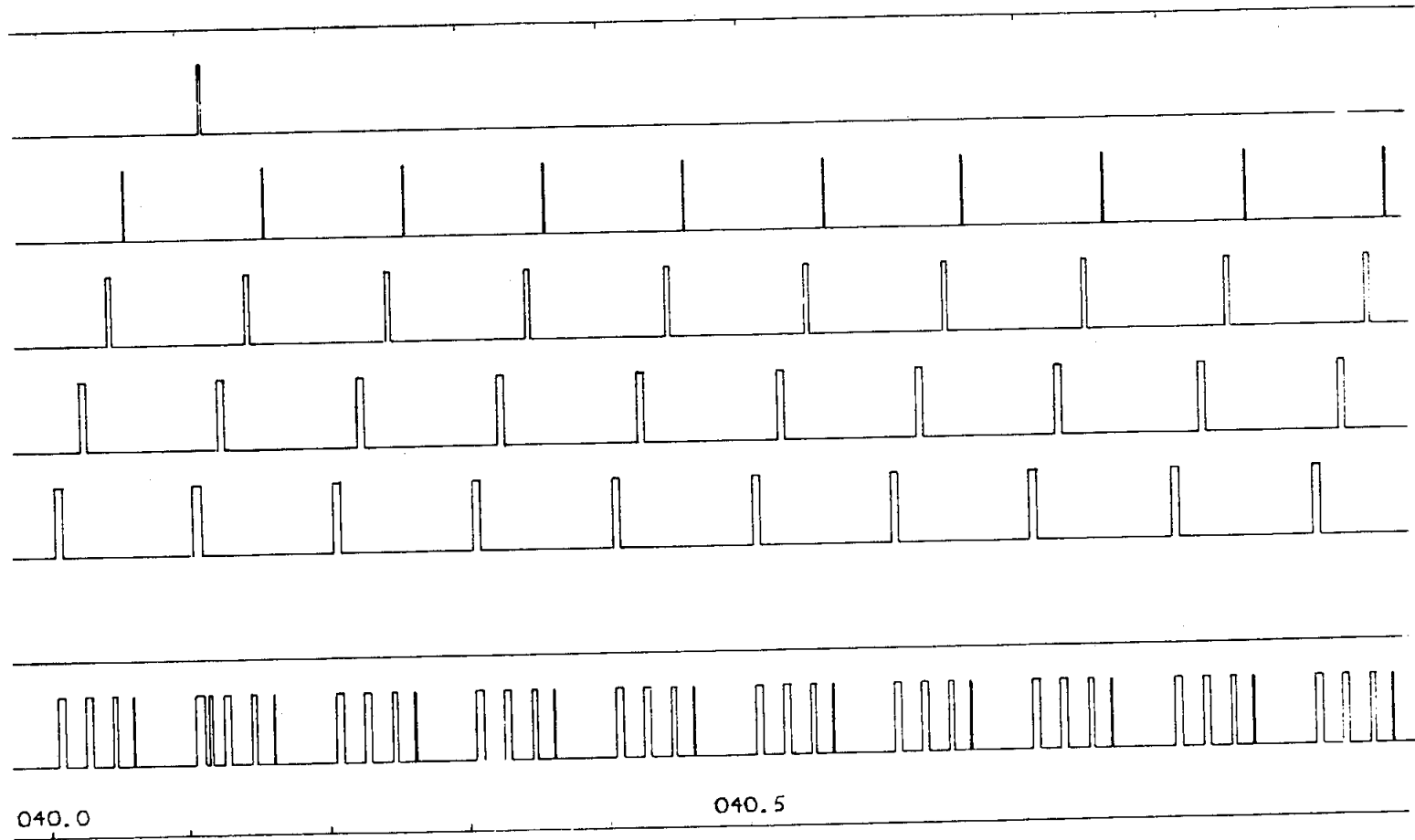


Fig. 3.2.11 DAP Timing -- Normal Run (Cont'd)

### 3.3 THRUST VECTOR CONTROL AUTOPILOT

by A. Engel, A. Penchuk, R. Schlundt, and G. Stubbs

During thrusting portions of flight, S/C attitude control in pitch and yaw is achieved by driving the gimbal servos of the SPS gimballed engine. The resulting offset of the thrust vector with respect to the vehicle center of gravity results in the generation of control torques about the S/C pitch and yaw axes. The computation of gimbal servo commands in response to angular-rate commands from the steering program (P40) is the function of the Thrust Vector Control Digital Autopilot (TVC DAP). A separate autopilot (TVC ROLL DAP) provides attitude and rate control in the roll axis by means of the RCS jets on the Service Module (SM).

The following is a summary outline of TVC pitch and yaw control:

- a. The CMC steering loop computations generate attitude-rate commands in inertial coordinates and transform them into body coordinates.
- b. The CDU angles are read and back differenced to give attitude rates in platform coordinates. These are transformed into body coordinates and subtracted from the CMC rate commands.
- c. The resulting attitude-rate errors are integrated to form the attitude errors in body coordinates.
- d. The respective attitude errors are fed to the pitch and yaw compensation filters, whose outputs are the commands to the engine-gimbal servos for pitch and yaw.

The TVC ROLL DAP is designed to provide attitude and rate control about the roll axis by use of the RCS jets. Its function is strictly attitude hold: the orientation of the S/C about the roll axis at the time of ignition is held within a specified deadband throughout the burn. The outer-gimbal angle (OGA) is read and processed to yield approximate roll-attitude and roll-rate measurements. A switching logic in the phase plane is then used to generate jet commands to the RCS jets.

The operation of the DAPs during an SPS burn is completely automatic, requiring no inputs from the astronaut. Before the burn, however, the astronaut may enter the CSM and LM weights or the estimated engine-trim angles in the pitch and yaw planes. (This entry is optional, to be made only should the astronaut be dissatisfied with values which have been pad-loaded, computed, or entered earlier after a vehicle configuration change such as the LM undocking). By entering V46 on the DSKY, the astronaut can change the CSM/LM filter during a burn. He must also determine ullage requirement and initiate timely ullage thrusting. Astronaut entries are discussed in paragraphs 3.3.2, 3.3.3, 3.3.4, and 3.3.5.

#### 3.3.1 TVC DAP Design Requirements

The TVC DAP programs must fulfill the primary requirement of providing, in conjunction with the external-guidance loop, satisfactorily small velocity-

pointing errors at thrust cutoff. The DAP programs must also limit excursions in vehicle attitude and in thrust-vector orientation in such a way as to minimize propellant usage and gimbal-servo clutch wear and to allow pilot monitoring. A simple roll-control program that holds the roll attitude within  $\pm 5$  degrees of the desired angle is sufficient to prevent adverse pitch and yaw cross-coupling. Cross-coupling could result in errors on the matrix transformations used to generate body-axis pitch- and yaw-attitude errors.

The DAP programs must operate with uncertainties in initial conditions and with vehicle characteristics, only roughly defined, that vary with flight time. These are discussed in paragraphs 3.3.1.1 and 3.3.1.2.

#### 3.3.1.1 Initial Conditions

The TVC DAPs will experience several initial perturbations at SPS ignition time:

- a. Initial turning rates in roll, pitch, and yaw. -- Off-nominal RCS-jet performance during ullage may lead to turning rates at SPS ignition time of up to 1 deg/sec.
- b. Initial lateral slosh-mass displacement. -- No specific data are yet available on the maximum possible displacements, but a value of 0.5 ft has been used for testing.
- c. Initial longitudinal propellant displacement. -- The DAP designs were based on a pre-burn ullage; therefore, no testing was conducted with initial conditions resulting from no-ullage propellant displacement.
- d. Thrust-vector misalignment. -- Before thrust initiation, the CMC supplies trim signals to the engine-gimbal servos in order to orient the thrust vector through the estimated c. g. position. It is very likely, however, that there will be some error in the alignment. There are two sources of thrust-vector misalignment, viz., uncertainties in the thrust vector positioning system and uncertainties in the estimation of the c. g. position. These sources have been described quantitatively in Ref. 3.1, which gives a  $3\sigma$  misalignment angle ranging from 1.4 deg (full) to 0.98 deg (empty), for the CSM, and 1.25 deg (full) to 0.710 deg (empty) for the CSM/LM.

In addition to the initial misalignment, there will be a time variation, because of fuel consumption, in the c. g. position. Also, there is a possibility of fluctuations in the thrust vector within the nozzle as a result of uneven erosion. The time variation of the c. g. position is given in Reference 3.2. The maximum predicted rates for the CSM/LM are about 0.003 deg/sec, in the pitch plane, and 0.003 deg/sec in the yaw plane. For the CSM, the figures are 0.0083 deg/sec, in the pitch plane, and 0.014 deg/sec in the yaw plane.

The thrust vector variation has been described in Ref. 3.3 and 3.4. It appears that the variation will be less than  $\pm 0.2$  deg in any 20-second interval and that the total variation over a long burn will be within  $\pm 0.3$  deg.

### 3.3.1.2 Variation in Vehicle Characteristics

The dynamic characteristics of the CSM/LM are sufficiently different from those of the CSM alone as to require the development of separate autopilot programs tailored to the characteristics of each vehicle. The three principal differences in the two vehicles are as follows:

- a. The bending mode frequencies of the CSM/LM are as low as approximately 2 cps; the bending mode frequencies of the CSM alone start at approximately 5.3 cps.
- b. The two vehicles differ substantially, both in the moment arm from the gimbaled engine to the center of gravity and in the vehicle moment of inertia. As a result, a given deflection of the gimbaled engine of the CSM alone can produce as much as four times the angular acceleration as the same deflection in the CSM/LM vehicle.
- c. The fuel and oxidizer slosh behavior in the CSM/LM vehicle is different than the CSM alone because of the additional slosh masses in the LM tanks, the effects of the increased mass and moment of inertia of the overall vehicle, and the differences in c. g. location. (See Ref. 3.5.)

The problem of minimizing the excitation of slosh modes and preventing any destabilization of these modes is of equal importance for both vehicles. The problem of avoiding the excitation of the bending modes and preventing their potentially destabilizing influence is primarily a problem in CSM/LM autopilot design.

### 3.3.2 Operating Procedures

During an SPS burn, the functioning of the TVC DAPs is automatic, but there are several important interfaces that must be properly established before the burn.

#### 3.3.2.1 R03 (Verb 48): Configuration and Initial Gains

Routine R03 (called from DSKY by Extended Verb 48) is normally executed before an SPS burn. The Noun 46 sequence of R03 -- in particular the CONFIG bits of R1 (DAPDATR 1) bits 15, 14, 13 -- provide information on vehicle configuration as follows:

$$\text{CONFIG (Bits 15, 14, 13 of DAPDATR1)} = \begin{cases} 000 & \text{CM (or no DAP)} \\ 001 & \text{CSM alone} \\ 010 & \text{CSM/LM} \\ 011 & \text{CSM/LM/SIVB} \\ 110 & \text{CSM/LM, ascent stage only} \end{cases}$$

Bits 15, 14, and 13 are used in the TVC DAP as follows: (1) by TVCDAPON initialization to select gains and sample rates; (2) by the PITCH DAP and YAW DAP to select the proper CSM or CSM/LM filter; (3) by TVCEXECUTIVE to perform the one-shot correction; (4) by TVCMASSPROP (as below).

The Noun 47 sequence of R03 provides CSM weight and LM weight (in pounds), and Noun 48 provides the values of PTRIM and YTRIM (in degrees). The vehicle weights are used by TVCMASSPROP, which is called by R03, to obtain the proper values of  $I_{xx}$ ,  $I_{AVG}$ , and  $I_{AVG}/Tl_x$ . These in turn are used to calculate the DAP filter gains. (See paragraph 3.3.4.)

PTRIM and YTRIM are used by the gimbal-drive test/trim sequence to position the engine for ignition. Also, TVCDAPON uses these same values to initialize the offset-tracker filters DELPBAR and DELYBAR, the double-precision trim trackers PDELOFF and YDELOFF, and the initial values of the DAP output commands PCMD and YCMD. The thrusting program (P40) also uses these values in computing vehicle alignment for ignition.

### 3.3.2.2 Gimbal-Drive Test and/or Trim (S40.6)

The gimbal-drive test/trim sequence (S40.6) prepares the digital-to-analog converter output interfaces for transmitting TVC DAP commands to the SPS engine actuators. The routine is entered automatically as part of the pre-ignition sequence of P40. Before execution of S40.6, the S/C CONT switch will have been put in the CMC position. (See Section 4 of this document.)

The routine provides for an optional test of the engine-gimbal actuators before the engine trim angles are commanded. If the astronaut wants the test, he keys in PROCEED at the appropriate time (see Section 4), and the test is performed. The test entails commanding a sequence of  $\pm 2$ -deg deflections, both in the pitch and the yaw gimbal actuators, which the astronaut should monitor on the SPS gimbal angle display. Upon completion of the test, the trim values are commanded in preparation for ignition. Should the astronaut wish to omit the test, he can key in ENTER instead of PROCEED, and the trim angles will be commanded in 4 seconds. The output interface between the autopilot and the engine actuators is established regardless of the option selected. This is in order that, at the end of S40.6, the SPS engine will have been aligned for ignition, and the actuators will be running. Figure 3.3.1 is a functional flow chart of S40.6.

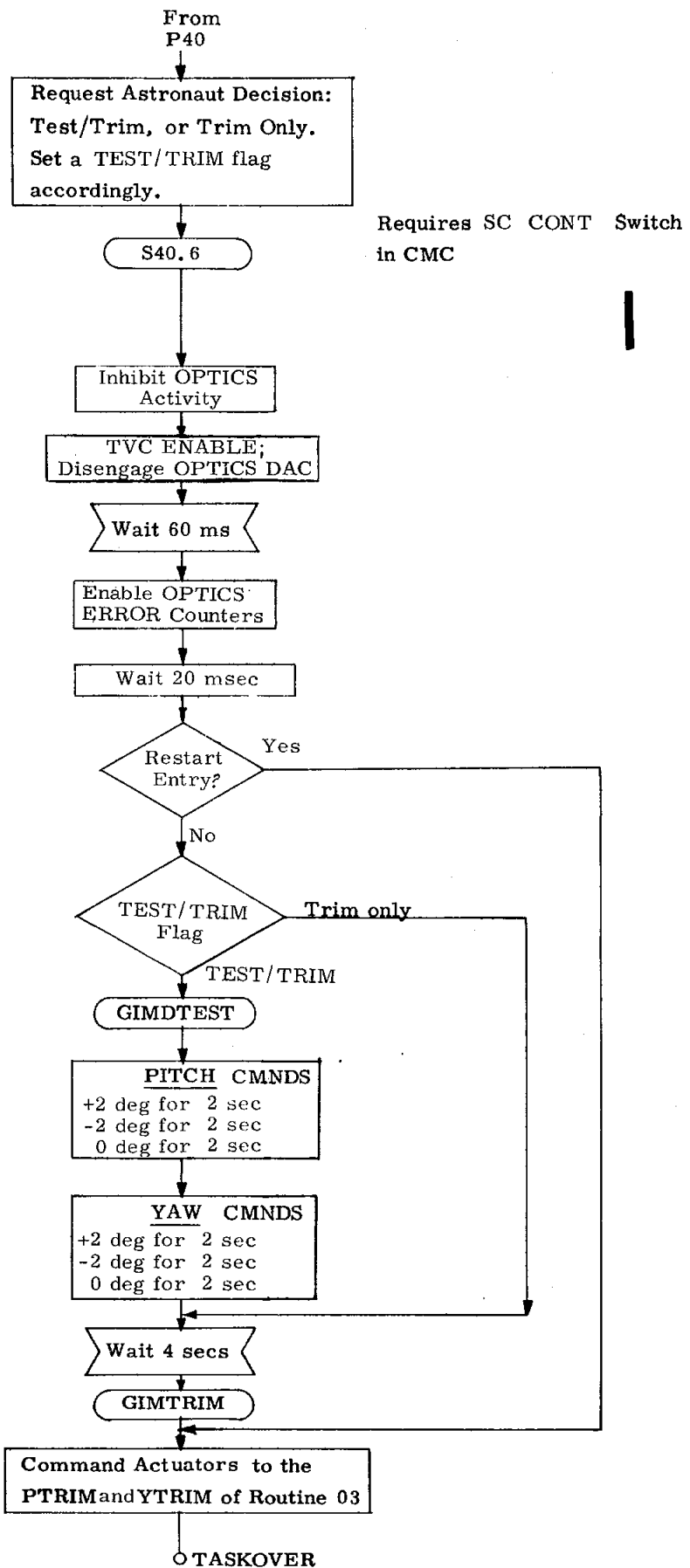


Fig. 3.3.1 Gimbal Drive Test/Trim

3.3-5

### 3.3.2.3 TVC DAP Start-up Sequence

After the completion of R03 and the gimbal trim sequence, the TVC DAPs are started by a call to TVCDAPON, which is the TVC initialization sequence. This call comes from the P40 routine (at DOTVCON), which is the controlling routine for engine ignition. All functions then proceed automatically. (Special events such as V46 switchover, and normal shutdown require special interfaces.) Following a 0.4-second delay after ignition, P40 sets the TVC restart phase indicators, sets the T5 bits (bits 15, 14 of FLAGWRD6) to indicate that TVC uses the T5 clock, and makes the call to TVCDAPON.

TVCDAPON performs all remaining TVC preparation: (1) it zeros the erasables for filter storage and other temporary locations; (2) it selects (based on LM-on or LM-off configuration) the DAP coefficients, gain, Thrust Misalignment Correction Loop (TMC) gain, and steering gain; (3) it initializes the offset-tracker filters, the double-precision trim trackers, the attitude-error integrators, and the DAP commands; and (4) it prepares the FDAI needles with a special initialization call to NEEDLER. The final operations of TVCDAPON are a 0.51 second WAITLIST call for TVCEXECUTIVE, and a TIME5 call for DAPINIT.

DAPINIT reads CDUY and CDUZ for the past CDU values of the pitch and yaw differentiators. DAPINIT then calls PITCHDAP, and DAP computations begin. From then on, PITCHDAP calls YAWDAP, which in turn calls PITCHDAP, etc., maintaining the sampling frequency. The time required for the IGNITION-TVCDAPON-PITCHDAP sequence is approximately 0.5 sec.

The routine TVCEXECUTIVE is self-perpetuating at 1/2-sec intervals. Among its functions are calling the ROLL DAP, calling NEEDLER to update the FDAI attitude-error needles, updating the variable gains, and making the one-shot and repetitive thrust-misalignment corrections.

Figure 3.3.2 is a time-line chart of the main DAP routines for the first few seconds of an SPS burn. The nominal time of ignition (TIG-0) was 180 sec. This time line is for illustration only, and should not be construed as DAP performance specification.

#### 3.3.2.4 Engine Shutdown

The engine shutdown sequence originates in the SERVICER routine, after the steering computations find that TGO (time to reach the desired velocity) is less than 4 sec. SERVICER computes the time for stopping the engine and calls P40 (at SPSOFF) to do the actual shutdown sequence. Following the SPS engine shutdown, there is a 2.5-sec delay while the TVC DAPs continue to function as the thrust level decays. There is an additional 0.6-sec delay before the RCS DAP is restarted (RCS DAPON). Jet firings start approximately 1 sec later.

At TVC DAP termination, an end-of-burn update of the trim estimates PACTOFF and YACTOFF takes place. The update occurs when the engine-off command is generated (SPSOFF) and consists of picking up the pitch and yaw DELFILTER values DELPBAR and DELYBAR and loading them into the trim registers PACTOFF and YACTOFF. The update is not permitted until DELPBAR and DELYBAR have been properly established after TVC initialization.

#### 3.3.3 TVC DAP Filters: Design and Implementation

##### 3.3.3.1 General

Seven major points regarding frequency response and stabilization of the system should be discussed before proceeding to a description of the individual autopilots:

1. All significant poles and zeros of the CSM and CSM/LM engine-vehicle system occur at frequencies that are well below half the lowest sampling frequency. Therefore, it is possible to treat the digital autopilot plus engine-vehicle system as if it were continuous and to apply the classical frequency-response approach to the designing and describing of the system.
2. Every significant bending and slosh mode of the CSM/LM vehicle results in a complex pole pair that is immediately preceded by a complex zero pair in the engine-vehicle transfer function (relating vehicle-attitude  $\theta$  to engine deflections). This makes it possible to apply the same phase-stabilization criterion to all bending and slosh resonances in the CSM/LM. The same zero-before-pole configuration occurs in the CSM for propellant loadings associated with the nominal lunar mission. For the off-nominal loading of 60 to 100 per cent, however, the fuel slosh in the sump tank produces a pole-before-zero configuration that has a frequency close to that of a zero-before-pole configuration caused by storage-tank fuel slosh. Fortunately, it turns out that the sump-tank slosh mass has a very small



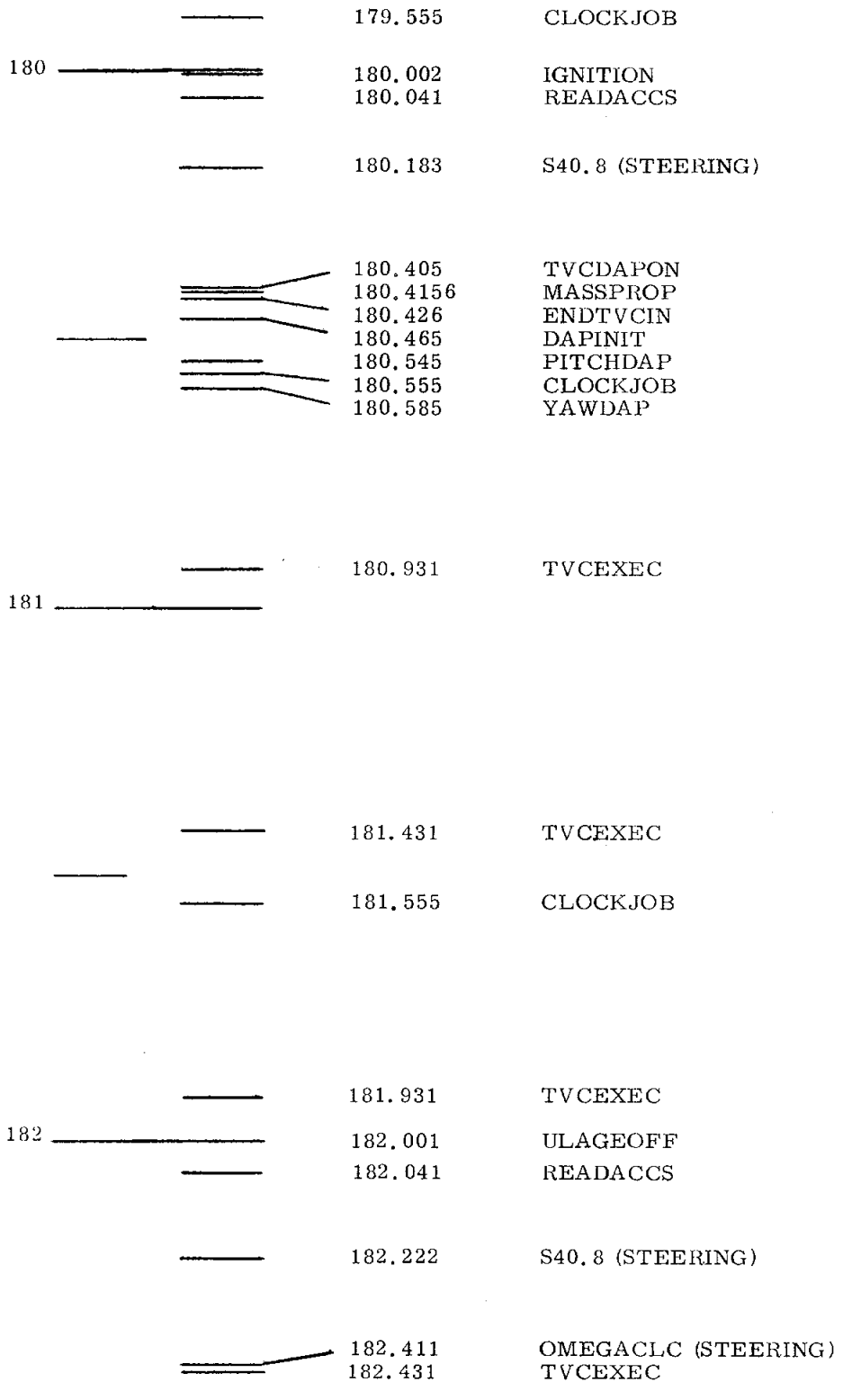


Fig. 3.3.2 TVC DAP Startup (CSM/LM, 80 msec sampling rate)

Revised

Added

GSOP # R-577

PCR # 1020

Rev. 10

Date 2/70

moment arm to the vehicle c.g. As a result, it is possible to phase-stabilize the more predominant storage-tank slosh mode without drastically destabilizing the sump-tank mode. In fact, the amplitude of the sump-tank oscillation grows only by a factor of three in the time taken to go from 100 per cent down to 60 per cent propellant loading, even with the pessimistic assumption of zero damping for the sump mode. With a small amount of positive damping (e. g., 0.005), this growth rate is much lower.

3. The effect of each of the zero-pole pairs on the stability of the system can be analyzed in terms of the magnitude and phase contribution to the overall open-loop gain versus phase plot of the system. Each zero-pole pair produces in this plot a closed contour that must be prevented from encircling the 0-dB, -180-deg point. This point corresponds to the -1 point on a Nyquist plot.
4. The values of the slosh and bending zero-pole pairs are dependent on the propellant loading; the remainder of the overall open-loop function is essentially independent of this loading (since the autopilot filter gain is compensated automatically for engine-vehicle gain changes). Therefore, it is convenient to analyze the effect of the changing zero-pole pairs by superimposing their varying gain-phase characteristics for different propellant loadings on the remaining unchanging portion of the open-loop function. This constant portion of the open-loop function consists of the rigid body, the autopilot, and the engine gimbal servo transfer functions. The portion will henceforth be referred to as the "rigid-body open-loop function," although it also includes the static gain effects of vehicle bending. The transfer function of the engine gimbal servo used in the design and analysis is

$$\frac{\delta}{\delta_c}(s) = \frac{5.12 \times 10^3}{(s + 19.62)(s^2 + 15.9s + 260)}$$

The deviations in gain and phase of the actual engine gimbal servo from the gain-phase characteristics of the above model will alter the stability margins reported here. (See Ref. 3.6.) The stability characteristics of the autopilot design are described in terms of the rigid-body open-loop function presented in Figs. 3.3.3 - 3.3.5, where the solid curve represents the autopilot-vehicle without the thrust-misalignment correction loop, and the dotted line shows the complete system.

5. All the zero-pole pairs of bending and slosh occur at frequencies above the main crossover frequency. Therefore, any potential encirclement of the 0-dB, -180-deg point would have to be the result of the resonance peaks

produced by the slosh and bending poles. These peaks may be prevented from reaching 0 dB by attenuation in the autopilot filter, or they can be phase shifted to prevent the peaks greater than 0 dB from encircling the 0-dB, -180-deg point. The former approach is called "gain stabilization"; the latter, "phase stabilization."

6. The frequency analysis required in order to design the autopilot filter for phase stabilizing the slosh and bending modes is greatly simplified by assuming that the zero-pole pairs for these modes have infinitesimal damping ratios. This assumption leads to autopilot designs that are slightly (but not excessively) conservative. With this assumption, each zero-pole-produced contour in the overall magnitude versus phase plot will cross 0 dB at  $\phi$  and  $\phi + 180$  deg, where  $\phi$  is the phase of the rigid-body open-loop function at the pole frequency. These crossovers may be prevented from straddling the 0-dB, -180-deg point by restricting  $\phi$  to a range, at the pole-frequency, as follows:

$$(\alpha - 180 \text{ deg}) < \phi < -\alpha.$$

Here,  $\alpha$  is a constant selected to achieve a desired minimum margin of stability. Henceforth,  $\alpha$  will be referred to as the "resonance stability margin."

7. If the required open-loop phase at a particular resonance frequency is produced by a preceding positive-phase excursion, the resonance is said to be lead stabilized; if the required phase is produced by a negative-phase excursion, the resonance is said to be lag stabilized.

### 3.3.3.2 CSM/LM Filter Design

The autopilot system employs two filter functions -- one in a high-bandwidth mode,  $D_h(z)$ , and one, for backup, in a low-bandwidth mode,  $D_l(z)$ .

The high-bandwidth filter stabilizes the bending modes by a combination of phase lag, for low frequencies, and attenuation for high frequencies. The filter takes advantage of the fact that the estimated minimum bending-mode frequency has been raised appreciably above the slosh frequencies. This increase in bending frequency allows the phase lead provided at the main crossover frequency to be extended well beyond this crossover point in order to stabilize the slosh modes without adversely reducing the large phase lag required to lag-stabilize the bending modes. As shown by the open-loop plots in Fig. 3.3.3, the filter lead-stabilizes the slosh modes out to 0.65 cps (with a resonance stabilization margin of 0 deg) and lag-stabilizes the bending modes down to 1.34 cps (with a resonance stabilization margin of 35 deg). The lower limit on bending stabilization is 65 per cent of the estimated minimum bending frequency.

Figure 3.3.3 shows the open-loop characteristics of the high-bandwidth mode with and without the effects of a thrust misalignment correction (TMC) loop. The filter stabilizes the slosh resonances for the CSM/LM propellant loadings encountered in the nominal lunar flight. The maximum stable slosh frequency is 0.65 cps (or 4.075 rad/sec), which is about 20% greater than the 0.54 cps (or 3.4 rad/sec) estimated maximum frequency for the CSM/LM in the nominal lunar mission. (The estimated maximum slosh frequency is the LM descent tank frequency in the last CSM/LM burn prior to detaching the fully loaded LM in lunar orbit.)

The rigid-body open-loop function for the low-bandwidth filter yields the magnitude-versus-phase characteristics shown in Fig. 3.3.4. The slosh modes are phase-lag stabilized (with a resonance stabilization margin of 0 deg) down to a frequency of 2.08 rad/sec. The gain margin is 6 dB, and the open-loop crossover frequency is 0.35 rad/sec. The bending modes are attenuated by more than 100 dB.

The TMC loop is to be used both in the high- and the low-bandwidth modes with a DELFILTER time constant of 8 seconds. When switchover to the low-bandwidth mode occurs, the output of the TMC loop is re-initialized to the value of the DELFILTER output just prior to the switchover. Concurrent with this TMC initialization, the low-bandwidth filter is switched in with a zero initial output. Thus, the TMC loop assumes the burden of providing the engine gimbal command at switchover. It is logical to make this command equal to the output of DELFILTER, which has been tracking the engine gimbal commands at the DAP sample rate.

The low-bandwidth mode has been retained for three reasons. First, a stable, low-bandwidth mode may be required for off-nominal propellant loadings where the slosh modes are not stabilized in the high-bandwidth mode. Second, the low-bandwidth mode is desirable as backup in the event that the present analytical slosh models are not accurately representative of stability conditions. Third, there is some uncertainty regarding the extent that engine-gimbal servo nonlinearities can destabilize large amplitude slosh oscillation in the high-bandwidth mode.

A separate filter function is used for the low-bandwidth mode because the great disparity between the modes makes impractical the use of one filter function sampled at different frequencies.

Since the low-bandwidth mode may not be needed to stabilize the slosh modes in most of the CSM/LM engine burns, it is best to switch to this mode only when an undesirable slosh oscillation is encountered. The astronaut must determine when a slosh mode is oscillating in an unacceptable manner and make the switchover with a V46E on the DSKY. The engine-angle indicator dials can be used to observe slosh oscillations. If these dials indicate oscillations at the slosh frequency (roughly 0.5 cps) and the oscillations grow to around  $\pm 1$ -deg amplitude about the mean value, then the

slosh mass is oscillating with approximately  $\pm 1$ -ft displacement. Though this is not serious in a structural sense, the astronaut may prefer to switch to the low-bandwidth mode. Details of the switchover implementation are in paragraph 3.3.3.4.2.

### 3.3.3.3 CSM/LM Filter Functions

Filter functions for the low- and high-bandwidth modes are described in Tables 3.3-I to 3.3-IV.

The gain factors of these filter functions ( $K_{wh}$ ,  $K_{wl}$ ,  $K_{zh}$ ,  $K_{zl}$ ) are given in terms of the product of each factor times the vehicle steady-state gain constant ( $K_g$ ), where

$$K_g \equiv [s^2 G(s)]_{s=0}$$

$$G(s) = \frac{\theta(s)}{\delta_c(s)} = \text{engine-vehicle transfer function.}$$

The value of  $K_g$  depends on the vehicle propellant loading and, therefore, varies during a burn. The low-frequency gain characteristics of the autopilot depend on the product of  $K_g$  and the low- and high-bandwidth filter gains. The variable-gain mechanization, which applies equally to CSM/LM and CSM, is discussed further in paragraph 3.3.4.

### 3.3.3.4 CSM DAP Filter

The CSM-alone DAP filter is a lead-lag function with the following transfer function:

$$D(z) = K_z \frac{1 - 1.480247z^{-1} + 0.553559z^{-2} - 0.057085z^{-3}}{1 - 2.062524z^{-1} + 1.565661z^{-2} - 0.401160z^{-3}}$$

The gain relationship is  $K_z(Tl_x/I_{AVG}) = 8.4 \text{ sec}^{-2}$ . The gain factor ( $K_z$ ) of the filter is selected to produce a 0-dB crossover of the open-loop transfer function at 2.0 rad/sec. During the thrusting periods, where  $Tl_x/I$  of the vehicle is changing with time, the CMC automatically changes  $K_z$  so as to maintain the crossover frequency at approximately this value. Thus,  $K_z$  varies from 3.75, for a full CSM, to 1.25, for a nearly empty vehicle.

The phase margin at the crossover frequency is 50 deg; the gain margin is 10 dB. (See Fig. 3.3.5.) The slosh modes are phase-lead stabilized. The rigid-body open-loop phase angle varies between -140 and -150 degrees over the slosh frequency range 3.2 to 4.8 rad/sec. This provides adequate phase stabilization for the predominant slosh modes.

TABLE 3.3-I

w - Transform of the High-Bandwidth Filter

$$D_h(w) = K_{wh} \left[ \frac{\prod_{i=1}^6 (w - w_{ci})}{\prod_{j=1}^6 (w - w_{dj})} \right]$$

$K_{wh} K_g$	$1.4530969 \times 10^{-1}$
$K_{ssh} K_g$	$5.50796355 \times 10^{-1}$
Zeroes of $D_h(w)$	$w = -1.9285714 \times 10^{-2}$ $w = -1$ $w = -1$ $w = -1$ $w = -5.2457143 \times 10^{-2} \pm j 5.2193893 \times 10^{-1}$
Poles of $D_h(w)$	$w = -1.6875 \times 10^{-1} \pm j 2.9266072 \times 10^{-1}$ $w = -1.6875 \times 10^{-1} \pm j 2.9266072 \times 10^{-1}$ $w = -6.5571429 \times 10^{-2} \pm j 3.212325 \times 10^{-1}$

Steady-State Gain Constants:

$$K_g = [s^2 G(s)]_s = 0$$

$$K_{ssh} = [D_h(w)]_w = 0 = [D_h(z)]_z = 1$$

Relationship between W and Z Transforms:

$$D_h(w) = [D_h(z)]_{z = \frac{1+w}{1-w}}$$

TABLE 3.3-II

w - Transform of the Low-Bandwidth Filter

$$D_1(w) = K_{w1} \left[ \frac{\prod_{i=1}^6 (w - w_{ai})}{\prod_{j=1}^6 (w - w_{bj})} \right]$$

$K_{w1} K_g$	$8.9 \times 10^{-5}$
$K_{ssl} K_g$	$4.38 \times 10^{-2}$
Zeroes of $D_1(w)$	$w = -4.8 \times 10^{-3}$ $w = -1$ $w = -1$ $w = -2$ $w = -1.3056 \times 10^{-2} \pm j 1.299048 \times 10^{-1}$
Poles of $D_1(w)$	$w = -4.2 \times 10^{-2} \pm j 7.284 \times 10^{-2}$ $w = -4.2 \times 10^{-2} \pm j 7.284 \times 10^{-2}$ $w = -1.632 \times 10^{-2} \pm j 7.99512 \times 10^{-2}$

Steady-State Gain Constants:

$$K_g = [s^2 G(s)]_{s=0}$$

$$K_{ssl} = [D_1(w)]_{w=0} = [D_1(z)]_{z=1}$$

Relationship between W and Z Transforms:

$$D_1(w) = [D_1(z)]_{z = \frac{1+w}{1-w}}$$

TABLE 3.3-III

z - Transform of the High-Bandwidth Filter

$$D_h(z) = K_{zh} \left[ \frac{\prod_{i=1}^6 (z - z_{ci})}{\prod_{j=1}^6 (z - z_{dj})} \right]$$

$K_{zh}/K_{wh}$	4.3116113
$K_{zh} K_g$	$6.2651890 \times 10^{-1}$
$K_{ssh} K_g$	$5.5079636 \times 10^{-1}$
Zeroes of $D_h(z)$	$z = 9.6215837 \times 10^{-1}$ $z = 0$ $z = 0$ $z = 0$ $z = 5.2520484 \times 10^{-1} \pm j 7.5638593 \times 10^{-1}$
Poles of $D_h(z)$	$z = 6.1026229 \times 10^{-1} \pm j 4.0321755 \times 10^{-1}$ $z = 6.1026229 \times 10^{-1} \pm j 4.0321755 \times 10^{-1}$ $z = 7.2056066 \times 10^{-1} \pm j 5.1868883 \times 10^{-1}$

Gain Constants:

$$K_{wh} = \text{gain factor of } D_h(w), \text{ defined in Table 3.3-I}$$

$$K_g = [s^2 G(s)]_{s=0}$$

$$K_{ssh} = [D_h(z)]_{z=1} = [D_h(w)]_{w=0}$$

Relationship between W and Z transforms:

$$D_h(z) = [D_h(w)]_{w = \frac{z-1}{z+1}}$$



TABLE 3.3-IV

z - Transform of the Low-Bandwidth Filter

$$D_1(z) = K_{z1} \left[ \frac{\prod_{i=1}^6 (z - z_{ai})}{\prod_{j=1}^6 (z - z_{bj})} \right]$$

$K_{z1}/K_{w1}$	10.15
$K_{z1} K_g$	$9.04 \times 10^{-4}$
$K_{ss} K_g$	$4.38 \times 10^{-2}$
Zeroes of $D_1(z)$	$z = 9.9044586 \times 10^{-1}$ $z = 0$ $z = 0$ $z = -3.333333 \times 10^{-1}$ $z = 9.4228732 \times 10^{-1} \pm j 2.4906071 \times 10^{-1}$
Poles of $D_1(z)$	$z = 9.1005219 \times 10^{-1} \pm j 1.3352035 \times 10^{-1}$ $z = 9.1005219 \times 10^{-1} \pm j 1.3352035 \times 10^{-1}$ $z = 9.5578068 \times 10^{-1} \pm j 1.5385608 \times 10^{-1}$

Gain Constants:

$$K_{w1} = \text{gain factor of } D_1(w), \text{ defined in Table 3.3-II}$$

$$K_g = [s^2 G(s)]_{s=0}$$

$$K_{ssl} = [D_1(z)]_{z=1} = [D_1(w)]_{w=0}$$

Relationship between E and Z transforms:

$$D_1(z) = [D_1(w)]_{w = \frac{z-1}{z+1}}$$

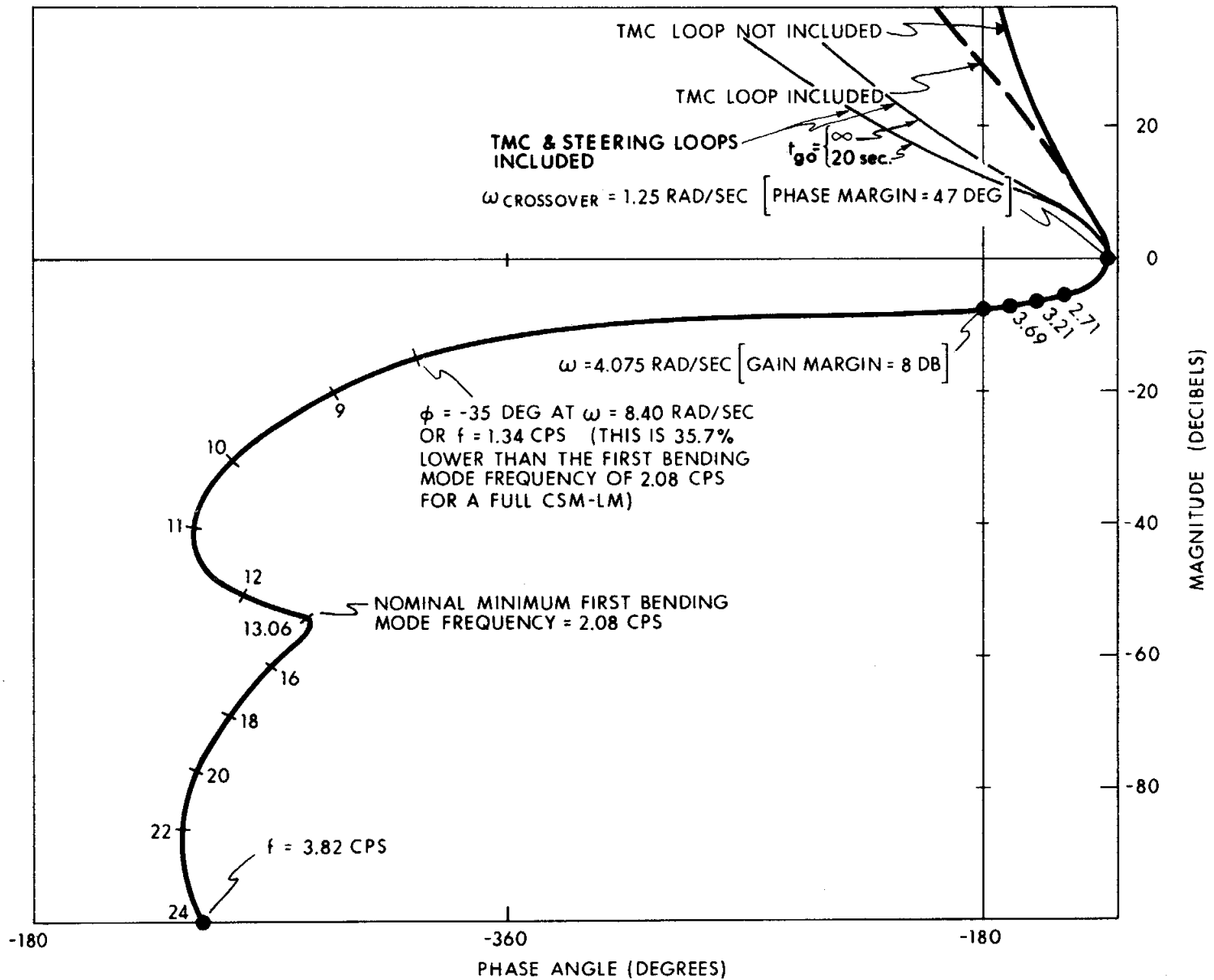


Fig. 3.3.3 CSM/LM, High-bandwidth Mode; Rigid-body Open-loop function, Magnitude versus Phase

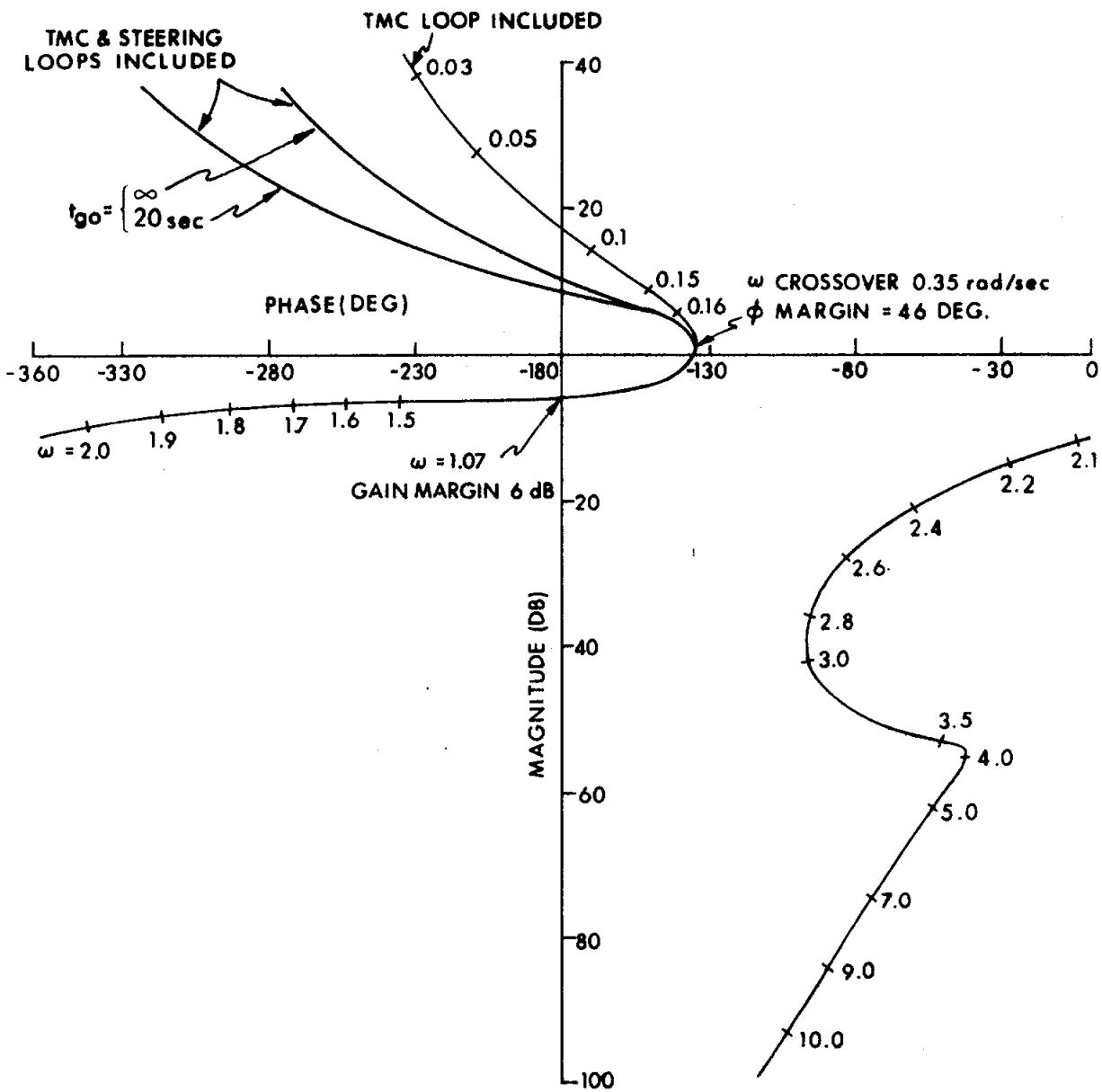


Fig. 3.3.4 CSM/LM, Low-bandwidth Mode; Rigid-body Open-loop function, Magnitude versus Phase

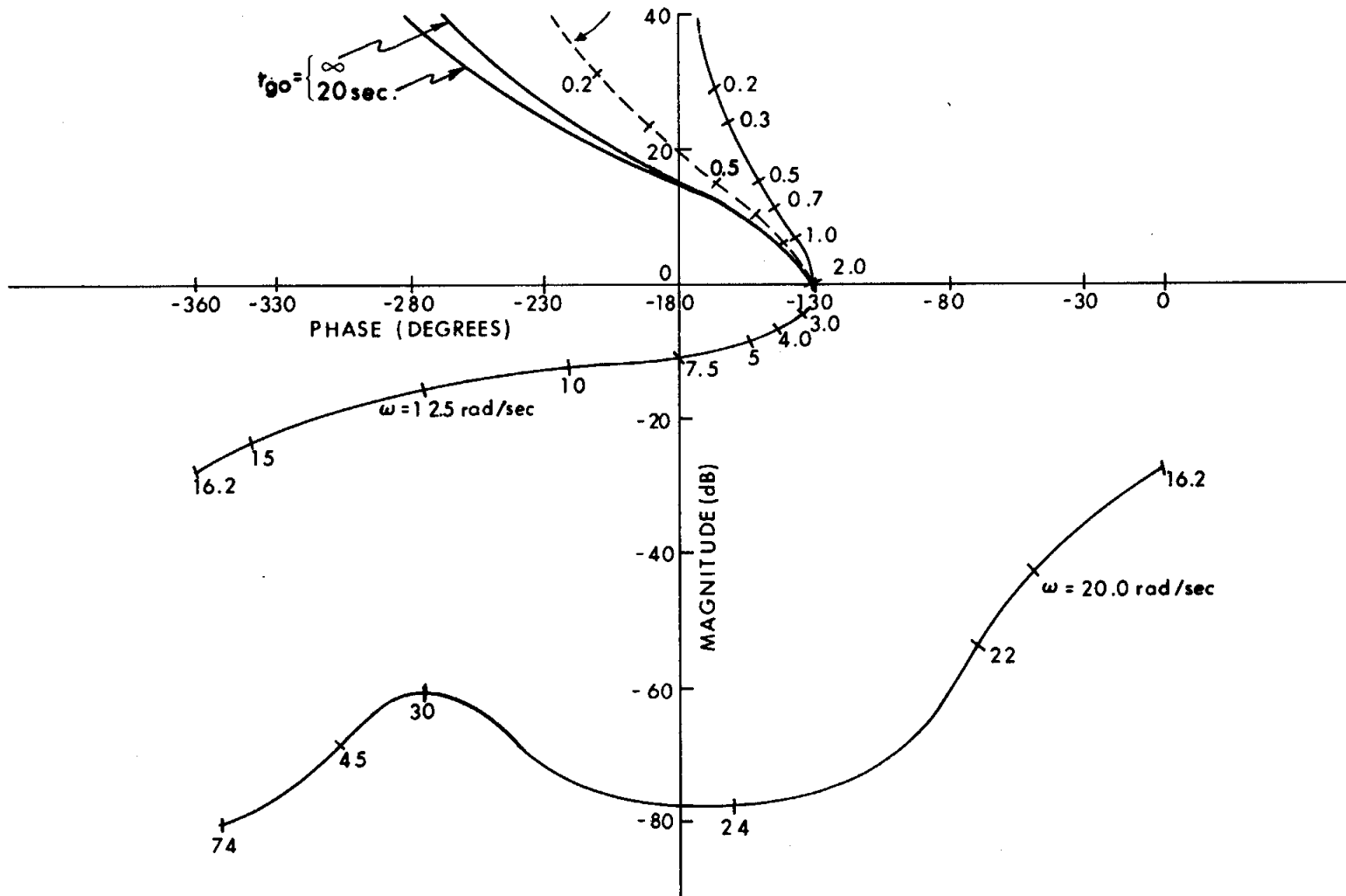


Fig. 3.3.5 CSM; Rigid-body Open-loop function, Magnitude versus Phase

For the nearly full CSM, the slosh masses in the sump tanks are ahead of the vehicle center of gravity. This produces a pole-zero pair having the pole at a lower frequency than the zero. This pole-zero configuration is destabilized by the phase-lead filter characteristic. The time constant of the divergent slosh oscillations, however, is an order of magnitude greater than the time required for the propellant to deplete behind the c.g., where the unstable condition will cease to exist.

According to the latest data available, the bending modes for the CSM vehicle occur above 5.3 cps, where the loop gain is well below 0 dB. Using the minimum expected value of 0.005 for the damping of bending resonances, the bending peaks should remain at least 20 dB below the 0-dB line; this ensures adequate gain stabilization of the bending modes.

3.3.3.4.1 Filter Implementation. -- Both the CSM configuration and the CSM/LM configuration use a generalized sixth-order filter which consists of three cascaded second-order sections. The CSM/LM mode uses all three sections; the CSM only two. Figure 3.3.6 illustrates the filter mechanization, showing the test for CSM or CSM/LM after the second cascade section. The difference equation for each of the cascade sections is given by

$$\text{OUT} = \text{N0(IN)} + [\text{N1(IN)}z^{-1} + \text{N2(IN)}z^{-2}] - [\text{D1(OUT)}z^{-1} + \text{D2(OUT)}z^{-2}]$$

where the transfer function is of the form

$$\frac{\text{OUT}}{\text{IN}} = \frac{\text{N0} + \text{N1}z^{-1} + \text{N2}z^{-2}}{1 + \text{D1}z^{-1} + \text{D2}z^{-2}}$$

The filter coefficients, which are loaded at the start of each burn in TVCINITIALIZE, are single precision numbers. The coefficients for the CSM and for the CSM/LM low-bandwidth mode are stored in fixed memory; the CSM/LM high-bandwidth coefficients are pad-load erasables. The filter gain coefficient  $K_z$ , i. e., (VARK), is a pad-load erasable for all three sets of coefficients. The filter storage variables are stored in double-precision, and computations are done by multiplying the SP coefficients by the appropriate DP storage values. The three sets of coefficients and gain factors are given in Table 3.3-V and Fig. 3.3.7.

The filter transfer functions in the z-domain are described in terms of the second-order factors required for cascade mechanization. The coefficients are unscaled except for the first-order terms (N11, D11, N21, D21, N31, D31), which are scaled at one-half their actual value (Fig. 3.3.6). The scaling for the filter inputs, storage, and outputs is 180 degrees per full register.

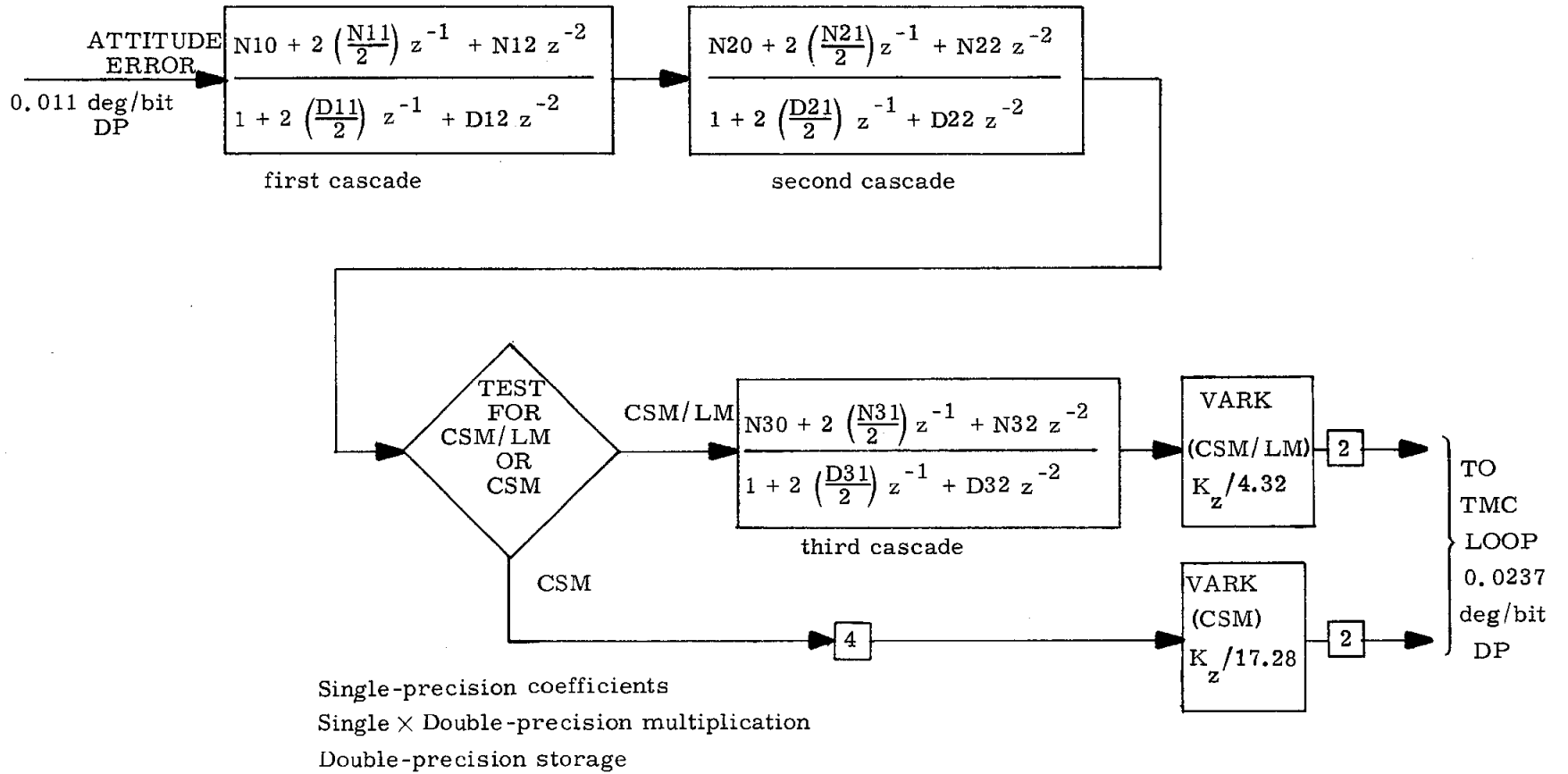


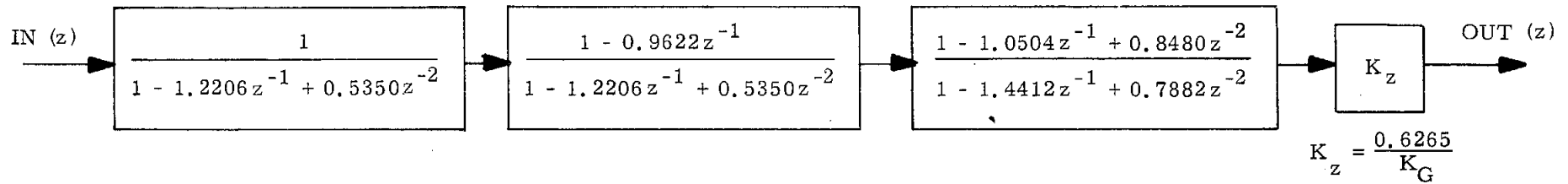
Fig. 3.3.6 Generalized Sixth-order Filter.

TABLE 3.3-V

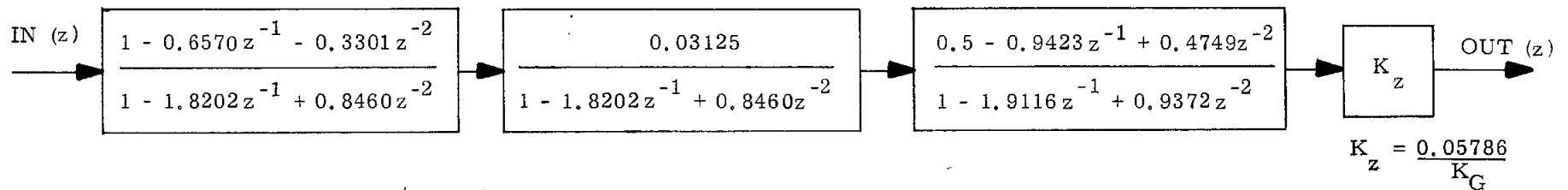
## TVC DAP FILTER COEFFICIENTS AND GAINS

	CSM	CSM/LM High-Bandwidth	CSM/LM Low-Bandwidth
N10	1.0	1.0 *	1.0
N11/2	-0.2549	0 *	-0.3285
N12	0.0588	0 *	-0.3301
D11/2	-0.7620	-0.6103 *	-0.9101
D12	0.7450	0.5350 *	0.8460
N20	1.0	1.0 *	0.03125
N21/2	-0.4852	-0.4811 *	0
N22	0	0 *	0
D21/2	-0.2692	-0.6103 *	-0.9101
D22	0	0.5350 *	0.8460
N30	—	1.0 *	0.5000
N31/2	—	-0.5252 *	-0.47115
N32	—	0.8480 *	0.4749
D31/2	—	-0.7206 *	-0.9558
D32	—	0.7882 *	0.9372
KTLX/I	8.40 *	0.6265 *	0.05786 *
REPFRAC	0.250 *	0.0375 *	0.0375
KPRIME	0.10 *	0.1500 *	0.0500
Sample Period	40 msec	80 msec	80 msec

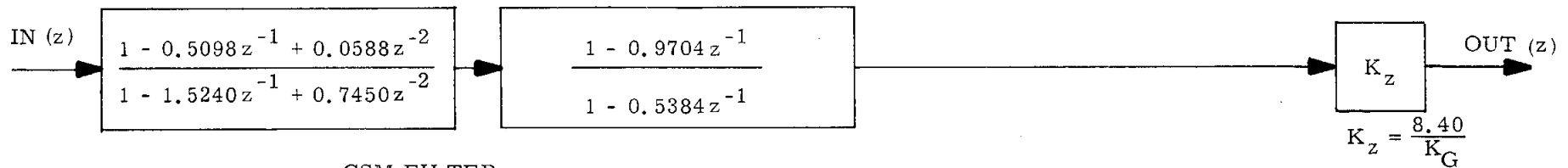
\*These are pad-load erasables, and are subject to change.



CSM/LM HIGH-BANDWIDTH FILTER (ERASABLE COEFFICIENTS)



CSM/LM LOW-BANDWIDTH FILTER



CSM FILTER

Fig. 3.3.7 Mathematical Block Diagram of the CSM/LM and CSM DAP Filter Configurations as Implemented in the CMC



Some care must be exercised in placing the second-order factors in the cascade sections. Generally it is best to group singularities having similar frequencies together in the same cascade section. If this is not possible (as in the CSM/LM low-bandwidth third cascade), an attempt should be made to keep the dc gains of the numerator and denominator from becoming too dissimilar. (The dc gain either of the numerator or the denominator is found simply by setting  $z = 1$  and adding the coefficient values.)

3.3.3.4.2 High-bandwidth to Low-bandwidth Switchover. -- In the CSM/LM mode, provision is made for a switchover from the normal high-bandwidth filter to a slower-acting low-bandwidth filter. This is effected only by the astronaut's keying in a V46E. Once entered, V46 tests for (1) TVC control of the T5 clock and (2) CSM/LM configuration. If both of these conditions are met, V46 transfers to TVCINITIALIZE to (a) zero the filter storage locations; (b) pick up the DELFILTER values and load these into the trim registers PDELOFF and YDELOFF; (c) load the low-bandwidth coefficients from fixed memory into the filter coefficient erasables; (d) load new values for the DAP gain, the TMC loop gain, and the steering gain; and (e) set the switchover flag (bit 15 of FLAGWRD9) to indicate that switch-over has occurred.

If Condition 1 is not met (TVC is not in control of T5 clock), V46 will either set up the RCS DAP or the SATURN Takeover Mode; if Condition 2 is not met (CSM-only configuration), a V46E merely illuminates the OPR ERR light.

No provision is made for switching back to the high-bandwidth mode once the V46 switchover has taken place. On the next burn, however, the high-bandwidth coefficients will be loaded from erasable memory.

#### 3.3.4 TVC DAP Variable Gains

The TVC DAP filter design -- in particular the selection of the filter gains -- is based upon the vehicle dynamics and gains at some selected, "design-nominal" flight condition. The design is such that the changes in vehicle dynamics associated with other flight conditions do not affect the stability of the control loop. Changes in vehicle gain  $Tl_x/I$  do, however, affect control-loop stability and, therefore, must be compensated by inversely proportionate changes in the DAP filter gain. The goal is to maintain a constant, overall open-loop gain and, hence, a constant bandwidth.

The open-loop gain is proportional to the product of the DAP filter gain ( $K_z$ ) and the vehicle gain ( $Tl_x/I$ ), as expressed by the following equations:

$$\begin{aligned}
 K_z(Tl_x/I) &\cong K_z(Tl_x/I_{AVG}) && (3.3-1) \\
 &= \text{Constant} \triangleq (KTLX/I) \text{ (design nominal),}
 \end{aligned}$$

where

$$I_{AVG} = (I_y + I_z)/2$$

Equation (3.3-1) relates the optimum gain to the significant mass properties of the vehicle, and may be used both to establish the initial gain and to vary the gain during a burn as  $T\ell_x$  and  $I_{AVG}$  vary.

The actual gain relationship for the TVC DAP is given by

$$VARK = KTLX/I (I_{AVG}/T\ell_x),$$

where the pad-loaded registers ECTLX/I, ECTLX/I+1, and ECTLX/I+2 contain the constants that are the product of the DAP gains ( $K_z$ ) and vehicle gains ( $T\ell_x/I$ ) for the CSM, CSM/LM high-bandwidth, and CSM/LM low-bandwidth modes, respectively.

Variable gains for the ROLL DAP are implemented similarly. The desired roll gain (1/CONACC) is a function of roll moment of inertia:

$$(1/CONACC) = \frac{2\pi}{M} (I_{xx}), \quad (3.3-2)$$

where  $M$  is the roll jet torque of 1400 ft-lb.

The gains for the roll autopilot and TVC DAP filters are established initially and updated using a small AGC program called TVCMASSPROP. This program, which is called every 10 seconds by TVCEXECUTIVE, computes piecewise-linear approximations to the curves of  $I_{xx}$ ,  $I_{AVG}$ , and  $I_{AVG}/T\ell_x$  versus CSM propellant weight (CW). These curves are given in parametric form, with LM mass as the parameter. (See sketch in Fig. 3.3.8.) Using A for ascent stage, D for descent stage, F for full, E for empty, and X for off; the vehicle weights used in constructing the fixed curves are as follows: CSM dry weight = 23,956 lb LM (AF, DF) = 32,000 lb; LM (AF, DE) = 14,116 lb; LM (AF, DX) = 9,965 lb; LM (AE, DX) = 4,938 lb; (See Ref. 3.7.)

The functioning of TVCMASSPROP is as follows:

- a. It checks to see whether LM is attached (by checking bit 13 of the word DAPDATR1).
- b. If LM is on, TVCMASSPROP uses the pad-loaded variable LEMMASS to calculate the desired piecewise-linear curve from the family of curves of parameter versus CW for each of the three output variables. This means that, for each variable, a breakpoint parameter value is computed, as well as the slopes to the left and right of the breakpoint. Note that for the three output variables eight quantities are computed

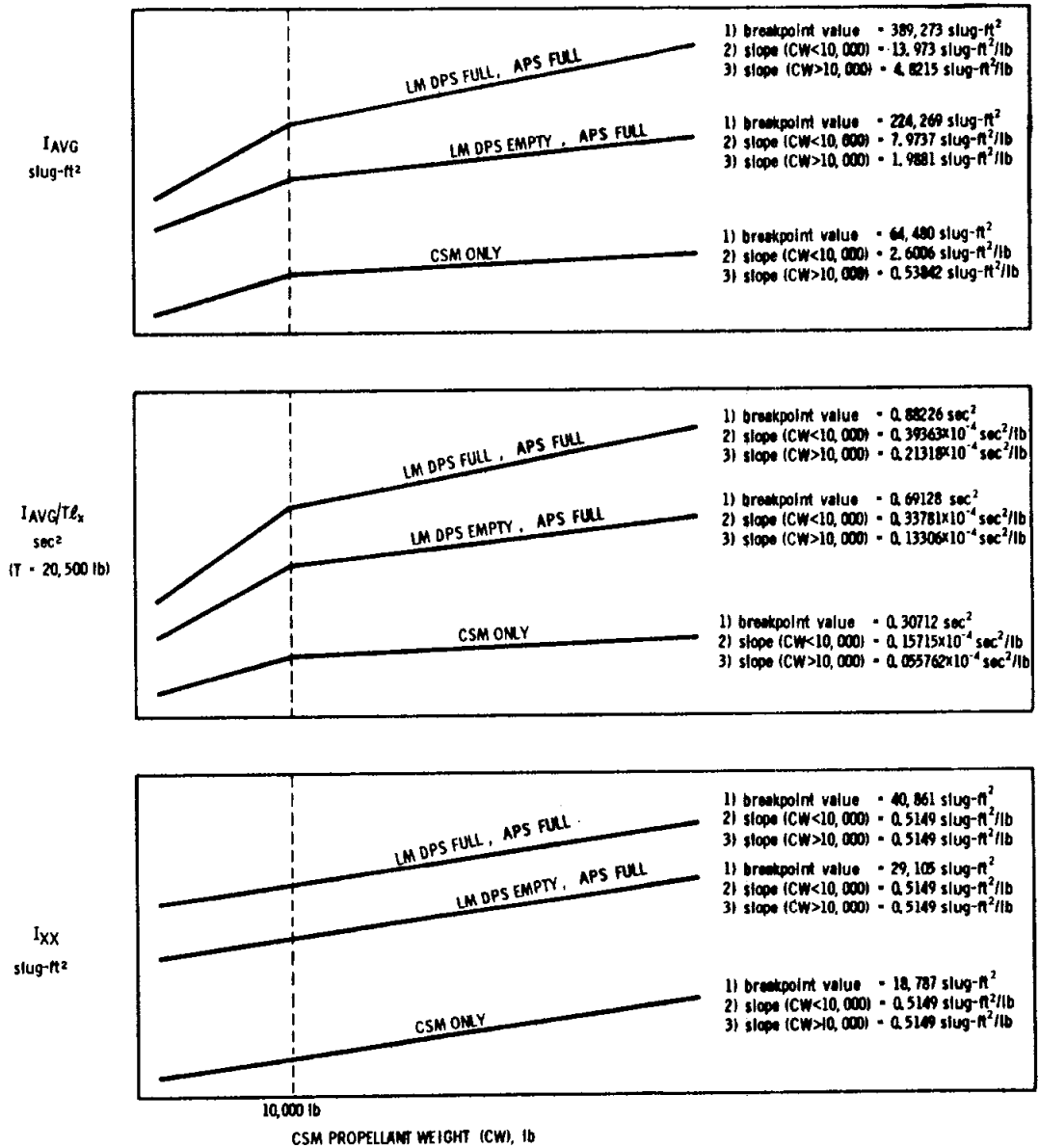


Fig. 3.3.8 Sketch of Curves Used by Program TVCMASSPROP To Calculate  $I_{xx}$ ,  $I_{AVG}$ , and  $I_{AVG}/T_{Lx}$

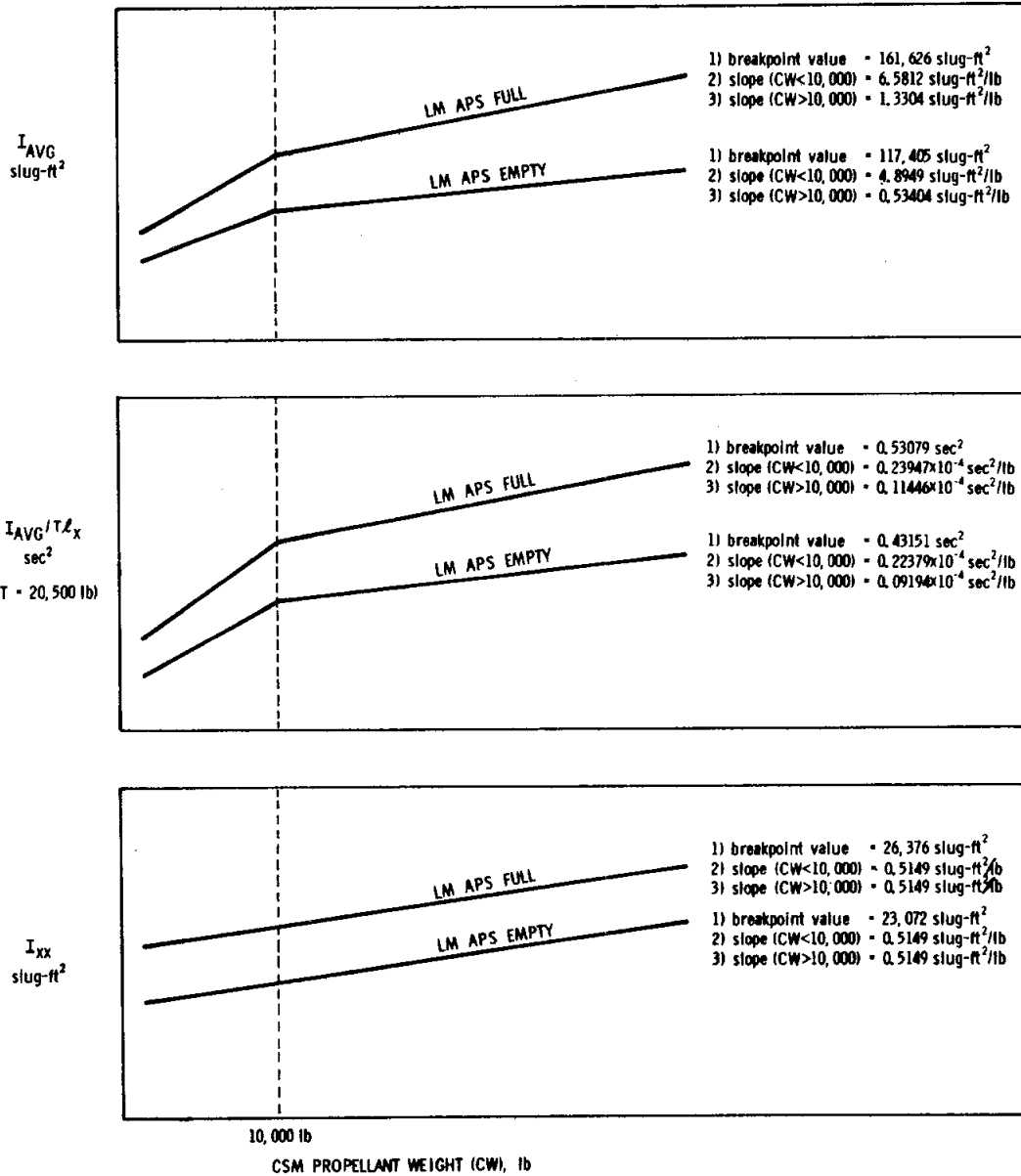


Fig. 3.3.9 Mass Properties Approximations:  
CSM Docked with LM Ascent Stage Only.

using LEMMASS. These are (1) a breakpoint value and two slope values for  $I_{AVG}$  versus CW, (2) a breakpoint value and two slope values for  $I_{AVG}/Tl_x$  versus CW, and (3) a breakpoint value and a single slope value for  $I_{xx}$  versus CW. (See Fig. 3.3.8.)

If LM is not on, the eight quantities are still calculated, but they then define the curves for CSM alone.

- c. Once a specific curve has been chosen for each output variable, the pad-loaded variable CSMASS is used to determine the actual operating point on each of the curves. This defines the current value of the three output variables.
- d. Before returning control to TVCEXECUTIVE or R03, TVCMASSPROP also updates the total vehicle mass, called WEIGHT/G. This is done by simply summing the variables LEMMASS and CSMASS. (The value of CSMASS is updated in TVCEXECUTIVE immediately after TVCMASSPROP is finished. This is done by subtracting a pad-load constant equal to the assumed engine-on mass flow over a 10-second period.) Because of the way WEIGHT/G is updated, it is correct only at the end of the 10-second interval, and will be somewhat lower than the actual value during the interval. At the end of a burn (or in case of engine fail) CSMASS is corrected for the unused portion of propellant in that particular 10-second interval.

Provision is made for the special case of the CSM docked with the LM ascent-stage only (no descent stage). For TVCMASSPROP to function correctly in this mode, the astronaut must change the CONFIG bits of the erasable word DAPDATR1 (bits 15, 14, 13) to 1, 1, 0, and must load in a new value of LEMMASS (ascent-stage weight). The three outputs of TVCMASSPROP are then calculated as in the nominal case, except that corrections are made to the curves of  $I_{AVG}$  and  $I_{AVG}/Tl_x$ . The curves for  $I_{xx}$  will be computed correctly using only LEMMASS; no additional correction is needed.

The curves of the three outputs versus CW for this special case are shown in Fig. 3.3.9.

TVCMASSPROP will give output values that match the NASA data package (see Ref. 3.7), with worst-case errors of less than 12 percent.

This includes any range of propellant loadings for the LM ascent stage, descent stage, or the special case of no descent stage, discussed above.

Once the three outputs of TVCMASSPROP are obtained, they are used by TVCEXECUTIVE, as in Eqs (3.3-1) and (3.3-2).

If a restart occurs during TVCMASSPROP computations, there is nothing that needs protecting; the program will simply be called again as soon as TVCEXECUTIVE is restarted.

The astronaut is not required to enter any data in connection with the autopilot variable gains. In R03, however, he is asked to monitor the DSKY for a display (V06 N47) of CSM and LM weight in pounds. If he is not satisfied with these values, he can enter new values, thereby both altering TVCMASSPROP and the autopilot gains.

The 10-second intervals for the call to TVCMASSPROP are determined by a simple counter within TVCEXECUTIVE. The loop-gain change at CSM/LM switchover corresponds to a reduction of the design-nominal gain  $KT\ell_x/I$  (Eq 3.3-1) for the pitch and yaw gains. This is done automatically as part of the switchover logic in V46 and TVCINITIALIZE.

### 3.3.5 Trim Estimation

Accurate engine-actuator trim (steady-state pitch- and yaw-actuator offset) is necessary for good performance of the TVC DAP. Ideally, the trim values are such that when the pitch and yaw commands from the autopilots are both zero, the actuators position the engine bell such that the thrust vector is aligned with the vehicle center of gravity as to result in zero control accelerations. The ideal trim values depend on the location of the c.g., which tends to shift slowly during the burn. Thus, the problem of trim estimation involves initial estimates of the trim values and updating of the estimates as the c.g. is observed to move with shifts in fuel loading.

Three sources of trim information are provided to the TVC DAPs: (1) astronaut loads of PTRIM and YTRIM in Routine R03 (Verb 48); (2) a single-shot correction shortly after ignition (CSM only), followed by repetitive corrections (see paragraph 3.3.5.2); and (3) an end-of-burn update at the engine-off command (see paragraph 3.3.2.4). Each of these sources provides (potential) updates of the trim variables PACTOFF and YACTOFF (equivalent to the upper registers of the double-precision words PDELOFF and YDELOFF), which are the AGC registers containing the trim information.

### 3.3.5.1 Astronaut Loads via R03

The final sequence of R03 (Noun 48) displays the current trim estimates in registers 1 and 2, referred to as PTRIM and YTRIM. These are merely conversions (to degrees) of the DAP registers PACTOFF and YACTOFF. These registers are used by the thrusting program (P40) -- to adjust the vehicle burn attitude for the R60 maneuvers (accounting for c. g. position) and to do the gimbal-drive test/trim routine, positioning the engine for ignition. The astronaut can accept the displayed values, or he can load new values from vehicle-mass tables. Thus, the astronaut has ultimate control over any internally generated values before the burn.

The gimbal-trim values are the angular offsets of the engine-gimbal servos (pitch and yaw) necessary to align the thrust vector through the vehicle c. g. This alignment may be achieved by supplying trim commands to each gimbal servo, where the commands are expressed as follows:

$$\delta_{\text{OFFSET}} = \delta_{\text{cg}} + \delta_{\text{E}} - \delta_{\text{MECH}}$$

The values of the  $\delta$  terms differ in the pitch and yaw planes: the variable  $\delta_{\text{cg}}$  is the angular offset of the c. g. relative to the vehicle center line, as measured in the given pitch or yaw plane; the variable  $\delta_{\text{MECH}}$  is the mechanical offset of the engine gimbals; and  $\delta_{\text{E}}$  is the error in the orientation of the actual thrust vector relative to the commanded orientation of the engine bell. Several sources contribute to  $\delta_{\text{E}}$ , including misalignment of the thrust vector, relative to the engine-bell center line, and nonlinearities and biases in the engine-gimbal servo system. Only the intentional mechanical bias ( $\delta_{\text{MECH}}$ ) is known precisely. Tabulated estimates of  $\delta_{\text{cg}}$  versus vehicle mass are available, but no initial estimates of  $\delta_{\text{E}}$ . The autopilot tracks the actual  $\delta_{\text{OFFSET}}$  with an offset-correction loop whose measurement of  $\delta_{\text{OFFSET}}$  increases in accuracy as the burn progresses.

The recommended procedure is to assume  $\delta_{\text{E}} = 0$  and to trim the engine initially according to tabulated estimates of  $\delta_{\text{cg}}$  and the given  $\delta_{\text{MECH}}$ . Then, after one or more engine burns, a more accurate engine trim can be obtained by using the stored estimate of  $\delta_{\text{OFFSET}}$  provided by the offset correction loop at the end of the previous burn: the longer the previous burn, the more accurate the correction-loop estimate of  $\delta_{\text{OFFSET}}$ .

The procedure for aligning the vehicle assumes that the position of the engine thrust vector relative to the vehicle center line is given by  $\delta_{\text{OFFSET}} + \delta_{\text{MECH}}$  (as obtained for the pitch and yaw axes). This assumption neglects the fact that a commanded gimbal trim equal to  $\delta_{\text{OFFSET}}$  results in a thrust-vector error ( $\delta_{\text{E}}$ ). The alternative to this approach would be to assume that the thrust vector is aligned with the vehicle c. g. according to the tabulated  $\delta_{\text{cg}}$  estimates. It turns out, however, that the values of  $\delta_{\text{E}}$  are comparable to the errors in  $\delta_{\text{cg}}$ , with the result that the two vehicle alignment approaches produce nearly the same system errors. Therefore, for simplicity in programming,  $\delta_{\text{OFFSET}}$  is used as a basis for aligning both the vehicle and the engine. In this connection, we should point out that, with the present autopilot, the transients resulting from an error in engine alignment can produce as much as five times the velocity pointing error as the same angular error in vehicle alignment.

In checking the R03 display, the astronaut has the responsibility to ensure that the trim values are reasonable - - in particular, that they do not exceed the limit  $\pm 9$  deg imposed by the capacity of the optics error counters used to generate the signals for the engine actuators. No AGC coding checks against this limit are made in either the prethrust program or the engine-gimbal test/trim routine. Should this limit be exceeded, the DAPs lose track of the engine command by the excess amount.

### 3.3.5.2 Single-shot and Repetitive Corrections

To reduce the attitude and velocity errors, it is necessary to add an estimation and correction scheme for compensating the thrust misalignment. A functional block diagram of the corrector is shown in Fig. 3.3.10. Basically, the effect of the corrector is - -

- a) to estimate the mistrim and make a one-shot correction a few seconds after ignition (CSM only -- see Table 3.3-VI); then
- b) to become an effective proportional-plus-integral compensation for canceling initial estimation errors and for tracking any c. g. motion or thrust-vector variation.

The input to the correction loop is the filtered actuator command signal coming from DELFILTER, as shown in Fig. 3.3.10. The filter time constant is either 4 or 8 seconds, depending on the DAP sample rate. This is enough lag



3.3-32

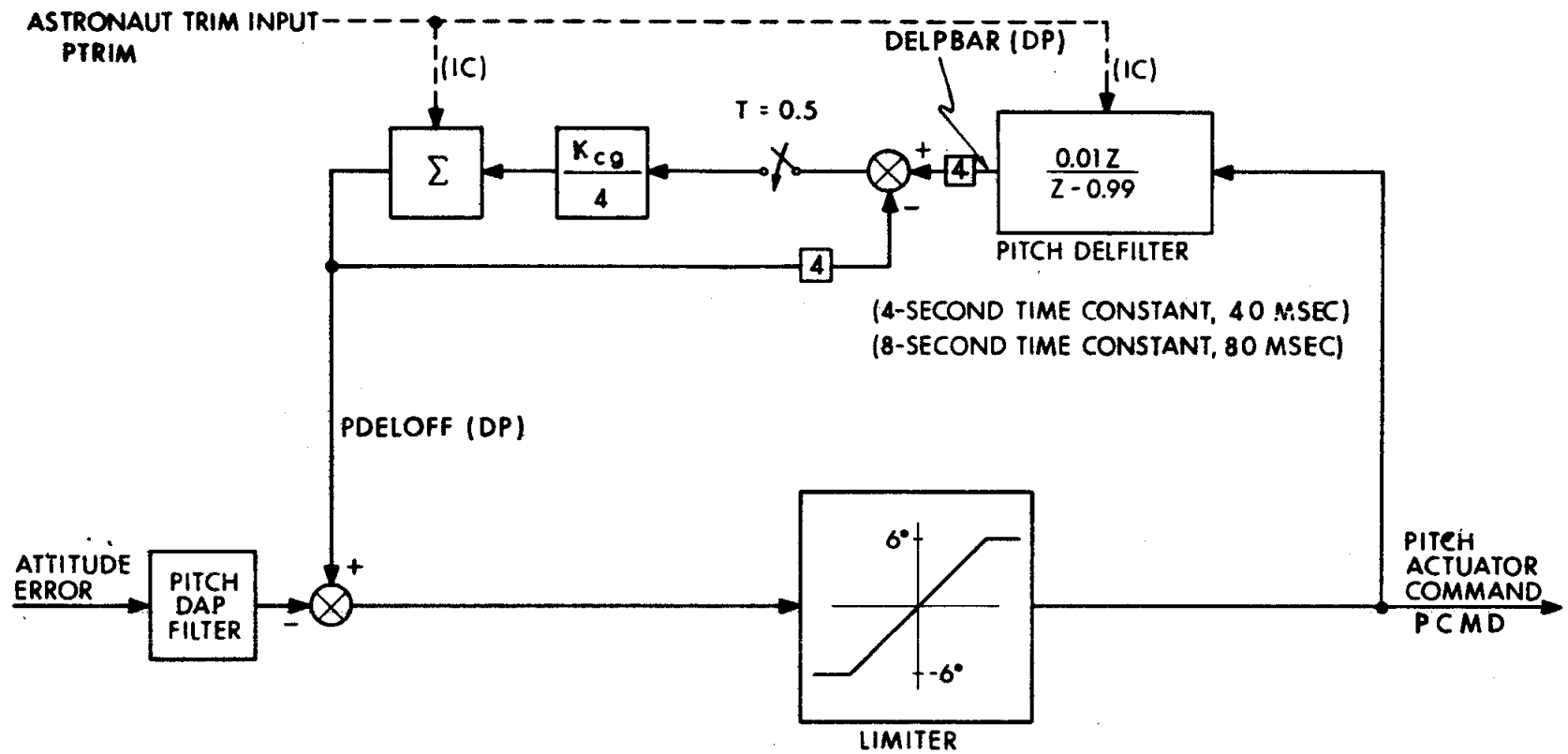


Fig. 3.3.10 Block Diagram of Pitch-axis Thrust Misalignment Correction (TMC) Loop

to provide significant smoothing of the effects of slosh oscillations and initial attitude rates.

The synchronized samplers in the correction loop do not close for their first sample until a specified time (TCORR) after DAP startup. For this first sample, the gain  $K_{cg}$  of the correction loop has a unique value (CORFRAC). After the first sample, which produces the one-shot correction, the samplers continue to work, with a sample period of 0.5 second, and the gain  $K_{cg}$  is dropped to a new constant value (REPFRAC). This lower steady-state value of  $K_{cg}$  is the result of a compromise between stability and improved tracking. REPFRAC is a pad-loaded quantity for CSM (EREPRAC) and CSM/LM high-bandwidth (EREPRAC + 1). The REPFRAC value for the low-bandwidth CSM/LM mode is fixed.

Table 3.3-VI summarizes the operation of the TMC loop (in terms of parameter values) both for the CSM and the CSM/LM configurations. The dynamic effect of the TMC loop can be seen by looking at the equivalent s-plane dynamics as shown in Fig. 3.3.11. Table 3.3-VII gives the pole-zero values for the CSM and CSM/LM configurations. The effects of these additional dynamics on the system gain-phase plots are shown as dotted lines on Figs 3.3.3 and 3.3.5.

### 3.3.6 TVC ROLL DAP

Roll control during SPS thrusting periods is achieved by firing RCS roll-jet pairs. Phase-plane switching logic is used to select the jets and to control the duration of jet firings. The control policy calls for maintenance of outer gimbal angle (OGA) within a  $\pm 5$ -deg deadband tolerance of a desired OGA (OGAD), which is simply the value of OGA at SPS ignition. ROLL DAP performance is monitored via the FDAI roll-attitude error needle, which is driven by the FLY-TO OGA error:

$$AK = OGAD - OGA. \quad (3.3-3)$$

Needle updates are made at the ROLL DAP sample rate of 1/2 second.

OGA control closely approximates direct body-axis roll-attitude control, provided that the middle gimbal angle (MGA) is small. The body-axis roll-rate equation shows that cross-coupling of inner-gimbal-angle (IGA) rate is a second-order effect for small middle gimbal angles (MGA):

TABLE 3.3-VI

PARAMETERS OF THRUST-MISALIGNMENT ESTIMATOR  
LOOP FOR THE CSM AND CSM/LM CONFIGURATIONS

DESCRIPTION	AGC CODE VARIABLES	CSM	CSM/LM HIGH-BW	CSM/LM LOW-BW
time of initial correction*	TCORR (fixed)	3 sec	0 sec	---
gain $K_{cg}$ at initial correction	CORFRAC (fixed)	$\frac{2}{2(\text{CORFRAC})}$	$\frac{1}{(\text{CORFRAC})}$	---
sample period of estimation loop	---	0.5 sec	0.5 sec	0.5 sec
gain $K_{cg}$ after initial correction	REPFAC	$\frac{0.250}{\text{EREPFRAC}}$ (pad-load)	$\frac{0.0375}{\text{EREPFRAC}+1}$ (pad-load)	0.0375 (fixed)

\*Time from first pass of TVCEXECUTIVE, which occurs approximately 0.93 sec after IGNITION. Note that the CSM/LM one-shot correction occurs approximately 0.4 sec after the first PITCHDAP pass. At this early time the DELFILTER response remains essentially unchanged from its initial value, thus the one-shot correction value is effectively zero.

 Revised AddedGSOP # R-577PCR # 1020Rev. 10Date 2/70

TABLE 3.3-VII

EQUIVALENT s-DOMAIN TRANSFER FUNCTION FOR  
THRUST-MISALIGNMENT ESTIMATOR LOOP

VEHICLE CONFIGURATION	TRANSFER FUNCTION
CSM            40 msec ( $K_{cg} = 0.250$ )	$\frac{(s + 0.25)(s + 0.50)}{s(s + 0.750)}$
CSM/LM       80 msec High-bandwidth ( $K_{cg} = 0.0375$ )	$\frac{(s + 0.125)(s + 0.075)}{s(s + 0.20)}$
CSM/LM       80 msec Low-bandwidth ( $K_{cg} = 0.0375$ )	$\frac{(s + 0.125)(s + 0.075)}{s(s + 0.20)}$

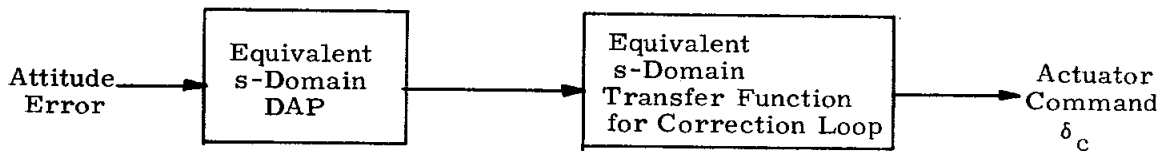


Fig. 3.3.11 Equivalent s-Domain Transfer Function of Thrust-misalignment Estimator Loop

$$p = \overline{OGA} + \dot{IGA} \sin(MGA). \quad (3.3-4)$$

The roll autopilot is shown in Fig. 3.3.12. The phase-plane switching logic is shown in Fig. 3.3.13. It is an adaptation of the LM phase-plane switching logic discussed in Ref. 3.8. Phase-plane OGA error and OGA rate are required inputs to the switching logic. Phase-plane OGA error is the negative of FLY-TO FDAI needle error, and OGA rate is derived by a simple first-order back difference of OGA:

$$\begin{aligned} \text{OGAERROR} &= \text{OGA} - \text{OGAD} = -AK, \\ \text{OGARATE} &= \frac{\text{OGA} - z^{-1}\text{OGA}}{T}, \end{aligned} \quad (3.3-5)$$

where  $z^{-1}$  is short-hand notation for "the past value of," and  $T$  is the ROLL DAP sample period of 1/2 second.

The phase plane is divided by the switching logic into three regions: jet firings for negative torque, jet firings for positive torque, and coast (no jet firings). OGAERROR and OGARATE establish the operating point within one of these regions, thus defining a particular control activity (+, -, or zero torque). The jet firing time to reach the coasting region from the operating point is a function of the control acceleration (CONACC) and the required change in velocity (DOGARATE - OGARATE), where DOGARATE (desired OGARATE) is the OGA rate at the coast-region penetration point of the control parabola through the operating point. The switching logic determines DOGARATE, and a running estimate of CONACC is available, as explained below. Firing time is given by the following:

$$\Delta T = \left| \frac{\text{DOGARATE} - \text{OGARATE}}{\text{CONACC}} \right| \quad (3.3-6)$$

Several operational constraints are applied to the  $\Delta T$  firing time in order to increase reliability, to conserve fuel, and to minimize control activity:

- a. The duration of a particular jet firing shall not exceed 2.5 seconds. (Long maneuvers consist of repeated 2.5-second bursts of control activity.)

3.3-37

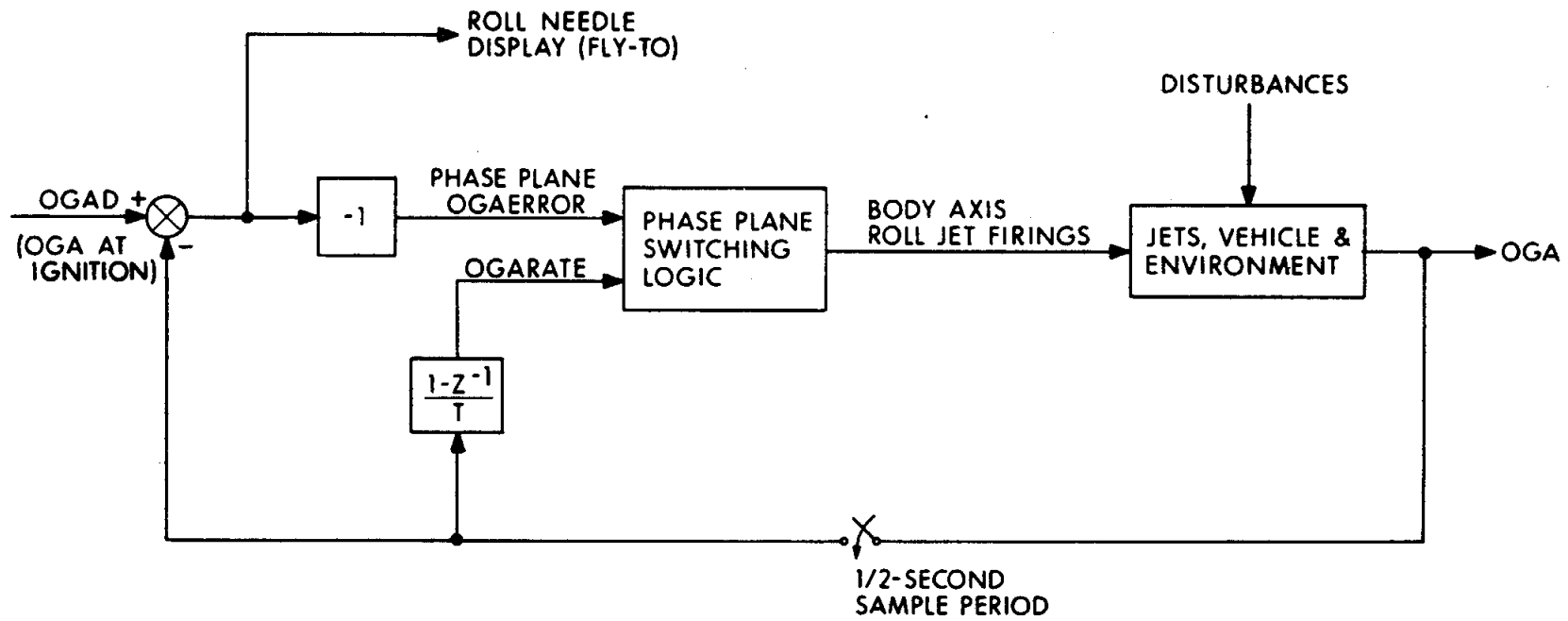


Fig. 3.3.12 TVC ROLL Digital Autopilot

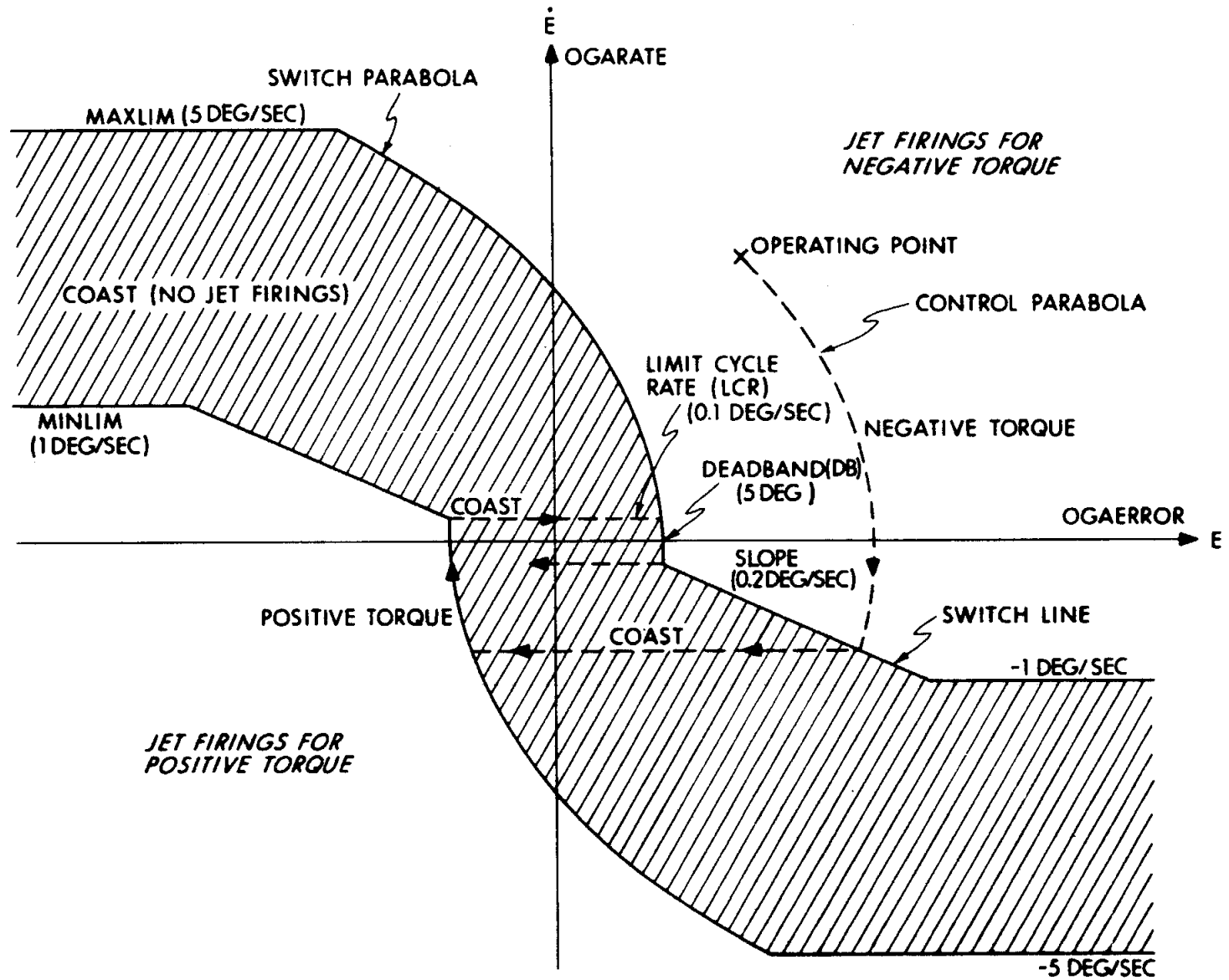


Fig. 3.3.13 Phase-plane Switching Lines for the TVC ROLL DAP

- b. A delay of at least 0,5 second shall separate jet firings. (Periods of zero torque enhance rate estimates and prevent excessive control activity.)
- c. Successive periods of the same sign of control torque shall fire jet pairs (for each torque sign there are two pairs) alternately. (Effect of jet failures, even combined jet failures, is minimized.)
- d. Subsequent re-evaluation of a jet-firing duration may decrease, but not increase, the total firing time (conserves fuel, especially with jet failures, and prevents excessive control activity).
- e. Jet firings shall not be shorter than 14 ms (minimum impulse).

The parabolic portions of the switching lines (Fig. 3.3.13) are ideal: they are constant-torque trajectories (control parabolas), at least within the ability of the CMC to track  $I_{xx}$ . Limit-cycle operation can thereby be achieved in truly optimal fashion, with but one or, at most, two jet firings if there are no sampling delays. (See also the firing duration constraints above.) Generation of the ideal switching parabola requires a knowledge of control acceleration:

$$\frac{Fd}{I_{xx}} = \frac{M}{I_{xx}} \triangleq \text{CONACC} \equiv (1/\text{CONACC})^{-1} \text{ rad/sec}^2, \quad (3.3-7)$$

where  $\underline{M}$  is the RCS roll-jet-pair torque ( $\approx 1400$  ft-lb). The ROLL DAP gain  $(1/\text{CONACC})$  tracks the roll inertia with 10-second up-dates (see paragraph 3.3.4) and thus permits construction of the ideal parabolas.

The switching trajectories (Fig. 3.3.13) are composed of parabolic, linear, constant-OGARATE, and constant-OGAERROR segments, as shown in Fig. 3.3.14. Analytic expressions for each segment are given. Also shown are the 12 subset regions that make up the 3 control regions of Fig. 3.3.13. The region of "jet firings for negative torque," for example, is composed of Subset-regions I, III, and VI'. The region of "jet firings for positive torque" is composed of Subset-regions I', III', and VI. The remaining subset regions (II, II', IV, IV', V, and V') constitute the coasting region.

Identifying the operating point with a particular control region is accomplished by the process of elimination illustrated in Fig. 3.3.15. Tests for subset regions are used as building blocks. Each subset region is bounded



3.3-40

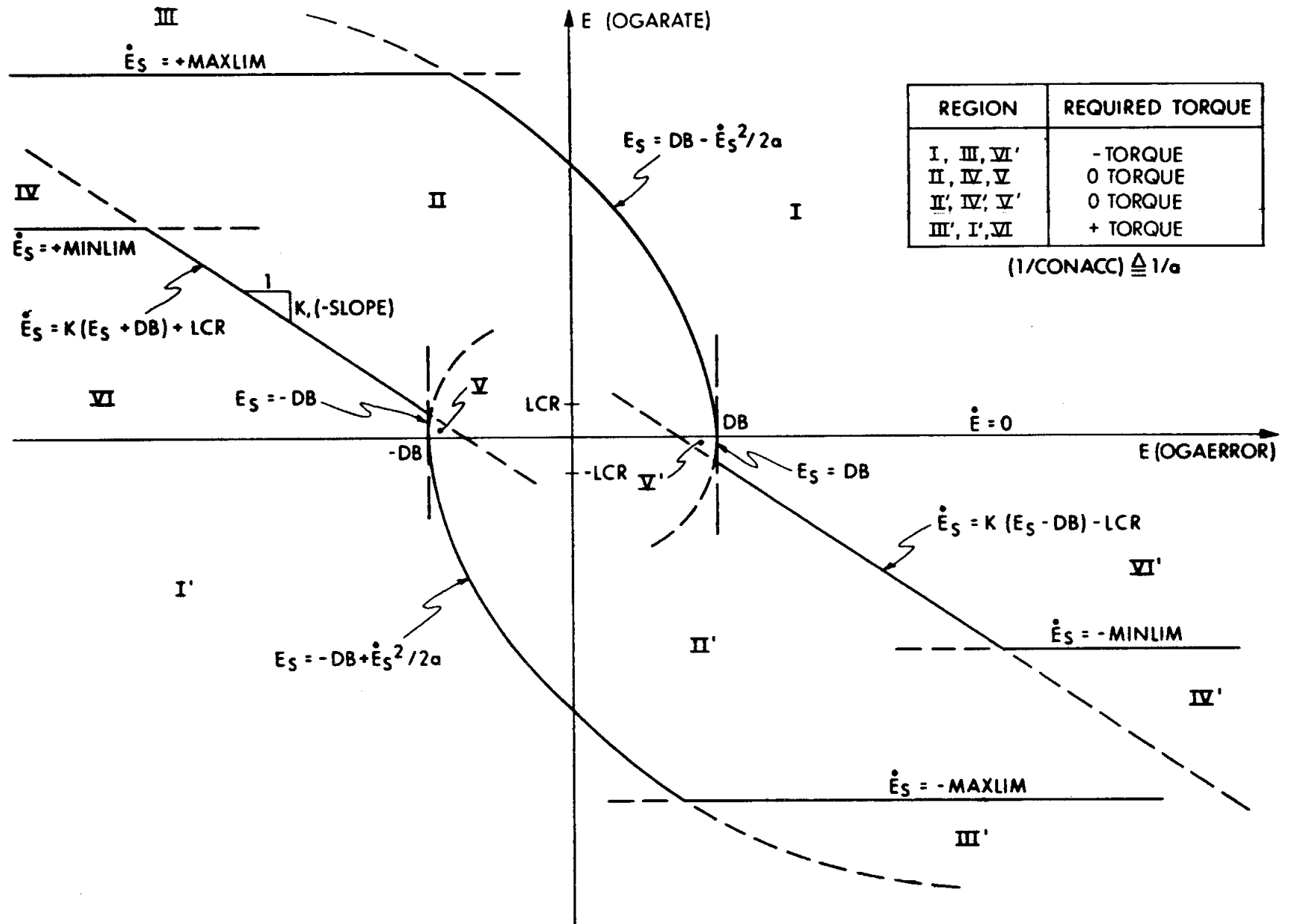


Fig. 3.3.14 Analytic Switching Lines and Control Regions in the TVC ROLL DAP Phase Plane

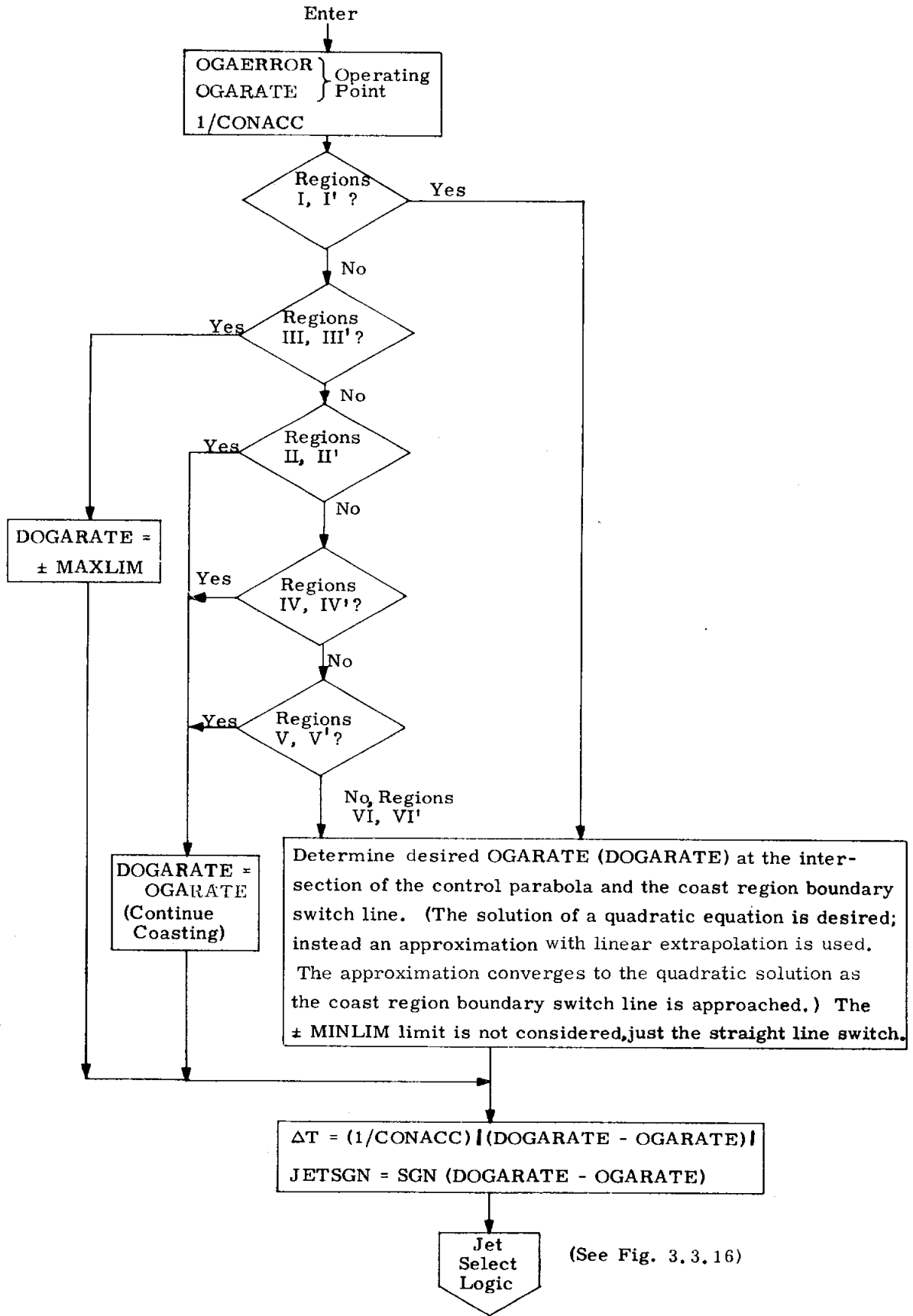


Fig. 3.3.15 TVC ROLL DAP Phase-Plane Switching Logic

by combinations of the switching-line segments and the abscissa axis and is thus describable in terms of simple analytic inequalities, which are then used to make the indicated tests.

This subset logic is used to determine desired OGA rate (DOGARATE). For operating points in the coasting region, DOGARATE is simply the current OGARATE (continue coasting). For operating points in Subset-regions III and III', DOGARATE is the OGARATE at the point that the parabolic trajectory penetrates the coast region. Thus, for Subset-regions III and III', DOGARATE is simply  $\pm$ MAXLIM, the appropriate rate-limit maximum.

For Subset-regions I and VI' (or I' and VI), DOGARATE is determined by the intersection of the control parabola with the straight-line switching line. This requires solution of a quadratic equation, for which is introduced an approximation that simplifies the quadratic equation to a linear one and has the desirable property of converging to the quadratic solution as the switching line is approached. The approximation involves substituting a straight line (i. e., the tangent to the control parabola) for the actual control parabola for operating points in Regions VI and VI'. The problem is then to solve for the intersection of the tangent and the constant-slope switch line. (For operating points in Region I or I', a dummy operating point is constructed in Region VI or VI', and the tangent taken at that point. The dummy point is located just off the control parabola at a fixed distance (0.1 deg/sec) from the x-axis.)

The equation used to solve for the intersection of the two lines (and hence solve for DOGARATE) is

$$\text{DOGARATE} = \text{NUM}/\text{DEN},$$

where

$$\begin{aligned} \text{NUM} &= \text{KY}^2(1/\text{CONACC}) - \text{K}[\text{DB} - \text{X SGN}(\Delta)] + \text{LMCRATE} \\ \text{DEN} &= \text{KY}(1/\text{CONACC}) - \text{SGN}(\Delta), \end{aligned}$$

and

$$\text{X, Y} = \text{OGAERROR}, \text{OGARATE}$$

$$\text{DB} = \text{Deadband} = 5 \text{ deg}$$

$$\text{LMCRATE} = \text{Limit cycle rate} = 0.1 \text{ deg/sec}$$

$$\text{K} = (-\text{slope}) = 0.2 \text{ deg/sec/deg}$$

$$\begin{aligned} \Delta &= \text{horizontal distance between operating point and control parabola} \\ &= \text{X} - [\text{DB} - \text{Y}^2(1/\text{CONACC})/2] \text{SGN}(\text{Y}). \end{aligned}$$

(This approximation is further described in Reference 3.9.)

Once DOGARATE is obtained, the jet-firing duration is determined by the relation:

$$\Delta T = (1/\text{CONACC}) |\text{DOGARATE} - \text{OGARATE}|, \quad (3.3-8)$$

where  $1/\text{CONACC}$ , the ROLL DAP gain, is the estimate of the control acceleration. (See Eq. 3.3-7.)

Figure 3.3.16 shows the jet-select logic that applies the jet firing-duration constraints, sets up the task to terminate the jet firings at the proper time, and actually fires the jets.

Restart protection for the ROLL DAP consists simply of starting it over; there are no copycycles, phase-points, etc. The original desired OGA is maintained. Table 3.3-VIII lists numerical values for the significant ROLL DAP parameters.

### 3.3.7 TVC DAP Interfaces

#### 3.3.7.1 Input Interface

Cross-product steering (see paragraph 5.3.3.4, Section 5 of this document) produces a vector-rate command (deg/sec) in reference coordinates by the following relationship:

$$\underline{\omega}_{c\text{REF}}^T = K'T(1 \underline{VG} \times 1 \underline{MDT}),$$

where  $\underline{MDT} = - \underline{DELVREF} + c_b \Delta t$ .

$K'$  is the steer-law gain, and  $\underline{VG}$  is the velocity-to-be-gained vector. The vector is transformed to body (NAVBASE) coordinates via the transformations REFSMMAT and SMNB:

$$\underline{\omega}_{c\text{BODY}}^T = (\text{SMNB}) (\text{REFSMMAT}) \underline{\omega}_{c\text{REF}}^T.$$

Figure 3.3.17 is a functional block diagram of the TVC DAP input interface. The rate-feedback signals to the autopilot are formed by first taking

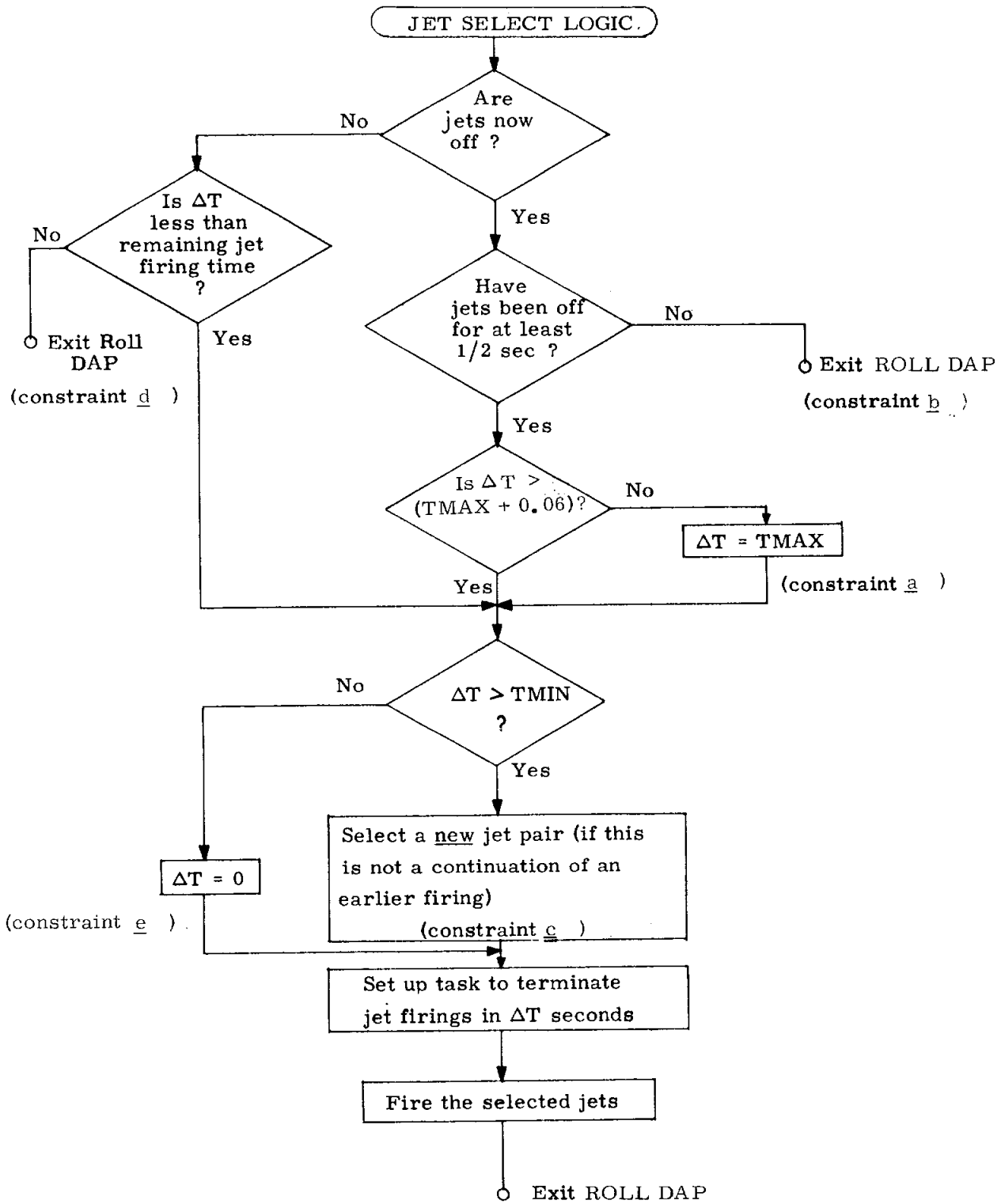


Fig. 3.3.16 TVC ROLL DAP Jet Selection Logic

TABLE 3.3-VIII  
ROLL DAP PARAMETERS

Symbol	Identity	Value
T	TVC ROLL DAP Sample Rate	1/2 second
M = Fd	Roll Jet Torque (per pair)	1400 ft-lb
DB	Deadband	$\pm 5$ deg
LCR	Limit-Cycle Rate	$\pm 0.1$ deg/sec
MAXLIM	Maximum Rate Limit	5 deg/sec
MINLIM	Minimum Rate Limit	1 deg/sec
K, (-slope)	Slope of Straight-line Portion of Switch Logic	0.2 (deg/sec)/deg
a, (1/CONACC) <sup>-1</sup>	Parameter of the Parabolic Portion of the Switch Logic: a = CONACC = M/IXX, where 1/CONACC is the ROLL DAP gain	variable
TMAX	Maximum Firing Duration	2.5 seconds
TMIN	Minimum Firing Duration	15 ms

the back difference of the CDU angles. These differences are then passed through a limiter whose output is linear (unity gain) up to 2.33 degrees but is zero for greater magnitudes. The purpose of this limiter is to protect the vehicle against a spurious setting of the 11.25-degree bit in the CDU read counters, \* which would produce an effective 11.25-degree step input to the TVC DAP filter. The read counters would countdown the 11.25-degree error at their 70-deg/sec rate, which would give a CDU difference of 2.82 degrees per 40-msec DAP sample period. Rather than the full 2.82 deg/sample, we used the lower number of 2.33 deg/sample as the limit. This number represents a compromise between the desire to reject most of the possible 11.25-degree step error and the requirement that actual vehicle tumbling be monitored and controlled.

After passing through the limiter, the CDUDOTs are transformed into body coordinates:  $\omega_B^T = (\dot{N}) \underline{CDUDOT}$ , where  $\underline{CDUDOT} = \underline{CDU} - z^{-1} \underline{CDU}$ .

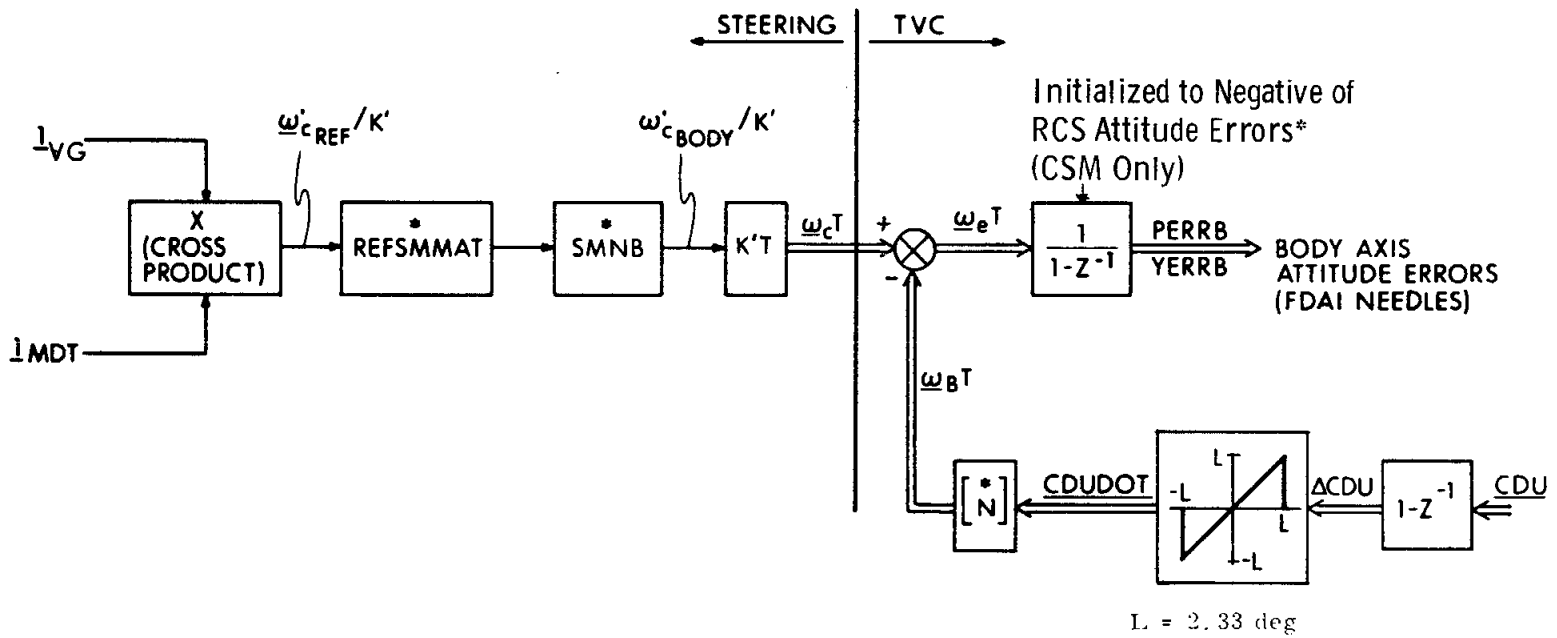
Scaling of the DAP-Steering interface is complicated by the implementational expediency of lumping the  $T$ s of the integrator and the differentiator into the steering gain  $K'$ , such that the effective scaling is inversely proportional to the DAP sample rate.

The three standard matrix transformations are  $SMNB^*$ ,  $REFSMAT^*$ , and  $\dot{N}^*$ . ( $\dot{N}^*$  is given in Fig. 3.3.18.) The sines and cosines for  $\dot{N}^*$  and  $SMNB^*$  are updated every second by the routine QUICTRIG, which is called by P40 (CLOCKJOB).

A limiter, set for limiting the output at 45 deg, or 1/8 revolution, operates on each body-axis error integrator. The limiter is of the analog-feedback type: the input to the integrator is nulled when the output is at the limit. The purpose of the limiter is to assist scaling of the DAP filters.

---

\* This bit is more sensitive than are the others to electrical noise in the CDU environment; it is possible, therefore, though not likely, for the bit to be set by a noise pulse.



\*Limited to  $\pm 1.5$  deg

Fig. 3.3.17 Interface Between Cross-product Steering and TVC DAP



$$\omega_B = (N)^* \underline{CDUDOT}$$

$$(N)^* = \begin{pmatrix} 1 & \sin \psi & 0 \\ 0 & \cos \phi \cos \psi & \sin \phi \\ 0 & -\sin \phi \cos \psi & \cos \phi \end{pmatrix}$$

$\phi$  = outer gimbal angle

$\psi$  = middle gimbal angle

$\theta$  = inner gimbal angle

Fig. 3.3.18 CDU Rates to Body Rates Transformation

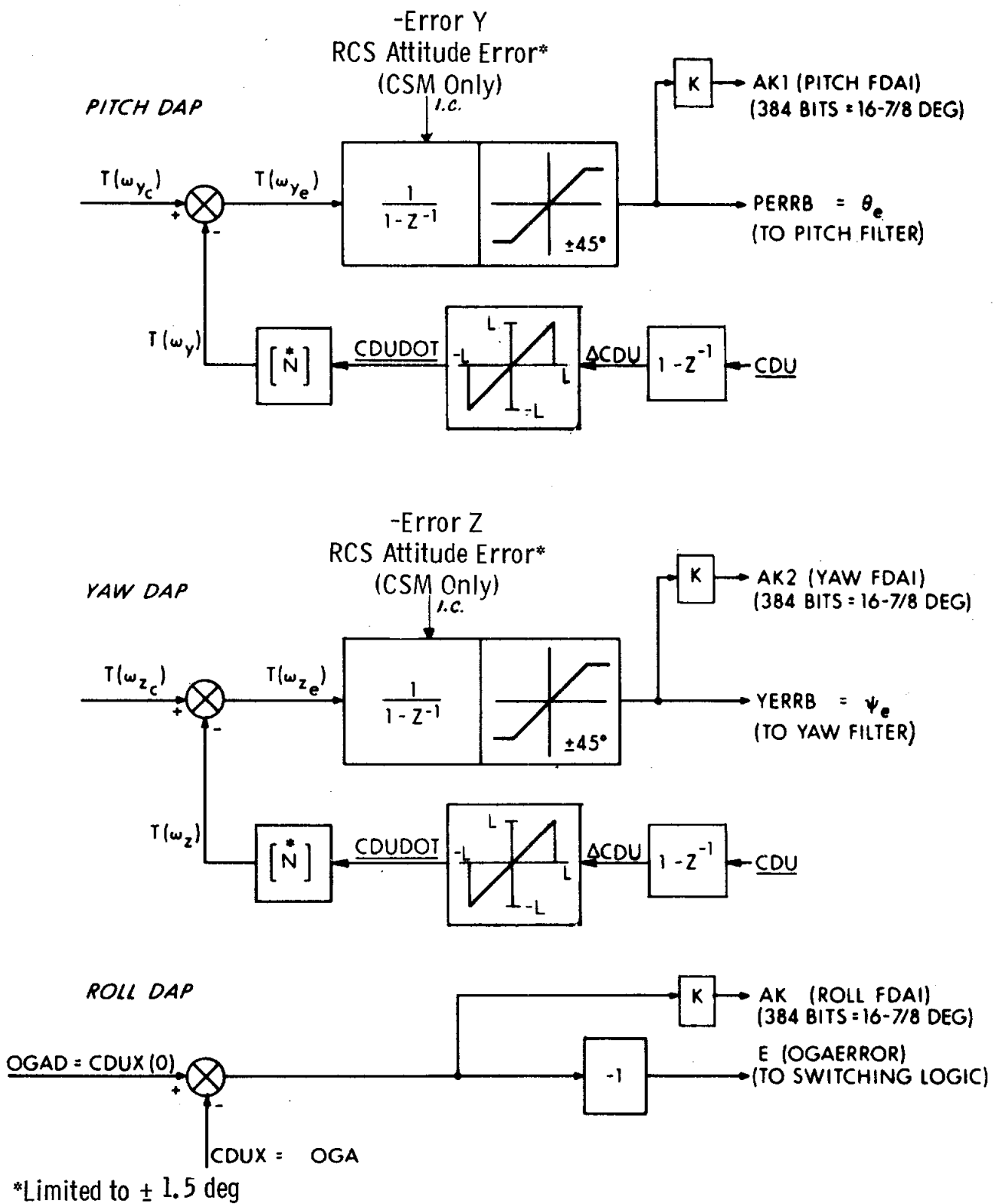


Fig. 3.3.19 FDAI Needle Variables

3.3-50

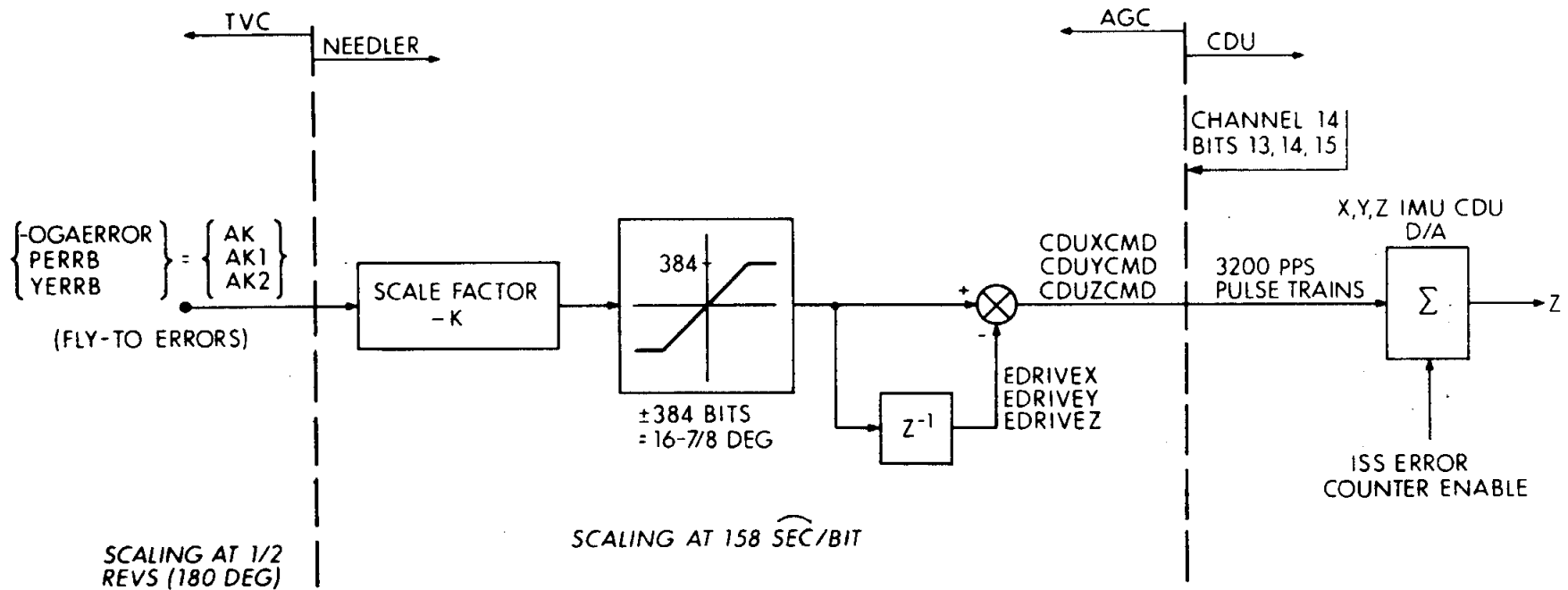


Fig. 3.3.20 Error Needles Interface for TVC DAP

Initial conditions are required by the pitch and yaw differentiators and integrators. The subroutine DAPINIT, called one sample period before the first pass through the pitch DAP, reads the CDUs for the initial values of CDU-past for the differentiators. Initial conditions for the attitude-error integrators are established for the CSM by picking up the negative RCS attitude errors for pitch and yaw (ERRORY, ERRORZ) just before TVCDAPON is called. The values, subject to a  $\pm 1.5$ -degree limit, are then loaded into the TVC attitude-error registers PERRB and YERRB after the TVC zeroing loop has been completed. For the CSM/LM configuration, the attitude-error integrators are initialized to zero to avoid possibly large engine excursions at ignition.

### 3.3.7.2 Output Interface

The D/A sections both of the IMU and the OPTICS CDUs are involved in TVCDAP output: the IMU CDUs display attitude-error signals on the FDAI needles, and the OPTICS CDUs generate the analog signals that drive the SPS gimbal actuators.

3.3.7.2.1 FDAI Needle Displays. -- Pitch and yaw body-attitude errors are displayed on the pitch and yaw needles; outer-gimbal-angle (OGA) error is displayed on the roll needle. The signal pickoffs are shown in Fig. 3.3.19. Each of the DAP variables (AK = -OGAERROR, AK1 = PERRB, and AK2 = YERRB) are scaled at the normal CDU scaling (full register = 180 deg). All three variables are FLY-TO errors, positive in the sense:

$$\text{Error} = \text{Commanded Attitude} - \text{Measured Attitude.}$$

Processing of the AK signals is handled by the subroutine NEEDLER associated with the RCS DAP. Basic functions of this subroutine include preparing the IMU error counters (initialization and enablement), scaling the AKs for full-scale needle deflection of  $16\frac{7}{8}$  deg, generating incremental commands, and releasing the pulse trains to the counters. These operations are shown schematically in Fig. 3.3.20.

Display is effected by a special initialization call to NEEDLER, followed by calls from TVCEXECUTIVE every  $1/2$  second. The DAPs compute values for PERRB and YERRB every 40 (or 80) ms and update AK1 and AK2 with the new values. NEEDLER is called only once every  $1/2$  second, however, and the needle updates are made with the then-current AKs.

During the changeover from RCS to TVC in the CSM configuration, there will be a short period of approximately  $1/2$  to 1 second during which the needles will be zeroed. After this period, the errors are re-established with the values left by the RCS DAP, subject to the  $\pm 1.5$ -deg limit as discussed in paragraph 3.3.7.1. For the CSM/LM, the needles are not re-established with the RCS errors.

3.3.7.2.2 Actuator Commands via the Optics CDUs. -- The D/A portions of the OPTICS shaft-and-trunion CDUs generate the dc-analog signals that drive the pitch and yaw SPS gimbal actuators in response to the ACG-generated

actuator commands PCMD and YCMD. Figure 3.3.21 is a schematic diagram of the actuator-command generation, within the AGC, and of the generation, by the CDU, of the analog signals to drive the actuators. Note that the AGC output consists of incremental changes in command:

$$\Delta \text{PCMD} = \text{PCMD} - z^{-1} \text{PCMD}$$

These increments are stored into the AGC output-counter registers TVCPITCH and TVCYAW. When the 3200-pps pulse trains are released, the error counter accumulates (sums) them, and the associated D/A ladder and demodulator transforms them into the proportional signal that drives the actuator amplifiers.

Scaling for the AGC command registers is set by the CDU interface, where, nominally, one bit represents 85.41 arc-seconds (or 0.0237 deg) of engine deflection. Derived from this ratio is the so-called actuator scaling revolution (ASCREV):

$$1 \text{ASCREV} = \frac{85.41 \times 16384}{3600 \times 360} = 1.0797511 \text{ rev}/(\text{full register}).$$

Note that there is a difference in scaling between the DAP input interface, where a full register equals 180 deg, and the output interface, where a full register equals 388.3 deg (360 x 1 ASCREV). This difference amounts to an inherent dc gain across the DAP of 2 ASCREV (or 2.1595). This factor is accounted for in the gain factor VARK.

To drive the gimbal servos, the CDU must be in the thrust-vector-control mode. To initiate this mode, the SC CONT switch on the main control panel must be set to the CMC position. This generates the GN&C autopilot-control discrete and sets up the actuator amplifier to receive voltages from the OPTICS CDU. In the CDU, the discrete arms, but does not energize, the thrust-vector-control relays. The TVC ENABLE discrete from the computer to the CDU energizes these relays, thereby switching on the dc-error signals to drive the actuator amplifiers. The computer must also send the OPTICS ERROR COUNTER ENABLE discrete that enables the error counter to track the command increments received by the CDU. These increments are released from TVCPITCH and TVCYAW by setting the OPTICS ACTIVITY bits. Preparation of the CDU (activating these discrettes subject to certain timing constraints) is normally handled by the Gimbal Drive Test and/or Trim Program S40.6.

### 3.3.8 Restart Protection of the TVC DAP

Computer restarts fall into two categories -- hardware restarts, which cause many channels (including those used for TVC) to be reset to zero; software restarts, which do not affect the TVC channels. Both kinds of restarts cause WAITLIST task information to be lost, thereby preventing the TVC DAP subroutine TVCEXECUTIVE from perpetuating itself at 1/2-second intervals.

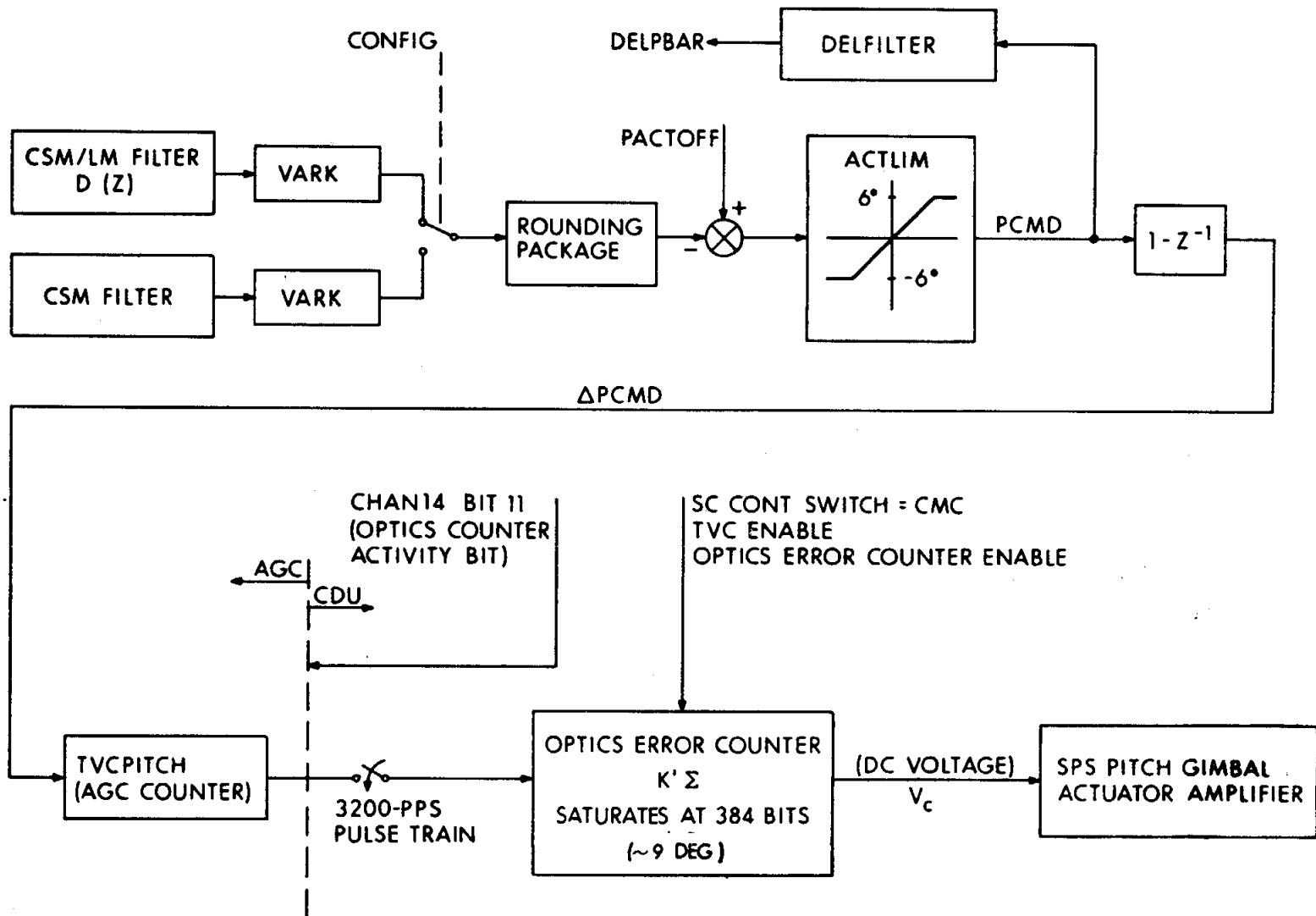


Fig. 3.3.21 TVC Actuator Command Interface: Pitch Channel

Hardware Restarts. -- In the event of a hardware restart during an SPS burn, the most important requirement from the point of view of TVC DAP operation is to re-establish the D/A interface between the DAPs and the engine-gimbal servos. This must be done quickly, as a hardware restart deactivates the OPTICS ERROR counters and resets TVC ENABLE. This action drives the engine servos to their electrical-null positions, since the driving voltage drops to zero. Depending on the flight condition, the electrical-null positions could be several degrees off the desired engine-trim positions. Therefore, nulling the engines could result in a large transient moment of the vehicle. To minimize this transient, the output-error counters for pitch and yaw are reset to their previous values as soon as the D/A interface is reactivated. Commands go to the servos even before the DAP computation resumes. These tasks are performed by the TVC restart package (REDOTVC).

In addition to re-establishing the D/A interface, restart protection must be provided against the loss of information in the working registers (A, L, Z, Q): counters, integrators, and computations involving past values of quantities must all be protected. This is accomplished by storing the quantities in temporary locations as they are computed. The temporary locations are then copied into the permanent locations during copy cycles that follow the computation sections. Accordingly, the DAP logic includes several copy cycles, each following a major computation section. Should a restart occur during a copy cycle, the copy cycle is repeated. Should restart occur during a computation period, the restart logic determines whether to recompute only the computation section or to repeat the entire DAP cycle.

Hardware restarts also affect guidance equations and AGC executive routines that must be re-established. This means that there will be some delay before the DAPs can resume their operations. Simulation tests have shown a delay of  $\approx 0.1$  second between restart initiation and the re-establishment of the D/A interface with the previous actuator-command values. Another DAP sample period (40 or 80 ms) elapses (for re-establishing CDU rates) before the DAPs generate further incremental commands. The effect, however, of this transient on the vehicle attitude is negligible.

Hardware restart protection of the TVC DAP coding requires a special TVC restart package. REDOTVC, called from the standard AGC restart routine, reactivates the TVC DAP interfaces, re-establishes the waitlist priority of TVCEXECUTIVE, determines where in the TVC DAP coding the TVC DAP computations can be safely restarted, and, at the appropriate time, restarts the TVC DAP computations.

Software Restarts. -- TVC software restart protection is much simpler, involving only the re-establishing of the TVCEXECUTIVE waitlist task, accomplished by the AGC restart logic. Unlike hardware restarts, software restarts do not require special TVC restart logic.

REFERENCES FOR SUBSECTION 3.3

- 3.1 Smith, E., "Initial Uncertainty in the SPS Thrust Vector Direction Due to Random Errors in the APOLLO Block II TVC Digital Autopilot (DAP) Systems," NASA Memorandum EG23-67-36, March 1967.
- 3.2 Kubiak, E. T., "Presentation of Mass Properties Data to MIT," NASA Memorandum EG23-67-106, June 1967.
- 3.3 Lum, B. T., "Block II G&C, SM RCS, and Spacecraft Dynamic Models," North American Aviation Internal Letter No. 190-420-ACA-67-006, May 1967.
- 3.4 Robinson, C. E., and Runyan, R. B., "Thrust Vector Determination for the APOLLO Service Propulsion Engine Using a Six-Component Force Balance," Arnold Engineering Development Center Report No. AECD-TR-65-250, December 1965.
- 3.5 Gille, J., "Slosh Parameters and Tank Dimensions," APOLLO Block II CSM G&C Data Book, No. 2.5.3.2, North American Submittal No. NAA-S-75, March 16, 1966.
- 3.6 Penchuk, A., and Stubbs, G., "Limits on Engine Gimbal Servo Frequency Response Imposed by Autopilot Stability Requirements," MIT Instrumentation Laboratory SAD Memo. No. 68-11, July 29, 1968.
- 3.7 CSM/LM SPACECRAFT Data Book, Vol 3, NASA Document SNA-8-D-027, March 1968; also Amendment 1, April 24, 1968.
- 3.8 Cherry, G., and O'Connor, J., "Design Principles of the Lunar Excursion Module Digital Autopilot," MIT Instrumentation Laboratory Report R-499, July 1965.
- 3.9 Danforth, W. C., "TVC Roll Autopilot," MIT Instrumentation Laboratory SUNDISK Flowchart FC-0460, December 1967.



### 3.4 ENTRY AUTOPILOT AND MISSION CONTROL PROGRAMS by Robert R. Bairnsfather

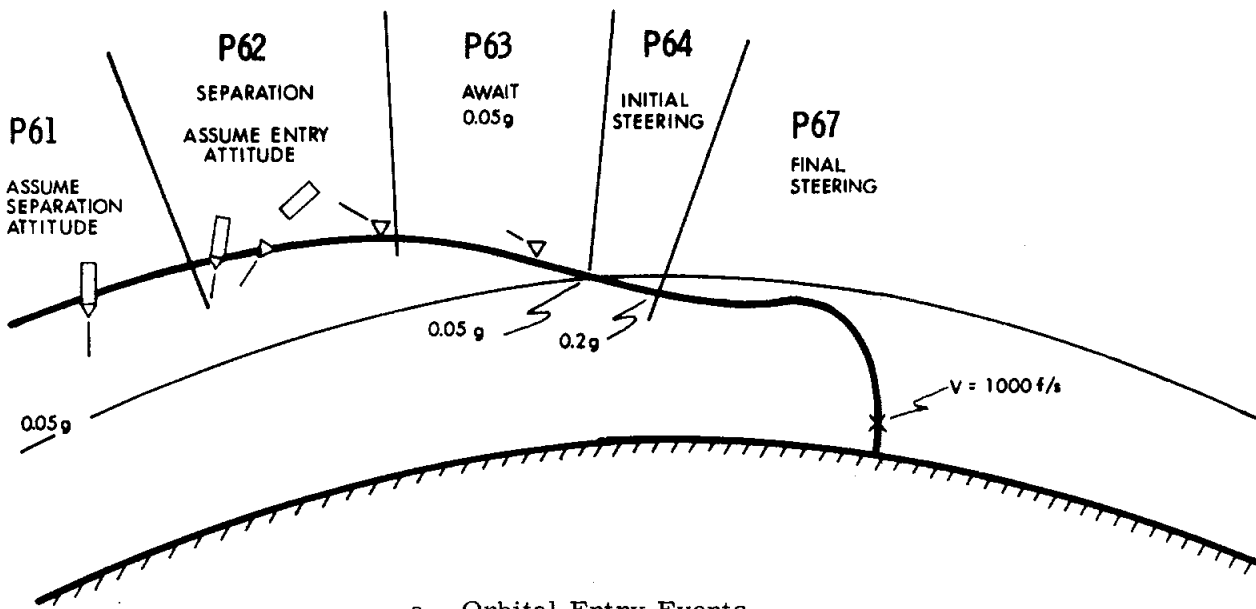
#### 3.4.1 Atmospheric Reentry - An Overall View

The Entry programs cover the phases of spacecraft flight commencing with the maneuver to SM-CM separation attitude and continuing until drogue chute deployment. A typical trajectory for orbital reentry is illustrated in Fig. 3.4.1a. A lunar trajectory appears in Fig. 3.4.1b. The trajectory is broken into segments, each identified by a Mission Program number from P61 through P67\*. From the standpoint of the Entry DAP, trajectory portions above the 0.05 g contour are serviced by the extra-atmospheric mode of DAP operation, and those below by the atmospheric mode of DAP operation. The contour is sensed by Entry Guidance which clears the switch .05GSW to zero if above the contour, and sets .05GSW to one if below. In the atmospheric mode, the DAP performs rolling maneuvers such that the CM rolls about the vector direction of velocity relative to air mass by causing yaw rate to be coordinated with roll rate. (See also Entry Guidance, Section 5, this document.)

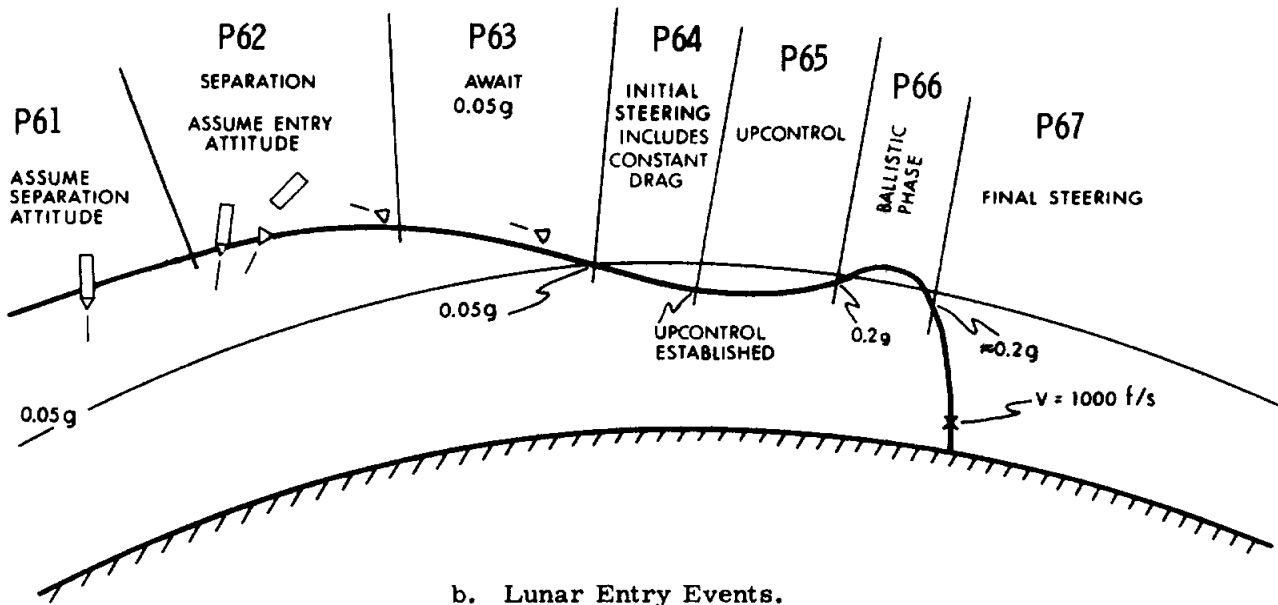
A brief summary of the P60's follows:

- P61 The CM is maneuvered to the SM-CM separation attitude. DSKY display provides information to initialize the Entry Monitor System (EMS).
- P62 Crew performs CM-SM separation. DAP establishes attitude hold after separation until crew specifies initial Entry roll attitude. DAP initiates and performs maneuver to bring CM into Entry trim attitude with respect to relative velocity vector.
- P63 Initialize Entry Guidance. DAP maintains Entry attitude. Await onset of 0.05 g.
- P64 Entry Guidance awaits onset of 0.05 g. If velocity at 0.05-g point is less than 27,000 ft/sec, P67 is entered when 0.2 g occurs. If velocity at 0.05-g point is greater than 27,000 ft/sec, Entry Guidance establishes the up-control reference trajectory. DAP follows roll commands issued by Entry Guidance and performs coordinated rolling with rate damping.
- P65 When constant-drag control has reduced the predicted range to within 25 n.mi. of the desired range, the up-phase is entered, and Entry Guidance steers along a self-generated reference trajectory to a controlled skipout condition. DAP follows roll commands issued by

\*The P60 mission-control programs and the Entry Guidance programs described in paragraphs 3.4.1 through 3.4.3 are included for information only. They provide the reader with a convenient linkage between the DAP (GSOP Section 3), Entry Guidance (GSOP Section 5), and the P60 mission-control programs (GSOP Section 4). The control documents for the non-DAP functions are GSOP Sections 4 and 5.



a. Orbital Entry Events.



b. Lunar Entry Events.

Fig. 3. 4. 1 Typical Entry Events.

Entry Guidance and performs coordinated rolling with rate damping. If, however, altitude rate is negative and if velocity is low enough, P67 is entered.

- P66 When drag acceleration has become less than  $Q7 \text{ ft/sec}^2$ , the ballistic phase of steering is entered and Entry Guidance ceases to generate new commands ( $R_c$ ). The DAP maintains roll attitude at the existing  $R_c$  and continues to perform pitch and yaw damping. If the CM leaves the atmosphere, then when drag\_level becomes less than 0.05g. Entry DAP changes to three-axis attitude control in order to keep the CM in the attitude of trimmed flight with respect to the relative velocity vector. Also,  $R_c$  is set to zero to command full lift up, providing a horizon check. During the second reentry when 0.05g is exceeded, Entry DAP resumes rate damping in pitch and yaw. The end of the ballistic phase occurs when drag exceeds  $6.5 \text{ ft/sec}^2$  (approximately 0.2g).
- P67 Entry Guidance generates steering commands  $R_c$  to fly the final phase pre-stored reference trajectory to target. DAP follows roll commands as issued and performs coordinated rolling with rate damping. Entry Guidance stops updating roll command when the relative velocity  $< 1000 \text{ ft/sec}$ . DAP maintains roll attitude hold and rate damping until P67 is terminated by crew.

The portion of reentry of interest to the Entry DAP begins with SM-CM separation (P62). Adequate clearance between CM and SM is needed before initiating the CM reorientation maneuver. In the interval while clearance is being established, the CMC Mode switch on the instrument panel should be moved to FREE to prevent the RCS DAP, whose software is still active, from firing the CM thrusters or else re-contact may result. After the interval, the Entry conditions are established as commanded attitude angles: roll attitude as was specified by keyboard entry, zero yaw, and trim angle of attack. The extra-atmospheric DAP maneuvers to satisfy these conditions and holds the attitude obtained. After the 0.05 g contour is encountered (P63), the atmospheric DAP takes control; it follows roll commands issued by Entry Guidance, discussed in the following paragraph, and performs coordinated turns with rate damping.

Return to earth at a specified landing point is achieved by Entry Guidance, utilizing atmospheric aerodynamic lift. The transition from extra-atmospheric control to atmospheric control is signified when Entry Guidance senses that the acceleration has exceeded 0.05 g and sets the switch, .05GSW. The guidance equations determine proper orientation of the lift vector relative to the trajectory plane as the means of control in achieving the desired landing point. The component

of lift in the plane of the relative velocity and the position vector controls the down-range flight. Cross range is controlled by the out-of-plane component of lift. By rolling the CM about the velocity vector, orientation of the lift vector is achieved such that the desired in-plane component obtains. The out-of-plane component of lift causes lateral drift of the vehicle. This sidewise motion is used for plane changing, if any is needed. Otherwise lateral drift is an unwanted by-product of the steering, and is constrained by causing the CM to roll so as to reverse the sign of the out-of-plane component of lift. Since the in-plane component is the fundamental controlled quantity, it is important that its sign be unchanged during lateral reversals or switchings. In effect this demands that the CM roll predominantly through the smaller of the two possible angles at lateral switching time. In certain critical cases, Entry Guidance insists on rolling over the top without regard for the angle size, and the switch LATSW is set to inform the roll DAP. Thus Entry Guidance provides a single output quantity, commanded roll angle  $R_c$ , to be achieved by the CM. This output quantity is supplemented by two switch settings: that of LATSW and of .05GSW.

Within the atmosphere the CM is aerodynamically stable, a property that simplifies the autopilot design. In pitch and yaw, since stability is no problem, simple rate dampers are used. Furthermore, aerodynamic forces are utilized to do most of the work during a coordinated roll. The vehicle roll attitude in response to applied roll RCS torque can be represented adequately by considering only the torque due to moment of inertia. Damping and cross-coupling torques are negligible. Therefore, a simple predictive autopilot utilizing the phase plane is used.

TABLE 3.4-I OUTLINE OF ENTRY EVENTS

<u>EVENT</u>	<u>CONTROLLING ACTION</u>	<u>DAP FUNCTION</u>
<u>Separation</u>	Load $R_c, \beta_c, \alpha_c$ with $R, \beta, \alpha$ , Load $R_H$ with $R$	3-axis ,Attitude Hold
<u>Establish Entry condition</u>	Set $R_c$ : Specified By Key Board (used as roll command except as noted) $\beta_c = 0$ $\alpha_c = \alpha_t$ (expected trim)  (Unless specified, use $R_c$ for roll command.)	$ \alpha  > 135$ Roll Damping using $p$ . Load $R$ into $R_H$ . Attitude Control in $\beta, \alpha$ using $r, q$ .
		$45 <  \alpha  < 135$ Attitude Control in $R, \beta, \alpha$ using $r, p, q$ . (Use $R_H$ for roll command)
		$ \alpha  < 45$ Attitude Control in $R, \beta, \alpha$ using $p, r, q$ . If in roll deadzone: $R_H \leftarrow R_c$
$D > .05g$	$R_c$ given By Entry Guidance	Attitude Control in $R$ . $q, r$ Damping (coord.) .
$V < 1000 \text{ ft/s}$	$R_c$ Remains Constant	Attitude Control in $R$ . $q, r$ Damping (coord.) .
Drogue	DSKY Response	Disable DAP

### 3.4.2 Reentry - System Point of View

The present section is intended to provide an overall view of the system of Entry programs. Portions having to do with initialization and sequencing will be discussed in detail; autopilot operation is deferred until later.

The Entry autopilots are designed to perform automatically all maneuvers for all phases of Entry flight starting with positioning the CM in the Entry attitude and continuing until drogue chute deployment. Such capability requires several modes of operation. These modes are illustrated schematically in the block diagram in Fig. 3.4.2 where the two basic modes are atmospheric and extra-atmospheric. In the extra-atmospheric mode, the CM has three-axis attitude control based on the Euler set  $R, \beta, \alpha$  (defined in Fig. 3.4.13). The commanded values of the attitude angles ( $R_c, \beta_c, \alpha_c$ ) correspond either to those for attitude hold or to those required to bring the CM into trim with respect to the velocity vector measured relative to the atmosphere. Each of the errors associated with the Euler angles is assigned to the body axis that exerts the most effective control. The atmospheric mode is selected whenever atmospheric drag exceeds 0.05 g. Attitude control in roll  $R$  is maintained using the p-jet axis while the q- and r-jet axes are used for pitch and yaw dampers. The yaw damper also enforces a coordinated roll maneuver.

The basic steering cycle is done every two seconds and is described using the atmospheric mode as the example.

The cycle begins with Navigation. Integrating accelerometers (PIPA's) provide the velocity increments which are used by AVERAGEG to update the state vector. New body attitude angles are computed by CM/POSE and the cycle ends with Entry Guidance providing a new roll command  $R_c$ . The roll digital autopilot also operates on a two-second basis. It uses this command, together with present estimate of body rate and attitude angle which are provided each 0.1 sec., to control the CM over a two-second interval. Concurrently, the pitch and yaw dampers operate each 0.1 second. The effect of the jet thrusters on the CM is reflected by the IMU, thus closing the control loop. The same general cyclic behavior applies to the extra-atmospheric mode.

Timing is important in the description of measurement, steering and control. A simplified timing diagram for the Entry DAP is given in Fig. 3.4.3. The column headed STEERING is executed every two seconds. Program READACCS (Fig. 3.4.16) reads the PIPA's and, during Entry, saves quantities to allow program CM/POSE (Fig. 3.4.17) to update the attitude angles. READACCS initiates a delayed task SETJTAG (Fig. 3.4.27) to call the roll DAP CM/RCS (Fig. 3.4.34), and also initiates the navigation program AVERAGEG (GSOP, Sec. 5) to update the state vector. AVERAGEG exits directly to CM/POSE which calculates a fresh set of CM body attitude angles,

3.4-7

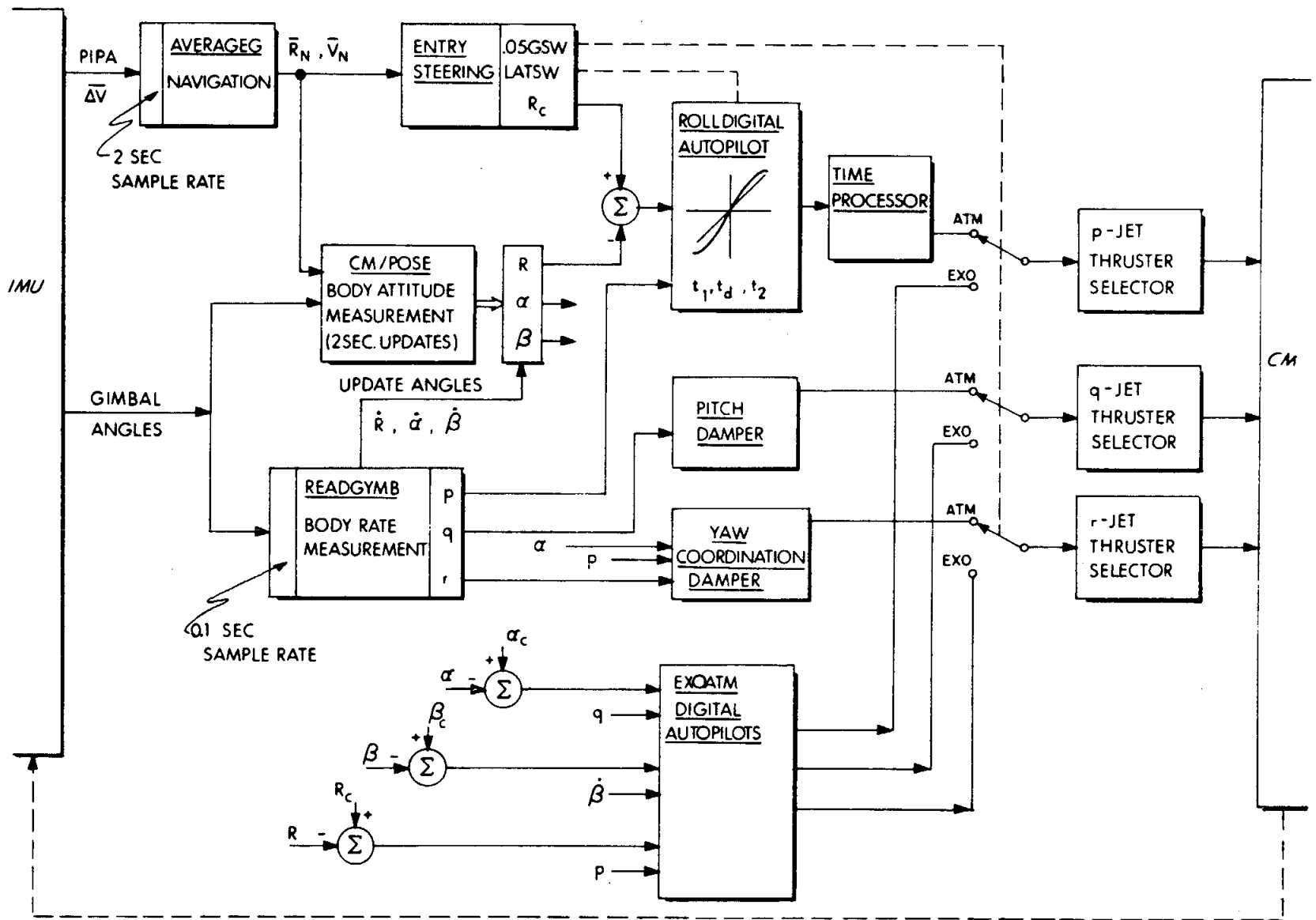


Fig. 3.4.2 Block Diagram of ENTRY Digital Autopilot

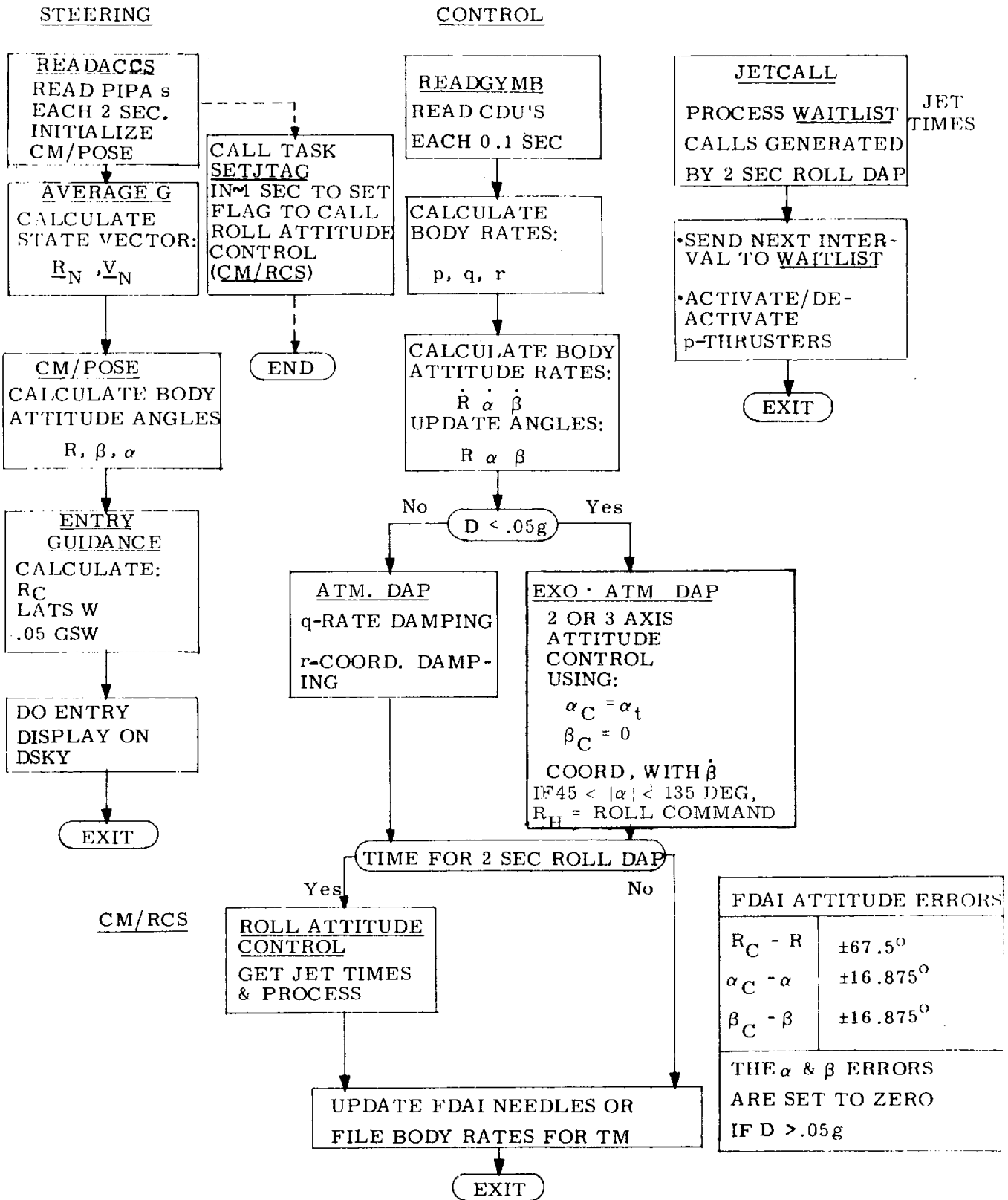


Fig. 3.4.3 Timing Diagram For Entry DAP.



corrected for time lapse since READACCS. CM/POSE has a variable exit that contains an appropriate address in the Entry Guidance program. The Entry calculations establish a new commanded roll angle  $R_c$ , and also two switch settings used by the DAP. Entry Guidance ends each cycle with the current Entry DSKY display, a display that changes with the internal Entry mode. The resulting roll command  $R_c$  is valid back at PIPA read time; however, to maintain uniform timing of the roll DAP (CM/RCS) and to allow time for computation, examination of  $R_c$  by the DAP is delayed by about one second. The roll DAP operates every two seconds but is initiated in sync with the faster DAP's.

The column headed CONTROL is executed each 0.1 second. The initial calculations measure the control variables. Program READGYMB (Fig. 3.4.28) reads the CDU's and continues to calculate CM body rates and body attitude rates. The body attitude angles are integrated between the CM/POSE two second updates. Depending on the setting of .05GSW, q- and r-damping are done or else the appropriate attitude control is done. This may be either two- or three-axis control; the choice depends on the magnitude of  $\alpha$  as is discussed in a later section. Following this, a switch is interrogated to see if the two-second roll DAP CM/RCS is to be executed on this pass. If not, it is omitted. The roll DAP uses  $R_c$  to predict the jet firing policy for the two seconds until a fresh  $R_c$  is available. The jet firing policy exists in the form of time intervals associated with particular p-jet thrusters. The CONTROL cycle ends by either updating the FDAI attitude error needles or by saving the current CM body rates in a list for telemetering. The additional CONTROL function of processing the roll-jet firing policy is done on an irregular basis. The Program JETCALL (Fig. 3.4.38) may be entered up to three times in a 2-second interval to enforce the jet firing policy.

### 3.4.3 Reentry -Mission Oriented View

The present section will cover in detail the Mission Control program interaction with the Entry DAP from the point of view of program operation, but not of program content. This includes topics such as start-up and shut-down sequences. For complete Mission Control Program description of the P60's, see Section 4 of this GSOP.

Program P61's primary function is the display of data to the crew for initializing the Entry Monitor System (EMS) and is therefore omitted here. (See GSOP Section 4. ) The only DAP-related operation in P61 is to set HEADSUP to -1 to specify lift-up attitude at the beginning of entry. The crew has the option in display noun N61 to change this specification.

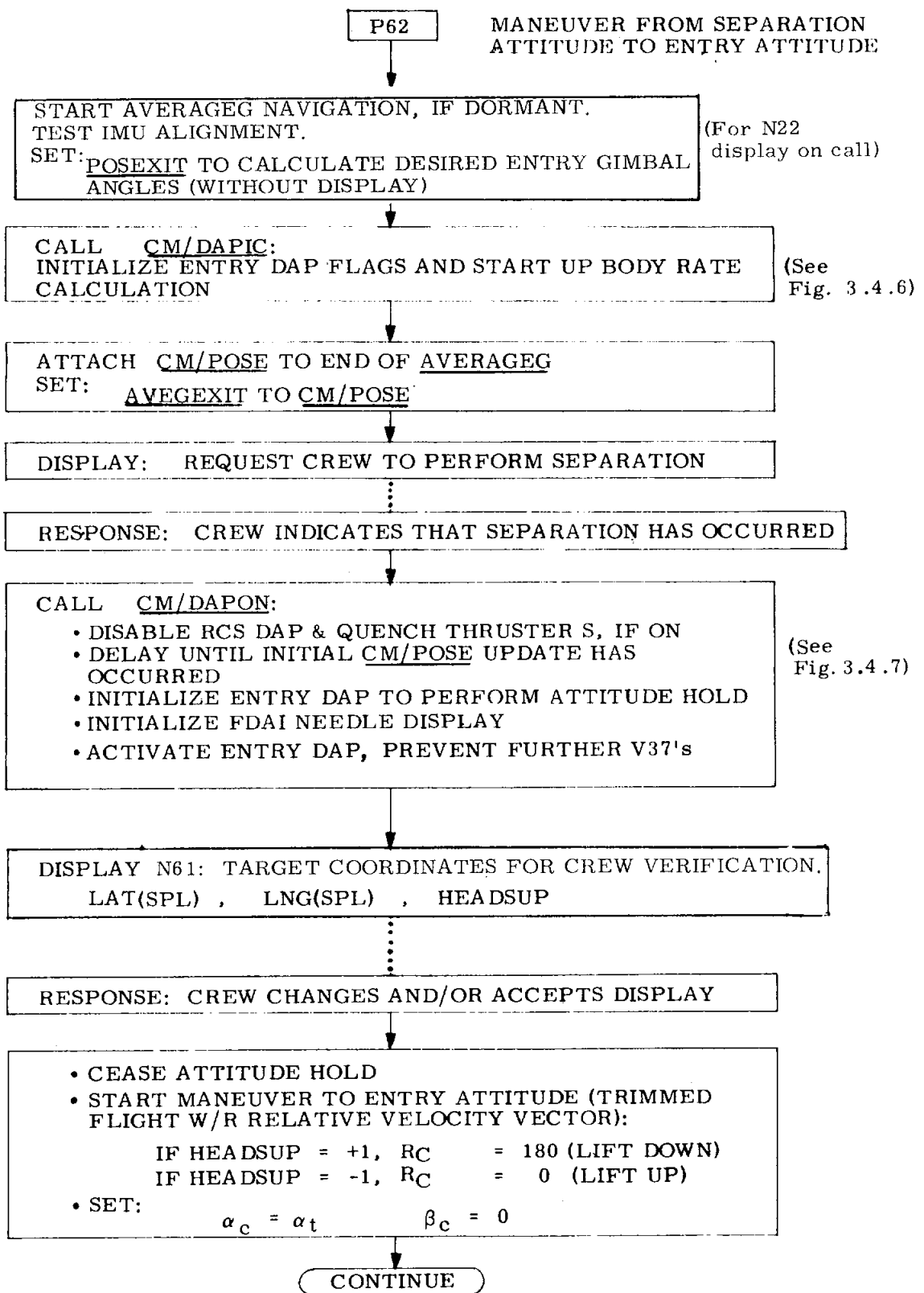


Fig. 3.4.4 Events in Mission Control Program.

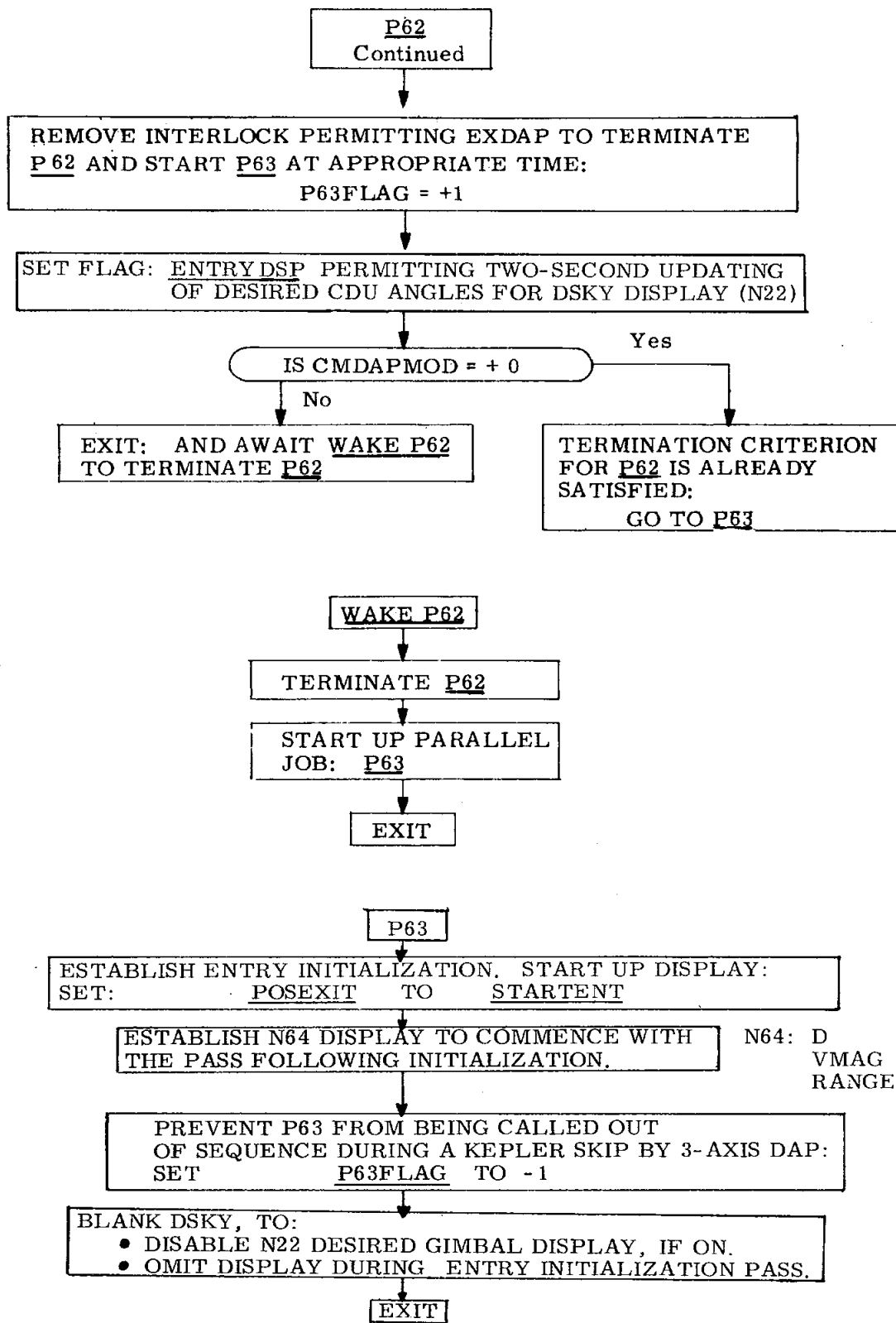


Fig. 3.4.5 Transition from Program P62 to P63.

Program P62 is outlined in Fig. 3.4.4 and Fig. 3.4.5. P62 can be entered directly from P61, or by way of the DSKY. In the event of the latter, AVERAGEG will be inactive; a short delay occurs before it is activated, while the state vector is brought up to date. The IMU alignment is checked and an alarm code is displayed on the DSKY either if

- a. the IMU is reversed, yielding a reversed rotation for the FDAI ball, or
- b. the IMU is more than 30° away from normal (or reversed) alignment.

Program CM/POSE (Fig. 3.4.17) will be activated shortly so its exit address must be set. Initially CM/POSE is caused to calculate desired (trim attitude) CDU angles for N22 display on call before exiting via the standard Entry Guidance logic that maintains restart protection. Next, the Entry DAP is initialized by calling CM/DAPIC, Fig. 3.4.6. The basic DAP program READGYMB, Fig. 3.4.28, is started up in sync with READACCS, Fig. 3.4.16, but delayed by half an autopilot update period, or 0.05 sec. This distributes the load on the T3 clock in order to avoid the stacking of interrupt tasks. Once started, READGYMB is self-perpetuating until disabled on finding the switch CM/DSTBY is zero. CM/DAPIC also initializes the following DAP switch bits to zero:

GAMDIFSW, GYMDIFSW	first pass indicators
CMDAPARM	indicates DAP not armed
.05GSW	above .05 g contour

Two switches are set to one:

LATSW	no roll over top demanded
CM/DSTBY	indicates DAP is active

Some computational quantities are zeroed here and restart protection provided.

Several jobs and tasks operate in parallel with P62. Those affected by CM/DAPIC are described here.

READGYMB - The basic Entry DAP cycle is initiated each 0.1 sec by READGYMB, Fig. 3.4.28. If the CDU's are not in fine align, the program re-initializes itself to an initial-pass status and exits. Otherwise, it reads the CDU's and forms gimbal angle differences. If CM/DSTBY = 1, the program continues on to test whether this is a first pass or not. If so, certain DAP variables are initialized and the program exits. Otherwise, computation continues at BODYRATE, Fig. 3.4.29, to calculate the CM body rates. If CMDAPARM = 0, the DAP cycle is terminated. Thus, CM/DAPIC starts the Entry DAP going and allows it to maintain a measure of CM body rates.

The entire Entry DAP operates in interrupt: the initial portion just described operates from the T3 clock and all subsequent calculations will be done from the T5

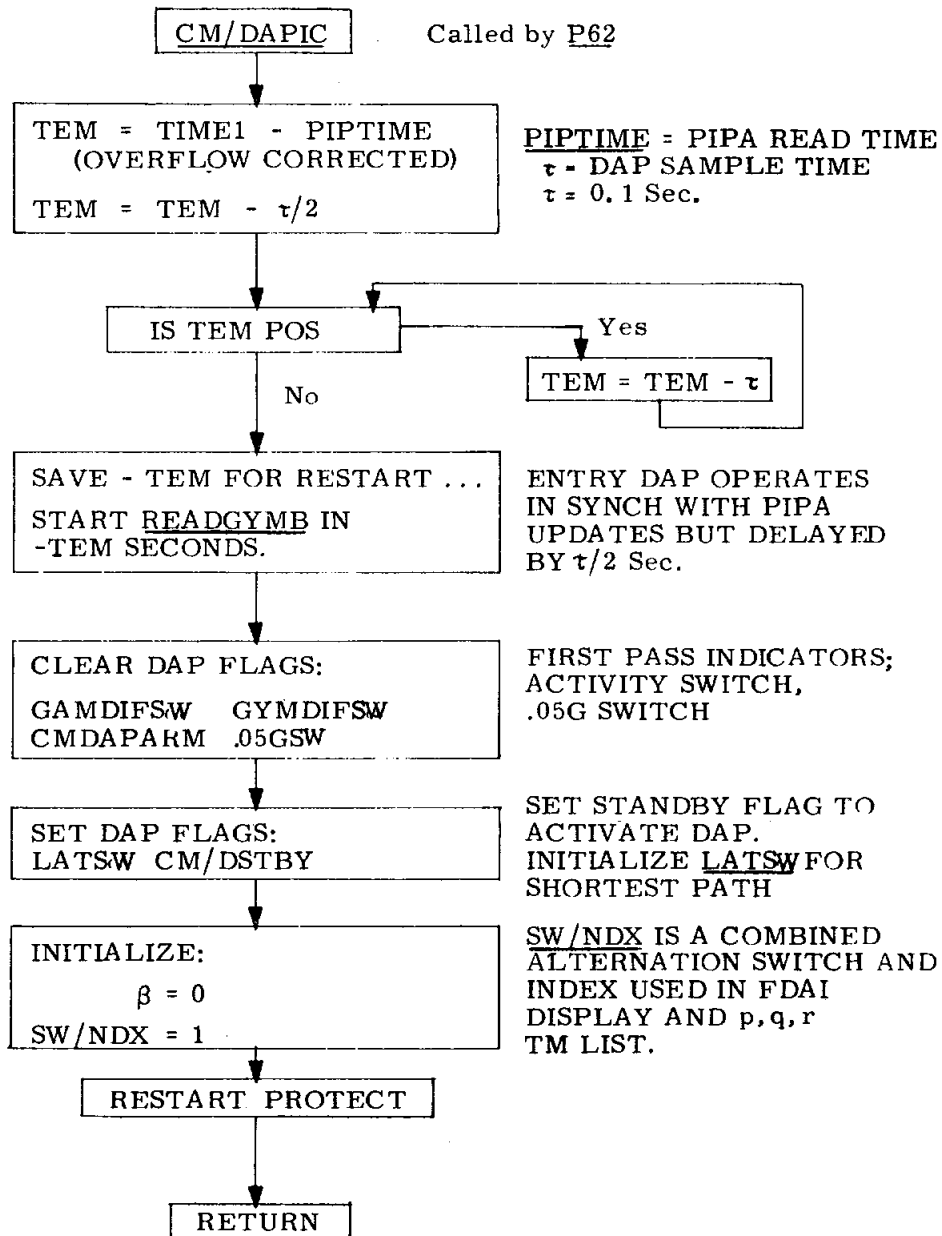


Fig. 3.4.6 Entry Digital Autopilot Initialization.

clock. This division is chosen so that the T3 calculation utilizes about 7.5 milliseconds. The 10-ms window between the ending of T3 portion and the start of the T5 portion allows any waiting interrupts to be processed. In particular, it assures servicing of down-rupts.

READACCS - The secondary DAP cycle operates on the two-second basis established by READACCS, Fig. 3.4.16, and consists of

- a. generation of body attitude angles by CM/POSE, (Fig. 3.4.17)
- b. generation of roll command  $R_c$  by Entry Guidance, (Section 5)
- c. generation of p-axis jet commands by the predictive roll DAP, CM/RCS, (Fig. 3.4.34)

Items (a) and (b) operate in cascade with READACCS and AVERAGEG as already pointed out. Item (c) is triggered by READACCS.

When READACCS finds CM/DSTBY = 1, it performs several functions pertinent to the Entry DAP. Attitude and gimbal angles are saved so that CM/POSE is able to update body attitude angles and correct for computation time loss. A DAP restart protection function is performed. The sync of the predictive roll DAP, CM/RCS, to the READACCS cycle is effected by causing a flag to be set after about a 1-second delay. (The exact value depends on CMC timing; for COLOSSUS 2, 1.2 sec is used.)

Returning to P62 in Fig. 3.4.4, the variable address AVEGEXIT of AVERAGEG is set to continue at CM/POSE. The exit for CM/POSE has been established already.

In digression, consider the operating situation before the AVEGEXIT above is set. If READACCS falls due while P62 is being performed, then READACCS will interrupt and be performed. If CM/DSTBY is non-zero, then certain quantities relating to Entry DAP are established. READACCS then proceeds to establish the execution of AVERAGEG at a higher priority than that of P62. Thus AVERAGEG will go to completion before P62 is resumed. Since we assumed AVEGEXIT was not yet changed, CM/POSE is omitted. However, P62 on resuming will change AVEGEXIT so that all subsequent updates of AVERAGEG will continue on to CM/POSE.

Returning once again to P62, the crew is requested via DSKY to perform SM-CM separation. The program flow will halt here until the crew responds with PROCEED. The purpose of the hold is to allow the crew full control over separation: when it is to be performed and when it is judged to be completed. Regarding DAP operation, it is noted here that even though the Entry DAP has been started up, it is in a stand-by condition. Prior to separation the RCS DAP is active. At separation the CMC Mode switch should be put at FREE to disable the RCS jet

firings before activating the CM Entry fuel system. Otherwise the RCS DAP can fire the CM jet thrusters because, even though separation has occurred, the RCS DAP software remains active until after the crew has responded with PROCEED.

Receipt of PROCEED by P62 causes CM/DAPON, Fig. 3.4.7, to be called. There, the RCS DAP is disabled and the jet channels zeroed. The program must idle until the first-pass flag GAMDIFSW = 1, indicating that CM/POSE has done at least one update and that valid body attitude angles exist. Normally GAMDIFSW will be non-zero by this time. An interlock flag for terminating P62 is established. The DAP is made to do attitude hold by loading the attitude commands with the present attitude angles. CMDAPARM switch is set to 1. This allows the Entry DAP to continue beyond updating CM body rates and to go to completion. Since T5 was being used by the RCS DAP, it was not possible before now to update the attitude rates and angles. As a result the attitude angles will be slightly inaccurate until the next CM/POSE update.

When CM/DAPON is over, the program returns to P62 to do the DSKY display of target coordinates and initial roll angle for crew verification or change. Upon receipt of PROCEED the DAP is caused to cease doing attitude hold and to commence the maneuver to Entry attitude, defined by: initial roll angle as specified, zero beta, and the trim value of  $\alpha$ . The interlock flag is removed to permit termination of P62. This flag was required to prevent premature termination of P 62 as a result of manual maneuvering. The entry display flag is set, allowing the computation of desired CDU angles to be displayed on the DSKY each 2 seconds. The display is done by the normal Entry Guidance exit display.

The termination criterion for P62 depends on estimating the end of the maneuver to entry attitude. If at this point in P62 the DAP mode indicator CMDAPMOD shows that the Entry DAP has already left the mode where the estimate is made, then P62 will go directly to P63. If, on the other hand, the maneuver to Entry attitude is in progress, then P62 effectively goes to sleep until the termination criterion is satisfied. The criterion for terminating P62 is based on the state of completion of the Entry attitude maneuver: when  $\alpha$  becomes less in magnitude than  $45^\circ$ , the time required by the CM to reach trim  $\alpha$  is estimated using an average pitch rate. When this time has elapsed the task WAKEP62, Fig. 3.4.5, is initiated to terminate P62 and start up P63, Fig. 3.4.5. It is possible in rare circumstances for P63 to be started up twice... by a restart, for example. However, the second pass through P63 is harmless.

The functions that P63 performs are to establish the variable verb-noun code for the Entry Guidance DSKY display, and to cause CM/POSE to exit directly to STARTENT in Entry Guidance and to prevent P63 from being called out of sequence. As is seen in Fig. 3.4.8, STARTENT initializes the Entry steering equations. It

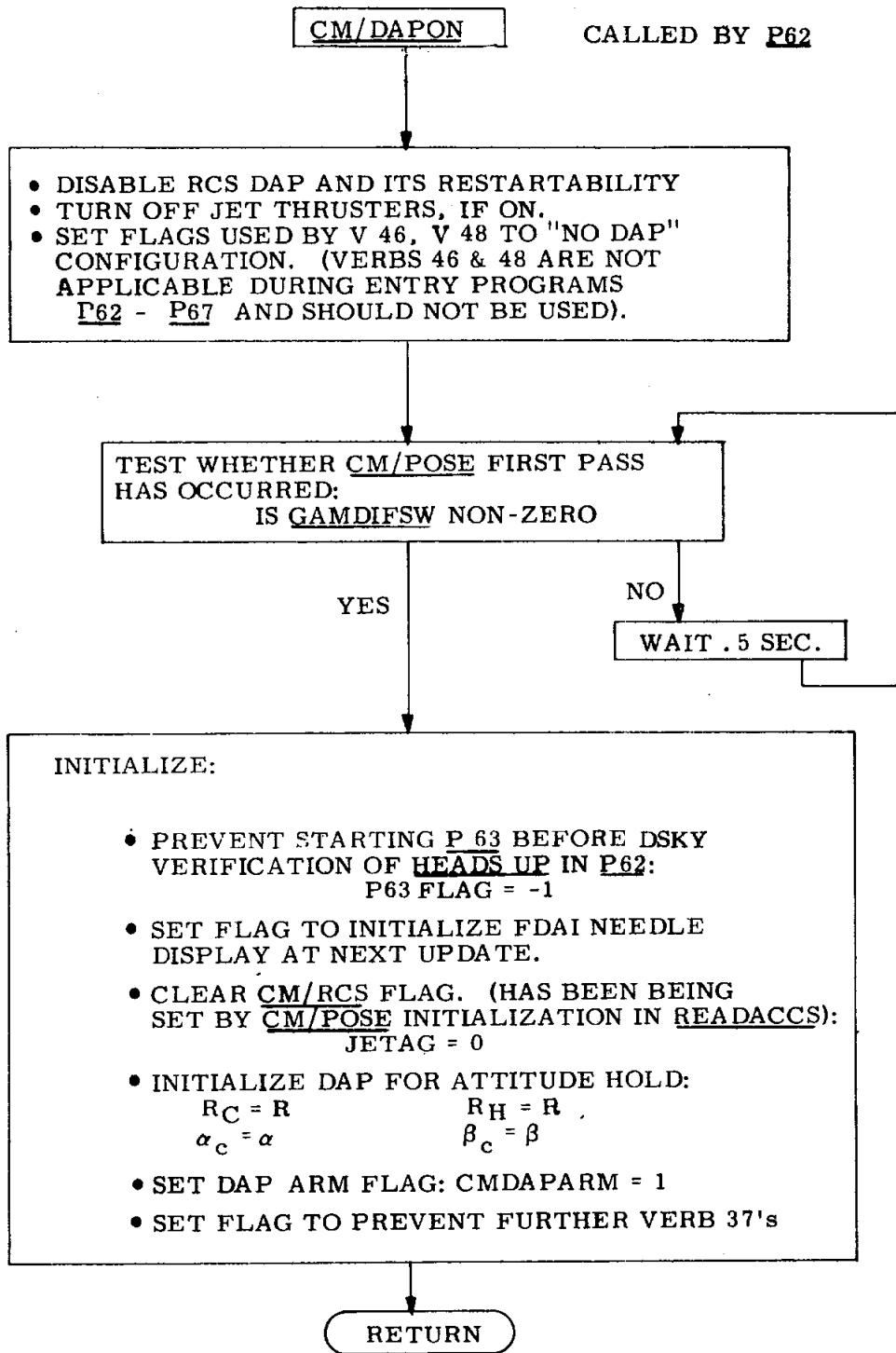


Fig. 3.4.7 Entry DAP Starting Sequence.



**INTERACTION BETWEEN ENTRY GUIDANCE AND ENTRY DAP**  
(Refer to Section 5 for Entry Guidance)

<u>Event</u>	<u>Action</u>
<u>STARTENT</u>	<ul style="list-style-type: none"> <li>• Initialize Entry. Includes the Switches:  <div style="margin-left: 40px;">LATSW = 1 .05GSW = 0</div> </li> <li>• At End of Pass, Set:  <div style="margin-left: 40px;">Mode to INITROLL POSEXIT to TARGETING</div> </li> </ul>
<u>TARGETING</u>	<ul style="list-style-type: none"> <li>• Preamble to Entry Guidance, entered once each pass. When Drag Acceleration exceeds 0.05 g's, set .05GSW = 1; otherwise, set = 0.</li> </ul>
<u>INITROLL</u>	<ul style="list-style-type: none"> <li>• Initial Phase of Entry.</li> </ul>
<u>KEPLER</u>	<ul style="list-style-type: none"> <li>• Ballistic Phase of Entry.</li> </ul>
<u>NEGTEST</u>	<ul style="list-style-type: none"> <li>• When <math>D &gt; C20</math>, Enforce Roll Over Top. Set:  <div style="margin-left: 40px;">LATSW = 0</div> </li> <li>• Roll DAP will Reset LATSW Each Update</li> </ul>
<u>PREDICT 3</u>	<ul style="list-style-type: none"> <li>• When <math>V &lt; 1000</math> ft/sec, Stop Steering.</li> <li>• Start Up Parallel Job P67.1 Set:        Mode to P 67.2</li> </ul>
<u>P67.2</u>	<ul style="list-style-type: none"> <li>• Calculate Present Latitude, Longitude for Display in P67.1</li> <li>• Exit without Doing Entry Display</li> </ul>
<u>SERVEXIT</u>	<ul style="list-style-type: none"> <li>• Program to terminate computation cycle that began with READACCS.</li> </ul>

Fig. 3.4.8 Milestones in Reentry Steering.

also sets the internal Entry mode selector to INITROLL and POSEXIT to TARGETING. Thus CM/POSE will go directly to TARGETING, the common preamble for all phases of Entry Guidance. As described in Section 5 of this GSOP, the various Entry phases are chosen based on Mode. Note that the entry display is omitted during STARTENT; this is because the range-to-go display is gross. (Two to three iterations yield convergence.)

A summary of Entry Guidance actions that affect the DAP operation is given in Fig. 3.4.8. As indicated, the switch  $\delta$ .05GSW is established in TARGETING. Generally, it will change during INITROLL and KEPLER phases causing the DAP mode to be atmospheric or extra-atmospheric. NEGTEST decides when the vehicle should roll over the top and clears LATSW accordingly. PREDICT3 senses when the relative velocity becomes less than 1000 ft/sec and terminates steering. When this occurs, the DAP maintains attitude hold using the more recent value of  $R_c$ . The steering calculations are replaced by a calculation of present latitude and longitude (P67.2) which are to be displayed in a parallel job of lower priority, P67.1, Fig. 3.4.9. The terminal phase of Entry consists of attitude hold in roll to  $R_c$ , and rate damping in pitch and yaw. During descent, as shown in P67.1, the crew can monitor the flashing display: range to target, present latitude and longitude. This phase is terminated at crew option, but can last until drogue chute deployment. Crew response is PROCEED (TERMINATE is equivalent). On receipt of PROCEED, Entry Guidance is disabled by removing CM/POSE from the "go to" address of AVERAGEG. The Entry DAP is disabled by clearing the flag CM/DSTBY. The clearing of GYMDIFSW is optional. The computer idle routine R00 is entered signifying termination of the Entry Guidance phase.

The actual de-activation of the Entry DAP Software is delayed until the switch CM/DSTBY is examined at the next regularly scheduled update. The shutdown procedure of the DAP is completely specified by the stand-by switch. At the next READGYMB update, if CM/DSTBY = 0, all CM jet thrusters are quenched; the restart mechanism is disabled to clear the restart Group and to prevent restarting the DAP; and READGYMB is not re-established in the WAITLIST. These actions will terminate the DAP cycle. If a restart should occur before the DAP restart mechanism were disabled, the effect would still be the same since CM/DSTBY would be unchanged. The second use of the stand-by switch is to nullify any roll jet activity that is pending. WAITLIST calls to JETCALL, Fig. 3.4.38, are ignored as they fall due, and the p-axis jets are left off. The third use of CM/DSTBY is in READACCS. Those operations performed there relating to the Entry DAP are omitted if CM/DSTBY = 0. Thus, after receipt of PROCEED, the cyclic DAP action ceases within 0.1 second (or 0.2 second if a restart occurred), and all DAP related operations cease within 2 seconds.

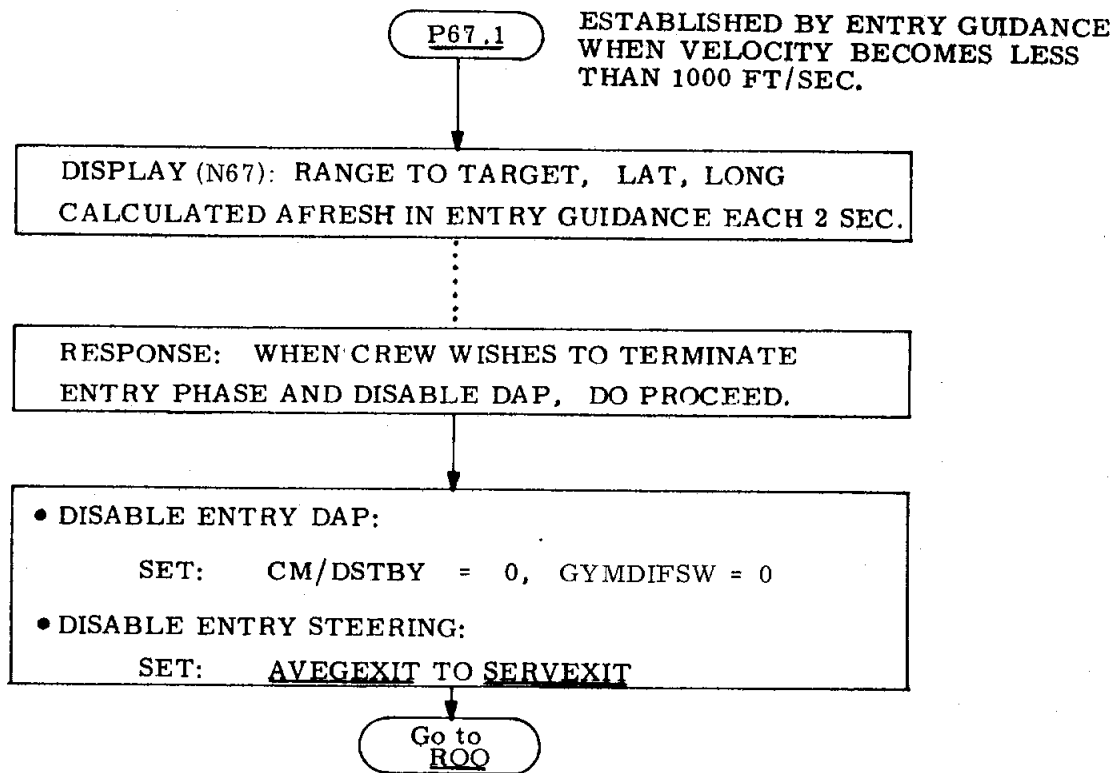


Fig. 3.4.9 Termination of Entry Control (P60s)

### 3.4.4 Entry Autopilot - Introduction

#### Interfaces

The CM interface topics will be discussed before taking up the analytic and computational aspects of the autopilot.

Entry Displays - The DSKY displays associated with the P60's are defined in Section 4 of the present GSOP. In addition, the autopilot is required to provide a display presentation to the FDAI attitude error needles as follows:

Extra Atmospheric DAP - The three attitude errors  $R_c - R$  (or  $R_H - R$ ),  $\beta_c - \beta$ , and  $\alpha_c - \alpha$  are presented each 0.2 second. The error used by the autopilot to fire the p-jets is displayed on the roll needle, the error used to fire the q-jets on the pitch needle, and the error used for the r-jets on the yaw needle. If  $|\alpha| > 135$  deg, the roll DAP does rate damping only, and the roll needle is zeroed every 2 sec.

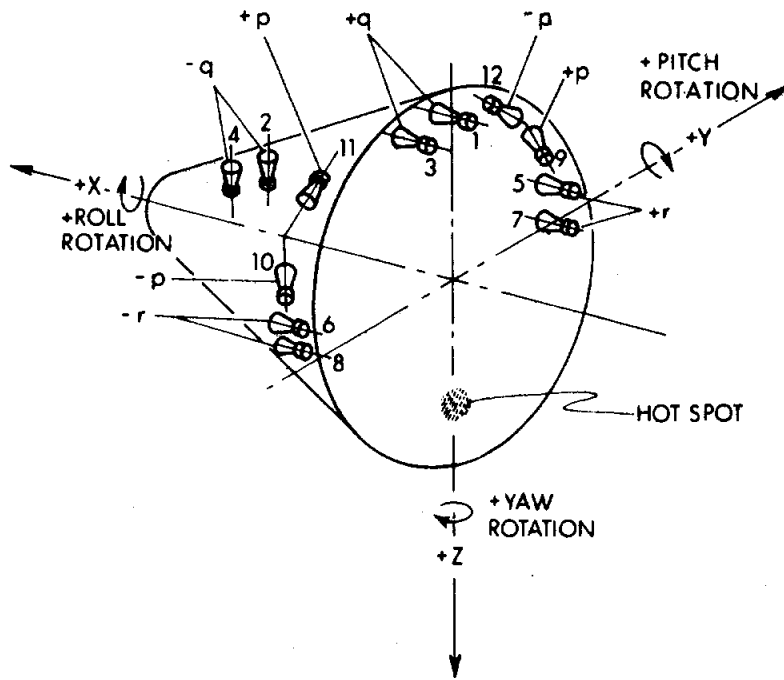
Atmospheric DAP - The only presentation is roll error, corrected for shortest angular path, on a 0.2-second basis. The pitch and yaw error needles are not driven and are at null.

The maximum deflection provided by the CMC to the error needles is  $67.5^\circ$  for roll (p-axis) and  $16.875^\circ$  for pitch and yaw (the q- and r-axes), corresponding to the full-scale calibration 50/15.

Manual Modes for DAP - The Entry DAP operates as though it were autonomous. The CMC Mode switch (HOLD, AUTO, FREE) is not examined. Manual takeover by the pilot will not affect DAP operation nor its display presentation. That is, the DAP will continue to present errors to the FDAI attitude error needles and to put out jet discrettes based on the current CM attitude and rates and the current commands. The disabling of the DAP jet discrettes is effected by hardware outside the CMC. Manual takeover is accomplished by turning the Translation Hand Controller clockwise to bypass the CMC. Control of the vehicle is then exercised by means of the Rotational Hand Controller via the SCS backup. Whenever manual control is relinquished by releasing the THC, the CMC will commence to direct the CM in accordance with current commands and current attitudes and rates.

Jet Thruster Configuration - The control forces exerted on the CM are generated by jet thrusters whose locations are shown schematically in Fig. 3.4.10. The coordinate system is a body-axis triad. The accompanying table identifies the relationship between the principal body rate produced by a given jet, the jet number, the fuel system, the channel number, and the channel bit assignment.

The following sections are devoted to analytical and computational description of the autopilot.



BODY RATE GENERATED	SYSTEM A			SYSTEM B			JOINT OCTAL CODE
	JET NO.	CMC CHAN	BIT	JET NO.	CMC CHAN	BIT	
+ p	9	6	1	11	6	3	00005
- p	12	6	2	10	6	4	00012
+ q	1	5	1	3	5	3	00005
- q	2	5	4	4	5	2	00012
+ r	5	5	5	7	5	7	00120
- r	8	5	6	6	5	8	00240

Fig. 3.4.10 CM Thruster Schematic.

### 3.4.5 Aerodynamic Attitude and Body Rate Estimation

#### Trajectory Triad

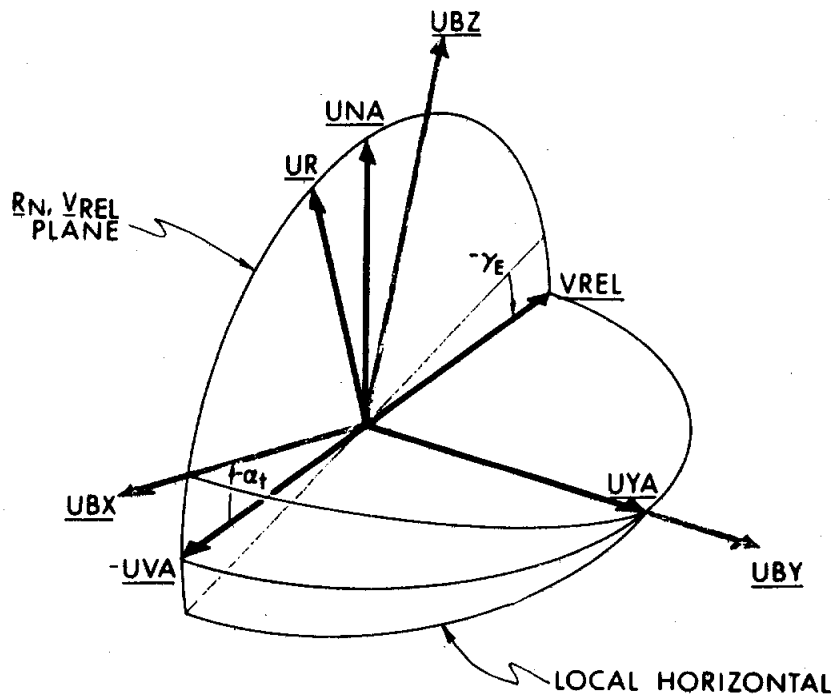
The Inertial Measurement Unit is the source of input data for Entry Guidance and the autopilots. Accelerations in the form of velocity increments are provided by the PIPAs, and the gimbal angle values are communicated by the CDU's. The coordinate system used during Entry is defined in Fig. 3.4.11. During entry the axis of symmetry of the CM is pointed backward along the trajectory and the triad used by the autopilots is - UVA, UYA, UNA. In the figure, the body axis set UBX, UBY, UBZ is shown for  $R$  corresponding to lift-up and for  $\alpha = \alpha_t$  (corresponding to trimmed flight). The Entry angle  $\gamma_E$  is defined as the angle between the local horizontal and the relative velocity vector. The trajectory triad is calculated in CM/POSE, Fig. 3.4.17.

#### Body Triad

The body axis triad of the CM is defined relative to the platform axis set in Fig. 3.4.12 in terms of the three gimbal angles. When all three gimbal angles are zero, the body set UBX, UBY, UBZ and the platform set UPX, UPY, UPZ coincide. At other times the body set is obtained from the platform set by using the Euler gimbal sequence: inner, middle, outer, abbreviated I, M, O. These rotations are pictured in Fig. 3.4.12 along with the transformation equations, (I). The CM unit body triad UBX, UBY, UBZ, expressed in platform coordinates, is computed from equations (II). The body triad is calculated in CM/POSE, Fig. 3.4.17.

#### CM Body Attitude

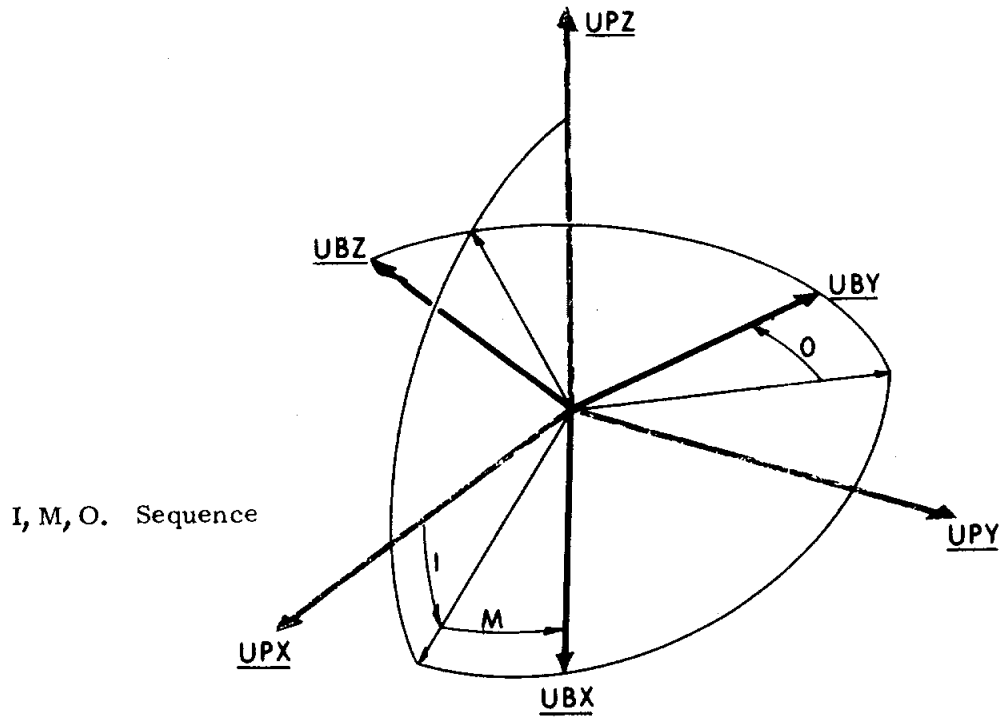
To control the CM in attitude, a measure of attitude is needed. Certainly the gimbal angles form an adequate set. However, the  $R, \beta, \alpha$  Euler angles of Fig. 3.4.13 are another equally valid and in some ways a more desirable set. The CM is to be posed relative to a velocity vector (for Entry, it is the velocity relative to the atmosphere) and the angles  $R, \beta, \alpha$  are a measure of the pose assumed. Entry Guidance will generate commanded roll angles  $R_c$  which are defined in the same way as  $R$ . The angles  $\alpha$  and  $\beta$  are pitch and yaw angles, becoming during atmospheric trim the angle of attack and angle of side slip. These angles are trajectory-related and independent of platform alignment. Computationally it makes little difference whether CM attitude control uses a set of desired gimbal angles or the set  $R\beta\alpha$ . Both are Euler sets and must be treated in some artificial way in order to be used in the phase-plane logic based on a control (or body) axis set. The  $R\beta\alpha$  set has the advantage of providing a continual indication of trajectory-related CM attitude information which is of general use. In addition, some simplification accrues from the overlapping control requirements of the atmospheric and extra-atmospheric DAP's. Briefly, this may be indicated by the attitude rate equations in Fig. 3.4.14. In the third equation,  $R\dot{\beta}$  tends to be negligible under DAP influence so that the  $\alpha$  error and  $\dot{\alpha}$  are assigned to the q-axis. For  $\beta$  error and  $\dot{\beta}$ , p- or r-axis control is



BODY AXES DRAWN FOR LIFT UP ( $R = 0$ )

$$\begin{aligned}
 \underline{UR} &= \text{UNIT}(\underline{R}_N) \\
 \underline{VREL} &= \underline{V} - KWE \underline{UNITW} \times \underline{UR} \\
 \underline{UVA} &= \text{UNIT}(\underline{VREL}) \\
 \underline{UYA} &= \text{UNIT}(\underline{UVA} \times \underline{UR}) \\
 \underline{UNA} &= \underline{UYA} \times \underline{UVA}
 \end{aligned}$$

Fig. 3.4.11 Entry Autopilot Coordinate Triads



$$\begin{pmatrix} \underline{UBX} \\ \underline{UBY} \\ \underline{UBZ} \end{pmatrix} = \begin{pmatrix} 1 & 0 & 0 \\ 0 & \text{CO} & \text{SO} \\ 0 & -\text{SO} & \text{CO} \end{pmatrix} \begin{pmatrix} \text{CM} & \text{SM} & 0 \\ -\text{SM} & \text{CM} & 0 \\ 0 & 0 & 1 \end{pmatrix} \begin{pmatrix} \text{CI} & 0 & -\text{SI} \\ 0 & 1 & 0 \\ \text{SI} & 0 & \text{CI} \end{pmatrix} \begin{pmatrix} \underline{UPX} \\ \underline{UPY} \\ \underline{UPZ} \end{pmatrix} \quad (I)$$

Body triad expressed in platform coordinates

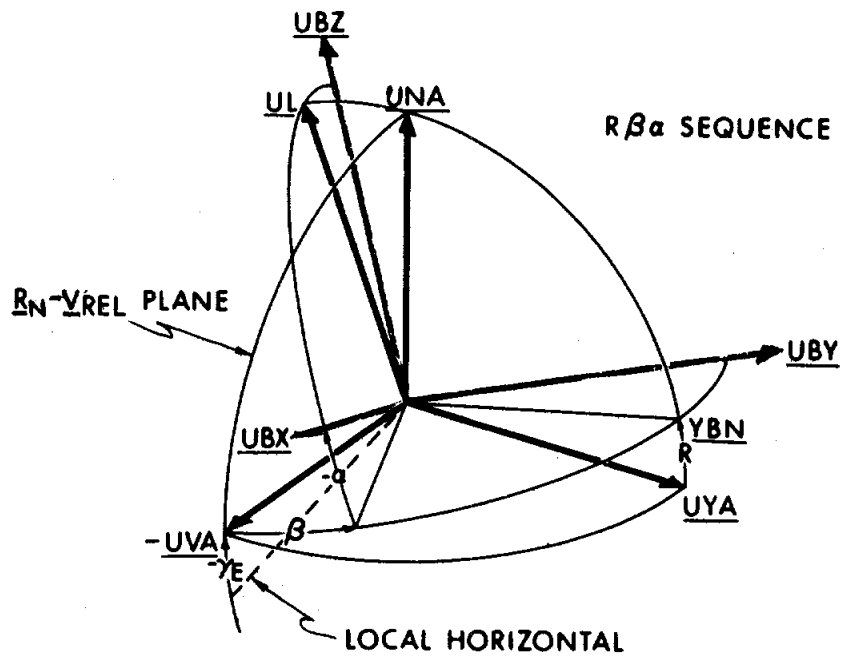
$$\begin{aligned} \underline{UBX} &= (\text{CM CI}, \quad \text{SM}, \quad -\text{SI CM}) \\ \underline{UBY} &= (-\text{CO CI SM} + \text{SO SI}, \quad \text{CO CM}, \quad \text{CO SI SM} + \text{SO CI}) \\ \underline{UBZ} &= (\text{SO CI SM} + \text{CO SI}, \quad -\text{SO CM}, \quad -\text{SO SI SM} + \text{CO CI}) \end{aligned} \quad (II)$$

Body angular velocities

$$\begin{aligned} p &= \dot{O} + \dot{I} \text{ SM} \\ q &= \dot{I} \text{ CM CO} + \dot{M} \text{ SO} \\ r &= -\dot{I} \text{ CM SO} + \dot{M} \text{ CO} \end{aligned} \quad \text{Where SM} = \text{SIN M, etc.} \quad (III)$$

Fig. 3.4.12 Platform to Body Transformation





$$\begin{pmatrix} \underline{UBX} \\ \underline{UBY} \\ \underline{UBZ} \end{pmatrix} = \begin{pmatrix} C\alpha & 0 & -S\alpha \\ 0 & 1 & 0 \\ S\alpha & 0 & C\alpha \end{pmatrix} \begin{pmatrix} C\beta & S\beta & 0 \\ -S\beta & C\beta & 0 \\ 0 & 0 & 1 \end{pmatrix} \begin{pmatrix} 1 & 0 & 0 \\ 0 & CR & SR \\ 0 & -SR & CR \end{pmatrix} \begin{pmatrix} -\underline{UVA} \\ \underline{UYA} \\ \underline{UNA} \end{pmatrix} \quad (I)$$

Fig. 3.4.13 CM Body Attitude Angles - Definition

Combine matrices in Fig. 3.4.13 into single matrix. Calculate attitude angles as for CALCGA. (See Chapter 5)  
 Obtain body angles from

$$\underline{UL} = \text{Unit} (- \underline{UVA} \times \underline{UBY})$$

$$CR = \underline{UL} \cdot \underline{UNA}, \quad SR = -\underline{UL} \cdot \underline{UYA}$$

$$S\beta = \underline{UVA} \cdot \underline{UBY}$$

$$C\alpha = \underline{UL} \cdot \underline{UBZ}, \quad S\alpha = -\underline{UL} \cdot \underline{UBX}$$

For updating angles  $R, \beta, \alpha$  between matrix calculation, integrate the rate equations

$$C\beta \dot{R} = p C\alpha + r S\alpha$$

$$\dot{\beta} = -p S\alpha + r C\alpha$$

$$\dot{\alpha} = q + \dot{R} S\beta$$

Thus

$$R \leftarrow R + \dot{R}\tau$$

$$\beta \leftarrow \beta + \dot{\beta}\tau$$

$$\alpha \leftarrow \alpha + \dot{\alpha}\tau$$

Fig. 3.4.14 Computation of CM Body Attitude Angles

determined by the predominant term of  $\dot{\beta}$ , but generally this choice can be made based on only  $\alpha$ . The remaining attitude rate  $\dot{R}$  is assigned to the alternate axis, by symmetry of the equations. Another viewpoint is that DAP influence on  $\beta$  error and  $\dot{\beta}$  tends to keep  $\dot{\beta}$  small. This is equivalent to a coordinated roll maneuver, and effectively decouples the  $\dot{R}$  and  $\dot{\beta}$  control axes.

The CM attitude angles are defined relative to the trajectory triad -UVA, UYA, UNA and the body triad UBX, UBY, UBZ. Both are expressed in platform coordinates. The defining Euler sequence  $R, \beta, \alpha$  is pictured in Figure 3.4.13 along with the transformation equations (I). When all angles are zero, UBX points away from the heat shield along -UVA, the negative relative velocity vector; UBY lies along UYA, the normal to the trajectory plane; and UBZ lies in the trajectory plane and points along the lift vector. The condition  $R = 0$  corresponds to positive lift or lift up. Rotation of the body triad by rolling about UBX (or -UVA) through the angle  $R$ , causes the lift to have a component out of the trajectory plane. The direction of UBZ can be called UL since it points in the direction of the lift vector. The direction of UBY can be called YBN since for any  $R$  it points in the desired direction for UBY. That is, it is normal to the relative velocity, lying in the UNA, UYA plane. The second rotation is yaw about UL through the angle  $\beta$ . The last rotation is pitch about UBY through the angle  $\alpha$ , shown negative in the picture. The result of the final rotation is to locate the actual CM unit body triad UBX, UBY, UBZ relative to the trajectory triad -UVA, UYA, UNA in terms of the Euler attitude angles  $R, \beta, \alpha$ . The equations for calculating the angles  $R, \beta, \alpha$  and also their derivatives are summarized in Figure 3.4.14.

For the approximations involved in mechanizing the attitude rate equations, see the block diagram, ATTRATES, Fig. 3.4.30.

During almost all of the Entry trajectory, the angular velocity of the trajectory triad is negligible so that control of the CM with respect to the trajectory triad is possible even though the body rates are measured relative to the platform and the body attitude angles are measured relative to the trajectory triad. However, near the end of Entry, the trajectory bends down quite sharply and its curvature can no longer be neglected. For the DAP to continue to control the CM with respect to the trajectory triad, it becomes necessary to measure both the body rates and attitude rates relative to the trajectory triad. This is accomplished by noting that the triad rotation is essentially due to  $\dot{\gamma}_E$ . The equations of Figure 3.4.14 neglected the effect of  $\dot{\gamma}_E$ . By using  $\dot{\gamma}_E$  as a measure of trajectory triad angular velocity, the relative body rates and attitude rates are approximated by the equations in Figure 3.4.15. Use of the relative body rates prevents the DAP from firing jets to oppose the atmospherically generated  $\dot{\gamma}_E$ . A proper

To approximately correct for  $\dot{\gamma}_E$  in rate control relative to relative velocity vector, use

$$\text{prel} = p - S\alpha SR \dot{\gamma}_E$$

$$\text{qrel} = q - CR \dot{\gamma}_E$$

$$\text{rrel} = r + C\alpha SR \dot{\gamma}_E$$

With these, the attitude rate equations keep the same form

$$C\beta \dot{R} = \text{prel} C\alpha + \text{rrel} S\alpha$$

$$\dot{\beta} = -\text{prel} S\alpha + \text{rrel} C\alpha$$

$$\dot{\alpha} = \text{qrel} + \dot{R} S\beta$$

Fig. 3.4.15 Gamma Dot Correction to CM Body Rates

measure of attitude angles is retained by integrating the relative attitude rates between the CM/POSE updates. By correcting the body rates and then using the corrected values wherever required in the DAP, control of the CM with respect to the velocity vector is maintained. The level above which  $\dot{\gamma}_E$  correction is applied is  $\dot{\gamma}_E \text{ min.}$

The computation of equations in Figure 3.4.11 through Figure 3.4.14 is performed in CM/POSE, Figure 3.4.17 and Figure 3.4.18. CM/POSE is entered each two seconds directly from AVERAGEG and uses the new position and velocity to generate the trajectory triad. The body triad is generated using the gimbal angles that were saved during READACCS. Thus the Euler attitude angles which are extracted ( in the figure:  $NEW_R$ ,  $NEW_\beta$ ,  $NEW_\alpha$  ) were valid at the time at which position and velocity were valid: at the PIPA read time. To obtain the present attitude angles, the NEW angles must be corrected for any increment accrued in the interval between PIPA read time and the present. This is easily done since an independent integration of attitude rates is done each 0.1 second to maintain  $R, \beta, \alpha$ . When the NEW values are corrected, they replace  $R, \beta, \alpha$ . Thus CM/POSE prevents accumulation of error in attitude resulting from integration by providing a fresh reference each 2 seconds.

In addition to updating  $R, \beta, \alpha$ , CM/POSE tests to see if the magnitude of the relative velocity  $V$  is less than 1000 ft/sec to provide a warning that subsequent calculations of UYA will be unreliable because UR and UVA approach co-linearity. If the velocity is less than 1000 ft/sec, the last calculation of UYA will be used for the remainder of the flight. The error committed in using an old value of UYA affects only the measure of roll, and is not important at this stage of the flight. The calculation for  $\dot{\gamma}_E$  is chosen to be more accurate in the region where  $\dot{\gamma}_E$  is of possible interest.

Misalignment of IMU. -- The CMC state vector is carried in basic-reference coordinates. When the IMU is not exactly aligned, the CMC matrix REFSMMAT, relating the basic-reference coordinate system to the desired stable-member coordinate system, is in error since the matrix does not define the actual platform alignment. During AVERAGEG navigation, the PIPA  $\Delta v$ 's are measured in stable-member coordinates and must be transformed via REFSMMAT<sup>T</sup> into basic-reference coordinates for integration. A state-vector error accumulates with each integration step as the CM decelerates during entry. The body-attitude angles are defined with respect to the relative-velocity vector and deteriorate progressively but are usable for most of the flight. Near the end of the flight, however, when the actual velocity has fallen to a couple of thousand feet per second or less, deterioration is much more rapid. In these latter stages of entry, even though the roll angle is in error and the steering is based on a bad state vector, the roll axis remains stable. Error in  $\beta$  has little direct effect, since it is used only in the  $\dot{\alpha}$  calculation. (See Fig. 3.4.14.) It is the pitch angle  $\alpha$  that tends to be the most in error; it also has the greatest effect on DAP operation since both the roll-attitude DAP and the yaw damper are affected. (a) The roll-attitude rate equation in Fig. 3.4.14 shows that as  $\alpha$  approaches 90 degrees, the  $p$  contribution due to body roll rate vanishes. The roll DAP, by using  $\cos \alpha$  as a gain factor, recognizes this fact and ceases attitude maneuvers while continuing rate damping. During the period of roll damping, the CM will drift in attitude at deadzone velocities. When  $\alpha$  leaves 90 degrees, the roll DAP will resume attitude control--and with the proper sign. (b) If the on-board estimate of  $\alpha$  were used in the yaw damper, yaw rate errors in excess of the deadzone limit would be sensed if  $1/\cos \alpha$  became sufficiently large; these errors would cause continuous firing of the yaw jets. The jets are too weak to overcome the aerodynamic forces, and the main effect would be to deplete RCS fuel. Because the aerodynamic forces hold the CM in trim attitude, the yaw damper, as mechanized in Fig. 3.4.30, assumes that hypersonic trim applies. Thus, yaw coordination is insensitive to the on-board  $\alpha$  and remains valid during the variation in trim that occurs during transonic and subsonic flight.

#### Angular Velocity Measurement in CM Body Axes

The body angular velocities roll  $p$ , pitch  $q$ , and yaw  $r$  are measured in the positive sense about the respective axes UBX, UBY, UBZ and are obtained from the gimbal-angle rates using the sequence I, M, O of Fig. 3.4.12. When the gimbal angles are zero, body axes coincide with platform axes and the rates  $p$ ,  $q$ ,  $r$  are equal to the respective gimbal rates  $\dot{O}$ ;  $\dot{I}$ ,  $\dot{M}$ . When the gimbal angles are not zero, the body rates are obtained from equations (III) of Fig. 3.4.12.

Measurement of the gimbal rates, and hence of the body rates, is not continuous but occurs at regular time intervals as indeed do all calculations done by the CMC. The basic computation cycle for Navigation and Guidance is 2 seconds.

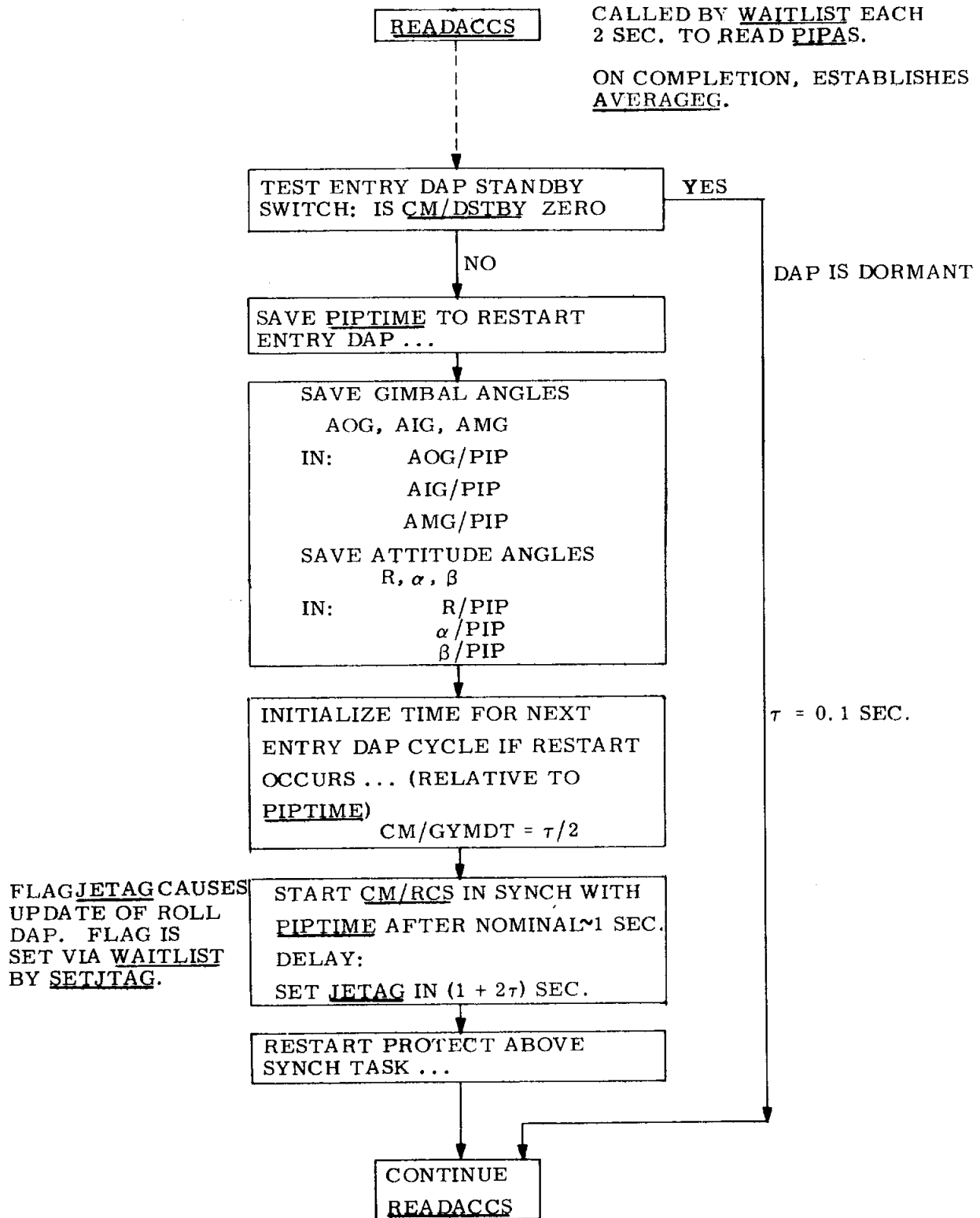
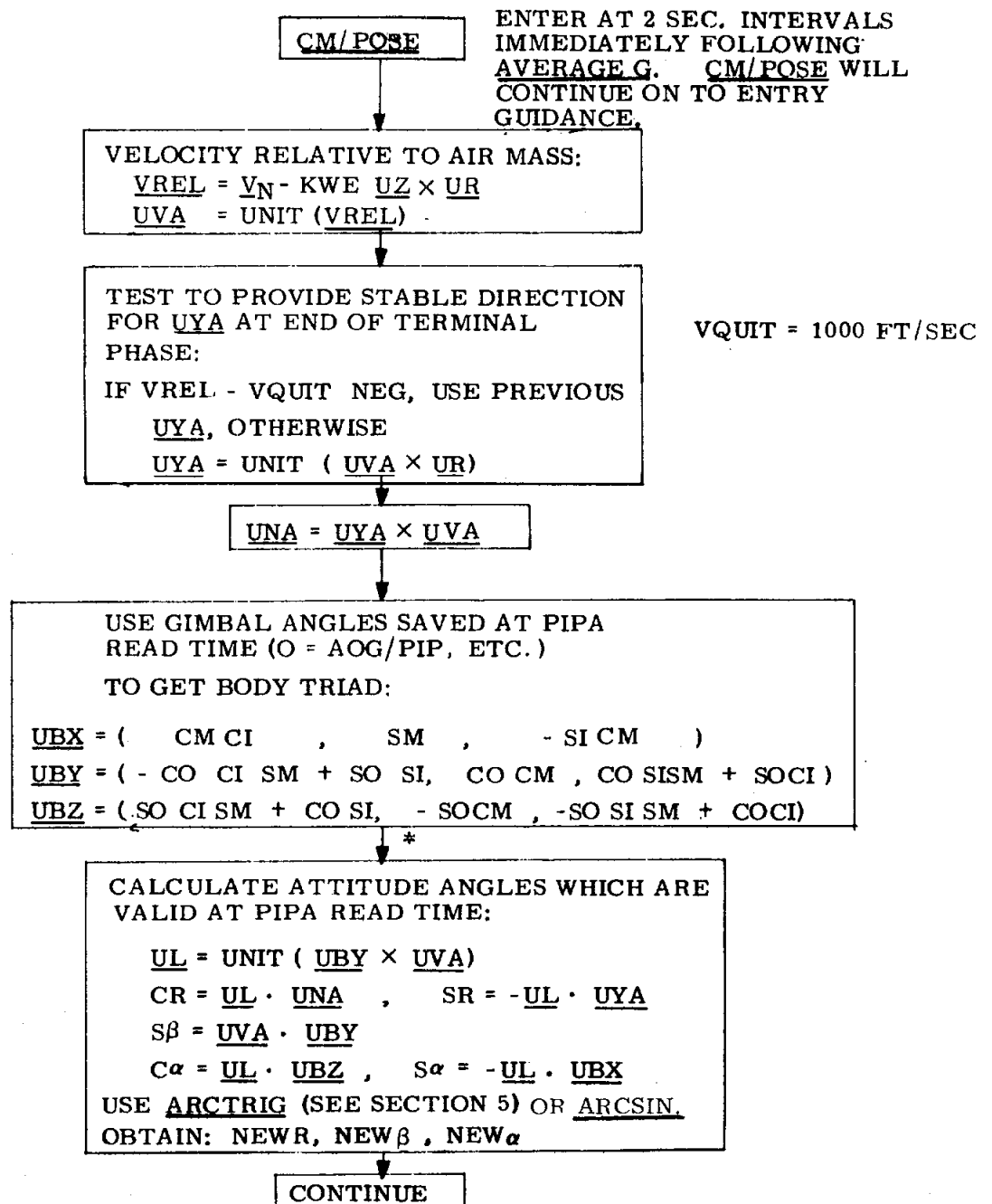


Fig. 3.4.16 Initialization of Body Attitude Calculation (CM/POSE).



\* REFSMMAT NOTE: For simplicity, the text is written using the IMU, or stable-member coordinate system. In the flight rope, however, the AVERAGEG state vector is in the basic-reference coordinate system, necessitating use of  $\text{REFSMMAT}^T$  at this point in order to transform the body triad from stable-member to basic-reference coordinates.

Fig. 3.4.17 Calculation of Attitude Angles.

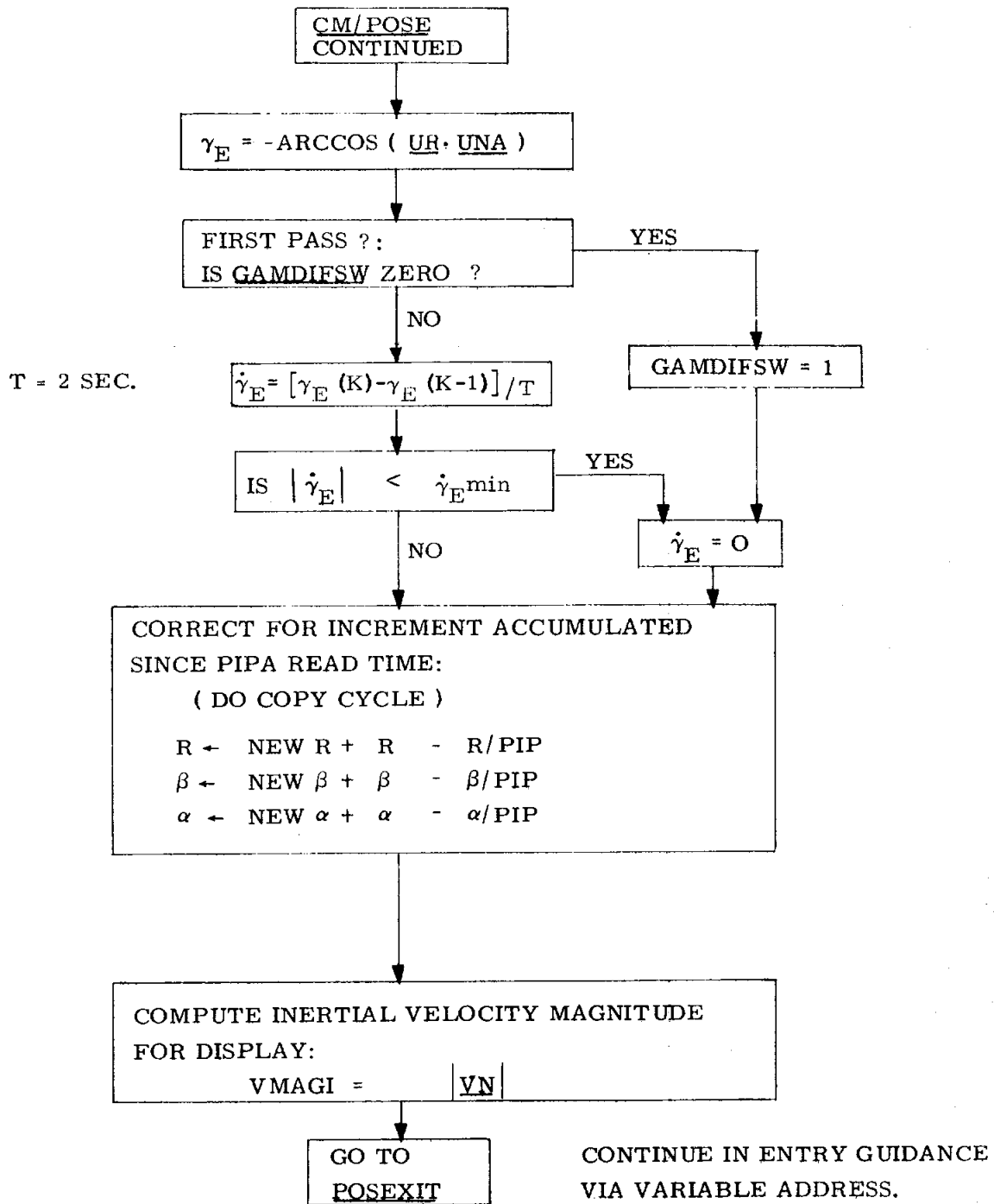


Fig. 3.4.18 Attitude Calculation, continued



Body rates must be determined more frequently, and the computation cycle time chosen is  $\tau$  (0.1 sec). Thus each interval  $\tau$ , the gimbal angular rates required by (III) are measured as CDU angular differences in the manner

$$\dot{O} \tau \approx \Delta O = O_k - O_{k-1}$$

and is illustrated in detail in READGYMB (Fig. 3.4.28). Using the measured gimbal differences  $\dot{O}\tau$ ,  $\dot{I}\tau$ ,  $\dot{M}\tau$ , (III) yield body rates as differences  $p\tau$ ,  $q\tau$ ,  $r\tau$ . These differences represent body rates that are exact only if the angular accelerations are zero. A better estimate is obtained from the measured  $p\tau$ ,  $q\tau$ ,  $r\tau$  by the simple algorithm which corrects for constant acceleration.

$$\dot{\theta} \tau \approx \Delta \theta = \Delta \theta_1 + \frac{\Delta \theta_1 - \Delta \theta_0}{2}$$

where the subscript 0 refers to the previous value of a difference and 1 refers to the present value. For each body rate in turn, substitute the present difference and the previous difference in place of the thetas, as shown in BODYRATE (Fig. 3.4.29). By previous difference, the previous result of (III) is meant, not the previous average. This fact is not made explicit in the referenced figure. The rate estimation program RATEAVG is shown in Fig. 3.4.33.

The CDU is a two-rate gimbal-angle readout device. If the gimbal angle rate exceeds about  $4^\circ/\text{sec}$ , the CDU will follow by alternating between high rate and low rate. The CDU angle indicated to the CMC as a result will contain a high-frequency sawtooth component of peak-to-peak amplitude about  $0.1^\circ$ . Therefore, the angular velocity estimates derived by differencing the CDU angles over a 0.1-sec interval will contain noise of the order of  $1^\circ/\text{sec}$  (when the vehicle rate exceeds  $4^\circ/\text{sec}$ ). Testing indicates this estimation error has no significant effect on autopilot performance.

The body angular velocities are calculated in BODYRATE, Fig. 3.4.29. After the averaged body rates are obtained from equations (III) of Fig. 3.4.12 with the aid of RATEAVG, the  $\dot{\gamma}_E$  correction is applied using the equations of Fig. 3.4.15. In this calculation, however, the estimated  $\alpha$  is replaced by a nominal value ( $\alpha_{\text{trim}}$ ) in order to reduce the  $\alpha$  body-rate error due to cumulative state-vector error. When the DAP is not in standby, the program picks up at ATTRATES, Fig. 3.4.30, and the body attitude rates are integrated to yield attitude angles as shown in Fig. 3.4.14. Since the integration occurs in interrupt and the rectification takes place under interrupt inhibit, there is no chance of an update being lost.

This is the end of the measurement portion of the DAP. The following paragraphs are devoted to the control portion.

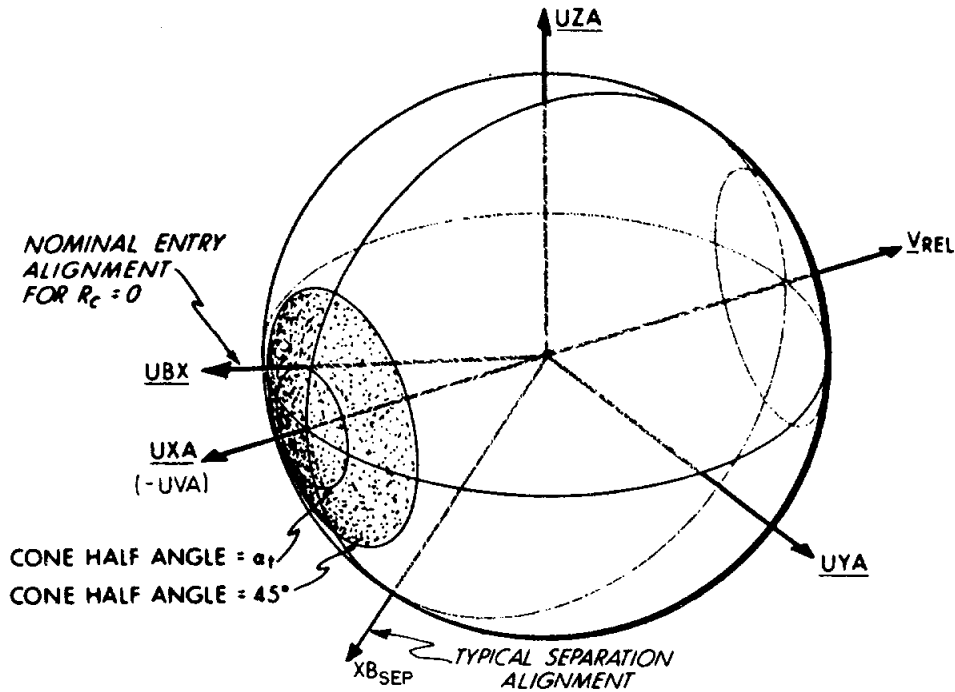
### 3.4.6 Extra-Atmospheric DAP

The CM autopilot function outside the atmosphere is fundamentally attitude control in all axes. Inside the atmosphere, attitude control is used only for roll, and rate damping is used for pitch and yaw. To minimize the size of the DAP software, multiple use is made of program logic wherever permissible.

It is convenient to categorize DAP action outside the atmosphere in terms of the size of  $\alpha$ , as is suggested by the attitude rate equations of Fig. 3.4.14. By quadranting  $\alpha$  relative to  $45^\circ$ , the attitude rates can be considered as being controlled by a single body rate. In  $\dot{\beta}$  for example, if  $|\alpha| > 135^\circ$  then  $r$  is the predominant term and  $\beta$  error can be assigned to the yaw axis. The control effectiveness of  $r$  diminishes if  $p$  is several times greater than  $r$  or if  $|\alpha|$  is near  $135^\circ$ . These restrictions do not seriously affect the present design, however. In Fig. 3.4.19, the assignment of Euler attitude errors in this manner to body axes is summarized. The region  $|\alpha| > 135^\circ$  is not expected to be entered, since nominal separation attitude is well outside the region. However, the DAP must be able to recover from any attitude, subject to restrictions of gimbal lock. (More will be said later of gimbal lock.) In the region of  $\text{CMDAPMOD} = -0$ , rate damping in roll is enforced to keep  $p$  small. Ideally, the roll maneuver from  $R$  to the initial entry value  $R_c$  should be performed completely, either before starting the pitch maneuver or after its completion. However, a maneuver of this type requires a predetermined sequence of maneuvers: do completely the roll maneuver about the body x-axis and then do the pitch, or do the pitch maneuver completely and then do the roll about the body x-axis. The present design elects to perform combined maneuvers where possible in a coordinated manner to remove the requirement of knowing when any one maneuver is fully completed. To this end, the roll maneuver is not initiated until the pitch maneuver enters the region  $|\alpha| < 45^\circ$  ( $\text{CMDAPMOD} = +0$ ). The  $\alpha$  and  $\beta$  attitude DAP is intended to execute maneuvers of  $2^\circ/\text{second}$ . Cross-coupling between thrusters, however, makes an upper bound necessary, and  $4^\circ/\text{second}$  is used. The phase plane logic (Fig. 3.4.20) of the 0.1-second DAP, used by both  $\alpha$  and  $\beta$ , is also used by  $R$  if  $\text{CMDAPMOD} = +1$ . Otherwise, the predictive phase plane (Fig. 3.4.24) of the 2-second DAP is used by  $R$ .

#### Overall Operation of EXDAP

The automatic maneuver from separation to entry attitude normally begins within the interval  $45^\circ < |\alpha| < 135^\circ$ . When separation is acknowledged by the pilot, the DAP is started up and maintains attitude hold as was described in P62, Fig. 3.4.4. On receipt of the new commands, the DAP will start the  $\alpha$  and  $\beta$  maneuvers and continue attitude hold in  $R$ . The reason for the latter is that the direction of the pitch maneuver in inertial space is determined by the roll angle  $R$ . Middle gimbal excursion is reduced in this way. In this region of  $\alpha$  ( $\text{CMDAPMOD} = +1$ ), the



	EXOATMOSPHERE			ATMOSPHERE
	$ \alpha  < 45 \text{ deg.}$	$ \alpha  > 135 \text{ deg.}$	$45 <  \alpha  < 135 \text{ deg.}$	$\alpha \sim \alpha_t$
CMDAPMOD	+0	-0	+1	-1
Roll	Attitude-control error = $\text{sgn}(C_\alpha)(R_c - R)$ rate = $p$ axis = $p$	Enforce rate damping error = 0	Attitude hold error = $\text{sgn}(S_\alpha)(R_H - R)$ rate = $r$ axis = $r$	Attitude-control error = $R_c - R$ rate = $p$ axis = $p$
Beta	Attitude-control error = $\text{sgn}(C_\alpha)(\beta_c - \beta)$ rate = $\dot{\beta}$ axis = $r$	rate = $r$	Attitude control error = $\text{sgn}(-S_\alpha)(\beta_c - \beta)$ rate = $\text{Sgn}(-S_\alpha)\dot{\beta}$ axis = $p$	Yaw-rate damp- ing with roll coordination rate = $r - p \tan \alpha$ axis = $r$
Alpha	Attitude- control error = $\alpha_c - \alpha$ rate = $q$ axis = $q$			Pitch-rate damp- ing rate = $q$ axis = $q$

Fig. 3.4.19 Entry Autopilot Attitude Modes.

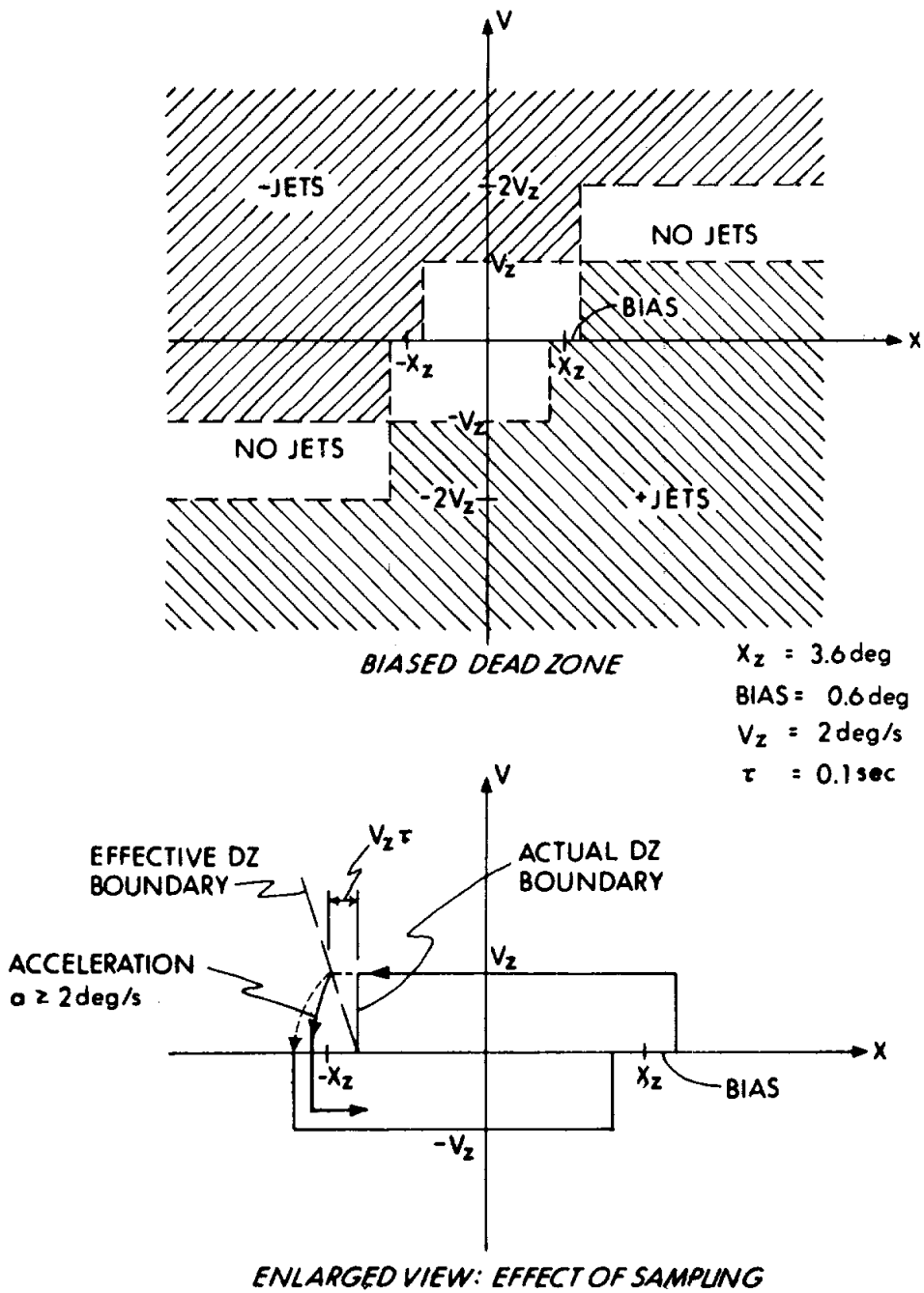


Fig. 3. 4. 20 Phase Plane Logic for CM Attitude DAP.

control axes for R error and  $\beta$  error are interchanged from the normal as shown in Fig. 3.4.19. All three axes are attitude controlled and obey the same phase-plane logic each 0.1 second. The rates when not in the dead zone will be between  $2^\circ/\text{sec}$  and  $4^\circ/\text{sec}$ .

In the interval  $|\alpha| < 45^\circ$  (CMDAPMOD = + 0); R error and  $\beta$  error return to their proper axes as shown.  $\alpha$  and  $\beta$  continue to share the same phase-plane logic, but roll control is changed from the 0.1-second update to the 2-second predictive attitude DAP (CM/RCS). A test is made to recognize the transition of  $|\alpha|$  across the  $45^\circ$  boundary and to assure that the p-jets are off. This is necessary since the time interval until the first CM/RCS update can be as much as 2 seconds. The WAITLIST call to WAKEP62 (Fig. 3.4.5) is also made at this transition. In general  $\beta$  will be zero by this time, so any remaining roll error will be nulled in a coordinated manner... a desirable feature should the CM encounter the atmosphere ahead of schedule.

The attitude commands for the extra-atmospheric phase of flight were discussed earlier, and are outlined in Table 3.4-I. The mechanization of the control portion of the extra-atmospheric DAP is EXDAP, Fig. 3.4.31.

#### Gimbal Lock

The subject of gimbal lock has been lightly treated since its avoidance is not a DAP function, but a crew procedure. The DAP will not generate abnormally large middle gimbal angles after a nominal separation. Large MGA excursion results from two things: a) roll angle accumulation during the uncontrolled interval following separation and b) the coordinated roll maneuver enforced during a  $180^\circ$  roll after  $|\alpha| < 45^\circ$ . Item (a) is unwanted, but is not serious unless the roll angle is large. For nominal IMU alignment, the desired condition at the start of the pitch maneuver is that the outer gimbal angle be near zero or  $180^\circ$ . The crew can reduce unwanted MGA excursion by manual maneuver prior to starting the automatic EXDAP pitch maneuver. If the crew maneuver is performed before the PROCEED signifying separation is keyed into the DSKY, the DAP will hold at the new attitude since, after separation, the ENTRY DAP does attitude hold in roll until  $|\alpha|$  becomes less than  $45^\circ$ . A large separation transient in roll can be corrected by rolling the CM to the nearest zero or  $180^\circ$  of the outer gimbal. The  $180^\circ$  roll maneuver can be done in the same way.

#### Manual Interaction

The manual over-ride properties of the DAP require some amplification. When first turned on in P62, the DAP performs the three-axis attitude hold. For pitch and yaw control, the commands  $\alpha_c$ ,  $\beta_c$  are set equal to present attitudes

$\alpha$ ,  $\beta$ . The present roll attitude is set into both roll command registers  $R_C$  and  $R_H$ . The reason for this is that two roll DAPs exist:

- a. the two-second DAP, using  $R_C$  as roll command, operates when  $|\alpha| < 45$  deg or  $|\alpha| > 135$  deg.
- b. the 0.1-second DAP, using  $R_H$  as its command, operates when  $45$  deg  $< |\alpha| < 135$  deg.

The contents of  $R_H$  will be maintained at values intended to provide continuity to the roll-axis control in the presence of manual override. This is accomplished by using current roll-attitude  $R$  when  $|\alpha| > 135$  deg, and by using roll-command  $R_C$  each time the deadzone is entered when  $|\alpha| < 45$  deg.

The CM will maintain attitude hold to the saved commands, with the following exception: when  $|\alpha| > 135$  deg, the roll DAP does only rate damping. (It considers that the attitude error is zero.) Thus, in the region  $|\alpha| > 135$  deg, if the crew manually rolls the CM, the DAP will accept the resulting attitude as defining the roll-command  $R_H$  to be used during the pitch maneuver to  $|\alpha| = 45$  deg. However, since the CM will pitch in the direction defined by  $R_H$ , the resulting roll attitude, above, should be either 0- or 180-deg outer-gimbal angle (assuming preferred entry IMU alignment) in order to avoid excessive middle-gimbal excursion. The attitude-hold mode is terminated when the crew responds to NOUN 61 in P62, and the entry trim values are established:

$$\begin{array}{l} \alpha_C = \alpha_t, \quad \beta_C = 0 \\ R_C \text{ as specified} \end{array} \left\{ \begin{array}{l} 0 \text{ deg for liftup} \\ 180 \text{ deg for liftdown} \end{array} \right.$$

When the CM approaches these conditions (either automatically or manually), the two-second roll DAP, on entering the deadzone, will save  $R_C$  in  $R_H$ . Thus, if manual override subsequently takes the CM from  $|\alpha| < 45$  deg back into the region  $|\alpha| > 45$  deg,  $R_H$  then contains the desired entry roll angle  $R_C$ , and roll-attitude hold will not be interrupted. On the other hand, if the override takes the CM into the region  $|\alpha| > 135$  deg, the DAP will put the current roll attitude into  $R_H$  in order to prevent having a large roll error as  $|\alpha|$  becomes less than 135 deg. The updating of  $R_H$  in the foregoing manner will provide some degree of roll-axis continuity and allow the DAP to be relatively insensitive to manual override. When manual control is relinquished, the DAP will pickup and will maneuver the CM into a condition of trim with respect to the present velocity vector. P63 will be started the first time that the DAP recognizes that  $|\alpha| < 45$  deg. Subsequent manual maneuvering will not initiate P63 again.

#### Detailed Description EXDAP

It is convenient to discuss the 0.1-second sampled DAP separately from the 2-second predictive roll DAP. The latter is included in the atmospheric section, even though its services are used outside the atmosphere.

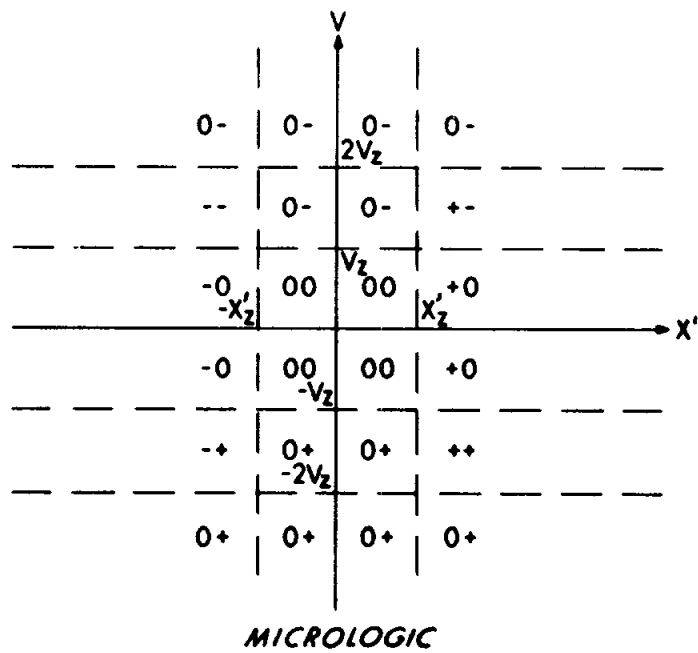
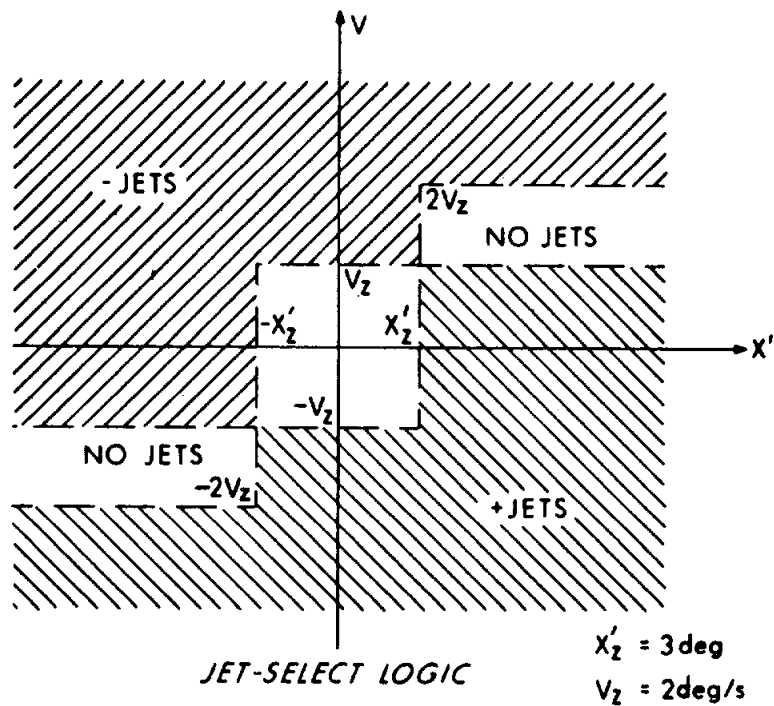


Fig. 3.4.21 Phase-Plane Logic (without Bias) for CM Attitude DAP.

The phase-plane logic for the sampled attitude DAP is common to all those axes operating at the  $\tau = 0.1$  second interval. The variables are attitude error, and rate error in the control axes. The phase plane logic is given in Fig. 3.4.20. A biased dead zone is employed to obtain a minimum limit cycle frequency. A closer view is in the lower part of the figure. Since the  $dz$  is used on a sampled basis, it is effectively enlarged by one sample time and proportionally to velocity. A point having velocity  $V_z$  traces the boundary trajectory, shown dotted. For the dead zone parameters chosen, a trajectory will always enter the negative half through the offset if the acceleration is greater than  $2^0/s/s$ . The degree of penetration depends on the actual value of acceleration over the number of samples. Typical values of acceleration for single-ring operation of the CM are between  $3^0/s/s$  and  $6^0/s/s$ . Symmetrical (theoretical) limit cycles have periods of the order of 60 seconds. But in practice steady state is not reached, yielding assymetrical cycling of potentially longer duration.

To render the description of the phase plane specific, let  $X = \beta_c - \beta$  be the error,  $V = \dot{\beta}$  be the velocity, and the jet axis be  $r$ . Further, let  $X' = X - \text{SGN}(V)$  BIAS. The equation for  $X'$  converts the unbiased  $dz$  into a biased one. The following description is based on the unbiased  $dz$  in Fig. 3.4.21.

Both  $X'$  and  $V$  are to be kept within specified limits: the range  $(-V_z, V_z)$  for  $V$  and the range  $(-X_z', X_z')$  for  $X'$ . Within the area bounded by these limits, jet thrusters are turned off. If  $|X'| < X_z'$ , but  $V > +V_z$ , negative jets are desired and are indicated by the minus sign. Similarly, if  $V$  exceeds the lower bound, positive jets are required. If  $|V| < +V_z$ , and  $X' > +X_z'$ , positive jets are required to establish a positive velocity to reduce the error  $X'$ . As indicated, the positive jets remain on until at a sample interval  $V$  has exceeded  $V_z$ , when all jets are turned off. The positive velocity causes the point  $(X', V)$  to drift leftward. At a subsequent sample instant,  $X'$  is observed to be less than  $X_z'$  but  $V > +V_z$  and negative jets are actuated. In this manner arbitrary initial conditions  $(X', V)$  of reasonable value are caused to enter the central box. If these were the only jet thrusters or if there were no cross coupling, this would be the whole story. However, coupling from thrusters on other axes as well as coupling of  $\alpha$  and body rates causes the velocity to increase above  $V_z$  by an undesirable margin. The addition of the upper bound at  $2V_z$  constrains  $V$  to have acceptable values.

In actual operation both  $X'$  and  $V$  are separately tested against limits. A tag is set to zero if the limit is not exceeded, and to  $\pm 1$  bit depending on the sign of the limit exceeded. In Fig. 3.4.21 the pairs of signs refer to the result of both tests, where the two tags are shown in the order  $(X', V)$ . The tags are combined in a "logical or" using ones complement arithmetic to generate a single tag. The resulting tag is used to select the proper jet code from a list for the axis being



controlled ( $r$  in the present example). When a jet code is executed, only the jets designated by the code are fired or are left on if already firing. All other jets are quenched. A tag of value zero quenches any jets that might be firing. Figure 3.4.10 which showed jet geometry also lists the jet codes but not in indexable form.

The flow diagrams that apply to the extra-atmospheric DAP are READGYMB Fig. 3.4.28, through RATEAVG, Fig. 3.4.33. Subsequent figures also apply when CM/RCS is used, but are not discussed yet. The diagrams are sufficiently annotated so as not to need further comment. Table 3.4-II lists jet codes in indexable form.

### 3.4.7 Atmospheric DAP

Before encountering the atmosphere, all CM body attitude errors will be at null or nearly so, and the DAP mode will be characterized by  $|\alpha| < 45^\circ$  (or CMDAPMOD = +0) in Fig. 3.4.19. When the 0.05-g level is sensed by Entry Guidance, a switch is set. The DAP observes the switch and changes the DAP mode to -1, and the  $q$  and  $r$  control to pitch and yaw dampers. The predictive roll system CM/RCS is already activated and performing and is ready to accept commands when issued by Entry Guidance. Later on, when the ballistic phase is entered, the switch .05GSW is cleared. The DAP is able to slip easily back into the mode +0 and as easily out again when .05GSW is once more set to 1 (see Fig. 3.4.19).

In the atmosphere, the CM is controlled during flight by orienting the lift vector. The amount of lift available for control purposes, i. e., the ratio of lift to drag (L/D), is determined by the c. g. location. Preflight ballast procedures ensure that the  $z_{cg}$  offset will give the desired L/D. The corresponding trim pitch angle is  $\alpha_t$ . The yaw trim results from the  $y_{cg}$  offset, and is kept as small as possible. In actual flight, the  $y_{cg}$  residual causes small  $\beta$  trim, of the order of a degree or so. For L/D of 0.3, the pitch trim  $\alpha_t$  is about -20 degrees, and remains relatively constant throughout hypersonic flight. As the transonic region is approached,  $\alpha_t$  increases about 8 degrees or so. When the CM goes subsonic,  $\alpha_t$  decreases to about 8 degrees below the hypersonic value and becomes a new trim value of around -12 deg. The DAP will tolerate such changes in  $\alpha_t$ .

#### Functional Behavior of Atmospheric Autopilots

In Entry Guidance, control is based on the components of lift in and normal to the trajectory plane, components that are specified in terms of an angle defined the same as  $R$  but having value  $R_c$ . If the CM is to achieve the desired lift direction, then the  $Y$  body axis UBY must lie along YBN, Fig. 3.4.13. This condition is met when  $\beta = 0$ . Thus one property of the Entry autopilot is to keep  $\beta = 0$  and another is to have the actual vehicle roll angle  $R$  agree with the desired value  $R_c$ .

Within the atmosphere, aerodynamic forces tend to keep  $\beta$  essentially zero, and  $\alpha$  assumes a trim value  $\alpha_t$  so that attitude control is required only in

roll. As the CM rolls, UB<sub>Y</sub> should remain normal to UVA. When  $\beta = 0$  and  $\alpha$  is constant, such a maneuver causes UB<sub>X</sub> to describe a cone of angle  $2\alpha$  about -UVA while UB<sub>Z</sub> similarly describes another cone about +UVA. This condition of rolling about the velocity vector; or making a coordinated roll, is equivalent to requiring that the CM angular velocity vector lie along -UVA. In the atmosphere, then, coordinated roll maneuvers are enforced by the angular rate autopilots already required to damp pitch and yaw body rates caused by dynamic behavior of the CM.

Figure 3.4.13 shows that for the ideal case,  $\beta = 0$ , only roll and yaw rate are present if the body angular velocity is to lie along -UVA. Further, this angular velocity is equal to the rate of change of roll angle R. A third property of the atmospheric autopilot is that it enforce the proper proportionality between yaw and roll rate necessary to produce coordinated roll.

Table 3.4-II Table of Jet Codes

TABLE NAME	JET AXIS	OCTAL CODE
Yaw Code	+r jets on	00120
	jets off	00000
	-r jets on	00240
Roll Pitch Code	+p, +q jets on	00005
	jets off	00000
	-p, -q jets on	00012

(See also Fig. 3.4.10)

NOTE . -- Sign convention of Fig. 3.4.21: Positive tag selects positive jets.

-- Sign convention of DAP flow charts: Positive tag selects negative jets.

In the atmospheric mode, rate damping is used to maintain pitch and yaw angular velocities within prescribed limits. The digital autopilots perform this function in a discontinuous manner by producing a control action each time new input data are available. Thus, the pitch and yaw autopilots are exercised each 0.1 second immediately following the measurement of angular velocity.

#### Pitch Damper DAP

The pitch-axis autopilot for the CM performs rate damping action using the simple logic of Fig. 3.4.22a, which is the single axis representation of Fig. 3.4.21. As long as sampled pitch rate is less than  $2^\circ/\text{sec.}$ , no action is taken and the jet thrusters are off. Whenever sampled pitch rate exceeds  $2^\circ/\text{sec.}$ , the jet thrusters are activated to produce opposing torque. The jets remain firing until the pitch rate is observed to be less than  $2^\circ/\text{sec.}$  Because of the digital nature of rate measurement, jet switching is based on the value of the rate at the time of measurement, which in general will not be exactly  $2^\circ/\text{sec.}$  Hysteresis, a result of the 0.1-sec interval between control actions, is present at the nominal  $2^\circ/\text{sec}$  switching discontinuity and prevents the formation of high frequency limit cycles in the presence of pitch acceleration. The hysteresis zone is of variable width and can be as large as twice the total  $\Delta V$  achievable by the jets in one sample time (Fig. 3.4.22b).

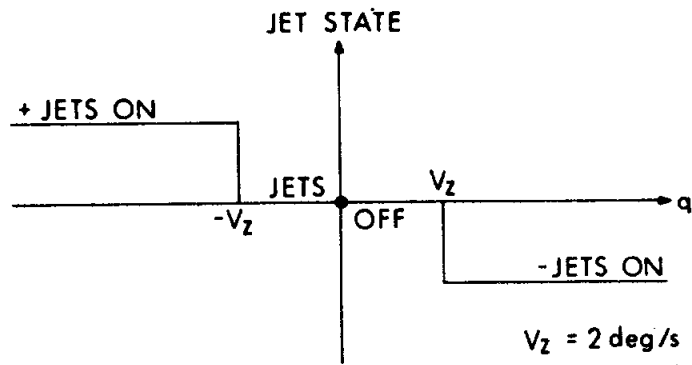
#### Yaw Damper DAP

The yaw axis requirements are somewhat different than pitch. The CM must roll about the velocity vector in order to maintain nominal trim attitude and to keep the stagnation point in a fixed region on the heat shield. Figure 3.4.23 illustrates the situation in the UBX, UBZ plane. The UBY component of  $\underline{V}_{REL}$  is kept essentially zero by the aerodynamic force so that the velocity shown can be considered to be the total velocity  $\underline{V}_{REL}$ . In the coordinated turn illustrated, the angular velocity vector lies along  $-\underline{V}_{REL}$  if the angular velocities in yaw and roll are related by

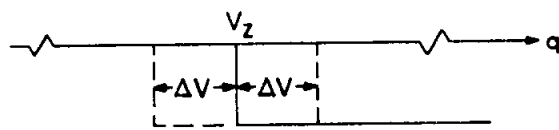
$$r = p \tan \alpha$$

and if pitch angular velocity  $q = 0$ . Even when the latter condition is not exactly fulfilled, the equation is still useful. Since cumulative state-vector error may eventually cause the indicated  $\alpha$  to be grossly wrong, however, the coordination term  $[\tan(\alpha)]$ , is replaced by  $\tan(\alpha_{trim})$  in the flight rope. This ensures yaw control throughout the expected range of aerodynamically enforced trim, and is independent of the onboard measure of  $\alpha$ .

During periods of angular acceleration in roll, a corresponding acceleration in yaw is quickly established and supported by aerodynamic forces. We utilize these forces to encourage the CM to make a coordinated turn. The bulk of the work is done by the aerodynamics with the yaw jet thrusters operating only as needed according to Fig. 3.4.23. The jets fire when necessary to keep the vehicle within the central band. This allows  $r$  to be proportional to  $p$  and at the same time keeps yaw oscillations damped to within  $\pm 2^\circ/\text{second}$ .

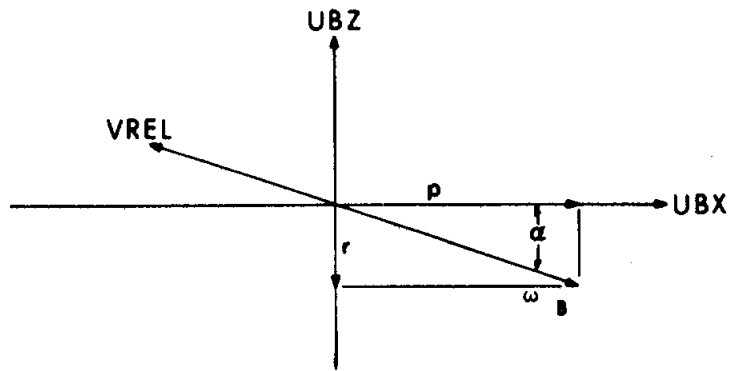


a. *PITCH RATE DAMPER*



b. *HYSTERESIS EFFECT*

Fig. 3.4.22 CM Pitch Rate Autopilot



Coordinated Roll

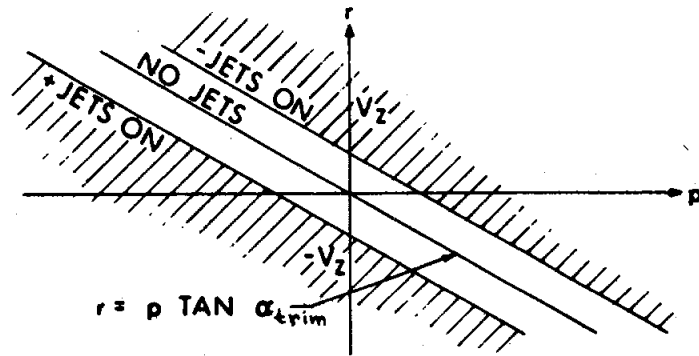


Fig. 3.4.23 CM Yaw Rate Autopilot

The yaw damper operates at the 0.1-second sample interval established by the angular velocity measurements and exhibits the same switching boundary hysteresis as the pitch damper.

The flow diagrams that apply to the atmospheric (damping) DAP for  $q$  and  $r$  are READGYMB, Fig. 3.4.28, through ATTRATES, Fig. 3.4.30.

#### 3.4.8 Roll Attitude Control - CM/RCS

Every 2 seconds during the entry phase, Entry Guidance provides a roll command  $R_c$ . To do this, it examines vehicle current position and velocity and also landing point position, decides on the proper orientation of the lift vector, and generates the commanded roll attitude of the CM necessary to achieve that orientation. The roll autopilot uses the command  $R_c$ , the present roll attitude  $R$ , and roll rate  $p$  to generate firing times for the jet thrusters. In general, there are three time intervals generated each 2 seconds. Two are thrust durations, and one is quiescent duration. Having obtained the time intervals, there remains the bookkeeping task of implementing the result of the calculations.

Bookkeeping consists of maintaining a short list containing pairs of entries: a jet thruster selection code and a time duration. The jet code specifies which jets are to be turned on or off and the time duration specifies the interval until the next change in jet activity occurs. Bookkeeping is carried out with the aid of the TIME3 preset timer (WAITLIST) in the CMC. The list contains only entries which can be executed within a single two-second interval.

#### Logic in Phase Plane with Control Line

The roll model for the CM is a simple inertia which makes the phase plane an attractive tool because motion is described by straight lines and parabolas. The  $(X, V)$  phase plane of Fig. 3.4.24 is used where  $X = R_c - R$ , and  $V = \dot{R}$ . When the CM has the commanded attitude, both  $X$  and  $V$  are zero, and the point  $(X, V)$  representing the state of CM motion is at the origin. Bear in mind that roll rate  $p$  is related to  $R$  by  $\cos \alpha$  in a coordinated roll. Although not necessary to the understanding of the roll DAP phase-plane logic, this knowledge is helpful when reading the flow chart mechanization. The DAP assumes that a coordinated roll obtains, and uses the current value of  $\cos \alpha$  to scale one axis of the phase plane so that velocity  $V$  and change in error  $\Delta X$  are compatible. Incompatibility results in overshooting the origin and costs fuel. The X-axis is selected for the  $\cos \alpha$  term in DAP mechanization, which means that  $V = p$ , and  $X = (R_c - R) \cos \alpha$  in the following discussion.

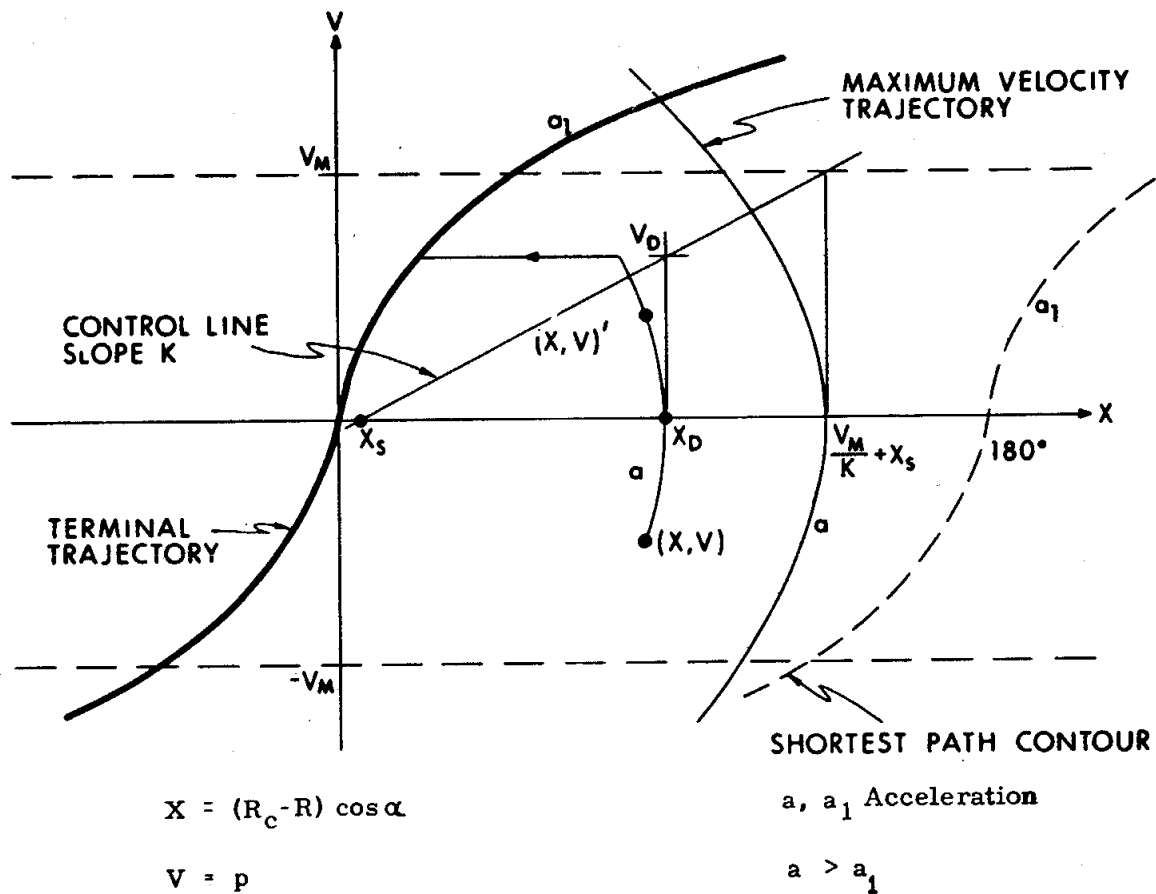


Fig. 3.4.24 Dual Gain Roll Attitude Phase Plane with Control Line

This choice was originally made for its simplicity because only the error  $X$  depends on  $\alpha$ ; velocity limits and deadzone limits are constants expressed in units of body rate. When platform misalignment is considered, however, and the state-vector error begins to accumulate, errors are introduced into the indicated body-attitude angles. The indicated  $\alpha$  can go through 90 degrees. In this region, the  $\cos \alpha$  in the DAP approaches zero and turns off the roll-axis attitude control. Since, in this region,  $p$ -effect on indicated roll attitude  $R$  is insignificant (Fig. 3.4.14), the DAP should not be used to generate roll rates. The CM will drift at deadzone values of  $p$ . When  $\alpha$  increases further,  $\cos \alpha$  becomes nonzero, and the DAP resumes control. The sign reversal of  $\cos \alpha$  maintains stability.

The salient feature of the control technique is the use of a line of slope  $K$  to determine the rate with which an error is reduced. This has several advantages. The fundamental and motivating one is that fuel consumption ( $\Delta V$ ) becomes somewhat proportional to error. The CM responds rapidly to large error and proportionately more slowly for small error. The slope  $K$  is chosen as small as is consistent with the rate of response needed during Entry. A by-product is that the equations involved are simplified. Furthermore, this system will efficiently follow ramp inputs by establishing the necessary rate.

A second facet is trajectory construction using parabolas of different acceleration, a gambit that minimizes the sensitivity of the control system to actual jet thruster acceleration. Choosing the lower acceleration ( $a_1$ ) to have a value near that of the single fuel-ring thrusters, and the larger acceleration ( $a$ ) to have a value slightly less than that of the dual fuel ring has the effect of providing good transient response with little penalty in fuel usage.

The following discussion applies to right of the terminal trajectory. In operation, the roll DAP has initial values ( $X, V$ ) as marked in Fig. 3.4.24. The DAP design is based on the trajectory indicated. Positive jet acceleration of exactly  $a$  causes the parabolic path shown to be generated. The jets will remain on until the specified drift velocity ( $V_d$ ) is reached, at which time the jets are turned off. The time duration of the first thrust interval ( $t_1$ ) is  $(V_d - V)/a$ . The trajectory drifts at constant velocity ( $V_d$ ) until the terminal trajectory is intercepted. The drift velocity is defined geometrically by the control line shown in the picture and is calculated as  $V_d = K(X_d - X_s)$ , where  $X_d = X + \frac{V^2}{2a}$ . When the terminal trajectory is reached, it is followed to the origin by using a second thrust interval having negative jet acceleration of exactly  $a_1$ . The time duration of the second thrust interval ( $t_2$ ) is  $V_d/a_1$ . The time duration of the drift interval ( $t_d$ ) is

$$[2X - t_1 (V + V_d) - t_2 V_d] / 2 V_d.$$



If the duration of the trajectory from the point  $(X, V)$  to the origin, which is the sum of  $t_1$ ,  $t_d$ , and  $t_2$ , exceeds the update interval ( $T$ ), then only the first  $T$  seconds of the trajectory is implemented. The roll DAP computes a completely new trajectory each  $T$  seconds from whatever  $(X, V)$  it finds. In this way, changes in command, noise in measurement, uncertainty and cross-coupling of jet acceleration and other disturbances are always taken into account. Now, suppose that the initial point were  $(X, V)'$  in the figure. The parabola would be extended backward to the x-axis to define  $X_d$ , and the same geometry applied as above.

The behavior described above will, of course, occur only if the first interval has acceleration  $\underline{a}$  and the second interval has acceleration  $a_1$ . In actual fact, both thrust intervals must use the same jet thrusters -- either the single-ring or the dual-ring thrusters. Consider the normal, single-ring operation: let  $a_1$  be the actual jet acceleration; then the first interval is computed using the value  $2 a_1$  for  $\underline{a}$ . In this case, the DAP control logic will predict the value of  $V_d$  and specify the first thrust duration. But the actual jet acceleration is only one-half of the expected value  $\underline{a}$ , so that at the end of the burn the actual velocity is half-way between  $V$  and  $V_d$ . For suitable values of  $K$ , the duration of the predicted trajectory to the origin will exceed  $T$ . During the time remaining in the  $T$  interval, the point will drift to the right or to the left, depending on whether the velocity achieved was negative or positive. When the next update occurs, the same process recurs, and, eventually, the point  $(X, V)$  will be to the left of the control line. Possibly several updates are required in order to achieve a suitable  $\Delta V$  for the first burn using  $\underline{a}$ , since, for each update, only one-half of the expected is achieved. The slowed response is the price paid for the independence of acceleration magnitude. Once across the control line, the first burn is generally absent, so that the predicted trajectory and the actual trajectory agree. The origin is approached directly and without overshoot.

On the other hand, consider that both fuel rings are active and that the dual-jet acceleration is  $\underline{a}$ ; then, to compute the second burn, the value  $\underline{a}/2$  is used for  $a_1$ . In this case, the predicted trajectory and the actual trajectory will agree until the second burn starts.

The higher acceleration will cause twice the  $\Delta V$  and result in undershoot of the origin. On the next update, the first burn is exact, and goes to a much reduced  $V_d$ . Thus the error due to the second burn is considerably reduced. Convergence is rapid, usually an extra cycle or two. The slowed response is again the price paid for independence from knowledge of actual acceleration. However, what is bought is stable operation over a 2:1 acceleration variation, a property that does not exist if both thrust intervals are based on the same (single-ring) acceleration.

Returning to Fig. 3.4.24, the shortest angular path test consists of asking whether the point  $(X, V)$  lies inside the contours at  $\pm 180$  or outside of them. In the nominal single fuel case, any point  $(X, V)$  inside the contours considers the origin as its terminal point. Points outside these contours should consider  $\pm 360$  as their origin. Such points  $X$  are shifted by  $-360 \operatorname{sgn}(X)$  and thereby appear inside the contours so far as the phase plane logic is concerned. Such a shift is necessary since physically  $-360, 0,$  and  $360$  are the same CM attitude. Furthermore it is necessary that the contour dividing the regions of stable nodes be dynamic rather than geometric. Otherwise there exists a region between the dynamic contour and the geometric one where points will initially head for the origin as node; but the trajectory will carry across the geometric contour and then head for  $360$  as the proper node. This results not only in taking the longer path, but also in taking a longer time to do it. The acceleration associated with the shortest path contour of Fig. 3.4.24 is that for the single-ring jets.

The dead zone utilized for the roll attitude is the parallelogram of Fig. 3.4.25. The shape is chosen to provide a smaller limit cycle amplitude for a given zone width  $X_B$ . The effective dead zone on a  $T = 2$ -second basis is nearly rectangular since  $X_B = Vz T$ . The intercept  $V_I$  is intended to keep the limit cycling velocity at a value less than  $Vz$  and is used to specify the control line intercept  $X_S$ .

Control policy is outlined in the three flow charts starting with CM/RCS, Fig. 3.4.34. In the first, roll error is established. Because of symmetry, the control equations are instrumented only for the rhp, where the plane is bisected by the terminal trajectory. To determine which half-plane contains  $(X, V)$ , evaluate the equation for the left-hand buffer curve, Fig. 3.4.26 at the initial point  $(X, V)$ . If the point is to the left, reverse the sign of the variables to reflect about the origin into the rhp and continue at the dead zone test. If not to the left, similarly evaluate the right-hand buffer curve. If the point is to the left of this curve, it is in the buffer zone. The zone is designed to pass trajectories that would nearly reach the origin. These trajectories, if not passed, would be reflected about the origin and caused to go through another two-burn cycle. Such near misses are principally due to noise in velocity measurement, or timing effects, or deviation in the actual single-ring acceleration from the DAP value  $a_1$ , or a combination of these. If the point lies in the buffer zone, it is treated as a second burn and caused to thrust to the X-axis.

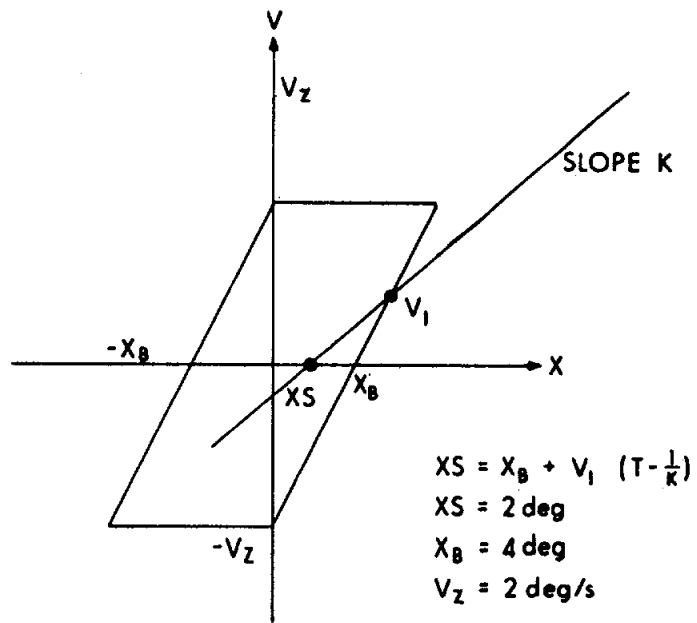


Fig. 3.4.25 Roll System Dead Zone

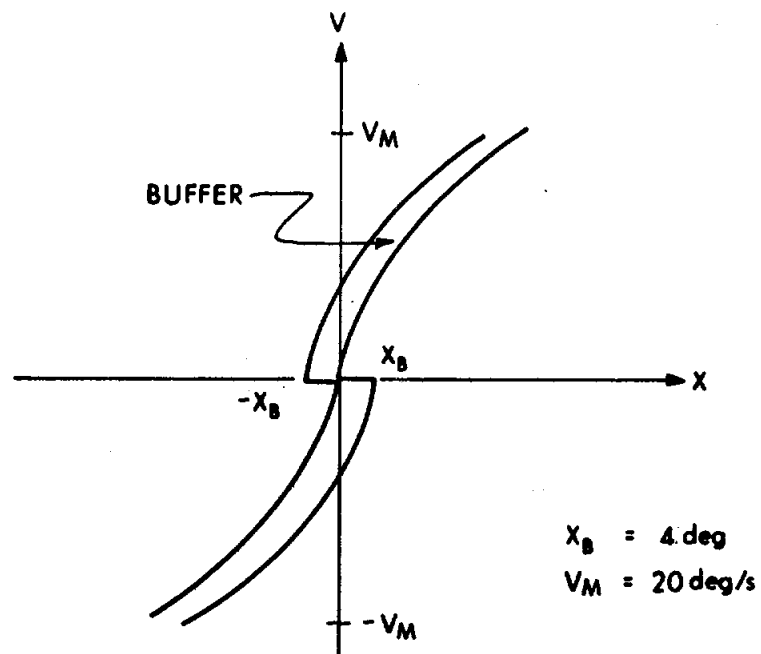


Fig. 3.4.26 Buffer Zone.

If it is not in the zone, then it is already in the rhp and the program continues at the dead zone test. Regarding the buffer zone, the branches that make it up are terminal trajectories suitably shifted.

Pick up at the dead zone test and continue past. If the point  $(X, V)$  is to the right of the maximum velocity trajectory through  $X = X_s + VM/K$ , then thrust up (or down) to  $V = VM$ . If the point is to the left, and below the control line, thrust up to  $V_d$ . But if the point is to the left and over the control line, keep the present velocity as the drift velocity if  $V_d < V$ . In all cases calculate the complete trajectory to the origin. The equations are summarized in the flow chart.

The result of the trajectory calculations are three time intervals:

$t_1$	the time to thrust from $V$ to $V_d$ (or $VM$ )
$t_d$	the time required to drift at $V_d$ (or $VM$ )
$t_2$	the time to origin on terminal trajectory from $V_d$ (or $VM$ )

Intervals  $t_1$  and  $t_2$  are firing intervals and  $t_d$  is a quiescent interval. The attitude system can generate three, two, one or none of the time intervals. None are generated if the point  $(X, V)$  lies within the deadzone at the origin. Jets are quenched, if on, and the program exits.

#### TIMETEST and JET CALL1

The program portion named TIMETEST, Fig. 3.4.37, examines each of three possible time intervals and prepares to execute each in sequence if

1. no interval is less than three centiseconds.
2. the sum of the interval and the previous intervals plus the time used in computation is not within 3 centiseconds of 2 seconds.

Each time interval that fails to meet the above requirements is ignored, but the jet codes corresponding to such intervals are appropriately executed.

The program portion named JETCALL1, Fig. 3.4.38, performs the actual bookkeeping with the jet list, executing the jet codes and establishing WAITLIST calls as required. These calls return via JETCALL to be processed.

#### 3.4.9 DAP Displays and Telemetry

The program CM/FDAI, Fig. 3.4.39, is a general exit routine for the Entry DAP's. It is passed through at the end of each 0.1-second DAP cycle and services all FDAI attitude error needles on alternate passes. On the intervening passes, the three CM body rates are listed in the UPBUFF area of erasable for telemetering. The list format is: time of latest initialization of list, a combined switch and index, and five sets of body rates spaced 0.2 second apart and in the order p, q, r. The magnitude of the index designates the latest set of rates filed, because the telemetering cannot interrupt the DAP. The telemetering portion of CM/FDAI is self-cycling, but it is forced to recycle after each CM/RCS update.

#### 3.4.10 Restart Protection of Entry DAP

In the Entry DAP, restart protection is quantized in units of updates. That is, the WAITLIST call for READGYMB is restart protected relative to READACCS time and to the number of DAP cycles that have been performed since that time. Should a restart occur during DAP computation, the entire update is lost. Otherwise no interruption to DAP operation occurs. But since a restart turns off all jets, there is always a momentary interruption to DAP control. The CM/RCS DAP has a flag, JETAG, to signify that a 2-second DAP update is due. The flag is cleared in CM/RCS to indicate that the DAP was indeed called. Clearing of the flag is placed as near the end of CM/RCS as possible. Should a restart occur before the flag is cleared, then the next 0.1-second update will once again call CM/RCS and the update is not lost. However, if restart occurs after the flag was cleared, the 2-second roll update is lost. Again, restart has turned off the jets, so no DAP control problem exists. The loss of updates is not critical and has a negligible effect on an entry trajectory, even when restarts occur at a moderate rate.

#### 3.4.11 DAP Flow Chart Summary

The Entry DAP is described by the flow charts starting with READGYMB, Fig. 3.4.28, and continuing through CM/FDAI, Fig. 3.4.39. This chain of events starts with gimbal angle readout and is followed by body rate calculation, attitude rate calculation, and attitude angle integration. Immediately following this the sampled DAP is entered. Covered in the next two figures are those autopilot functions that are implemented on the 0.1-second basis: the rate dampers and EXDAP. The next two figures are the subroutines BIASED DZ and RATEAVG used in the foregoing figures. The 2-second predictive roll DAP CM/RCS starts with Fig. 3.4.34 and continues through the processing of waitlist time calls, Fig. 3.4.38. CM/FDAI, Fig. 3.4.39, is the DAP display program. This set of diagrams is presented as a block since it represents the complete sequence of events associated with DAP updates. Initialization of the DAP is covered by CM/DAPIC, Fig. 3.4.6, and CM/DAPON, Fig. 3.4.7. Timing of CM/RCS is established by SETJTAG, Fig. 3.4.27. Of importance also are the calculations that are required to establish the body attitude Euler angles: CM/POSE, Fig. 3.4.17 and Fig. 3.4.18, in conjunction with READACCS, Fig. 3.4.16. The program for these calculations runs somewhat independently of the DAP. All constants used by the ENTRY DAP appear in Table 3.4-III.

READACCS (AVERAGEG)  
Initiates SETJTAG Via  
WAITLIST After Nominal  
~1 Sec. Delay.

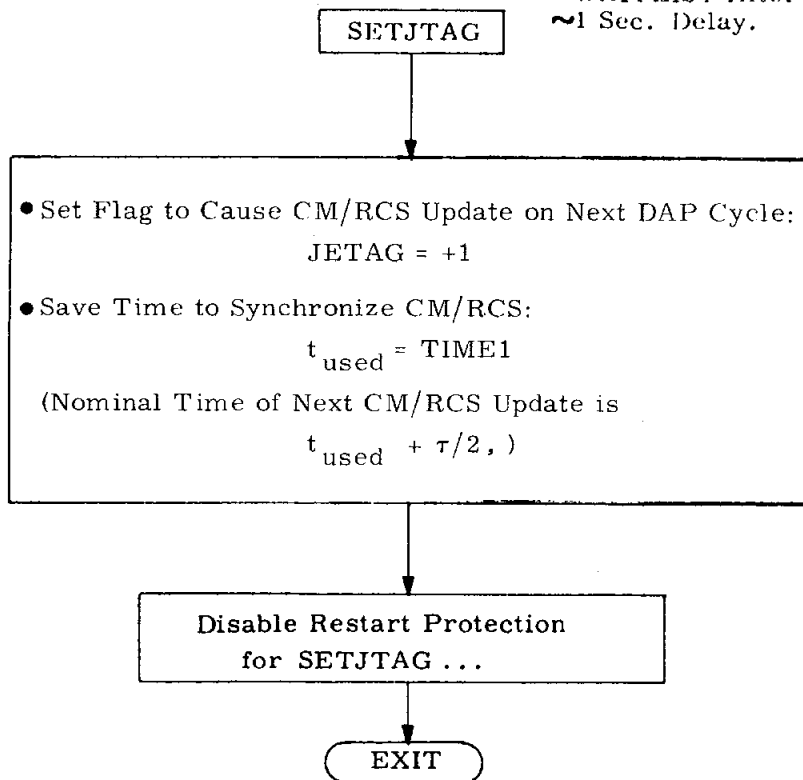


Fig. 3.4.27 Roll DAP Synchronizer.

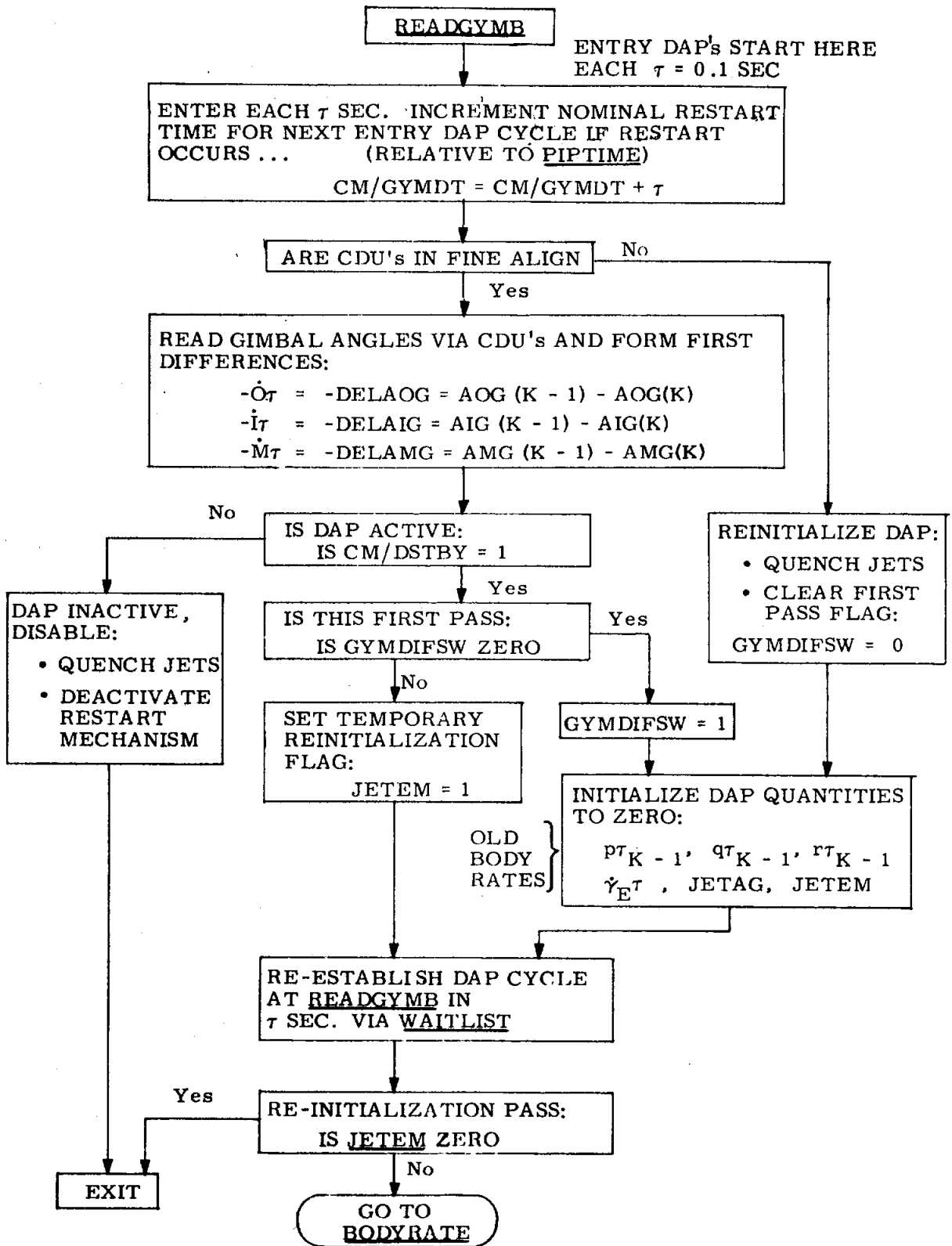


Fig. 3.4.28 Gimbal Angle Rates & Body Rate Initialization.

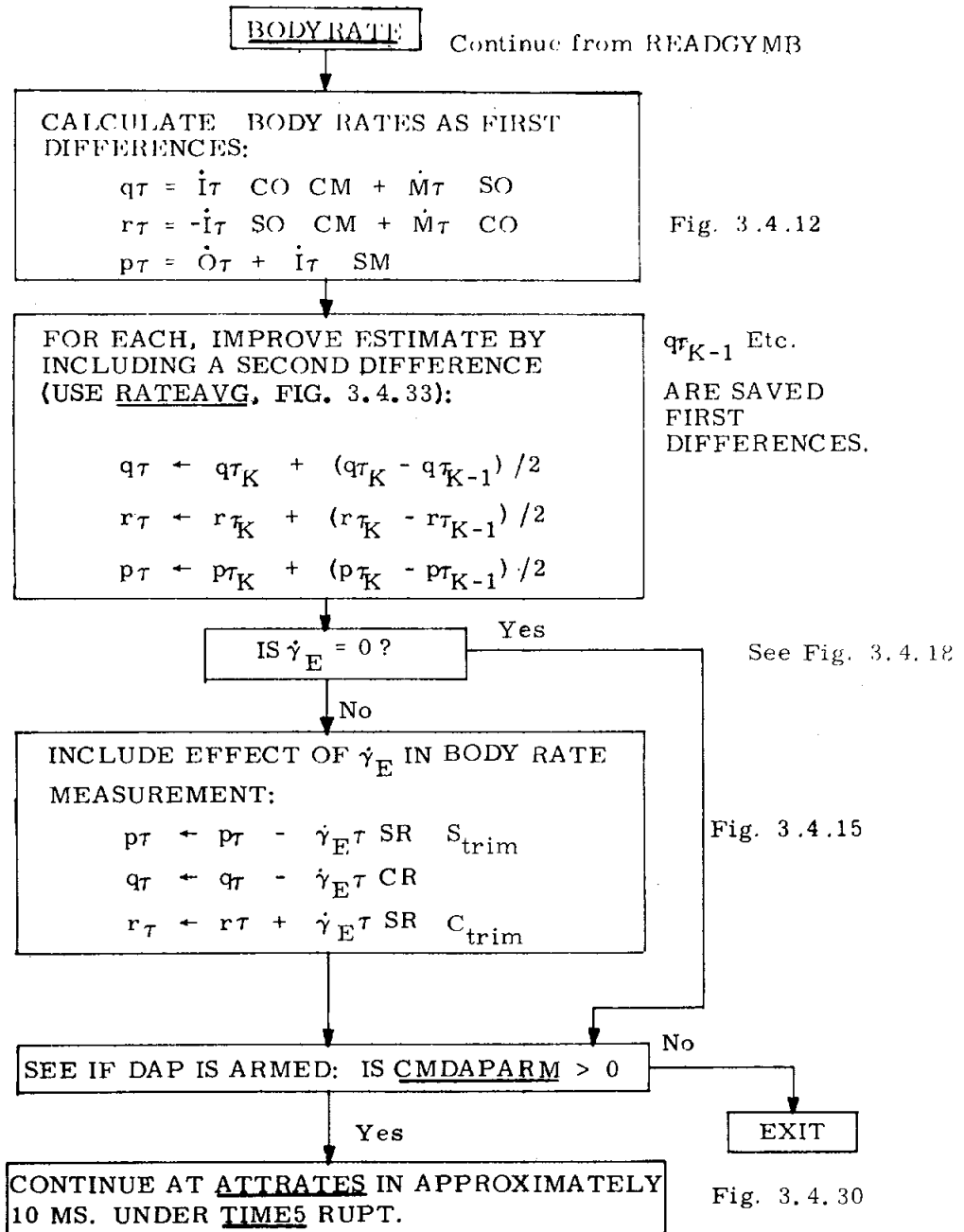


Fig. 3.4.29 CM Body Rates.



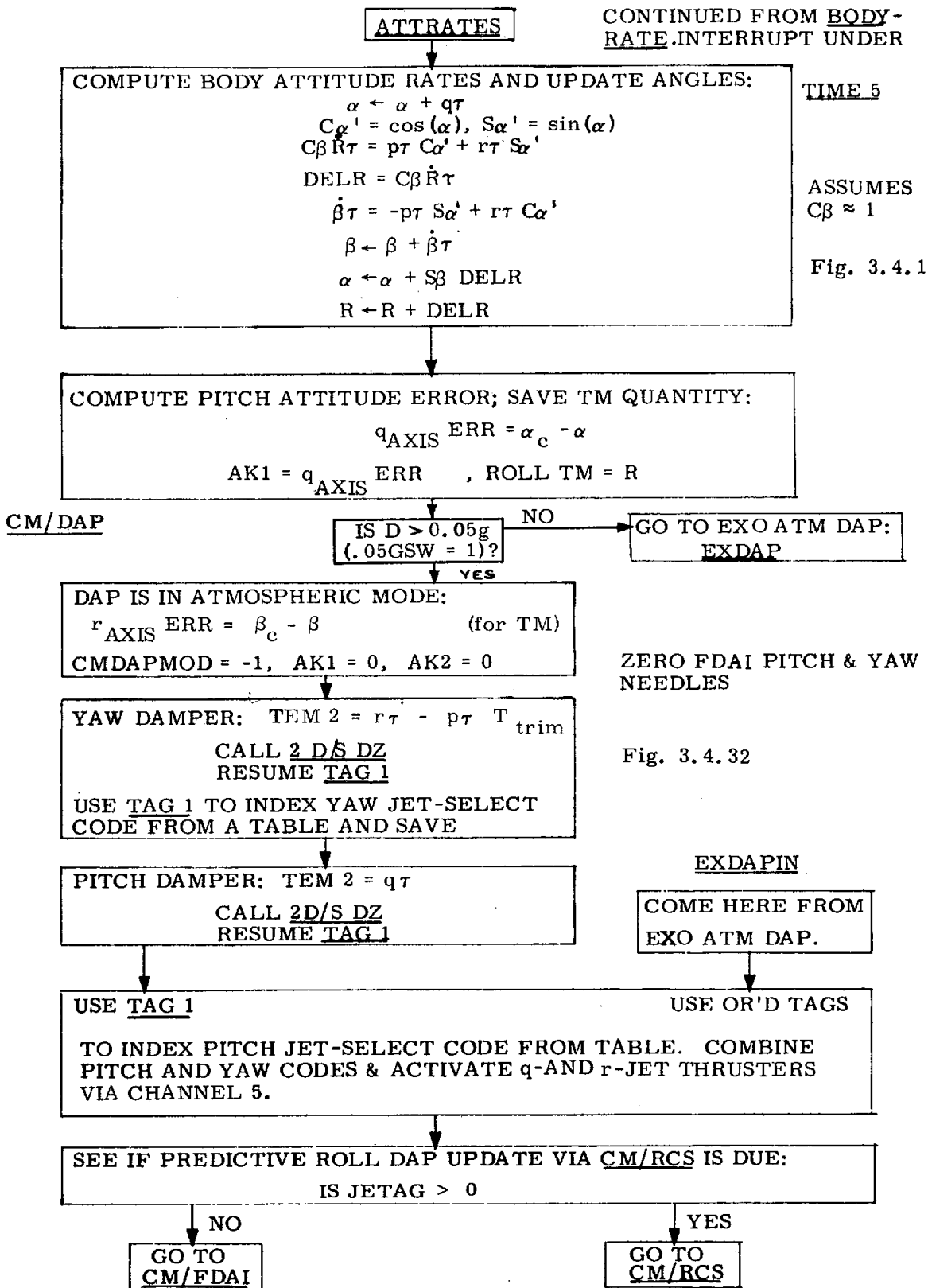


Fig. 3.4.30 CM Attitude Angles; Pitch and Yaw Dampers.

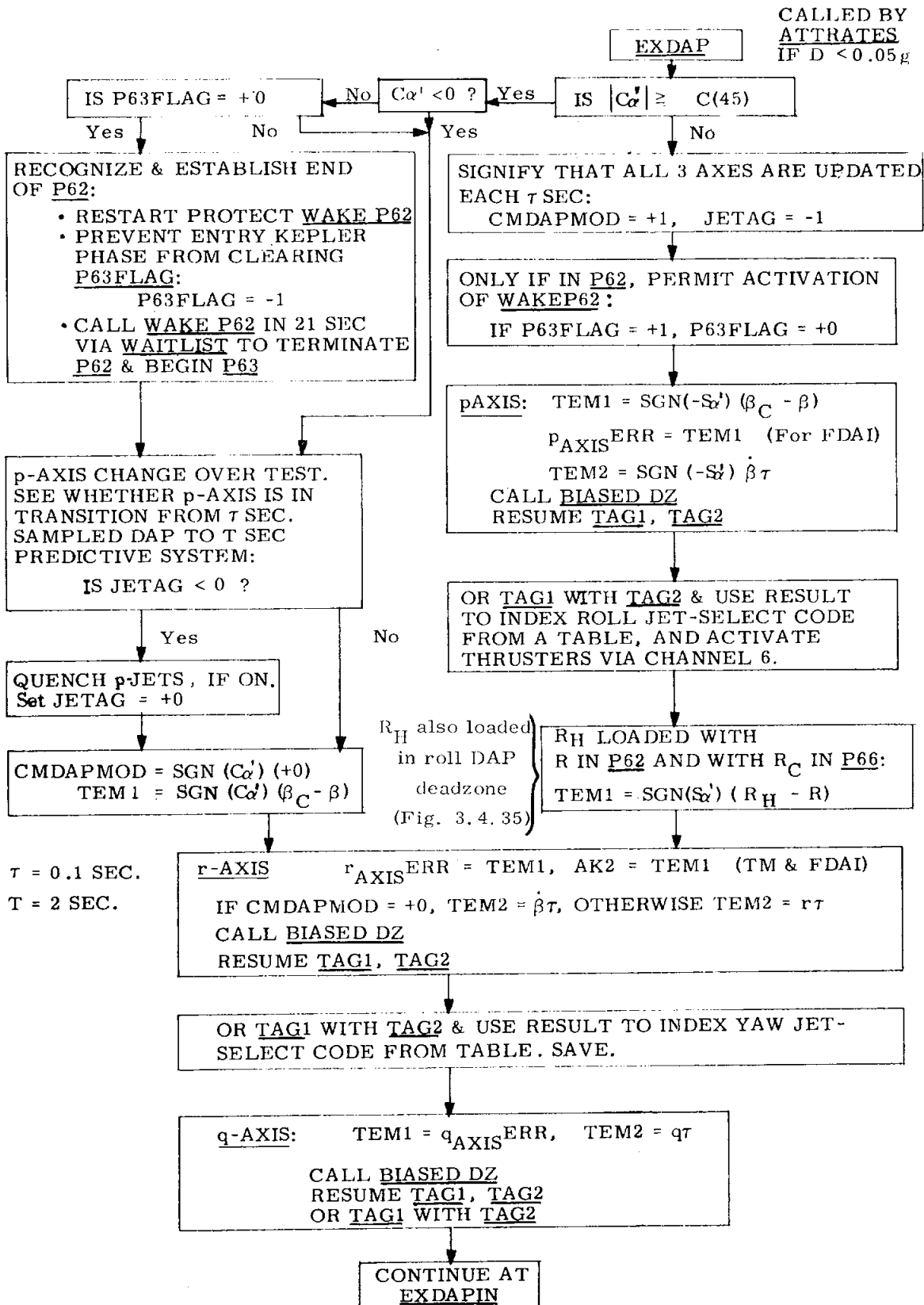
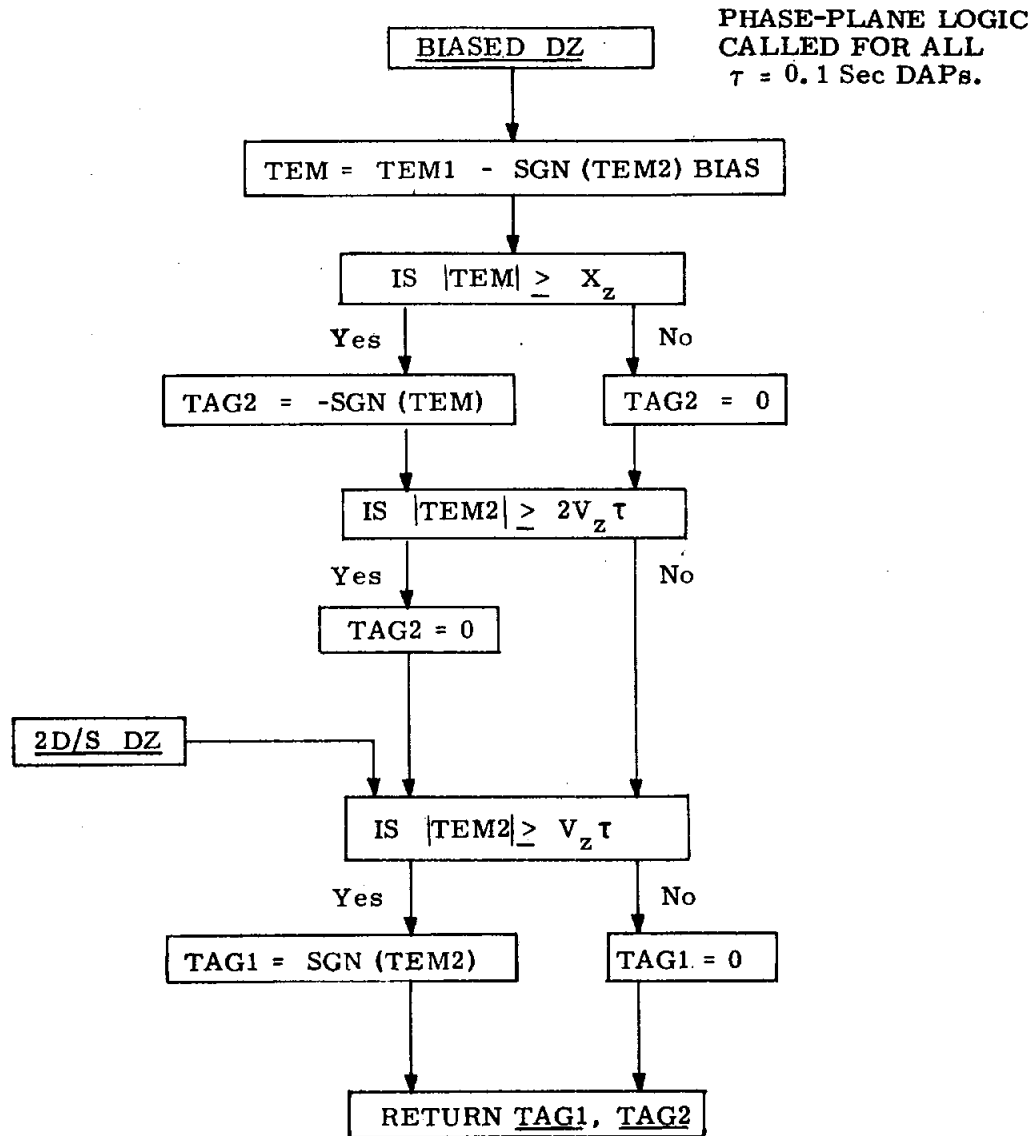


Fig. 3.4.31 EXO Atmospheric Attitude CM DAP.

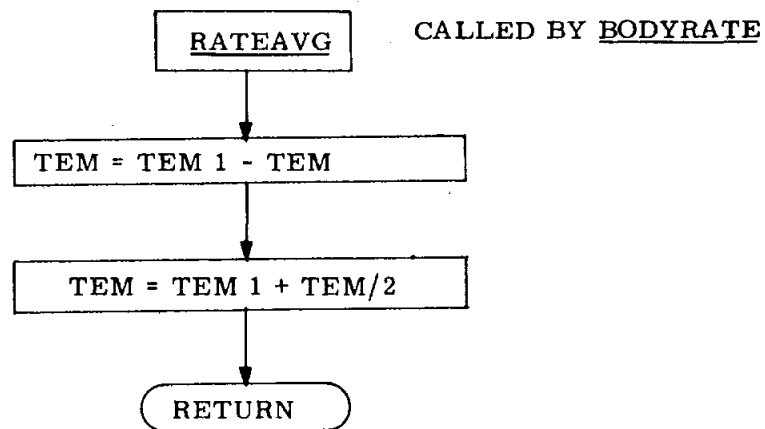


TEM1 = SIGNED ATTITUDE ERROR  
 TEM2 = SIGNED (ATTITUDE) RATE  
 TAG1 AND TAG2 TAKE ON THE VALUES  
 +1, 0, -1.

BIAS =  $0.6^\circ$   
 $X_z = 3.6^\circ$   
 $V_z = 2^\circ/s$

+1 WILL SELECT THE JET CODE  
 CORRESPONDING TO NEGATIVE  
 ACCELERATION.

Fig. 3.4.32 Biased DZ and Rate DZ for CM Attitude DAP.



ESTIMATE BODY RATES IN PRESENCE OF CONSTANT ACCELERATION.

TEM 1 = PRESENT VALUE OF ANGULAR INCREMENT.

( $p\tau$ ,  $q\tau$ , or  $r\tau$ )

TEM = LAST VALUE OF ANGULAR INCREMENT.

$\tau = 0.1$  SEC.

Fig. 3.4.33 CM Body Rate Estimation.

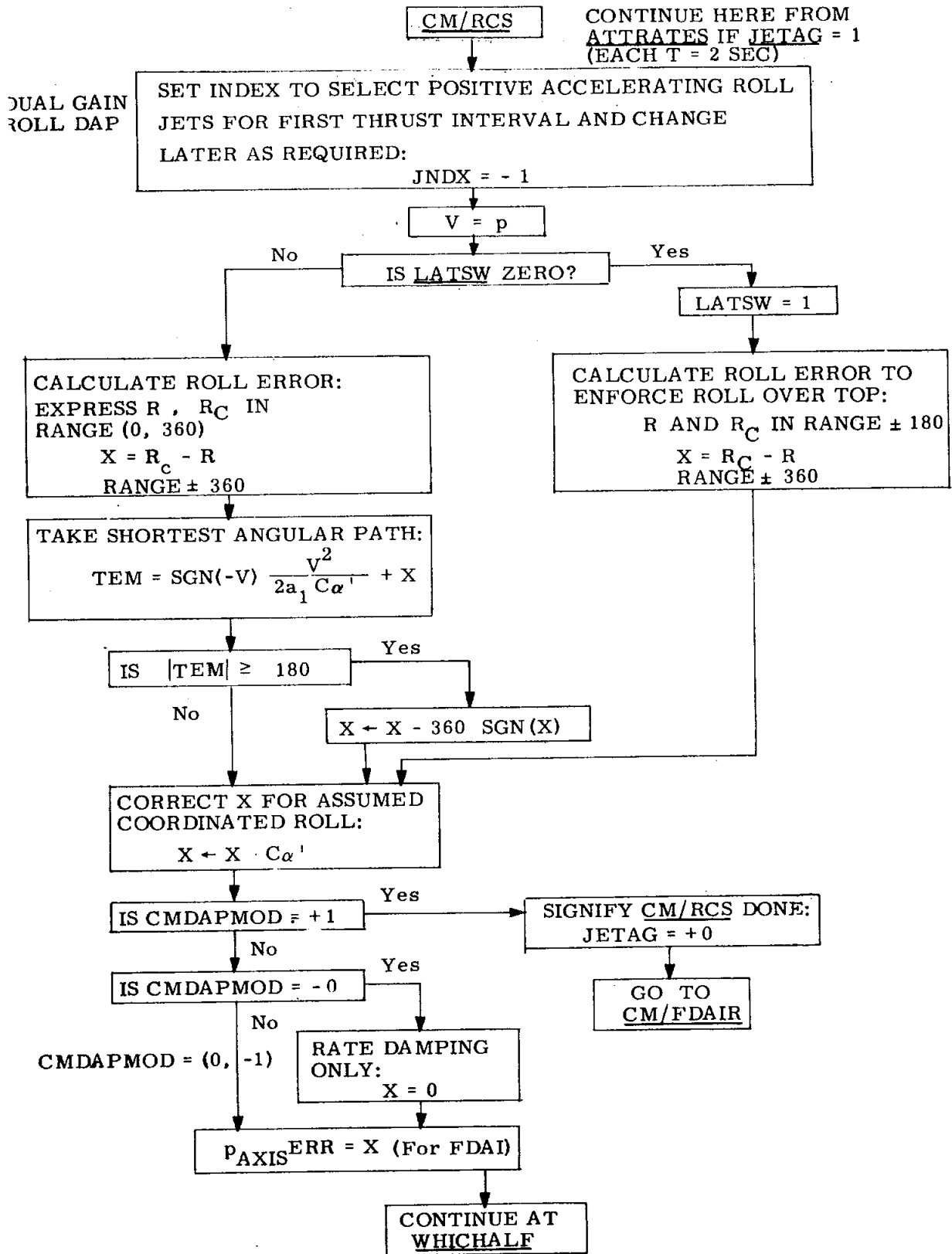


Fig. 3.4.34 Dual Gain Roll DAP - Error Calculation.

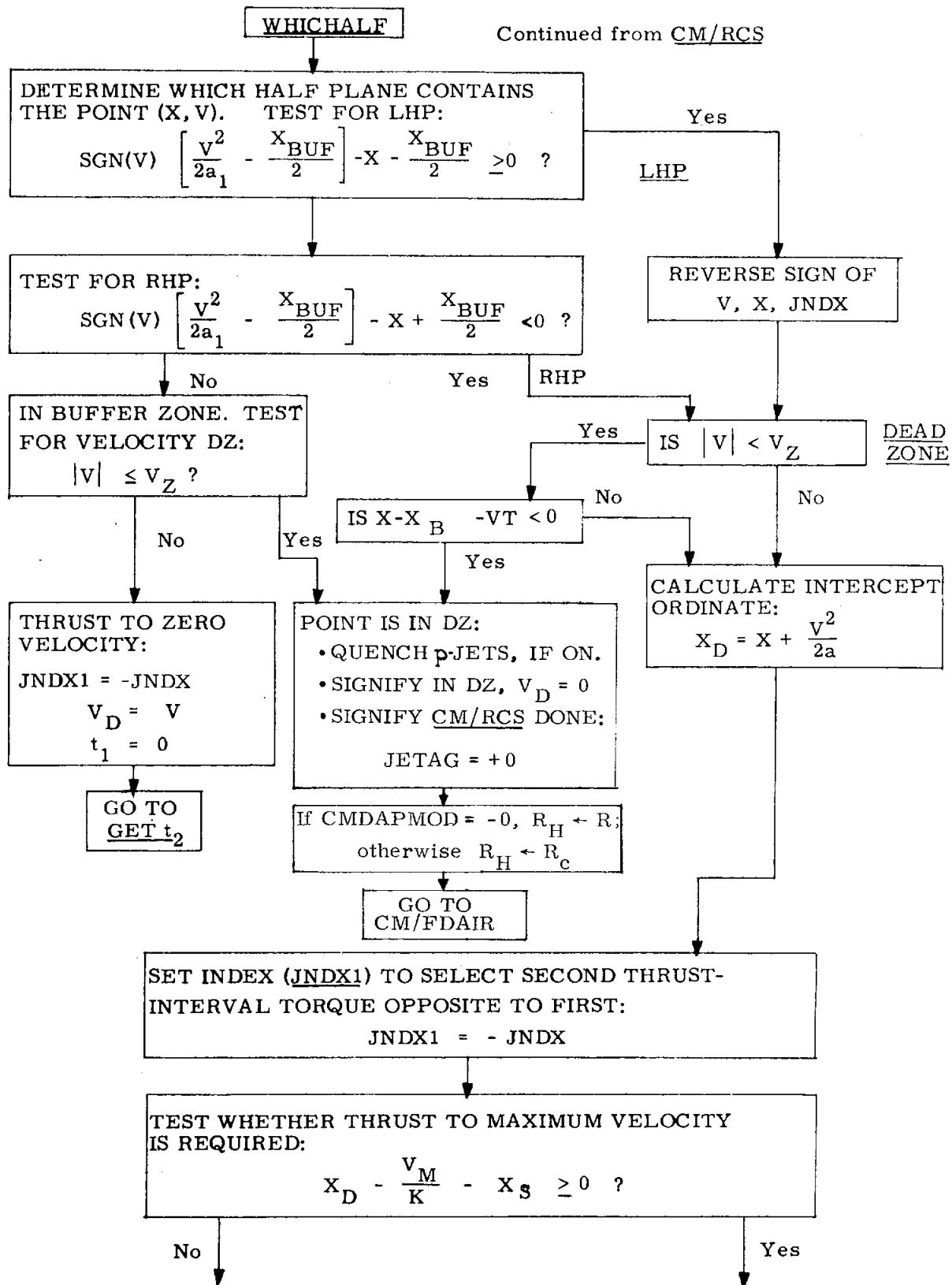


Fig. 3.4.35 Dual Gain Roll DAP - Initial Logic.

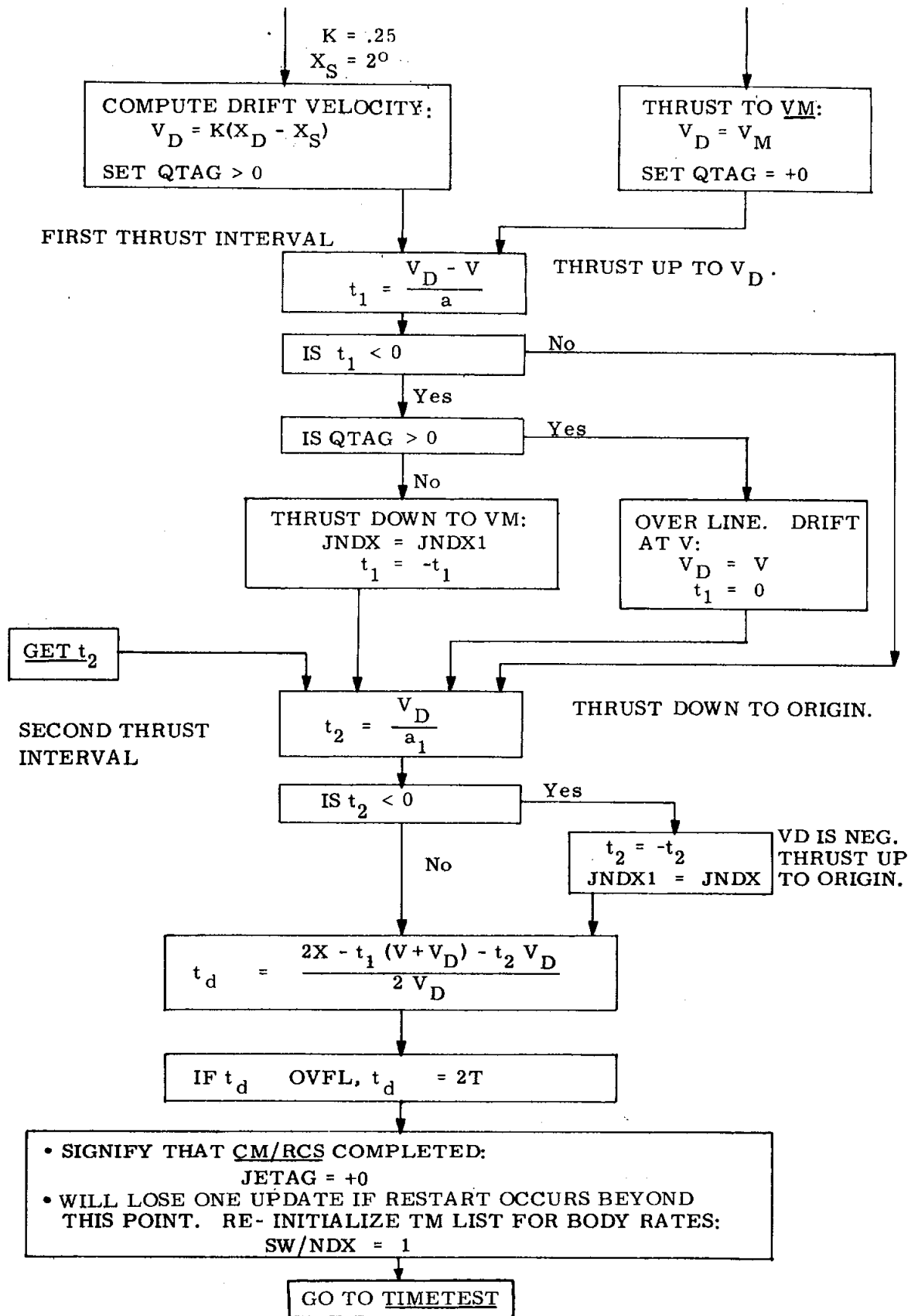


Fig. 3.4.36 Dual Gain Roll DAP - Time Calculations.

TIMETEST

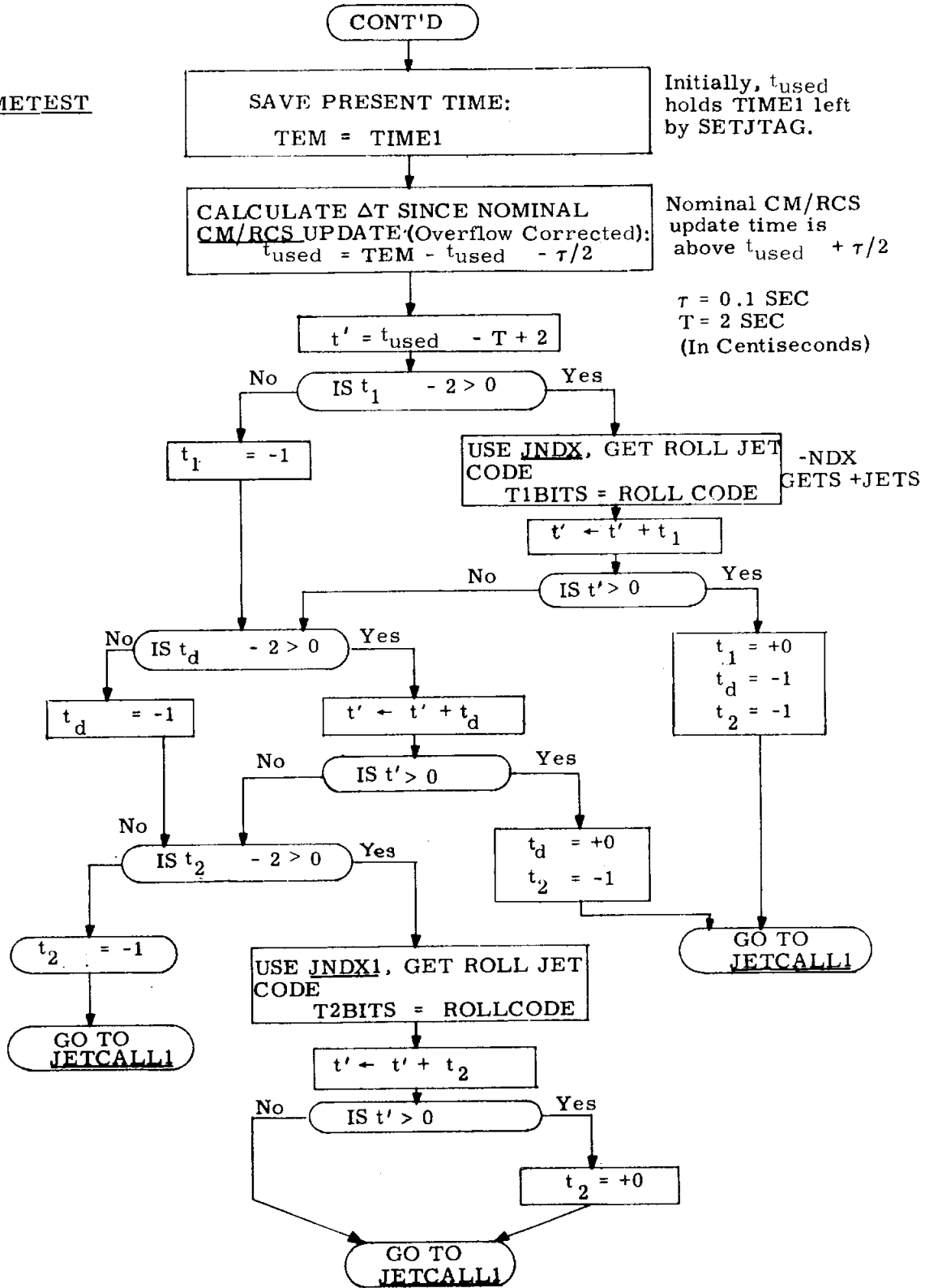


Fig. 3.4.37 Roll DAP - Time Interval Processing.



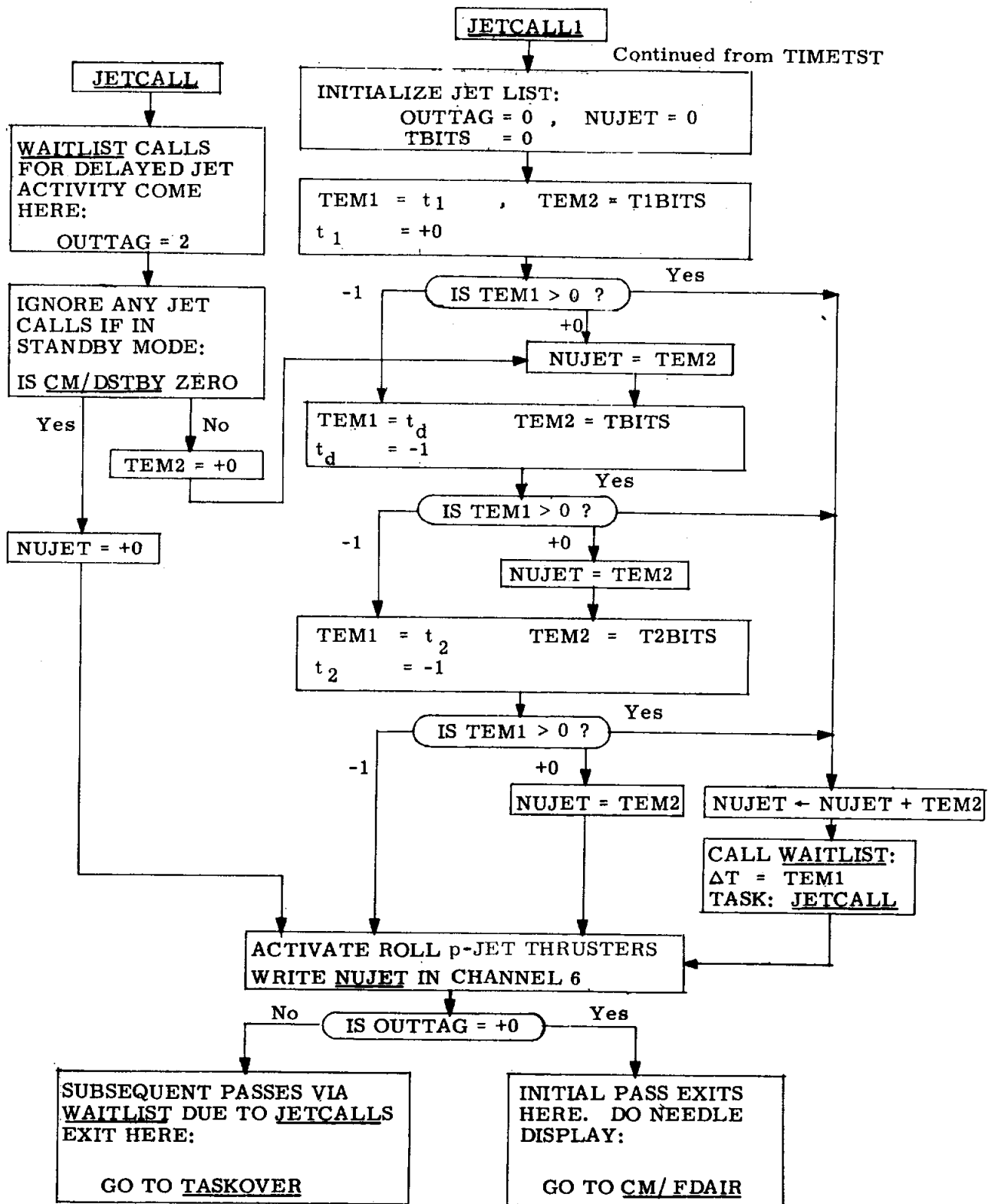


Fig. 3.4.38 Roll DAP - Time Interval Execution Logic.

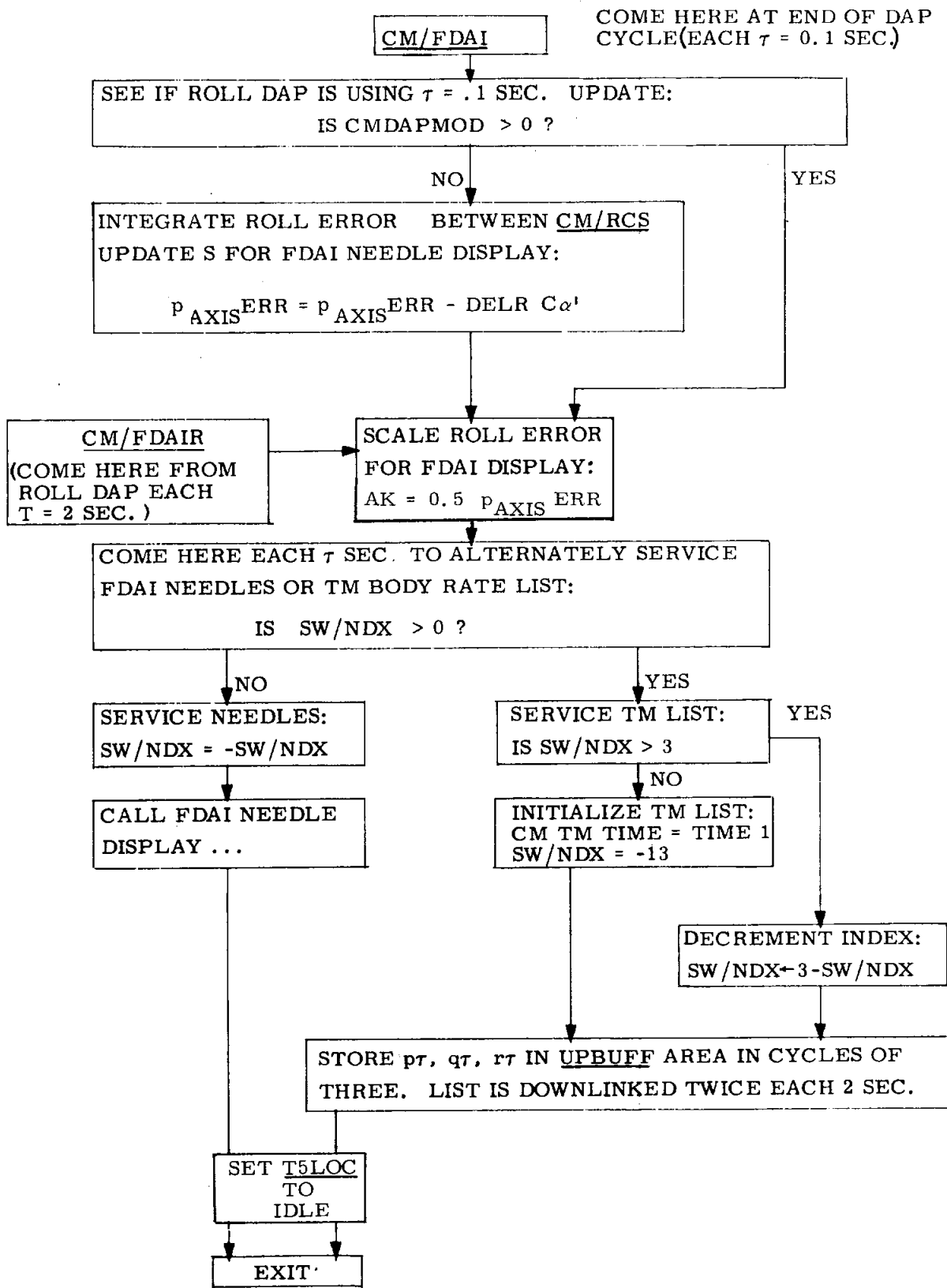


Fig. 3.4.39 Entry DAP Display and Telemetry Interface.

Table 3.4-III ENTRY DAP Constants

CONSTANT	VALUE
a	9.1 deg/sec <sup>2</sup>
a <sub>1</sub>	4.55 deg/sec <sup>2</sup>
α <sub>t</sub>	pad-loaded quantity, function of L/D.
α <sub>trim</sub>	- 20 deg
BIAS	0.6 deg
γ <sub>E</sub> <sup>min</sup>	0.5 deg/sec
K	0.25 sec <sup>-1</sup>
KWE	1546.70168 ft/sec = (.729211505 × 10 <sup>-4</sup> rad/sec)(21210604.46 ft)
T	2 sec
τ	0.1 sec
VQUIT	1000 ft/sec
V <sub>I</sub>	1 deg/sec
V <sub>M</sub>	20 deg/sec
V <sub>Z</sub> , V <sub>MIN</sub>	2 deg/sec
X <sub>B</sub> , X <sub>BUF</sub> , X <sub>MIN</sub>	4 deg
X <sub>S</sub>	2 deg
X <sub>Z</sub>	3.6 deg
X <sub>Z</sub> '	3 deg

### 3.4.12 Symbol Table

a	roll acceleration estimate for dual-rings; used by predictive roll DAP, CM/RCS.
$a_1$	single-ring roll acceleration estimate; used by CM/RCS.
AIG	inner gimbal angle, as read each $\tau$ second.
AIG/PIP	value of AIG that exists at PIPA read time and is saved for use in attitude calculation, CM/POSE.
AK	CM attitude error in body axes to drive roll FDAI needle.
AK1	CM attitude error in body axes to drive pitch FDAI needle.
AK2	CM attitude error in body axes to drive yaw FDAI needle.
AMG	middle gimbal angle, as read each $\tau$ second
AMG/PIP	value of AMG that exists at PIPA read time and is saved for use in attitude calculation, CM/POSE.
AOG	outer gimbal angle, as read each $\tau$ second.
AOG/PIP	value of AOG that exists at PIPA read time and is saved for use in attitude calculation, CM/POSE.
AVEGEXIT	variable exit address in AVERAGEG used to establish program flow.
AVERAGEG	program to perform navigation; generates $\underline{R}_N$ , $\underline{V}_N$ . See Section 5, GSOP.
$\alpha$	pitch attitude angle, used by ENTRY DAP. It is the third rotation of the CM body triad in the Euler sequence $R, \beta, \alpha$ , and is about <u>UBY</u> .
$\alpha$ /PIP	value of $\alpha$ that exists at PIPA read time and is saved for use in attitude calculation, CM/POSE.
$\dot{\alpha}$	rate of change of pitch attitude $\alpha$ .
$\alpha_c$	$\alpha$ attitude command, used by ENTRY DAP.
$\alpha_t$	the hypersonic value of $\alpha$ for the CM in trimmed flight, a pad-loaded quantity.
$\alpha_{trim}$	- 20 deg, approximately the hypersonic $\alpha$ for $L/D = 0.3$ .
BIAS	bias value used to offset the biased dead zone of EXDAP.
$\beta$	yaw attitude angle, used by ENTRY DAP. It is the second rotation of the CM body triad in the Euler sequence $R\beta\alpha$ , and is about <u>UBZ</u> .

$\beta$ /PIP	value of $\beta$ that exists at PIPA read time and is saved for use in attitude calculation, CM/POSE.
$\dot{\beta}$	rate of change of yaw attitude $\beta$ .
$\dot{\beta}\tau$	$\beta$ attitude increment due to $\dot{\beta}$ , calculated each $\tau$ second.
$\beta_c$	$\beta$ attitude command, used by ENTRY DAP.
CHANNEL 5	CMC channel for CM q- and r-jets.
CHANNEL 6	CMC channel for CM p-jets.
CMDAPARM	if switch bit is zero, DAP is in standby mode and only calculates body rates. If bit is 1, DAP exerts control on CM.
CMDAPMOD	a 4-position switch used by ENTRY DAP.
	-0 $ \alpha  > 135^\circ$ D < 0.05 g
	+1 $45^\circ <  \alpha  < 135^\circ$ D < 0.05 g
	+0 $ \alpha  < 45^\circ$ D < 0.05 g
	-1    D > 0.05 g
CMTMTIME	a register containing the time (TIME1) of initializing the list used for telemetering the body rates (see SW/NDX).
CM/DSTBY	switch bit is 1 if DAP is active. DAP will be turned off when bit becomes zero.
CM/GYMDT	register used by ENTRY DAP restart mechanism. Contains time of next DAP update relative to time when PIPAs were read.
CM/POSE	program to calculate CM body attitude angles.
CM/RCS	name of the predictive roll ENTRY DAP. Computations performed each T seconds.
CM CO, CI	{ short-hand notation for cos (M), cos (O), cos (I), where M, O, I are the gimbal angles.
$C_{trim}$	cos (-20°), nominal hypersonic trim $\alpha$ for L/D = 0.3
$C\alpha'$	DAP variable, cosine of the first approximation to $\alpha$ .
C20	maximum drag level for down-lift, used by Entry Guidance to determine LATSW setting. See Section 5, GSOP.
D	atmospheric drag acceleration, used in Entry Guidance. See Section 5, GSOP.
-DELAG	outer gimbal angle difference, generated each $\tau$ second and used in body rate calculation.

-DELAIG inner gimbal angle difference, generated each  $\tau$  second and used in body rate calculation.

-DELAMG middle gimbal angle difference, generated each  $\tau$  second and used in body rate calculation.

DELR roll attitude increment due to  $\dot{R}$ , calculated each  $\tau$  second.

GAMDIFSW switch is zero until gamma has been calculated once in CM/POSE, in order to assure that a valid difference can be computed. Switch may be reset to zero more than once.

GYMDIFSW switch is zero until CDUs have been read once by READGYMB, in order to assure that valid CDU differences exist. Switch is 1 otherwise. Switch may be reset to zero more than once.

$\gamma_E$  angle between local horizontal and  $\underline{V}_{REL}$ ; measured positive upward.

$\dot{\gamma}_E$  rate of change of  $\gamma_E$ .

$\dot{\gamma}_E^{min}$  minimum value of  $\dot{\gamma}_E$  for which the body rates are corrected for  $\dot{\gamma}_E$ .

HEADSUP a quantity set by the crew via DSKY to specify the roll attitude that the CM is to assume before entering the atmosphere.

I inner gimbal angle.

$\dot{i}$  rate of change of inner gimbal angle.

JETAG a switch used to control the time sequence of CM/RCS. If JETAG = +1, the roll DAP is updated. If JETAG = 0, DAP is omitted.

JETCALL }  
 JETCALL1 } { jet list processor, program to service the roll jets as required by CM/RCS. Initial pass uses JETCALL1; subsequent passes via WAITLIST use JETCALL.

JETEM temporary registers used by ENTRY DAP.

JNDX two-value quantity used in CM/RCS to specify sign of the roll acceleration to be used during the first thrust interval.

JNDX1 two-value quantity used in CM/RCS to specify the sign of the roll acceleration to be used during the second thrust interval.

K slope of the Control Line used in CM/RCS.

KWE the product of earth rate and earth radius used in approximating the coriolis term in the calculation of velocity of the CM relative to the air mass. Instead of  $\underline{W} \times \underline{R}$ , KWE  $\underline{UNITW} \times \underline{UR}$  is used. KWE  $\equiv 1546.70168$  ft/sec. See Section 5, GSOP: Entry Guidance.

LATSW	switch bit is zero if Entry Steering wants ENTRY DAP to roll over the top. DAP rolls through shortest angular path if bit is 1.
LAT(SPL)	latitude of desired landing site.
LNG(SPL)	longitude of desired landing site.
M	middle gimbal angle.
$\dot{M}$	rate of change of middle gimbal angle.
NEW $\alpha$	{ values of Euler set $R\beta\alpha$ as extracted by CM/POSE from the calculated sines and cosines of the attitude angles.
NEW $\beta$	
NEW $\gamma$	
NUJET	register containing roll jet code that is to be executed next by the jet list processor of CM/RCS.
O	outer gimbal angle.
$\dot{O}$	rate of change of outer gimbal angle.
OUTTAG	switch word used to mark the type of entry into the jet-list processor of CM/RCS.
p	roll rate, component of CM angular velocity vector along body X-axis, <u>UBX</u> .
$p\tau$	attitude increment due to p body rate, calculated each $\tau$ second.
$p_{K-1}$	{ previously calculated body rate (increment), saved for use in calculation of current body rate.
$p_{K-1}\tau$	
$p_{\text{AXIS}}^{\text{ERR}}$	CM roll attitude error in body axes generated by DAP and displayed on FDAI needle. Equivalent to AK.
$p_{\text{rel}}$	CM roll body rate, corrected for $\dot{\gamma}_E$ .
PIPTIME	time at which PIPAs were last read.
PITCH CODE	table of pitch jet codes.
POSEXIT	variable exit address in CM/POSE used to establish program flow.
P63FLAG	a flag used in sequencing the change to program P63 from P62.
q	pitch rate, component of CM angular velocity vector along body Y-axis, <u>UBY</u> .
$q\tau$	attitude increment due to q body rate, calculated each $\tau$ second.

$q_{K-1}$	}	{	previously calculated body rate (increment) saved for use
$q\tau_{K-1}$			
$q_{\text{AXIS}}^{\text{ERR}}$			CM pitch attitude error in CM body axes generated by DAP and displayed on FDAI needle. Equivalent to AK1.
$q_{\text{rel}}$			CM pitch body rate, corrected for $\dot{\gamma}_E$ .
$Q_7$			minimum drag for up-control phase of ENTRY Guidance (see Section 5.)
$r$			yaw rate, component of CM angular velocity vector along body Z-axis, <u>UBZ</u> .
$r\tau$			attitude increment due to $r$ body rate, calculated each $\tau$ second.
$r_{K-1}$	}	{	previously calculated body rate (increment) saved for
$r\tau_{K-1}$			
$r_{\text{AXIS}}^{\text{ERR}}$			CM yaw attitude error in CM body axes generated by DAP and displayed on FDAI needle. Equivalent to AK2.
$r_{\text{rel}}$			CM yaw body rate, corrected for $\dot{\gamma}_E$ .
$R$			roll attitude angle, used by ENTRY DAP. It is the first Euler rotation of the CM body triad about the negative relative velocity vector <u>-UVA</u> , along which <u>UBX</u> points.
$R/\text{PIP}$			value of $R$ that exists at PIPA read time and is saved for use in attitude calculation, CM/POSE.
$\dot{R}$			rate of change of roll attitude, $R$ .
$R_c$			roll attitude command issued by Entry Guidance and used by ENTRY DAP. It is defined as a rotation about the negative relative velocity vector, <u>-V<sub>REL</sub></u> .
READACCS			program to read integrating accelerometers (PIPAs), and to establish timing for ENTRY DAP and attitude calculations in CM/POSE.
READGYMB			program to read gimbal angles via CDUs and start ENTRY DAP sequence each $\tau$ second.
$R_H$			register used by EXDAP in roll attitude hold; contains desired roll attitude.
<u><math>R_N</math></u>			CM inertial position vector, generated by AVERAGEG navigation.
ROLL			same as $R$ .
ROLLC			same as $R_c$ .



ROLL CODE	table of roll jet codes.
SETJTAG	program to initiate CM/RCS by setting flag JETAG.
SM } SO, SI }	{ shorthand for sin (M), sin (O), sin (I), where M, O, I are gimbal angles.
S <sub>trim</sub>	sin (-20°), nominal hypersonic trim $\alpha$ for L/D = 0.3
SW/NDX	combined switch and index associated with FDAI display and with telemetering. The contents of SW/NDX is negated immediately before use. Then, if the contents of SW/NDX is positive, the attitude errors are sent to FDAI error needles. If SW/NDX is negative, the value is used as an index to file the three body rates in a list for telemetering.
S $\alpha'$	DAP variable, sine of first approximation to $\alpha$ .
t <sub>on1</sub>	same as t <sub>1</sub> .
t <sub>on2</sub>	same as t <sub>2</sub> .
t <sub>off</sub>	same as t <sub>d</sub> .
t <sub>1</sub>	first roll acceleration interval generated by CM/RCS.
t <sub>2</sub>	second roll acceleration interval generated by CM/RCS.
t <sub>d</sub>	roll drift interval generated by CM/RCS.
TBITS	register that contains roll jet code for no jets on.
T1BITS	register that contains the roll jet code for first acceleration interval.
T2BITS	register that contains the roll jet code for second acceleration interval.
t'	quantity used in TIMETEST in determining the useability of the time intervals t <sub>1</sub> , t <sub>2</sub> , and t <sub>d</sub> that are generated by CM/RCS.
t <sub>used</sub>	elapsed time since nominal update of predictive roll DAP, CM/RCS. Used to maintain sync of DAP by accounting for computation time and other delays.
T	sample period of predictive roll DAP, CM/RCS. The same period is used by the navigation cycle beginning with READACCS.
T <sub>trim</sub>	tan(-20), approximated by S <sub>trim</sub>
TAG1 } TAG2 }	{ three-value quantities generated by ENTRY DAP phase plane logic for use in selecting jet-axis codes from a table.
TEM } TEM1 } TEM2 }	{ temporary quantities used in flow charts for convenience. May be one or several actual computer registers.

<u>TIME1</u> , <u>TIME2</u>	CMC time; double-precision registers in the order <u>TIME2</u> <u>TIME1</u> . In general, to read time, both <u>TIME2</u> and <u>TIME1</u> must be read. However, in computing time differences, <u>TIME1</u> alone may be used provided account is taken of possible incrementing of <u>TIME2</u> by overflow of <u>TIME1</u> and the corresponding re-setting of <u>TIME1</u> to zero.
<u>T1</u>	same as <u>TIME1</u> .
<u>T2</u>	same as <u>TIME2</u> .
<u>TIME3</u>	a preset timer that is maintained by <u>WAITLIST</u> for the purpose of scheduling.
<u>T3</u>	same as <u>TIME3</u> .
<u>TIME5</u>	a preset timer, maintained by the user for the purpose of scheduling.
<u>T5</u>	same as <u>TIME5</u> .
$\tau$	sample period used for body rate calculations. All portions of <u>ENTRY DAP</u> , except <u>CM/RCS</u> , operate at this rate.
<u>UBX</u> } <u>UBY</u> } <u>UBZ</u> }	CM body triad.
<u>UL</u>	unit vector in direction of lift vector. It is normal to <u>-UVA</u> and rotated away from <u>UNA</u> by the angle <u>R</u> .
<u>UNA</u>	unit vector in trajectory plane, normal to both <u>-UVA</u> and <u>UYA</u> . Also called <u>UZA</u> .
<u>UNITW</u>	unit vector along earth's spin axis. Same as <u>UZ</u> .
<u>UPBUFF</u>	CMC erasable array assigned to the uplink program and used during <u>Entry</u> to telemeter CM body rates.
<u>UPX</u> } <u>UPY</u> } <u>UPZ</u> }	{ triad attached to stable platform; identical to body triad when all gimbal angles are zero.
<u>UR</u>	unit vector along <u>R<sub>N</sub></u> .
<u>UVA</u>	unit vector along <u>V<sub>REL</sub></u> .
<u>UXA</u>	same as <u>-UVA</u> .
<u>UYA</u>	unit vector normal to trajectory plane. It lies along <u>V<sub>REL</sub> × R<sub>N</sub></u> .

<u>UZ</u>	same as <u>UNITW</u> .
<u>UZA</u>	same as <u>UNA</u> .
V	phase-plane velocity used by CM/RCS. It is equivalent to p. It may also appear as the product VT.
V	generally used as ordinate when X is the abscissa in phase plane figures for the ENTRY DAP. In present application the error X is defined as (Command minus Actual) and the Command is considered to be constant. It is therefore convenient to define V as the rate of change of the Actual rather than as $\dot{X}$ , as is usual. The resulting phase planes are inverted from the usual.
V	magnitude of $\underline{V}_{REL}$ . Also called VREL.
$V_D$	roll drift velocity computed using the Control Line and a parabola having acceleration (a) by CM/RCS.
$V_I$	velocity intercept of Control Line of slope K and parallelogram dead-zone in CM/RCS.
$V_M$	maximum roll rate allowed by CM/RCS.
VMAGI	magnitude of $\underline{V}_N$ computed for a display.
$\underline{V}_N$	CM inertial velocity vector, generated by AVERAGEG navigation.
VQUIT	value of VREL at which Entry Guidance ceases generating $R_c$ and at which CM/POSE ceases computing <u>UYA</u> .
$\underline{V}_{REL}$	velocity of CM relative to air mass.
VREL	magnitude of $\underline{V}_{REL}$ .
VT	angular increment in CM/RCS, product of roll rate V and sample time T. See V.
$V_z$	velocity limit used in all dead-zone figures.
X	attitude error used in all DAP phase plane illustrations. (see also V.) It is the difference between Command and Actual attitude. For the predictive roll DAP CM/RCS, the error is corrected for assumed coordinated maneuver, $X = (R_c - R) C\alpha'$ .
$X_B$	x-axis intercept used in CM/RCS by both buffer-zone and the parallelogram dead-zone.
$X_{BUF}$	x-axis intercept of buffer-zone in CM/RCS, and is equivalent to $X_B$ .

$X_D$	x-axis intercept of parabola having acceleration (a) and commencing at the point (X, V). Used in CM/RCS.
$X_{MIN}$	x-axis intercept for parallelogram dead-zone in CM/RCS.
$X_B$	x-axis intercept of Control Line in CM/RCS.
$X_z$	x-axis intercept (in absence of bias) used in the biased dead-zone of EXDAP.
$X'_z$	X'-axis intercept used in the unbiased dead-zone figure used in description of EXDAP.
YAW CODE	table of yaw jet codes.
<u>YBN</u>	unit vector along desired direction for <u>UBY</u> . It is normal to <u>-UVA</u> and rotated away from <u>UYA</u> by the angle R.
.05GSW	switch bit is zero if atmospheric drag acceleration is less than 0.05 g.
$\omega_B$	angular-velocity vector of CM.

### 3.5

## TAKEOVER OF SATURN STEERING

by Oistein Eliassen and Jack C. Reed

A capability is provided that allows the command-module computer to provide steering signals to the SATURN S-IVB Instrumentation Unit (IU) autopilot. There are two modes of takeover operation -- Automatic Mode and Manual, or "Stick," Mode.

#### 3.5.1 Automatic Mode

The Automatic Mode of CMC - SATURN IU takeover provides the CMC with a backup capability of issuing steering commands to the IU autopilot during boost stages S-IC, S-II, and S-IVB. The mode provides polynomial guidance for the S-IC stage but provides attitude - hold commands, only, for the S-II and S-IVB stages. The Automatic Mode is available only during P11 and is entered by the crew's selecting the CMC position of the LV GUIDANCE panel switch.

Nominally the LV GUIDANCE switch is in the IU position, and the P11 attitude-error subroutine (Figures 3.5-4 and -5 of COLOSSUS GSOP Section 5) monitors the CDUs, computes the attitude error, and displays the error on the FDAI; upon the crew's selecting the CMC position, the takeover function begins, and the P11 subroutine begins issuing the appropriate commands to the IU autopilot. Takeover commands are then computed as follows: The error existing at takeover is stored as the attitude-error bias; this value is subtracted from the actual error computed on the succeeding cycles; and the resulting value is used to issue steering commands that attempt to maintain a constant error equal to that existing at takeover (see Figure 3.5.1):

$$AK = [(\text{desired attitude} - \text{measured attitude}) - \text{attitude-error bias}] \times \text{SATURN SF}, * \text{ where "desired attitude" is a function of time, i. e., pitch polynomial (GSOP Section 5, paragraph 5.3.5), until disabled by the crew's selection of another program.}$$

Returning the LV GUIDANCE switch to IU while still in P11 takes the CMC out of the SATURN steering loop. Should the CMC position be again selected, a new attitude-error bias will be stored for computing AK.

---

\*SATURN Scale Factor, an erasable constant for increasing the gain to the IU autopilot. The maximum scale value is 4.0, resulting in a maximum output of 1.2 volt/deg for pitch and yaw and 0.3 volt/deg for roll.

### 3.5.2 Manual Mode

The Manual (Stick) Mode of CMC - SATURN IU takeover provides the crew with a capability of issuing RHC commands, through the CMC, to the SATURN IU autopilot. To initiate the SATURN manual function, the crew must first set to "3" the CONFIG octal window of Noun 46 R1. This is done by means of Verb 48 (R03). The crew then executes Verb 46. The routine is disabled by setting the CONFIG window to "0" and repeating Verb 46.

Keying VERB 46 ENTR (with CONFIG = 3) during P11 terminates the attitude-error subroutine (automatic mode) and leaves only the RHC for issuing control signals to the IU. The RHC out of detent provides constant maneuver rates based upon stored erasable parameters.

The manual takeover mode is entered once each 100 ms by means of the TIME5 clock and interrupt mechanism. During each cycle, the RHC bits are sampled, and rate commands are generated that remain in force until updated by the next cycle. The commands are communicated to the SATURN IU autopilot by means of the IMU error-counter digital-to-analog converters.

Since the IMU error counters also drive the FDAI attitude-error needles, these needles will be driven by stick commands. Because the stick commands are implied rate commands, and the needles are designed to indicate attitude errors, the magnitude of the needle deflection is not meaningful; the sign of the needle deflection will be the opposite sense of the stick deflection.

### 3.5.3 Coarse Align Avoidance during SATURN Steering

If gimbal lock is detected ( $CDUZ > 85^\circ$  magnitude, either real or due to CDUZ transients) during SATURN powered flight (as indicated by CONFIG = 3 with AVEGFLG = 1), coarse aligning of the IMU is bypassed in order to preserve the integrity of the CMC/SATURN IU interface for possible use by the manual SATSTICK mode discussed in Section 3.5.2 above. Coarse align CDU moding uses the same error counters and digital-to-analog converters used by SATSTICK, so it is necessary to avoid this conflict. Stick capability is mandatory; therefore, coarse aligning must be avoided.

### 3.5.4 Restarts

Restarts in either Automatic or Manual Mode will

- (1) Disable SATURN TAKEOVER relay,
- (2) Return command values to zero,
- (3) Re-enable SATURN TAKEOVER relay.

In the Automatic Mode, the computation of attitude error resumes and a new attitude -error bias is stored at each restart.



### 3.5.5 S-IVB Engine-off Signal

The CMC issues the S-IVB engine-off "output" whenever the SPS engine is commanded off. The bit is always reset upon selection of any program.



3.6 COASTING-FLIGHT ATTITUDE MANEUVER ROUTINE (R60)  
by Donald W. Keene

3.6.1 Introduction

The purpose of the attitude maneuver routine (R60) is to automatically reorient the spacecraft during coasting flight. This maneuver process is illustrated in Fig. 3.6.1. The desired attitude to which the spacecraft is to be aligned can be specified in one of two ways:

- a) By a set of terminal desired gimbal angles,  $\underline{\theta}_c$ .
- b) By two unit vectors,  $\underline{u}_{DSM}$  and  $\underline{u}_{ANB}$ .

$\underline{\theta}_c$  is the set of desired (or commanded) gimbal angles defined by

$$\underline{\theta}_c = \begin{pmatrix} \theta_{co} \\ \theta_{ci} \\ \theta_{cm} \end{pmatrix} = \begin{pmatrix} \text{desired outer gimbal angle} \\ \text{desired inner gimbal angle} \\ \text{desired middle gimbal angle} \end{pmatrix}$$

$\underline{u}_{ANB}$  is a body-fixed axis vector,  $\underline{u}_A$ , with components in navigation-base coordinates.  $\underline{u}_{DSM}$  is a desired-direction vector,  $\underline{u}_D$ , with components in stable-member coordinates.  $\underline{u}_{DSM}$  specifies the direction in inertial space to which  $\underline{u}_{ANB}$  is to be aligned. A flag switch, FL<sub>3</sub>AXIS, is provided to specify which of the two types of inputs is to be used.

If the vector type of input is chosen, the routine known as VECPOINT is used to compute a set of desired gimbal angles,  $\underline{\theta}_c$ , based on the values of  $\underline{u}_{DSM}$ ,  $\underline{u}_{ANB}$  and the current gimbal angles,  $\underline{\theta}$ . In Routine 60, these desired gimbal angles are displayed to the crew. The crew then has the option of performing the maneuver either manually or automatically. If the automatic option is selected, R60 calls a routine known as KALCMANU which computes a set of parameters ( $\underline{u}_r$ , A) that determine how the reorientation is to be performed. The maneuver is performed by rotating the spacecraft about the axis of single equivalent rotation,  $\underline{u}_r$ , by the

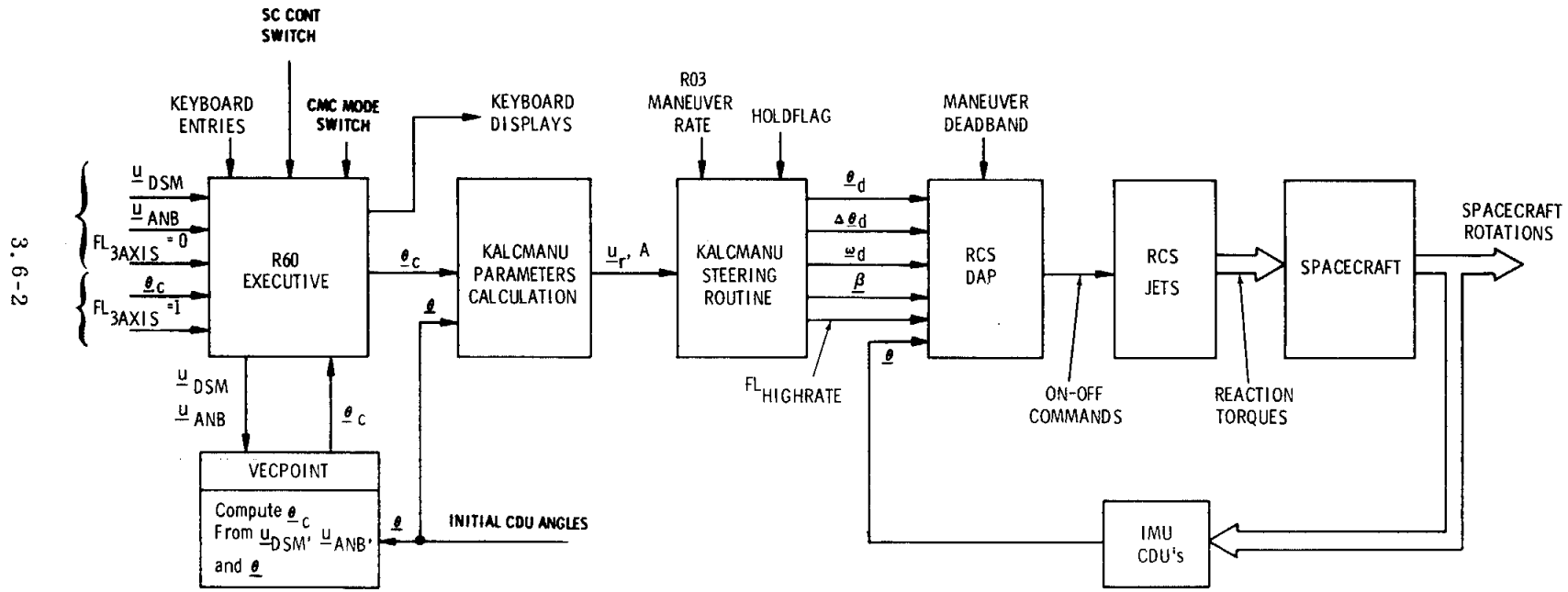


Fig. 3.6.1 R60 Information Flow

angle  $A$ .  $\underline{u}_r$  and  $A$  are completely determined by the initial orientation,  $\underline{\theta}$ , and the desired terminal orientation,  $\underline{\theta}_c$ . The rate at which the maneuver is performed is specified by the crew in R03.

The KALCMANU steering routine computes four sets of quantities for use by the RCS DAP in following the angular path defined by  $\underline{u}_r$ ,  $A$ . The first of these is a set of autopilot reference angles,  $\underline{\theta}_d$  (or intermediate desired CDU angles), which are updated once every second during the maneuver. To achieve a smoother sequence of commands between successive updates, the program also generates a set of incremental CDU angles,  $\Delta\underline{\theta}_d$ , to be added to  $\underline{\theta}_d$  by the RCS DAP. The steering routine also computes the component maneuver rates,  $\underline{\omega}_d$  (in spacecraft axes), and a set of bias angles,  $\underline{\beta}$ , to be used by the autopilot to prevent fuel-consuming overshoot when starting and stopping an automatic maneuver. The steering logic will also set a flag switch (FL<sub>HIGHRATE</sub>) if the largest maneuver rate is selected so that the autopilot will increase the frequency response of the rate filter and more effectively counteract the crosscoupling torques that may occur during the maneuver.

The aforementioned procedure allows the autopilot to establish and maintain a spacecraft rotation about the vector  $\underline{u}_r$  at a fixed rotation rate  $\underline{\omega}_d$ . The maneuvers are timed in open-loop fashion so that after a predetermined interval  $\Delta\underline{\theta}_d$ ,  $\underline{\omega}_d$ ,  $\underline{\beta}$ , and FL<sub>HIGHRATE</sub> are set to zero and the autopilot reference angles,  $\underline{\theta}_d$ , are set equal to the terminal angles,  $\underline{\theta}_c$ . Thus, upon completion of the maneuver, the spacecraft will finish up in a limit cycle about  $\underline{\theta}_c$ .

### 3.6.2 R60 Executive

The R60 Executive section of the attitude maneuver routine is illustrated in Fig. 3.6.2. The keyboard displays indicate the total FDAI ball-angle attitude required for the reorientation.\* If the vector option is selected by the calling program, the routine VECPOINT is used to compute the terminal desired gimbal angles  $\underline{\theta}_c$ . The crew has the option of either manually reorienting the spacecraft or having the maneuver performed automatically. If the crew elects to perform the maneuver manually, it may select the FDAI total attitude-error display (via V62) for additional visual cues in performing the maneuver. If the automatic option is to be used, the S/C CONT switch must be in the CMC position and the CMC MODE switch in AUTO. During the maneuver, the crew should monitor the FDAI ball for gimbal lock since KALCMANU has no provisions for avoiding gimbal lock. If the spacecraft attitude is approaching the gimbal-lock zone, the crew should stop the maneuver by switching to HOLD or simply by moving the hand controller and manually steering the spacecraft around gimbal lock. The maneuver may then be completed either automatically or manually.

The desired gimbal angles,  $\underline{\theta}_c$ , computed by VECPOINT are determined on the basis of minimizing the rotation angle required to align  $\underline{u}_{ANB}$  with  $\underline{u}_{DSM}$ . In general, this procedure will reduce the fuel required for the maneuver by not

\* For the command module, the FDAI ball angles are equivalent to gimbal angles.

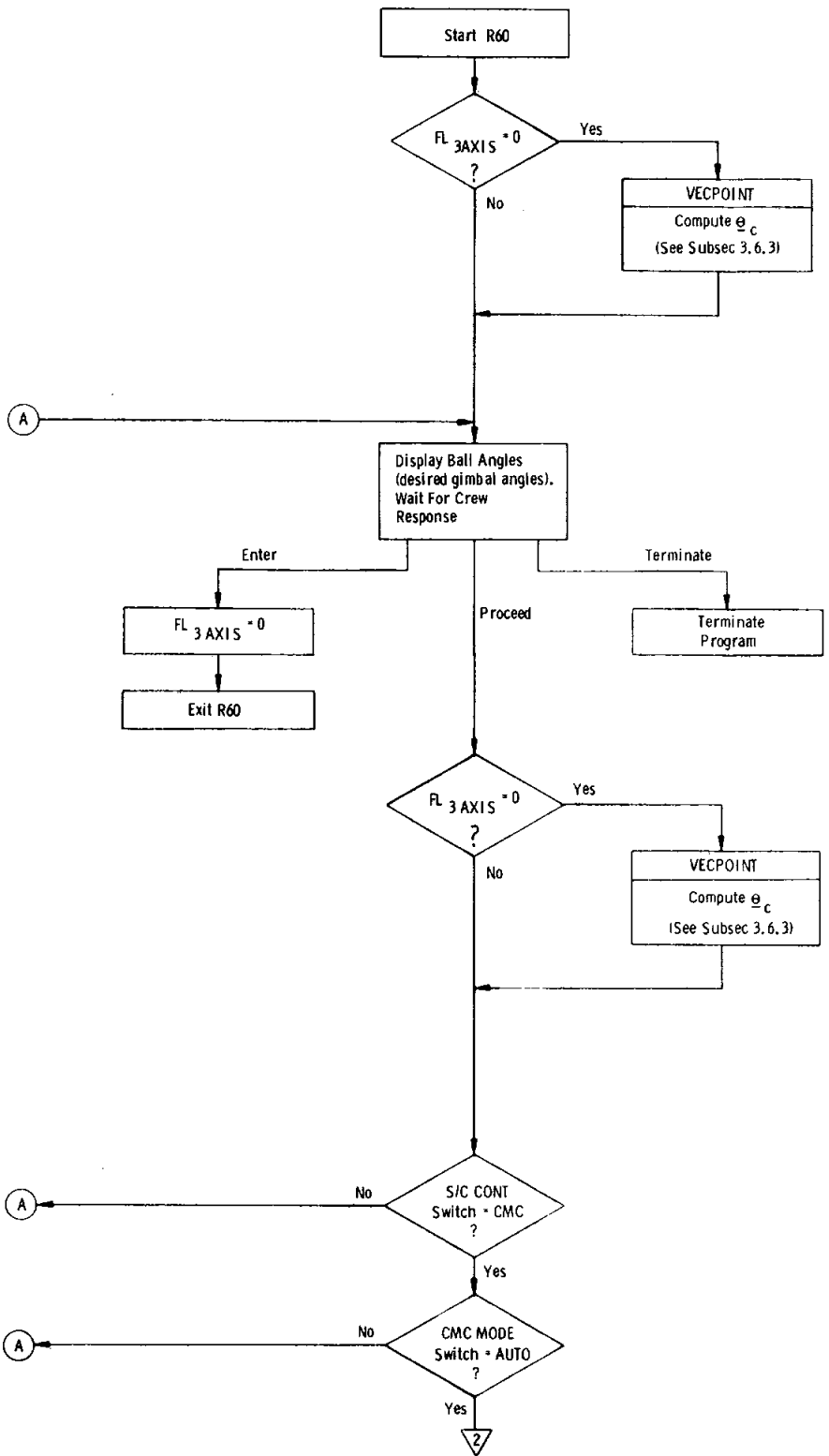


Fig. 3.6.2 R60 Executive (Sheet 1 of 2)

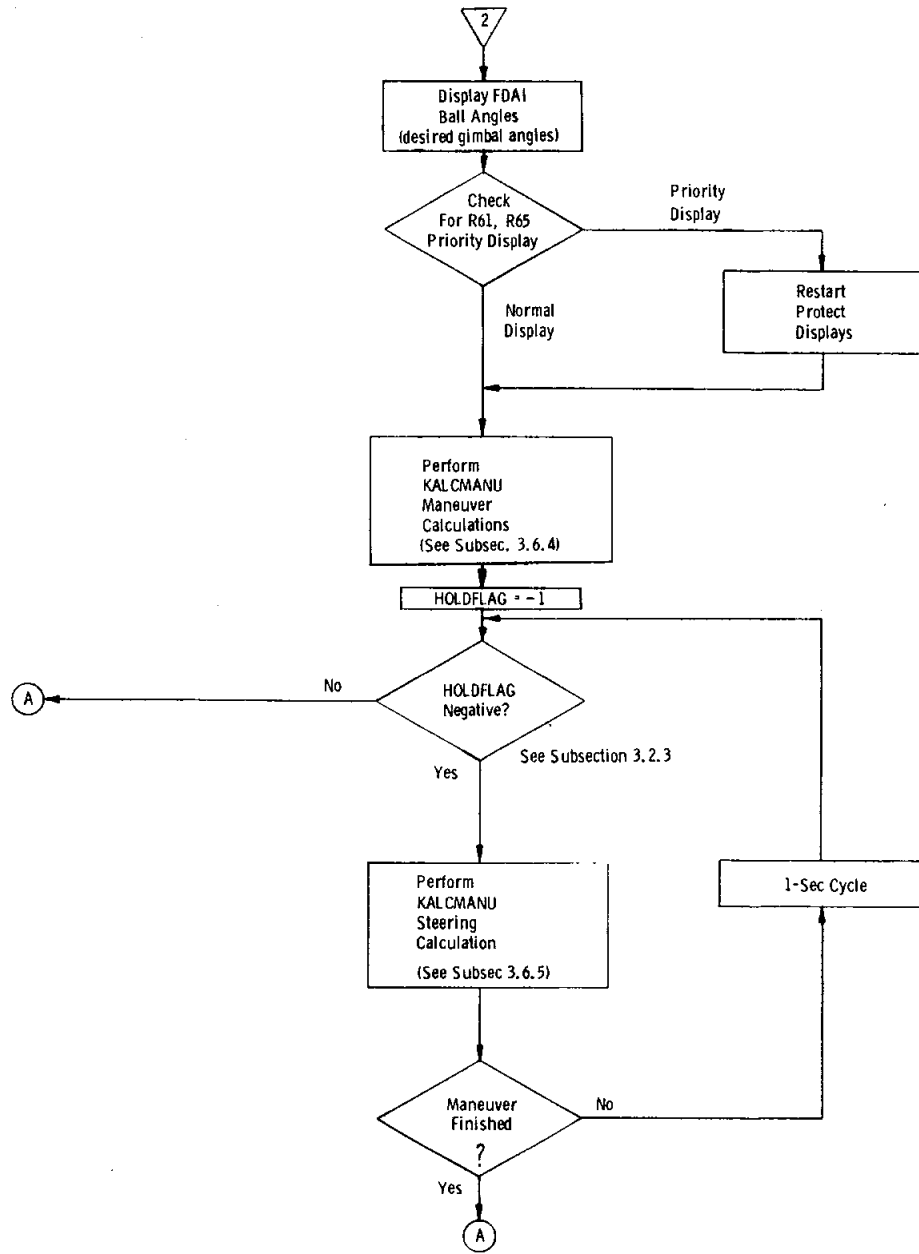


Fig. 3.6.2 R60 Executive (Sheet 2 of 2)



constraining the orientation of the spacecraft about the pointing axis\*, defined by  $\underline{u}_{\text{DSM}}$ . Additionally, the attitude about  $\underline{u}_{\text{DSM}}$  will be left unchanged. Consequently, the crew may specify the attitude about the pointing axis to satisfy additional communication, visibility, or thermal constraints, if desired. This is done by manually reorienting the spacecraft about the pointing axis either prior to or after the maneuver. If this procedure is done after the automatic maneuver, a final trim will usually be required to assure that  $\underline{u}_{\text{ANB}}$  is aligned with  $\underline{u}_{\text{DSM}}$ . If the trim is to be done manually, the crew should place the MODE switch in HOLD and PROCEED with the maneuver request so that the VECPOINT solution is recomputed from the new attitude.

### 3.6.3 VECPOINT

As mentioned in the preceding subsections, the VECPOINT routine is used to compute the desired gimbal angles,  $\underline{\theta}_c$ , based upon the values of  $\underline{u}_{\text{DSM}}$ ,  $\underline{u}_{\text{ANB}}$  and the current gimbal angles,  $\underline{\theta}$ . VECPOINT, in turn, uses a number of subroutines in its computations. These subroutines will be described first.

#### a) CDUTODCM Subroutine

This subroutine converts three gimbal angles,  $\underline{\theta}$ , to a direction-cosine matrix,  $\overset{*}{C}$ , that relates the corresponding spacecraft navigation-base orientation to the stable-member frame. The formulas for this conversion are

$$\overset{*}{C} = \begin{bmatrix} C_1 & C_2 & C_3 \\ C_4 & C_5 & C_6 \\ C_7 & C_8 & C_9 \end{bmatrix}$$

$$C_1 = \cos \theta_i \cos \theta_m$$

$$C_2 = -\cos \theta_i \sin \theta_m \cos \theta_o + \sin \theta_i \sin \theta_o$$

$$C_3 = \cos \theta_i \sin \theta_m \sin \theta_o + \sin \theta_i \cos \theta_o$$

$$C_4 = \sin \theta_m$$

$$C_5 = \cos \theta_m \cos \theta_o$$

$$C_6 = -\cos \theta_m \sin \theta_o$$

$$C_7 = -\sin \theta_i \cos \theta_m$$

---

\* See exception noted in Subsection 3.6.3.

$$C_8 = \sin \theta_i \sin \theta_m \cos \theta_o + \cos \theta_i \sin \theta_o$$

$$C_9 = -\sin \theta_i \sin \theta_m \sin \theta_o + \cos \theta_i \cos \theta_o$$

where

$\theta_o$  = outer gimbal angle

$\theta_i$  = inner gimbal angle

$\theta_m$  = middle gimbal angle

The interpretation of this matrix is as follows: If  $a_x$ ,  $a_y$ ,  $a_z$  represent the components of a vector in navigation-base axes, then the components of the same vector in stable-member axes ( $b_x$ ,  $b_y$ ,  $b_z$ ) are

$$\begin{pmatrix} b_x \\ b_y \\ b_z \end{pmatrix} = \overset{*}{C}(\underline{\theta}) \begin{pmatrix} a_x \\ a_y \\ a_z \end{pmatrix}$$

#### b) DCMTOCDU Subroutine

This subroutine extracts the CDU angles from a direction-cosine matrix,  $\overset{*}{C}$ , that relates the navigation-base axes to the stable-member axes. The formulas for this conversion are

$$\theta_m = \arcsin C_4$$

$$\theta_i = \arcsin (-C_7 / \cos \theta_m)$$

[ If  $C_1$  is negative,  $\theta_i$  is replaced by  $\pi \text{SGN}(\theta_i) - \theta_i$  ]

$$\theta_o = \arcsin (-C_6 / \cos \theta_m)$$

[ If  $C_5$  is negative,  $\theta_o$  is replaced by  $\pi \text{SGN}(\theta_o) - \theta_o$  ]

#### c) ROTCOMP Subroutine

This subroutine computes the direction-cosine matrix,  $\overset{*}{R}$ , that relates one coordinate frame to another frame that is rotated with respect to the first by an angle  $A$  about a unit vector  $\underline{u}_r$ . The formula for this matrix is

$$\overset{*}{R}(\underline{u}_r, A) = \overset{*}{I} \cos A + \underline{u}_r \underline{u}_r^T (1 - \cos A) + \overset{*}{U} \underline{X}_r \sin A$$

where

$$\begin{aligned} \overset{*}{I} &= \begin{bmatrix} 1 & 0 & 0 \\ 0 & 1 & 0 \\ 0 & 0 & 1 \end{bmatrix} \\ \underline{u}_r \underline{u}_r^T &= \begin{bmatrix} u_{rx}^2 & u_{rx} u_{ry} & u_{rx} u_{rz} \\ u_{ry} u_{rx} & u_{ry}^2 & u_{ry} u_{rz} \\ u_{rz} u_{rx} & u_{rz} u_{ry} & u_{rz}^2 \end{bmatrix} \\ \overset{*}{UX}_r &= \begin{bmatrix} 0 & -u_{rz} & u_{ry} \\ u_{rz} & 0 & -u_{rx} \\ -u_{ry} & u_{rx} & 0 \end{bmatrix} \end{aligned}$$

$\underline{u}_r$  = unit rotation vector resolved into spacecraft axes

A = rotation angle

The interpretation of  $\overset{*}{R}$  is as follows: If  $a_x, a_y, a_z$  represent the components of a vector in the rotated frame, then the components of the same vector in the original frame ( $b_x, b_y, b_z$ ) are

$$\begin{pmatrix} b_x \\ b_y \\ b_z \end{pmatrix} = \overset{*}{R}(\underline{u}_r, A) \begin{pmatrix} a_x \\ a_y \\ a_z \end{pmatrix}$$

The process used by VECPOINT in determining the terminal desired angles,  $\theta_c$ , is illustrated schematically in Fig. 3.6.3. VECPOINT uses three frames of reference: the L frame, the M frame, and the N frame - as well as the stable-member (SM) frame. The L frame is simply a base frame used as the starting



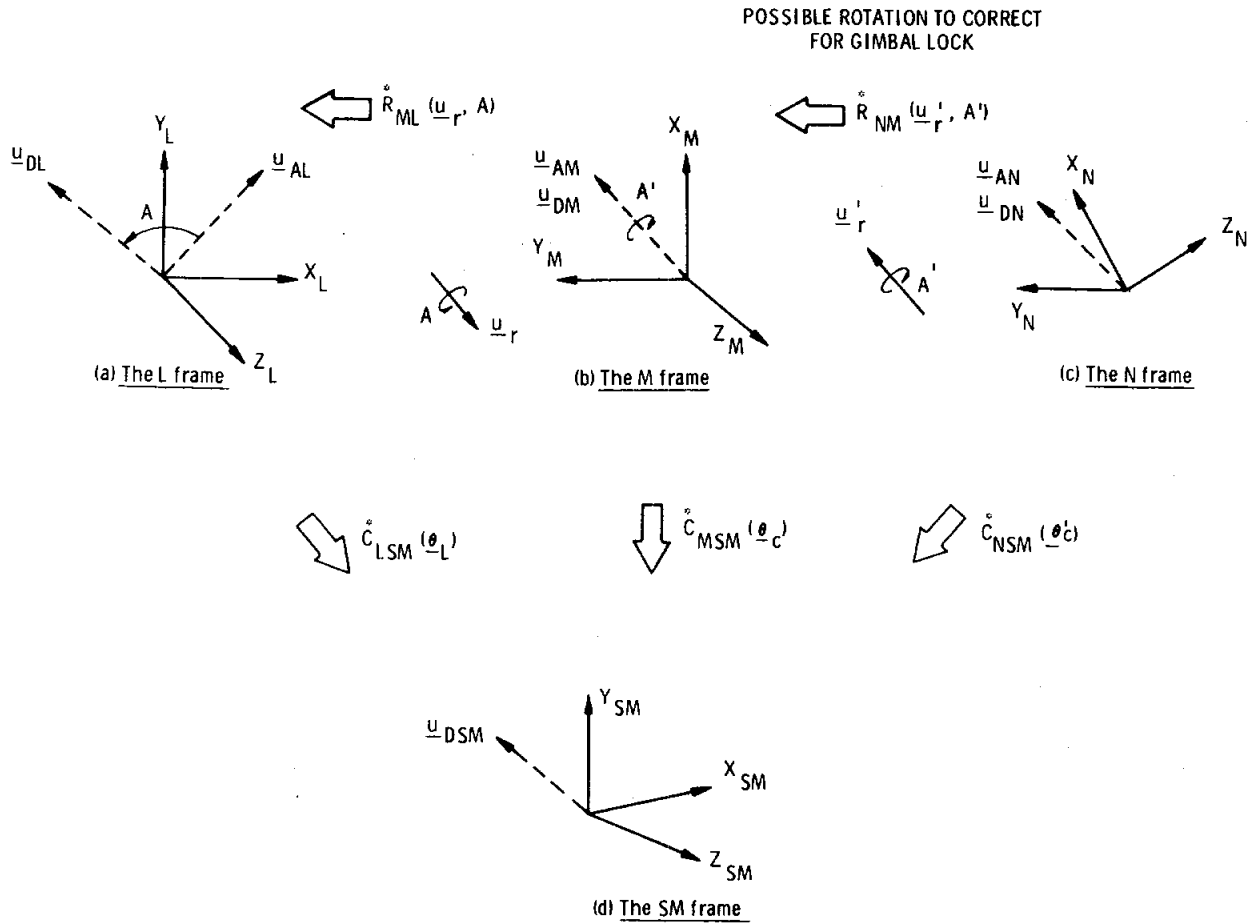


Fig. 3.6.3 The coordinate frames and transformations used in VECPOINT

point for subsequent rotations. In R60 VECPOINT computations, the L frame is the initial navigation-base frame computed from the initial gimbal angles,  $\theta$ . The vector  $\underline{u}_D$  is resolved from the stable-member frame as  $\underline{u}_{DL}$  † using the transformation  $\dot{C}_{LSM}^* \ddagger$ . The L frame is then rotated so that  $\underline{u}_{AL}$  and  $\underline{u}_{DL}$  are coincident. The rotation vector,  $\underline{u}_r$ , is defined by the cross product between  $\underline{u}_{AL}$  and  $\underline{u}_{DL}$ . If the two vectors are either parallel or antiparallel, a special computation of  $\underline{u}_r$  is performed (see below). Rotation about the cross-product vector will assure that spacecraft maneuvering will be minimized and that the rotation vector will have no component in the  $\underline{u}_{AL}$  or  $\underline{u}_{DL}$  directions.

In the M frame,  $\underline{u}_A$  is aligned with  $\underline{u}_D$  and normally the desired terminal angles can be extracted directly from the matrix  $\dot{C}_{MSM}^*$  that relates this frame to the stable-member frame. If, however, the M frame corresponds to a gimbal-lock orientation, an extra rotation about  $\underline{u}_{DM}$  (or  $\underline{u}_{AM}$ ) will be necessary to correct for the gimbal-lock condition.\*\* For VECPOINT, gimbal lock is defined when  $\underline{u}_{XM}$  is within 31 deg of the  $\pm y$  stable-member axis direction ( $\pm \underline{u}_{YSM}$ ), that is, when the magnitude of the desired terminal middle gimbal angle,  $|\theta_{cm}|$ , exceeds 59 deg. This situation is illustrated in Fig. 3.6.5, in which the shaded area represents the gimbal-lock region. As can be seen,  $\underline{u}_{XM}$  can be rotated out of gimbal lock by a sufficiently large rotation about  $\underline{u}_{AM}$ . Under some circumstances, however, no amount of rotation about  $\underline{u}_{AM}$  will correct for gimbal lock. This possibility may occur if the angle between  $\pm \underline{u}_{XM}$  and  $\underline{u}_{AM}$  is less than 31 deg. Whether or not gimbal lock can be corrected in such a case depends on the geometry of the problem. In order to simplify the VECPOINT calculations, however, it was decided that gimbal lock would be unavoidable under these circumstances. In fact, no correction will be made in VECPOINT if

$$\left| \underline{u}_{AM} \cdot \underline{u}_{XM} \right| \geq \cos 40.6 \text{ deg}$$

and  $\underline{u}_{XM}$  falls within the gimbal-lock region. Note that this criterion includes among others, the thrust vector for P40 pre-burn alignments. In this case, a platform realignment would be required before reorienting the spacecraft.

† The subscript L appended to the vector indicates the frame of reference into which the vector is resolved. Note that the components of  $\underline{u}_{ANB}$ ,  $\underline{u}_{AL}$ ,  $\underline{u}_{AM}$  and  $\underline{u}_{AN}$  are all numerically equal since they represent the same body-fixed vector.

‡  $\dot{C}_{LSM}^*$  is defined as the transformation from the L frame (or first subscript) to the stable-member frame (or second subscript).  $\dot{C}_{LSM}^{*T}$  is its transpose.

\*\* Note that, while there is logic in VECPOINT (see Fig. 3.6.4) to avoid a final middle gimbal angle causing gimbal lock, there is no logic in the KALCMANU calculation of maneuver parameters which ensures that the computed maneuver will not carry the vehicle attitude through gimbal lock during the maneuver.

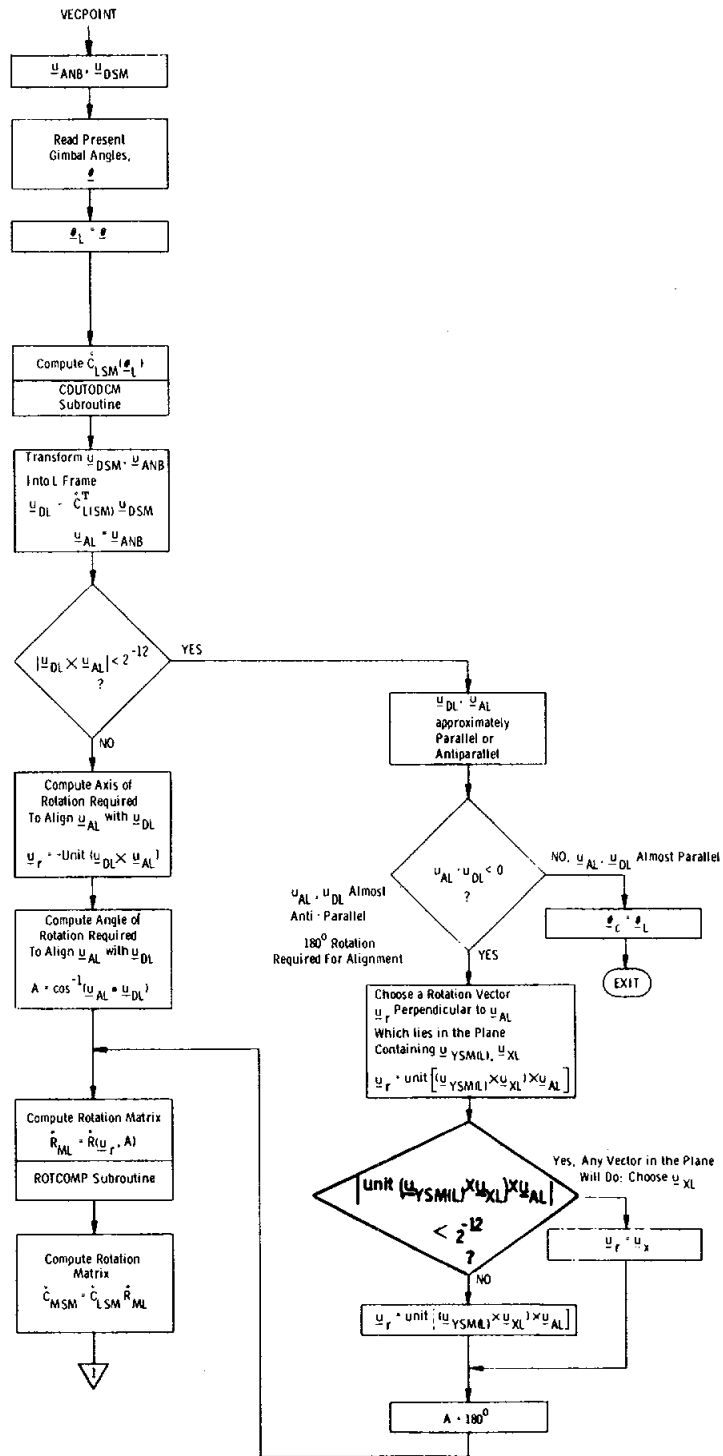


Fig. 3.6.4 VECPOINT logic flow (Sheet 1 of 2)

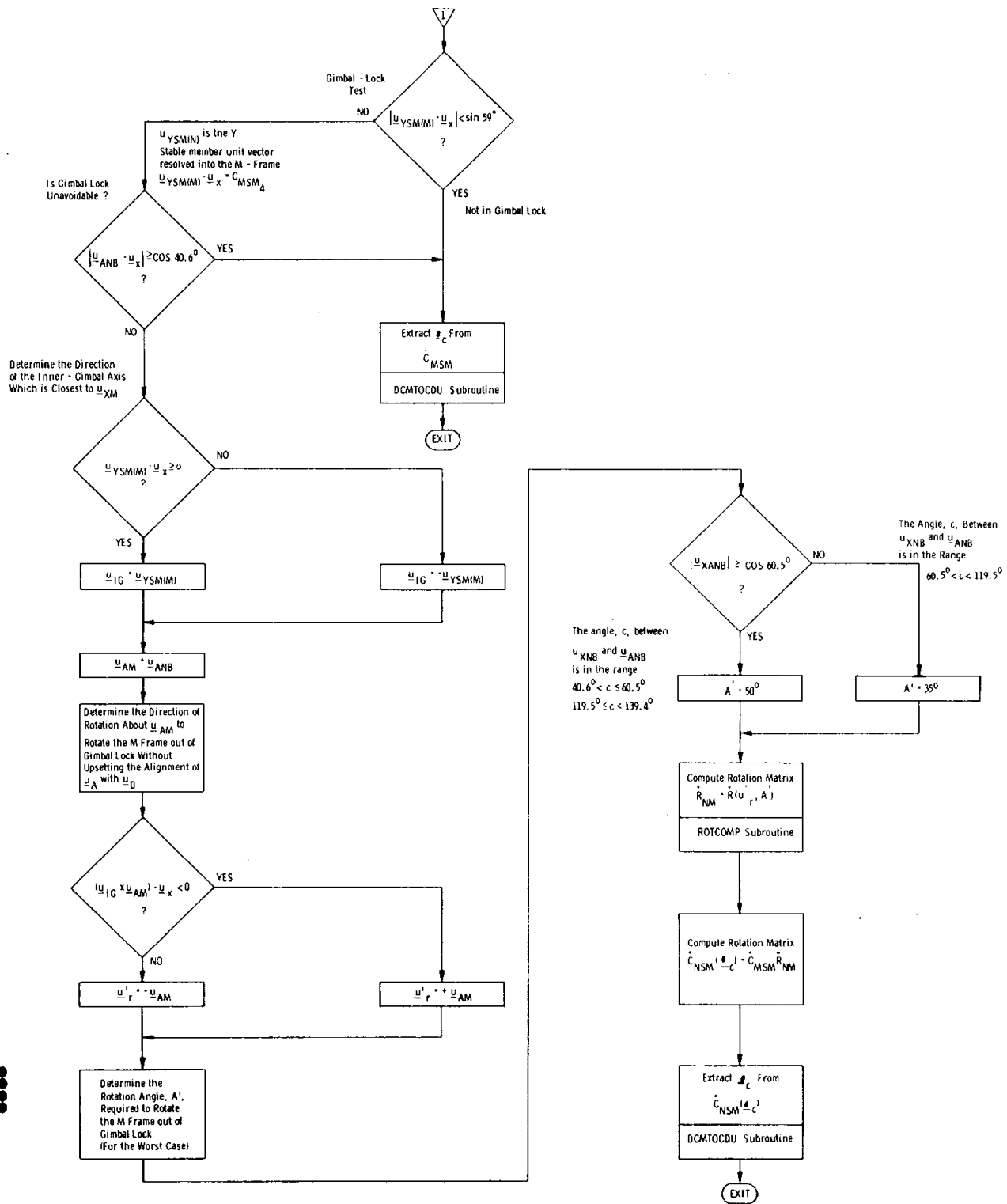


Fig. 3.6.4 VECPOINT logic flow (Sheet 2 of 2)

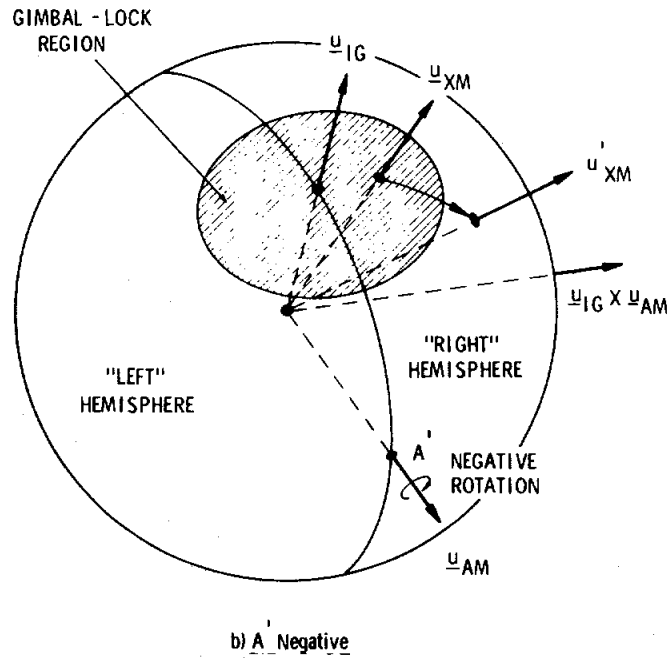
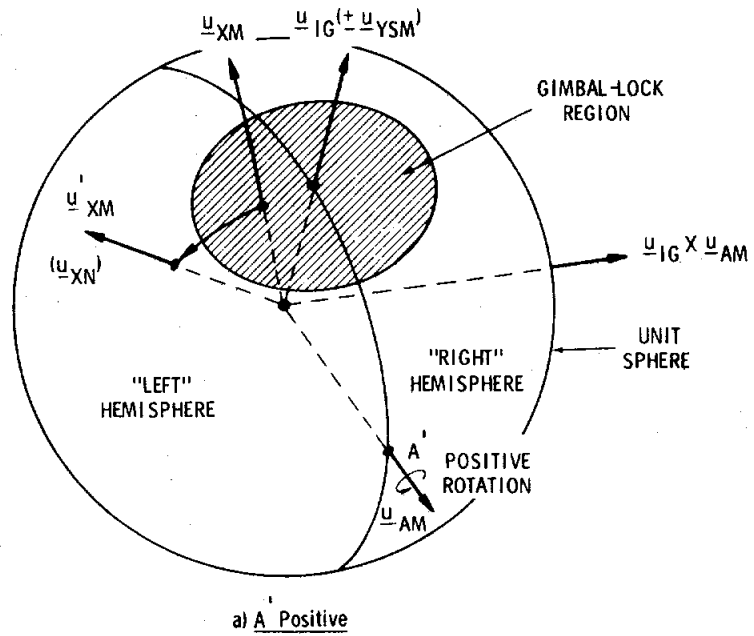


Fig. 3.6.5 Rotation to correct for gimbal lock



If it is found that the M frame can be reoriented to correct for gimbal lock, then the next step in the logic is to determine the direction of rotation about  $\underline{u}_{AM}$  and the magnitude of the rotation,  $A'$ , required for this reorientation. It is desirable to find the direction that minimizes the angular excursion through the gimbal-lock region. This is found by first locating the direction  $\underline{u}_{IG}$  of the inner gimbal axis ( $+\underline{u}_{YSM}$  or  $-\underline{u}_{YSM}$ ) that is closest to  $\underline{u}_{XM}$ . Referring to Fig. 3.6.5, if  $\underline{u}_{XM}$  lies to the "left" of the plane defined by  $\underline{u}_{IG}$  and  $\underline{u}_{AM}$ , then  $A'$  is positive. If, on the other hand,  $\underline{u}_{XM}$  lies to the "right" of the plane defined by  $\underline{u}_{IG}$  and  $\underline{u}_{AM}$ , then  $A'$  is negative. Note that if  $\underline{u}_{XM}$  lies in the plane of  $\underline{u}_{IG}$  and  $\underline{u}_{AM}$  then  $A'$  can be either positive or negative. For this case,  $|A'|$  is greatest for any fixed angular relation between  $\underline{u}_{IG}$  and  $\underline{u}_{AM}$ .

The remaining part of the problem is to determine the magnitude of the rotation required to correct for gimbal lock. Theoretically, one could determine the minimum rotation required to place  $\underline{u}'_{XM}$  exactly on the boundary of the gimbal-lock region. To simplify the problem, however, VECPOINT uses a predetermined set of angles that will assure that, even in the worst case,  $\underline{u}'_{XM}$  will always lie outside the gimbal-lock region. To define the worst-case conditions, examine the spherical triangle ABC shown in Fig. 3.6.6. The problem is to find the maximum value of the rotation angle,  $A$ , required to rotate  $\underline{u}_{XM}$  to the gimbal-lock boundary (point B), given the angle  $c$  between  $\underline{u}_{AM}$  and  $\underline{u}_{XM}$ . Clearly, the maximum value of  $A$  occurs when  $\underline{u}_{XM}$  falls in the "middle" of the gimbal-lock region, that is, when  $\underline{u}_{XM}$  lies in the plane of  $\underline{u}_{IG}$  and  $\underline{u}_{AM}$ . The following relationship holds for any spherical triangle:

$$\sin A = \sin a \frac{\sin C}{\sin c}$$

The maximum value of  $A$ ,  $A_{\max}$ , occurs when

$$\frac{dA}{dC} = \frac{\sin a}{\sin c} \frac{\cos C}{\cos A} = 0$$

or when  $\cos C = 0$ , that is,  $C = 90^\circ$ .

Thus,

$$A_{\max} = \sin^{-1} \frac{\sin a}{\sin c}$$

Note that the required rotation angle depends directly on the angle between  $\underline{u}_{XM}$  and  $\underline{u}_{AM}$ . If  $c$  is less than  $a$ , then  $A_{\max}$  is indeterminate; that is, gimbal lock may be unavoidable. To avoid calculating  $A_{\max}$  explicitly, VECPOINT divides the problem into three zones as defined in the following table.

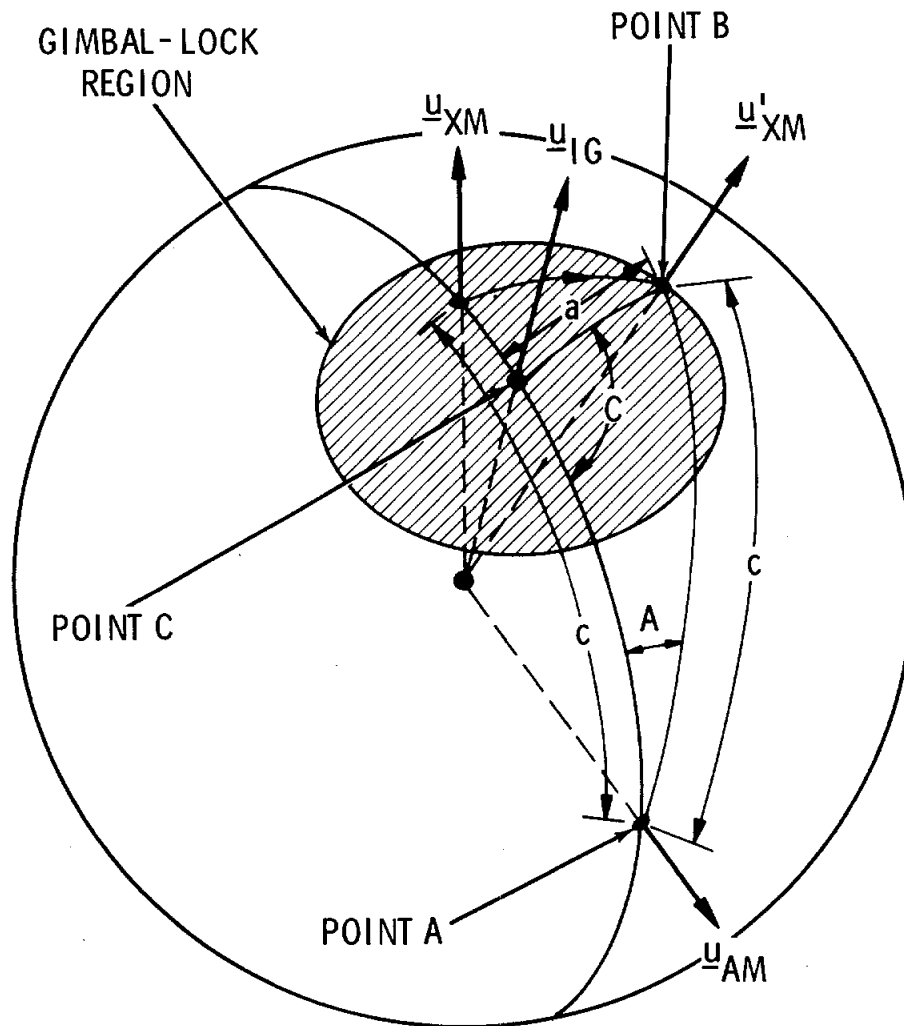


Fig. 3.6.6 Geometry for computing the maximum value of the angle A



c	A <sub>max</sub> (a ≈ 30°)
60.5° < c < 119.5°	35°
40.6° < c ≤ 60.5° 119.5° ≤ c < 139.4°	50°
0 ≤ c ≤ 40.6° 139.4° ≤ c ≤ 180°	INDETERMINATE

Note that the correction for gimbal lock will override the desire to minimize the rotation about the  $\underline{u}_A$  axis.

The one remaining item to be discussed concerning VECPOINT is the case when  $\underline{u}_{AL}$  and  $\underline{u}_{DL}$  are almost parallel or antiparallel. If  $\underline{u}_{AL}$  and  $\underline{u}_{DL}$  are almost parallel, then  $\underline{\theta}_c$  is set equal to  $\underline{\theta}_L$ . If the two vectors are almost antiparallel, then a 180-deg rotation is required for the alignment. In this case, the rotation vector is chosen so that  $\underline{u}_r$  is perpendicular to  $\underline{u}_{AL}$  and lies in the plane that contains  $\underline{u}_{YSM(L)}$  and  $\underline{u}_{XL}$ . If, however,  $\underline{u}_{AL}$  happens to be perpendicular to the plane, then any vector in the plane may be used for  $\underline{u}_r$ . In this event, the X axis is chosen. The computation of the M frame, the check for gimbal lock, and the extraction of the desired angles,  $\underline{\theta}_c$ , are then performed in the manner already described.

#### 3.6.4 KALCMANU Maneuver-Parameters Calculation

The KALCMANU routine is designed to generate commands for the CSM-RCS autopilot to reorient the spacecraft from an initial attitude to some desired attitude specified by  $\underline{\theta}_c$ . Although a number of authors have discussed optimal solutions to this problem, the task is a formidable one because of the nonlinear nature of rigid-body dynamics and the kinematics of rotational motion. Optimal solutions for a particular class of spacecraft configurations are treated in Reference 6.1. In this reference, the criterion for optimality is based upon the product of maneuver duration and fuel expenditure. Using the same criterion, previous design studies based upon a number of suboptimal approaches (Ref 6.2) have shown that a reasonable design compromise is to rotate the spacecraft about a single inertially fixed axis. This technique is employed in KALCMANU.



The process used by KALCMANU in computing the rotation axis,  $\underline{u}_r$ , and the rotation angle,  $A_m$ , is illustrated in Fig. 3.6.7. The program first computes the transformation between the initial spacecraft axes (at the time the KALCMANU routine begins) and the stable-member axes,  $\overset{*}{C}_{BSM}$ . The program also computes the matrix relating the desired terminal spacecraft attitude and the stable-member axes,  $\overset{*}{C}_{CSM}$ . The transformation between the desired and the initial attitude is  $\overset{*}{R}_{CB}$ , where

$$\overset{*}{R}_{CB} = \overset{*}{C}_{BSM}^T \overset{*}{C}_{CSM}$$

$\overset{*}{R}_{CB}$  can be partitioned into its symmetric and antisymmetric components as follows.

For the symmetric part,

$$\overset{*}{R}_S = (1/2)(\overset{*}{R}_{CB} + \overset{*}{R}_{CB}^T)$$

By comparing this with the equations described in the ROTCOMP subroutine (see Subsection 3.6.3) it can be seen that

$$\overset{*}{R}_S = \overset{*}{I} \cos A_m + \underline{u}_r \underline{u}_r^T (1 - \cos A_m)$$

For the antisymmetric part,

$$\overset{*}{R}_A = (1/2)(\overset{*}{R}_{CB} - \overset{*}{R}_{CB}^T)$$

or

$$\overset{*}{R}_A = \begin{bmatrix} 0 & -u_{rz} & u_{ry} \\ u_{rz} & 0 & -u_{rx} \\ -u_{ry} & u_{rx} & 0 \end{bmatrix} \sin A_m$$

The maneuver angle can easily be obtained from  $\overset{*}{R}_{CB}$  as

$$A_m = \cos^{-1} \left( \frac{\text{Trace}(\overset{*}{R}_{CB}) - 1}{2} \right)$$

The rotation vector,  $\underline{u}_r$ , is normally extracted from the antisymmetric part of  $\overset{*}{R}_{CB}$ ; that is,

$$\underline{u}_r = \text{unit} (-R_{A6}, R_{A3}, -R_{A2})$$

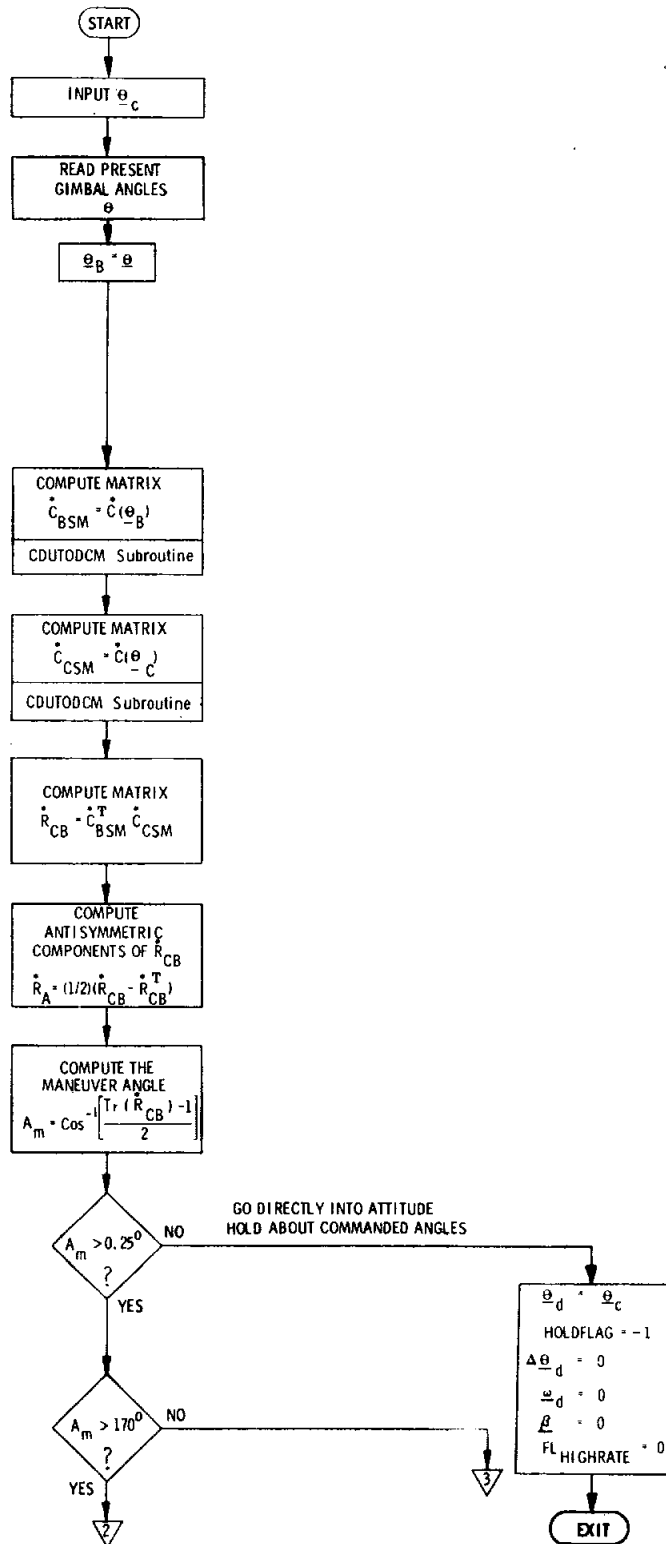


Fig. 3.6.7 Calculation of KALCMANU maneuver parameters (Sheet 1 of 3)

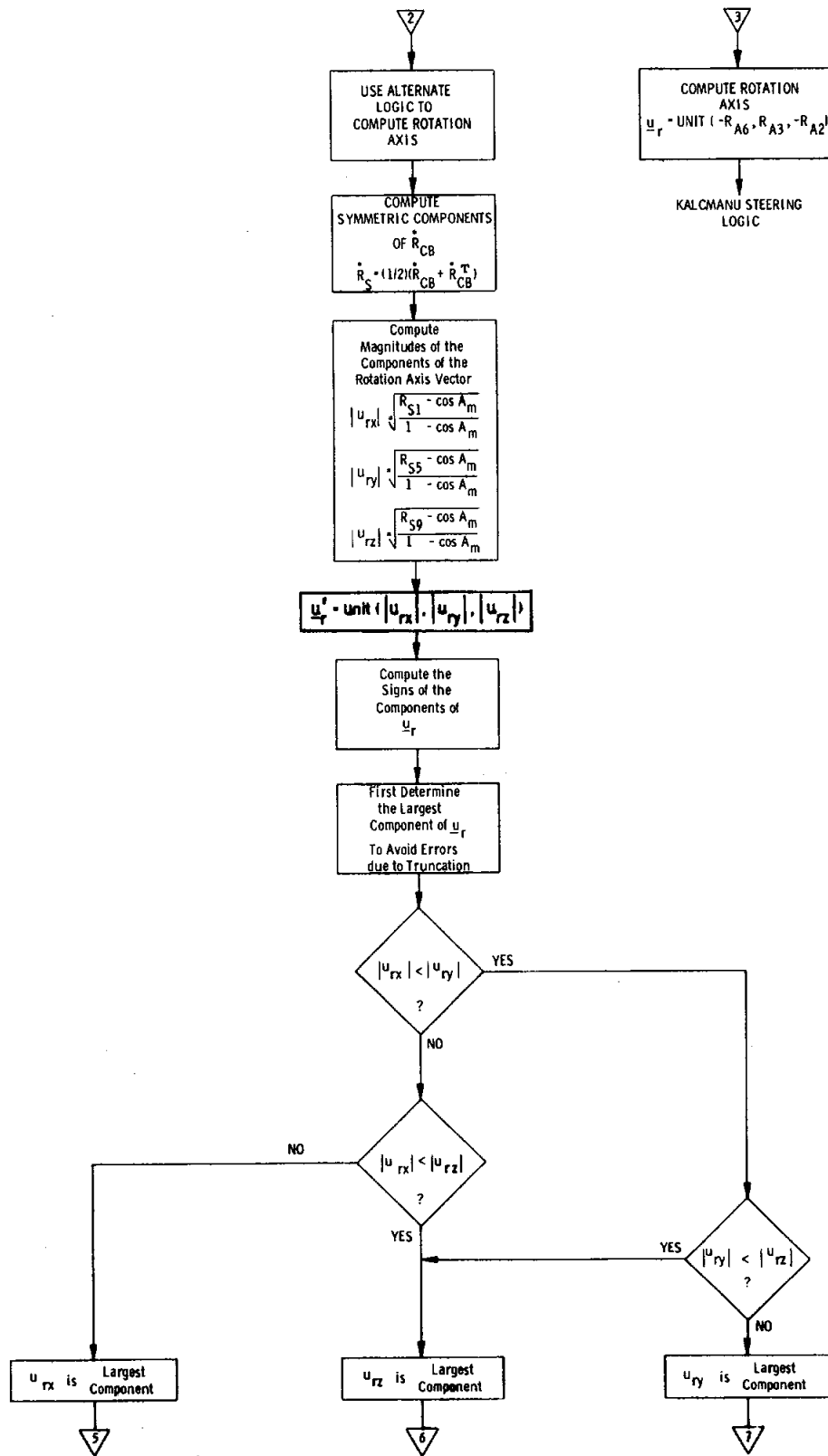


Fig. 3.6.7 Calculation of KALCMANU maneuver parameters (Sheet 2 of 3)



As  $\sin A_m$  approaches zero, however, the unit operation becomes indeterminate and an alternative calculation must be performed. If the maneuver angle is less than 0.25 deg, then no complicated automatic maneuvering is necessary and therefore one can simply set the autopilot reference angle,  $\theta_d$ , equal to the terminal desired angles  $\theta_c$  and exit. If  $A_m > 170$  deg, a method employing the symmetric part of  $\mathbf{R}_{CB}^*$  is used to determine  $\underline{u}_r$ , as illustrated in Fig. 3.6.7. The magnitudes of the components of  $\underline{u}_r$  are easily determined as

$$|u_{rx}| = \sqrt{\frac{R_{S1} - \cos A_m}{1 - \cos A_m}}$$

$$|u_{ry}| = \sqrt{\frac{R_{S5} - \cos A_m}{1 - \cos A_m}}$$

$$|u_{rz}| = \sqrt{\frac{R_{S9} - \cos A_m}{1 - \cos A_m}}$$

To obtain the signs of each component, it is first necessary to determine the sign of the largest component by referring to the values of  $\mathbf{R}_A^*$ . This is done to avoid the problem caused by truncation as  $\sin A_m$  approaches zero. If  $A_m$  is equal to 180 deg, then the sign of the largest component may be arbitrarily chosen. The signs of the remaining components may be determined by examining the off-diagonal terms in  $\mathbf{R}_S^*$ .

### 3.6.5 KALCMANU Steering

The KALCMANU parameter calculations described in the preceding subsection solve the problem of what angular path to take in order to reorient the spacecraft without excessive fuel expenditure. However, the problem of how to steer the spacecraft along this path must now be considered. One solution is to iteratively solve for  $\underline{u}_r$  and  $A_m$  explicitly as a function of the current spacecraft attitude and to control the spacecraft angular velocity,  $\underline{\omega}$ , by firing the RCS jets so that  $\underline{\omega}$  is parallel to  $\underline{u}_r$ . This approach, however, leads to several problems. First of all, because of the deadband requirements of the autopilot, and control inaccuracies, explicit guidance can lead to excessive changes in control commands as the spacecraft approaches the terminal attitude. This problem of terminal guidance is characteristic of explicit guidance schemes unless special consideration is given to the terminal-control problem. Secondly, there is a timing problem since the computation of  $\underline{u}_r$  and  $A_m$  is somewhat lengthy and would require an excessive amount of computer time. Instead, it is better to formulate the problem in terms of perturbations from a smooth reference trajectory that satisfies the end-point constraints. The procedure is to solve the global problem once via KALCMANU in order to establish a reference trajectory (defined by  $\underline{u}_r$ ,  $A_m$ ) and then have the autopilot solve

the micro-problem of controlling the spacecraft deviations from this reference trajectory, using small-angle approximations. This approach not only avoids the terminal-guidance problem and the timing problem but also provides "tighter" path control for satisfying other boundary conditions that may be placed upon the selection of the reference trajectory.

In order to determine the required steering interface between KALCMANU and the autopilot, it is first necessary to define the nature of the autopilot control variables. To simplify the discussion, the two-dimensional problem of rotation in a plane is considered first. There are two state variables of interest; namely, the attitude error,  $\theta_e$ , defined by

$$\theta_e = \theta - \theta_d$$

where

$$\theta = \text{actual vehicle attitude}$$

$$\theta_d = \text{desired vehicle attitude (constant)}$$

and the angular velocity of the vehicle,  $\omega$ . The "state" equations are

$$\dot{\theta}_e(t) = \omega(t)$$

and

$$\dot{\omega}(t) = f(\theta_e, \omega)$$

where

$f(\theta_e, \omega)$  is the control acceleration (applied by the jets) as determined by non-linear phase-plane switching logic. The control law is defined so that  $\theta_e$  and  $\omega$  will be nulled to within the control-law deadbands so as to maintain attitude hold about the reference attitude,  $\theta_d$ .

New state variables can be defined as follows:

$$\phi_e(t) = \theta(t) - \phi_d(t) + \beta$$

and

$$\omega_e(t) = \omega(t) - \omega_d$$

where

$$\phi_d(t) = \phi_d(t_0) + \omega_d [t - t_0]$$

$$\omega_d = \text{a constant}$$

$$\beta = \text{a constant}$$

$$\phi_d(t_0) \stackrel{\Delta}{=} \theta(t_0) = \text{constant}$$

The state equations for the new variables are

$$\dot{\phi}_e = \omega_e$$

$$\dot{\omega}_e = f(\phi_e, \omega_e)$$

With these control variables, the autopilot will attempt to null the rate error,  $\omega_e$ , thus forcing the spacecraft to rotate at a constant rate. With this simple transformation of variables, using the same control law as used for attitude hold, the autopilot can be converted to a constant-rate-command system. Note that at the beginning of the maneuver the desired angle  $\phi_d(t_0)$  is set equal to the initial angle  $\theta(t_0)$ . The constant,  $\beta$ , is added to the attitude error to prevent overshoot when starting and stopping the maneuver.  $\beta$  is computed as

$$\beta = -\frac{\omega_d}{m}$$

where

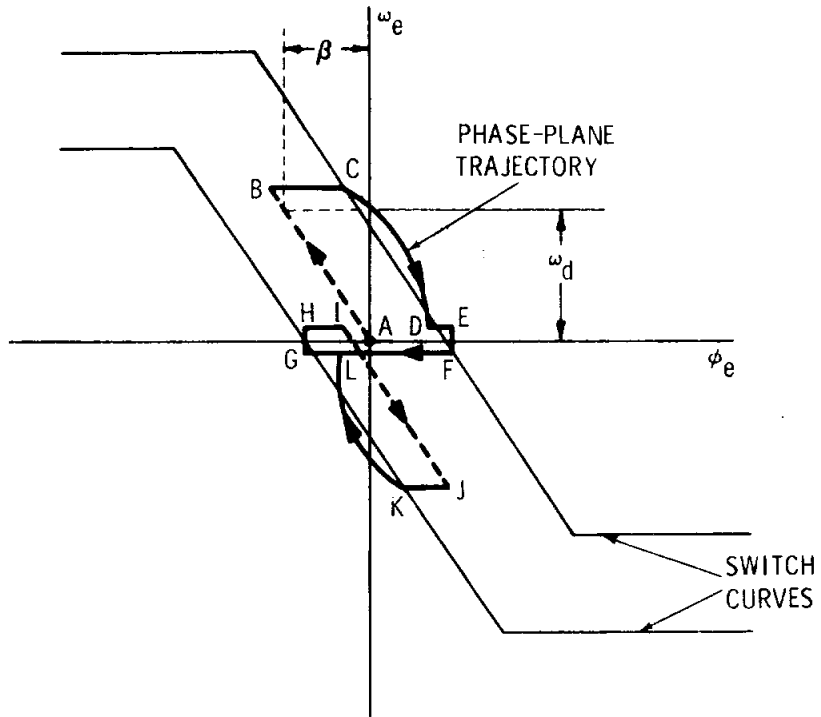
$m$  = slope of the phase-plane switch line (- 0.6 deg/sec/deg)

To interpret the effect of  $\beta$ , refer to Fig. 3.6.8a. This figure shows a simplified phase-plane logic and a typical phase-point trajectory. The maneuver starts at point A with  $\theta_e = 0$  and  $\omega = 0$ . With the application of steering commands, the phase point instantaneously jumps to a biased condition at B where  $\phi_e = \beta$  and  $\omega_e = -\omega_d$  ( $\omega_d$  is negative for the case illustrated). The phase point drifts to point C, where the control jets are turned on to reduce the rate error toward zero at point D. The trajectory then traverses a limit cycle EFGH until the maneuver finishes at point I, where the biases  $\beta$  and  $\omega_d$  are removed. At this point, the trajectory jumps to an unbiased condition at point J. Note that the actual rate is approximately equal to the desired rate and the phase point drifts to point K, where the jets decelerate the vehicle back into a limit cycle around the desired attitude. The situation without the angular bias,  $\beta$ , is illustrated in Fig. 3.6.8b. Note the fuel-consuming overshoot in this case. The inclusion of the bias term is based on the assumption that the initial rates are small and that the desired rates are achievable during the maneuver. For the three-dimensional problem, it must also be assumed that  $\beta$  is small enough so that the small-angle assumptions are not violated. For these reasons, CSM-LM docked automatic maneuvers should not exceed rates of more than 0.5 deg/sec.

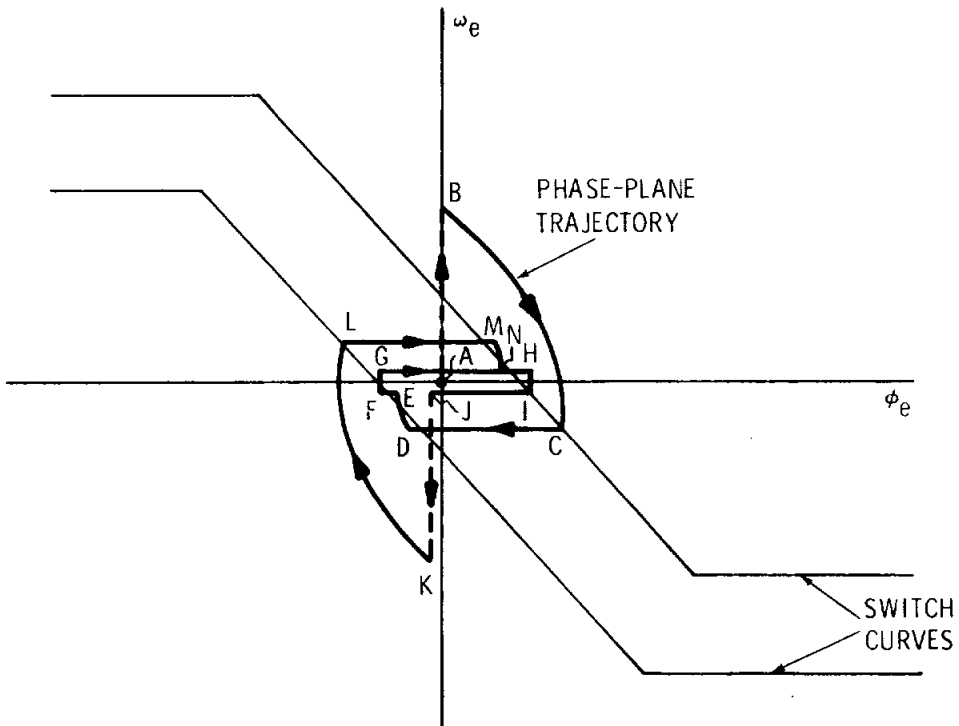
The logic flow for KALCMANU steering is shown in Fig. 3.6.9. The basic inputs are

- a)  $\underline{u}_r$ , the unit rotation vector.
- b)  $A_m$ , the rotation angle.
- c)  $|\omega_d|$ , the magnitude of the desired angular velocity as specified in R03.
- d) HOLDFLAG

The steering logic works on a cyclic basis. Every  $\Delta T_c$  (= 1 sec), the program issues new steering commands to the autopilot. On the first pass, a number of



a) Typical phase-plane trajectory with  $\beta$



b) Typical phase-plane trajectory without  $\beta$

Fig. 3.6.8 Maneuver phase-plane trajectories



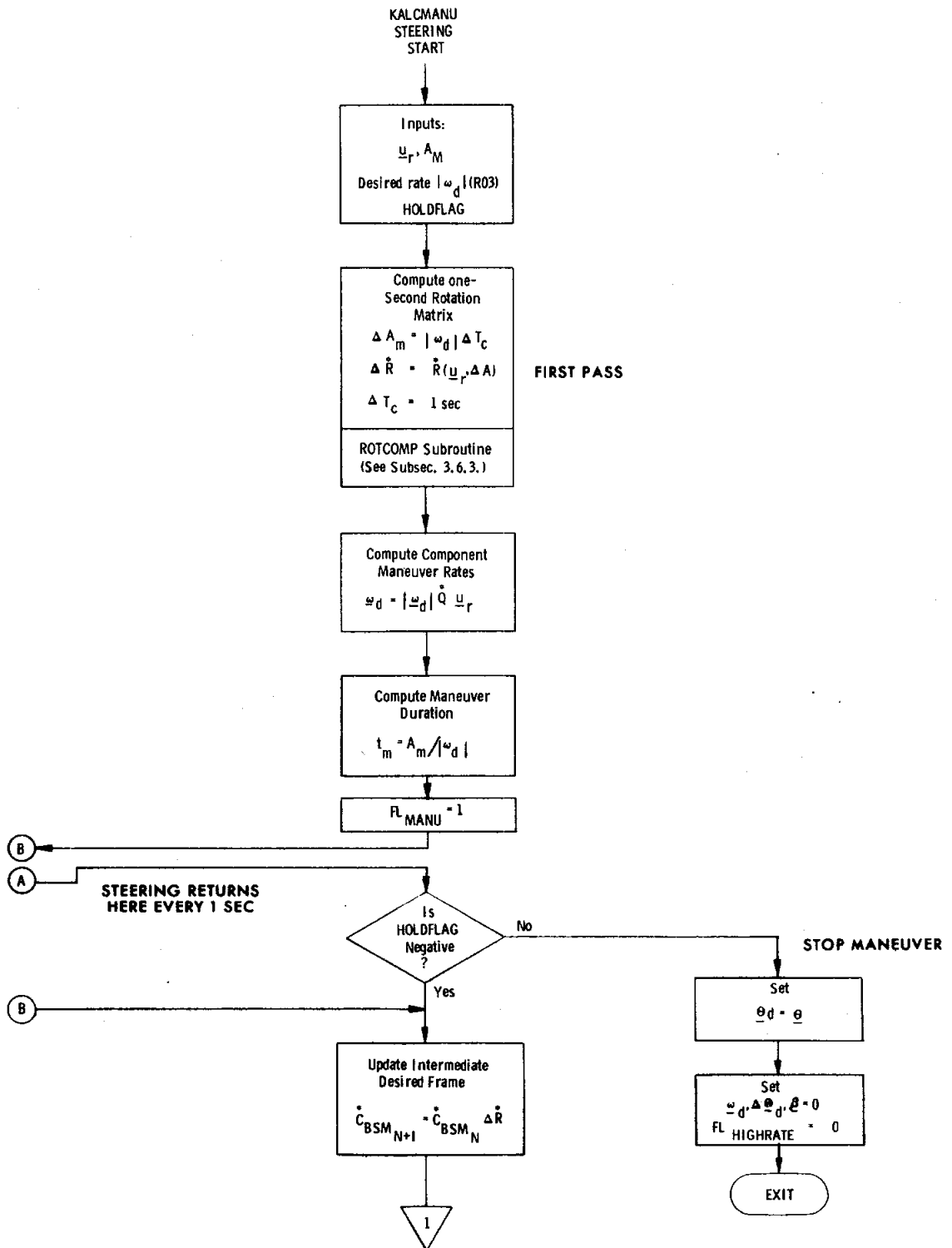


Fig. 3.6.9 KALCMANU steering logic (Sheet 1 of 4)

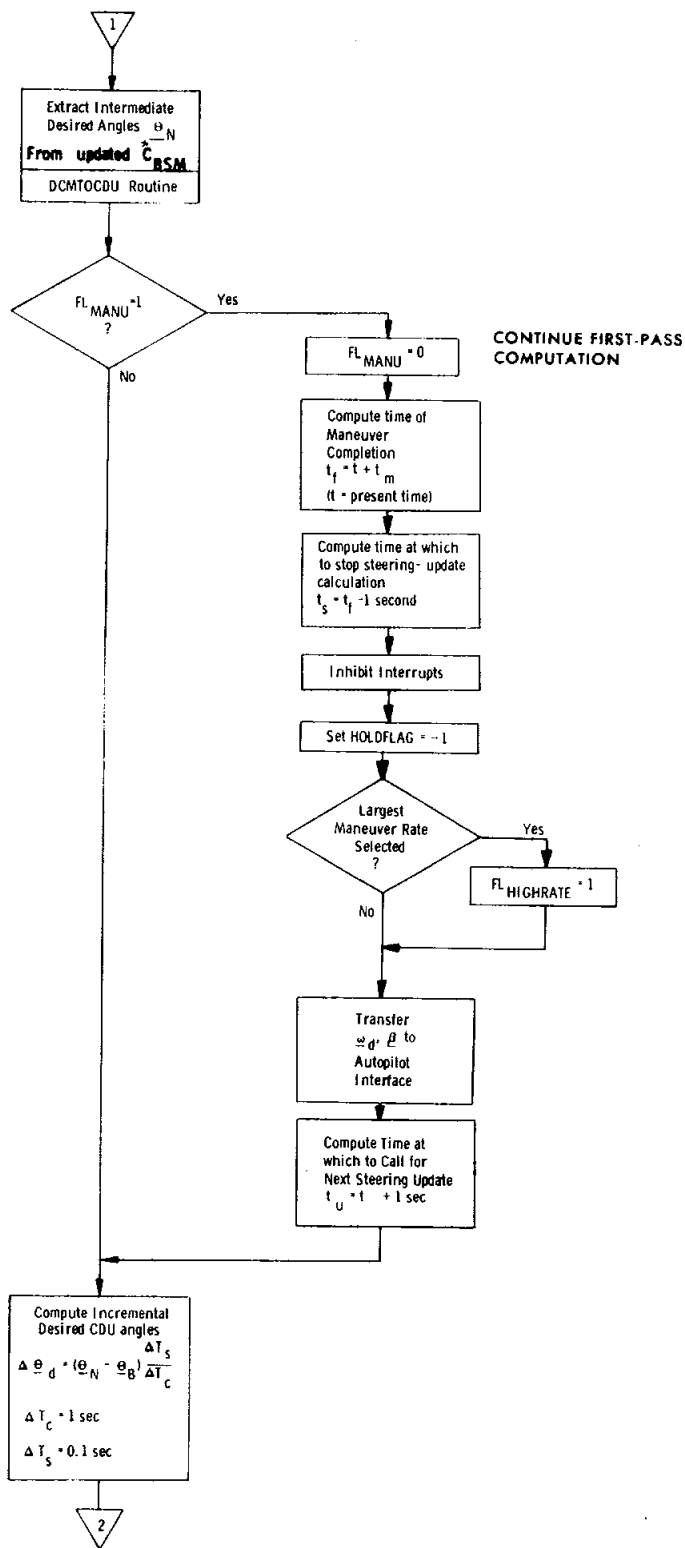


Fig. 3.6.9 KALCMANU steering logic (Sheet 2 of 4)

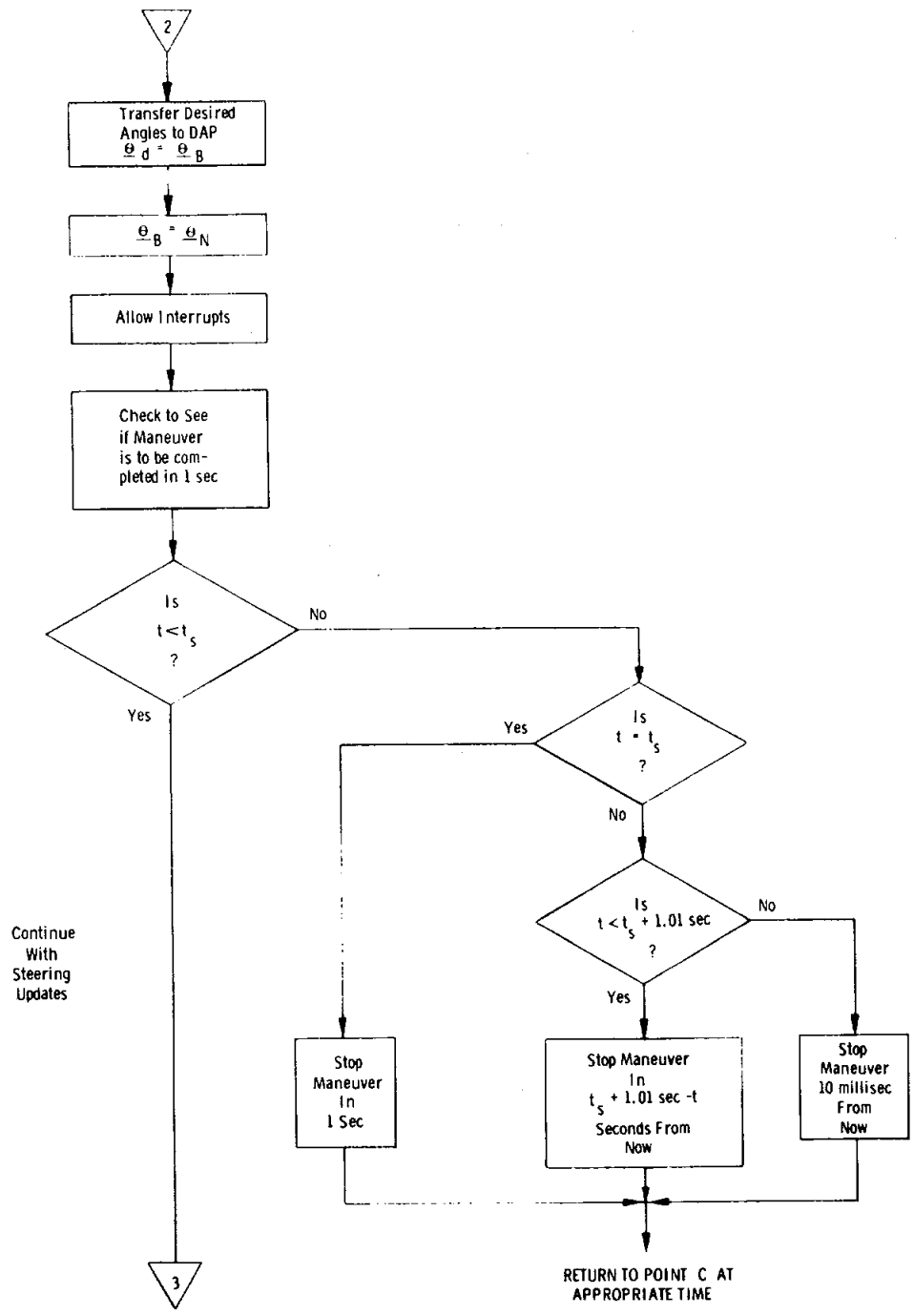


Fig. 3.6.9 KALCMANU steering logic (Sheet 3 of 4)

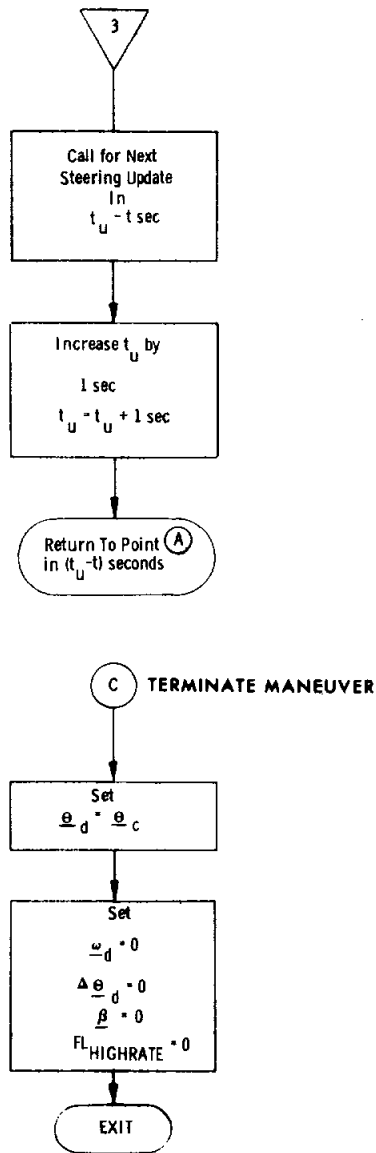


Fig. 3.6.9 KALCMANU steering logic (Sheet 4 of 4)

parameters are computed once and used during subsequent passes. One of these is the incremental rotation matrix,  $\Delta\mathbf{R}^*$ . This matrix corresponds to a one-second rotation of  $\mathbf{C}_{\text{BSM}}^*$ , the initial spacecraft orientation, about the rotation axis,  $\underline{u}_r$ . The magnitude of the rotation  $\Delta A_m$  is determined as

$$\Delta A_m = |\omega_d| \Delta T_c$$

For the first and all subsequent passes through the steering logic,  $\mathbf{C}_{\text{BSM}}^*$  is rotated by the angle  $\Delta A_m$ , and the autopilot reference angles  $\underline{\theta}_d$  are extracted from this matrix. The new desired reference matrix is simply

$$\mathbf{C}_{\text{BSM}_{N+1}}^* = \mathbf{C}_{\text{BSM}_N}^* \Delta\mathbf{R}^*$$

This iterative process generates the required reference trajectory  $\underline{\theta}_d(t)$ , which begins at the initial spacecraft attitude,  $\underline{\theta}_B$ , and terminates at  $\underline{\theta}_C$ . The desired rate is simply

$$\underline{\omega}_d = |\omega_d| \mathbf{Q} \underline{u}_r$$

where  $\mathbf{Q}^*$  is the transformation from navigation-base axes to the CSM-RCS autopilot control axes.  $\mathbf{Q}^*$  is defined as

$$\mathbf{Q}^* = \begin{bmatrix} 1 & 0 & 0 \\ 0 & \cos 7.25^\circ & -\sin 7.25^\circ \\ 0 & \sin 7.25^\circ & \cos 7.25^\circ \end{bmatrix}$$

$\underline{\omega}_d$  remains constant throughout the maneuver. The bias (or lag) angles are computed as

$$\beta_x = \frac{\omega_{dx}}{0.6}$$

$$\beta_y = \frac{\omega_{dy}}{0.6}$$

$$\beta_z = \frac{\omega_{dz}}{0.6}$$

These quantities also remain constant during the maneuver and are added to the attitude errors by the autopilot.

As mentioned in Subsection 3.6.1, the maneuver is timed in open-loop fashion and, for this reason, the first pass also computes the maneuver duration,  $t_m$ , as

$$t_m = \frac{A_m}{|\omega_d|}$$

The logic then sets a flag ( $FL_{\text{MANU}}$ ) to identify this as the first pass and, utilizing a section of coding common to both the first and subsequent passes, updates the desired reference angles  $\underline{\theta}_N$  ( $= \underline{\theta}_d$  projected 1 sec in advance) as described above.

With coding still unique to the first pass, the steering logic computes the time at which the maneuver will be completed as

$$t_f = t + t_m$$

where

$$t = \text{present time}$$

and the time at which to stop the steering-update process as

$$t_s = t_f - 1 \text{ sec}$$

The logic also computes the time  $t_u$ , at which the next update is to occur. If the maneuver is to be performed at the highest rate,  $FL_{\text{HIGHRATE}}$  is set to 1.  $HOLD\text{-}FLAG$  is then set equal to -1 to allow the autopilot to perform the maneuver. Note that all the initial commands are issued simultaneously to the autopilot with interrupt inhibited so that the maneuver will be started properly.

Returning to the common section of the coding, the logic then computes a set of incremental angles,  $\Delta\theta_d$ , for interpolation of the  $\theta_d$  reference angles between successive updates. This interpolation is required because the autopilot operates at a much higher sample rate,  $\Delta T_s$  (= 0.1 sec), than the steering ( $\Delta T_c = 1$  sec).  $\Delta\theta_d$  is computed as

$$\Delta\theta_d = (\theta_N - \theta_B) \frac{\Delta T_s}{\Delta T_c}$$

where

$$\theta_N = \text{desired reference angle projected 1 sec in advance}$$

$$\theta_B = \text{present desired reference angles}$$

These incremental angles are subsequently added to  $\theta_d$  by the autopilot, as explained in Subsection 3.2.  $\theta_d$  is then set equal to  $\theta_B$ , and  $\theta_B$  is replaced by  $\theta_N$  for use on the subsequent pass.

The logic then checks to see if the maneuver is to be completed within 1 sec. If not, the next steering cycle is called for in 1 sec, compensating for any delays between updates. If the maneuver is to be terminated, further updates are suspended and the program stops the maneuver at the appropriate time\*. To stop the maneuver, the program simply sets

$$\omega_d = 0$$

$$\Delta\theta_d = 0$$

$$\beta = 0$$

$$FL_{\text{HIGH RATE}} = 0$$

and sets  $\theta_d = \theta_c$  to eliminate any steering error. The crew can also intervene and stop the maneuver at any time by simply switching out of CMC AUTO or by moving the hand controller.

\*Actually delayed by approximately 10 millisc.

#### REFERENCES FOR SUBSECTION 3.6

- 6.1. Dixon, M., "Fuel-Time Optimal Spacecraft Reorientation," Ph.D. Thesis T-502, Instrumentation Laboratory, M.I.T., May 1968.
- 6.2. Crisp, R. and Keene, D., "Attitude Maneuver Optimization to Conserve Reaction Control Propellants," Report E-1832, Instrumentation Laboratory, M.I.T., August, 1965.
- 6.3. Crisp, R. and Keene, D., "Apollo Command and Service Module Reaction Control by the Digital Autopilot," Report E-1964, Instrumentation Laboratory, M.I.T., May 1966.
- 6.4. Keene, D., "Block II LGC Attitude Maneuver Routine: KALCMANU For Flight 206," Group 23 Internal Memo #8, Instrumentation Laboratory, M.I.T., November 1966.
- 6.5. Gorman, S. and Kimball, G., Apollo Software Information Memo 5-68-9, "VECPOINT Automatic Maneuvers for Program SUNDISK," U.S. Government Memorandum, May 1968.

Internal Distribution

Group 23A	<u>S. MacDougall</u> T. Brand P. Brennan P. Chin J. Higgins P. Kachmar	<u>IL 7-205</u> G. Levine E. Muller C. Pu M. Reber W. Robertson	10
Group 23B	<u>J. Kaloostian</u> A. Bancroft C. Beals N. Brodeur T. Crocker J. Goode R. Haslam	<u>IL7-221L</u> B. Ireland S. Jennings J. Laird N. Neville W. Ostanek R. Whittredge	12
Group 23B	<u>D. Lutkevich</u> C. Babicki G. Beck W. Danforth R. Daniel F. Decain R. Entes J. Flaherty J. Glendenning J. Good H. Hubbard	<u>IL7-228</u> H. Kana J. Klawnsnik H. Maher H. Nayar J. Reed (20) D. Reinke J. B. Smith F. Williams P. Wolff	38
Group 23B	<u>C. Taylor</u> N. Barnert B. Bramley A. Carter M. Cramer T. Crowley V. Demery D. Densmore S. Eliassen A. Engel	<u>IL7-221L</u> M. Hamilton D. Hsiung E. Hughes D. Lollar S. Rosenberg P. Rye N. Smith	16
Group 23H	<u>B. Lynn</u> S. Deutsch S. Goldberger	<u>IL7-234A</u> G. Kossuth J. O'Connor	4
Group 23C	<u>M. Erickson</u> R. Bairnsfather D. Fraser G. Kalan D. Keene	<u>IL11-102</u> A. Penchuk R. Schlundt R. Stengel J. Turnbull	8



Group 23D	<u>F. McGann</u> G. Dimock J. Dunbar I. Johnson R. Kiburz R. Metzinger E. Olsson	<u>IL7-332</u> R. Schulte A. Sewall S. Schroeder S. Smith F. Walsh W. Woolsey	12
Group 23D	<u>S. Prangley</u> J. Nevins	<u>IL7-209</u>	1
Group 23P	<u>C. Mitaris</u> S. Copps	<u>IL7-213</u> R. Larson	2
Group 23P	<u>A. Rubin</u> D. Hoag	<u>IL7-252</u> L. Larson	2
Group 23P	<u>E. Johnson</u> R. Ragan	<u>IL7-248</u> W. Stameris	2
Group 23S	<u>P. Amsler</u> M. Adams P. Felleman H. McOuat	<u>IL7-240</u> R. Strunce R. Werner R. White	6
Group 23T	<u>D. Farrell</u> W. Day G. Edmonds E. Grace K. Kido J. Lawrence R. Lones	<u>IL7-140</u> V. Megna J. Reedy N. Sears J. Silver J. St. Armand	11
Group 23N	<u>G. Grover</u> E. Blanchard L. B. Johnson	<u>IL11-202</u> G. Ogletree T. Parr	4
Group 33	<u>J. Hargrove</u> L. Drane K. Glick	<u>IL7-111</u> P. Mimno M. Johnson	4
Group 23P	<u>J. Sutherland</u> K. Greene	<u>IL7-266</u> G. Stubbs	2
APOLLO Library			2
MIT/IL Library			2

External Distribution List

MIT Instrumentation Laboratory P. O. Box 21025 Kennedy Space Center, Florida 32815 Attn: Mr. R. O'Donnell	(5)
MIT Instrumentation Laboratory Code EG/MIT Building 16 NASA Manned Spacecraft Center Houston, Texas 77058 Attn: Mr. Thomas Lawton	(3)
NASA MSC HW Building M7-409 Kennedy Space Center, Florida 32815 Attn: Mr. Frank Hughes	(10)
Mr. A. Metzger (NASA/RASPO at MIT/IL)	(1)
AC Electronics Division General Motors Corporation Milwaukee, Wisconsin Attn: Mr. J. Stridde Dept. 32-31 Attn: Mr. J. Kaiser Attn: Mr. W. Siarnicki Dept 38-02	(16)   (13) (2) (1)
Kollsman Instrument Corporation 575 Underhill Boulevard Syosset, Long Island Attn: Mr. F. McCoy	(1)
Raytheon Company Boston Post Road Sudbury, Massachusetts 01776 Attn: Mr. R. Zagrodnick	(6)
NASA/MSFC National Aeronautics and Space Administration George C. Marshall Space Flight Center Huntsville, Alabama Attn: J. Mack R-ASTR-5 Attn: V. Buckelew S&E-AERO-MFG A. Deaton R-AERO-DG F. Moore R-ASTR-N H. Hosenthien R-ASTR-F A. McNair I-MO-R D. Germany I-I/IB-E R. Barraza I-V-E W. Chubb R+ASTR/NG J. McCullough I-VE/T	(10)    (1) (1) (1) (1) (1) (1) (1) (1) (1) (1)
NASA/MSC National Aeronautics and Space Administration Manned Spacecraft Center Apollo Document Control Group (BM 86) Houston, Texas 77058 Attn: J. Williams, FS5 (letter of transmittal only)	300+2R

BELLCOMM	Bellcomm, Inc. 1100 17th Street N.W. Washington, D.C. 20036 Attn: Info. Analysis Section	(6)
LINK	LINK Group, GPSI SIMCOM 1740 A NASA Boulevard Houston, Texas 77058 Attn: Mr. D. Klingbell	(3)
TRW	H.V. Kienberger Bldg 82 Room 2045 TRW Systems Group One Space Park Redondo Beach, Calif 90278	(5)
NASA/GSFC	National Aeronautics and Space Administration Goddard Space Flight Center Greenbelt, Maryland Attn: Mr. Paul Pashby, Code 813	(2)
GA	Grumman Aerospace LEM Crew Systems Bethpage, Long Island, New York 11714 Attn: Mr. J. Marino (1) Attn: Mr. R. Pratt (1)	(2)
NAR	North American Rockwell Inc. Space and Information Systems Division 12214 Lakewood Boulevard Downey, California 90241 Attn: Apollo Data Requirements Dept. 096-340 Building 3, CA 99	(1 + 1R)
NASA/RASPO NAR	National Aeronautics and Space Administration Resident Apollo Spacecraft Program Office North American Rockwell, Inc Space and Information Systems Division 12214 Lakewood Boulevard Downey, California	(1)
NASA/KSC	National Aeronautics and Space Administration John F. Kennedy Space Center J. F. Kennedy Space Center, Florida 32899 Attn: Technical Document Control Office	(3)
NASA/RASPO GE	NASA Daytona Beach Operation P. O. Box 2500 Daytona Beach, Florida 32015 Attn: Mr. A. S. Lyman	(1)
NASA/HDQ	NASA Headquarters 600 Independence Avenue SW Washington, D. C. 20546 Attn: MAP-2 (4) Attn: Mission Director, Code MA (1) Attn: Robert Aller, Code MAO (1)	(6)

NASA/LEWIS	National Aeronautics and Space Administration Lewis Research Center Cleveland, Ohio Attn: Library	(2)
NASA/FRC	National Aeronautics and Space Administration Flight Research Center Edwards AFB, California Attn: Research Library	(1)
NASA/LRC	National Aeronautics and Space Administration Langley Research Center Langley AFB, Virginia Attn: Mr. A. T. Mattson	(2)
NAR/KSC	Kennedy Space Center, Florida 32815 M. S. O. B. North American Mail Station ZK69 Attn: Donald Matteson	(1)
NASA/RASPO GA	National Aeronautics and Space Administration Resident Apollo Spacecraft Program Officer Grumman Aerospace LEM Crew Systems Bethpage, Long Island, New York 11714	(1)
NASA/WSMR	National Aeronautics and Space Administration Post Office Drawer MM Las Cruces, New Mexico Attn: RH4 Documentation	(2)